



Lipoplexes recouverts d'acide hyaluronique pour le ciblage d'ARN interférant à des cellules tumorales surexprimant le récepteur CD44

Thais Leite Nascimento

► **To cite this version:**

Thais Leite Nascimento. Lipoplexes recouverts d'acide hyaluronique pour le ciblage d'ARN interférant à des cellules tumorales surexprimant le récepteur CD44. Pharmacie galénique. Université Paris Sud - Paris XI, 2015. Français. <NNT : 2015PA114834>. <tel-01367973>

HAL Id: tel-01367973

<https://tel.archives-ouvertes.fr/tel-01367973>

Submitted on 18 Sep 2016

HAL is a multi-disciplinary open access archive for the deposit and dissemination of scientific research documents, whether they are published or not. The documents may come from teaching and research institutions in France or abroad, or from public or private research centers.

L'archive ouverte pluridisciplinaire **HAL**, est destinée au dépôt et à la diffusion de documents scientifiques de niveau recherche, publiés ou non, émanant des établissements d'enseignement et de recherche français ou étrangers, des laboratoires publics ou privés.

UNIVERSITÉ PARIS-SUD

École Doctorale Innovation Thérapeutique : du Fondamental à l'appliqué

Pôle : Pharmacotechnie et Physico-chimie Pharmaceutique

Discipline : Pharmacotechnie et Biopharmacie

Lipoplexes recouverts d'acide hyaluronique pour le ciblage d'ARN interférant à des cellules tumorales surexprimant le récepteur CD44

Thèse de Doctorat

Thais Leite Nascimento

Série Doctorat N° 1331

Date de soutenance : 17/09/2015

JURY :

Prof. Elias FATTAL (Université Paris-Sud)

Dr. Hervé HILLAIREAU (Université Paris-Sud)

Prof. Nathalie MIGNET (Université Paris Descartes)

Prof. Didier BETBEDER (Université Lille 2 Droit et Santé)

Prof. Myriam TAVERNA (Université Paris-Sud)

Prof. Silvia ARPICCO (Università degli Studi di Torino)

Directeur de thèse

Co-encadrant de thèse

Rapporteur

Rapporteur

Examineur

Examineur

Sommaire

Abréviations	4
Introduction générale	8
Travaux antérieurs	12
Chapitre 1 - Nanoscale particles for lung delivery of siRNA	14
Chapitre 2 - Lipid based nanosystems for CD44 targeting in cancer treatment: recent significant advances, ongoing challenges and unmet needs	44
Travaux expérimentaux	80
Chapitre 1 - Supramolecular organization and siRNA binding of hyaluronic acid-modified lipoplexes for targeted delivery to CD44 receptor	82
Chapitre 2 - Efficient delivery of siRNA by hyaluronic acid-modified lipoplexes targeting CD44 receptors	110
Chapitre 3 - Study of the diffusion in respiratory mucus, lung distribution and in vivo gene silencing after intrapulmonary administration of hyaluronic acid-modified siRNA cationic lipoplexes	140
Discussion générale	164
Remerciements / Acknowledgements / Agradecimentos	178

Abréviations

AA	anisamide
AD	aerodynamic diameter
AS-ODN	antisense oligodeoxynucleotides
C3, C4, C5	complement components 3, 4, 5
CAM	cell adhesion molecules
CAP	calcium phosphate
CD24 / CD44	cluster of differentiation number 24 / 44
CD44v	variant isoforms of CD44
CE	capillary electrophoresis
CF	cystic fibrosis
CTGF	connective growth factor
DAPI	4',6-diamidino-2-phenylindole
DE	[2-(2-3didodecyloxypropyl)hydroxyethyl] ammonium bromide
DEAPA	diethylaminopropylamine
DiPhPE	diphytanoyl glycerophosphatidylethanolamine
DOPE	1,2-dioleoyl-sn-glycero-3-phosphoethanolamine
DOTAP	1,2-dioleyl-3-trimethylammonium-propane
DOTMA	n-[1-(2,3-dioleoyloxy) propyl]-n,n,n-trimethylammonium chloride
DPPE	dipalmitoyl phosphatidylethanolamine
DSC	differential scanning calorimetry
DSGLA	n,n-distearyl-nmethyl-n-2[n'-(n2-guanidino-l-lysiny)] aminoethyl ammonium chloride
DSRNA	double-stranded RNA
EDC	ethyl-dimethyl-aminopropyl-carbodiimide
EHV-1	equine herpes virus type 1
EPR	enhanced permeability and retention
ErbB2	receptor tyrosine-protein kinase
ERK1/2	extracellular signal regulated kinases
FITC	fluorescein isothiocyanat
GFP	green fluorescent protein
HA	hyaluronic acid
HA-LCS-NPs	hyaluronic-acid lipid-chitosan nanoparticles
HARE	HA receptor for endocytosis

HAase	hyaluronidase
HMW	high molecular weight
ICAM-1	intracellular adhesion molecule-1
IgG / IgM	immunoglobulin G / M
LMW	low molecular weight
LUC	luciferase
LYVE-1	lymphatic vessel endocytic receptor
MLV	multilamellar vesicle
MPP	mucus-penetrating particles
MPT	multiple particle tracking
MSD	mean square displacement
MW	molecular weight
M β CD	methyl- β -cyclodextrin
NLC	nanostuctured lipid carriers
PCL	poly(ϵ -caprolactone)
PCR	polymerisation chain reaction
PdI	polydispersity index
PE	phosphatidylethanolamine
PEG	poly(ethylene glycol)
PEI	polyethylenimine
PIV	parainfluenza virus
PLGA	poly(lactic-co-glycolic) acid
PS	polystyrene nanoparticles
PSA	poly(sebacic acid)
PVA	poly(vinyl alcohol)
qPCR	quantitative polymerisation chain reaction
RHAMM	receptor for hyaluronan-mediated motility
RISC	RNA induced silencing complex
RPMI	medium Roswell Park Memorial Institute
RSV	respiratory syncytial virus
SCLC	small cell lung cancer
SAXS	small-angle X-ray scattering
siRNA	small interfering RNA
SLN	solid lipid nanoparticles

SPARC	secreted protein, acidic and rich in cysteine
SPR	surface plasmon resonance
SUV	small unilamellar vesicle
TEM	transmission electron microscopy
TNF	tumor necrosis factor
VEGF	vascular endothelial growth factor

Introduction générale

Des progrès récents dans l'utilisation préclinique et clinique des petits ARN interférents (siRNA) ont montré leur potentiel en tant qu'inhibiteur de la synthèse protéique, et cela dans de nombreuses pathologies comme le cancer. L'administration des siRNA rencontre un certain nombre de problèmes liés à leur dégradation rapide dans les milieux biologiques, ainsi qu'à leur difficulté à pénétrer au sein des cellules cibles en raison de leur hydrophilie et de leur charge négative. Une des clés de l'amélioration de l'efficacité thérapeutique de ces molécules repose sur l'emploi de vecteurs. De nombreux vecteurs ont été formulés sur la base de systèmes colloïdaux que l'on dénomme aujourd'hui communément nanovecteurs ou nanomédicaments. Au cours de cette thèse, nous avons développé et optimisé des lipoplexes capables de protéger les siRNA contre la dégradation et de favoriser leur transport jusqu'aux cellules cibles. Ces lipoplexes, fonctionnalisés par de l'acide hyaluronique (HA), ont été conçus avec plusieurs objectifs, qui sont : (i) une complexation optimale des siRNA ; (ii) une toxicité limitée ; (iii) une capacité à cibler des cellules surexprimant le récepteur CD44, fortement impliqué dans les processus de développement tumoral et métastatique ; et (iv) un ciblage tumoral après administration par voie intraveineuse ou par voie intratrachéale. Pour ce faire, des lipoplexes recouverts d'HA ont été formulés, caractérisés d'un point de vue physico-chimique mais aussi du point de vue de leur *efficacité in vitro* et *in vivo*, pour la vectorisation active de siRNA vers des cellules tumorales surexprimant le récepteur CD44.

Le mémoire de la thèse comprend plusieurs parties. La première partie est bibliographique et se présente sous la forme de deux articles de revue, selon le plan suivant :

1. Le premier article, rédigé en tout début de la thèse, porte sur les caractéristiques des formulations de nanoparticules encapsulant les siRNA et les effets résultant de leur administration pulmonaire. La revue se concentre sur le transport de siRNA au sein de l'arbre pulmonaire, décrivant les différents obstacles à cette administration et la manière dont ils peuvent être contournés. Ce chapitre a été publié dans *Journal of Drug Delivery Science and Technology* en 2012.
2. Le deuxième chapitre concerne les nanoparticules à base de lipides (dont les liposomes) qui ont été utilisés pour le ciblage des récepteurs CD44. Dans cet article, nous décrivons le rôle de l'interaction entre l'HA et les récepteurs CD44 dans la prolifération et la migration cellulaire ainsi que l'inflammation et la croissance tumorale. L'effet de la modification de ces nanoparticules, par l'insertion d'HA, sur leurs propriétés physico-chimiques, leur activité biologique, leur interaction avec les récepteurs CD44, les voies d'internalisation cellulaire, la toxicité, l'activation du système complément/macrophages ainsi que la pharmacocinétique

est discutée. Ce chapitre a été soumis comme article de revue dans le journal *Nanomedicine* en 2015.

La seconde partie décrit les travaux expérimentaux sous la forme d'articles de recherche, organisés selon le plan suivant :

1. Dans un premier article, les lipoplexes vecteurs de siRNA ont été conçus et caractérisés. Pour atteindre le ciblage des récepteurs CD44, la structure des lipoplexes a été modifiée avec l'aide d'un conjugué entre l'HA et le lipide L-alpha-dioléylphosphatidyléthanolamine (DOPE). Une étude de la structure/morphologie de ces vecteurs a été réalisée en utilisant une combinaison de techniques telles que la diffusion dynamique de la lumière, l'électrophorèse capillaire, la cryomicroscopie et la résonance plasmonique de surface. L'organisation structurale du vecteur a été étudiée par diffusion des rayons X aux petits angles. Ce chapitre a été soumis comme article de recherche dans le journal *Soft Matter* en 2015.
2. L'activité *in vitro* et *in vivo* de la formulation optimisée de lipoplexes a été ensuite testée. La présence d'HA sur la surface des lipoplexes, et les effets de cette modification sur l'internalisation cellulaire ont été évalués. La capacité des lipoplexes à délivrer les siRNA a été démontrée en testant l'inhibition de l'expression génique de la luciférase sur lignée cellulaire de cancer du poumon A549-Luc, aussi bien *in vitro* qu'*in vivo* chez la souris par voie intraveineuse. Ce chapitre a été soumis comme article de recherche au journal *Nanomedicine NBM* en 2015.
3. Enfin, la diffusion des lipoplexes modifiés par l'HA au sein du mucus a été étudiée au cours d'un séjour au John Hopkins University dans l'équipe du Pr. Justin Hanes dans le but d'évaluer la faisabilité de l'administration locale (intratrachéale) de ces formulations pour le traitement de maladies pulmonaires. La diffusion des lipoplexes dans le mucus a été mesurée en utilisant la technique de 'multiple particle tracking'. Une étude *in vivo* chez la souris a aussi permis d'examiner la distribution des lipoplexes modifiés par l'HA, dans les poumons après administration intratrachéale. Ce travail sera soumis pour publication.

À la fin du manuscrit, une discussion générale reprend et développe tous les résultats obtenus au cours de cette thèse, et discute les perspectives scientifiques issues de ce travail.

Cette thèse de doctorat a été réalisée à l'Institut Galien Paris-Sud, sous la direction du Professeur Elias Fattal et du Docteur Hervé Hillaireau, grâce à l'octroi d'une bourse de la Fondation CAPES, du Ministère Brésilien de l'Éducation.

Travaux antérieurs

Travaux antérieurs

Chapitre 1 - Nanoscale particles for lung delivery of siRNA

Travaux antérieurs - Chapitre 1

Nanoscale particles for lung delivery of siRNA

Résumé

Les petits ARN interférents (siRNA) sont des molécules puissantes capables de bloquer l'expression des gènes après avoir atteint le cytoplasme de la cellule. Malgré leur grande efficacité, ils doivent être transportés par des nanovecteurs afin de les protéger contre la dégradation dans les fluides biologiques, accroître leur internalisation cellulaire et favoriser leur distribution subcellulaire. Plusieurs études ont mis en évidence le potentiel de l'administration locale de siRNAs dans les poumons pour le traitement de maladies pulmonaires. A cet effet, différents nanovecteurs ont été conçus pour le ciblage passif ou actif des cellules d'intérêt. Cette revue discute des possibilités de transporter les siRNA dans les poumons par ces nanosystèmes.

Chapitre publié sous forme d'article de review dans Journal of Drug Delivery Science and Technology, volume 22, 2012, 99-108. Auteurs : Thais Leite Nascimento, Hervé Hillaireau, Elias Fattal.

Literature review – Chapter 1

Nanoscale particles for lung delivery of siRNA

Abstract

Small interfering RNAs (siRNAs) are potent molecules capable of blocking gene expression after entering cell cytoplasm. Despite their strong efficacy, they need to be carried by nanoscale delivery systems that can protect them against degradation in biological fluids, increase their cellular uptake and favor their subcellular distribution. Several studies have highlighted the potential of local pulmonary delivery of siRNAs for the treatment of lung diseases. For this purpose, nanoscale delivery systems were addressed to target passively or actively the target cell. This review discusses the possibilities of approaching lung delivery of nanoscale particles carrying siRNAs.

Chapter published as a review article in Journal of Drug Delivery Science and Technology, volume 22, 2012, 99-108. Authors: Thais Leite Nascimento, Hervé Hillaireau, Elias Fattal.

Introduction

Since its discovery, the mechanism of RNA interference via small interfering RNA (siRNA) has developed rapidly into a powerful tool in molecular biology for studying the downregulation of gene expression. Due to their high efficiency and selectivity, siRNAs became rapidly interesting for medical applications like the treatment of severe diseases. There are a number of potential applications for targeted local delivery of siRNA to the lungs including the treatment of inflammatory, immune and infectious diseases, cystic fibrosis (CF), and cancer [1]. However, siRNAs face the same obstacles for a successful application as other nucleotide-based therapeutics like plasmid DNA or antisense oligonucleotides i.e., a poor cellular uptake and stability in serum and the lack of selectivity for the target tissue [1-4]. Therefore, carrier features of nanoparticulate delivery systems have been applied to address these limitations. Encapsulation and specific targeting of lung cancer cells thus offer the possibility of improving the treatment of lung diseases. This review focuses on the local delivery of siRNA to the lungs, describing the different barriers and the state-of-the-art ways they can be circumvented.

I. Mechanism of action of siRNA

siRNAs were discovered by showing that the introduction of long double-stranded RNA (dsRNA) into a variety of hosts could induce post-transcriptional silencing of all homologous host genes and/or transgenes [5-8]. Within the intracellular compartment, the long dsRNA molecules are metabolized to small 21-23 nucleotide interfering RNAs by the action of an endogenous ribonuclease: dsRNA-specific Rnase III enzyme Dicer [6, 9-12]. The siRNA molecules then assemble into a multiprotein complex, termed RNA-induced silencing complex (RISC) (Figure 1). Functional RISC contains four different subunits, including helicase, exonuclease, endonuclease, and homology searching domains. When siRNA binds to RISC, the duplex siRNA is unwound by helicase, resulting in two single strands (Figure 1) [13], allowing the antisense strand to bind to the targeted RNA molecule (Figure 1) [7, 14]. The endonucleases hydrolyze the target mRNA homologous at the site where the antisense strand is bound. RNA interference has an antisense mechanism of action as, ultimately, a single strand RNA molecule binds to the target RNA molecule by the Watson-Crick base pairing rules. Following binding, a cleavage enzyme present in RISC called argonaute 2, degrades the target RNA [15]. This mechanism makes feasible the use of small double stranded siRNA in therapeutics instead of AS-ODNs. When siRNA-mediated silencing occurs, the products are cleaved, released and degraded, allowing RISC complex to interact with other molecules from the mRNA pool [16]. It was also shown that small RNAs (called miRNAs for microRNAs) cause gene silencing in humans as well as in *Caenorhabditis elegans*,

Drosophila melanogaster, and plants [17, 18]. miRNAs are processed from extended RNA hairpins, whereas siRNAs are produced from a range of RNA precursors, such as viral, transposon RNAs and transgenes [19]. The mechanisms of siRNAs and miRNAs for RNA interference have some similarities, for example, the synthesis of both of them is related to the activity of Dicer, although there are significant differences between them, such as siRNAs cleaving mRNA, whereas miRNAs in some cases translationally repressed mRNA [20, 21].

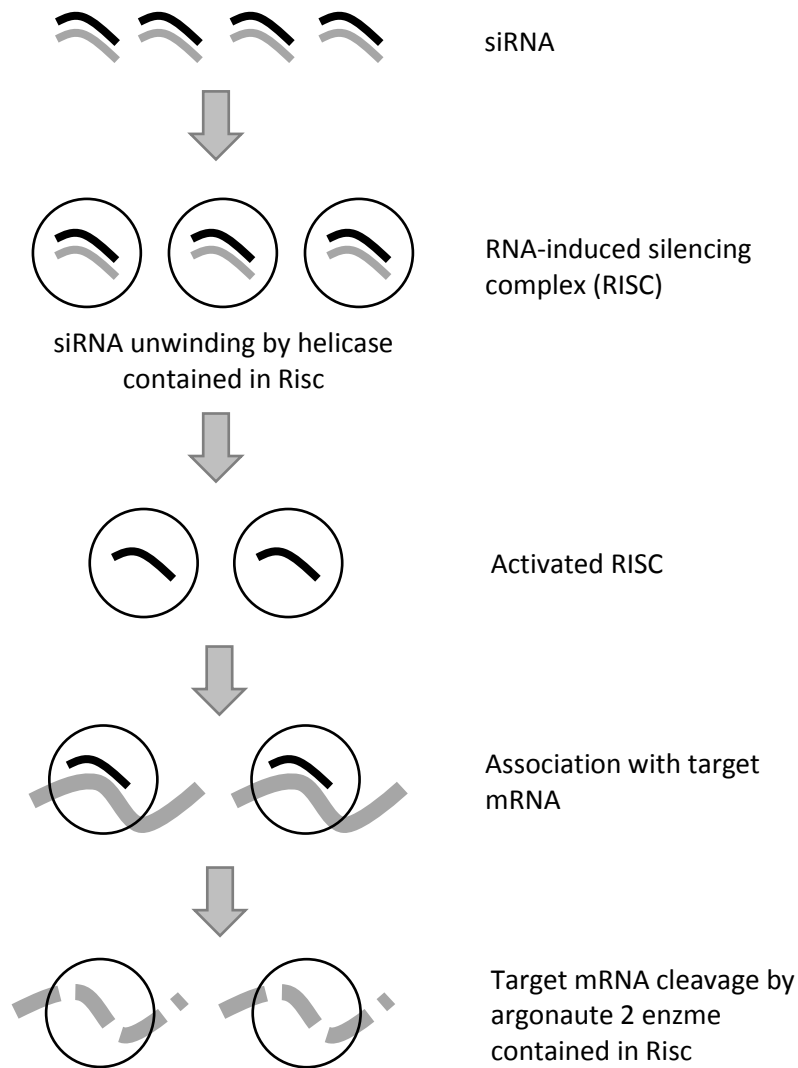


Figure 1. Mechanism of action of intracellular siRNA.

II. Barriers to siRNA delivery by inhalation

Direct instillation of siRNA into the lung offers several important benefits. As for any drug [22], the desired effect can be achieved with a total dose considerably lower than that required for systemic administration, resulting in a lower risk of toxicity and reduced adverse effects [23-24]. Also, instillation of siRNA (for instance as aerosol by intratracheal administration) offers direct access to lung epithelial cells, important cell types in a variety of pulmonary disorders and virus infections [22] and to the malignant cells on the respiratory tract, that cannot be achieved via systemic administration [25]. Finally, in the case of cancer treatment, the specificity of the siRNA would also result in much lower side effects when compared to conventional chemotherapy.

In this review, we will focus on local delivery to the airways of siRNA, which are large molecular weight molecules, both ionized and hydrophilic [4]. Despite a large interest, they present some hurdles for their *in vivo* administration (Table I). Indeed, even by lung administration, if the aerosolized solution reaches sites close to the target, the *in vivo* applicability of siRNA will be limited by the apparent siRNA instability in biological fluids and their inadequate cellular uptake (Table I). In biological fluids, the siRNA half-life is very short and varies from seconds to minutes [26]. This is predominately due to their rapid degradation by endogenous RNases and their rapid clearance [26]. To reach their cellular target, siRNAs need to cross the cellular membrane, but because of their negative charge and size [2], the incubation of unmodified free siRNA with mammalian cells does not result in effective knockdown of the target gene [27]. This is the reason why the most challenging innovation that is required for effective siRNA-mediated therapy in lung diseases is the targeting of siRNA to specific lung cell populations, using adequate delivery systems that will allow their delivery into the relevant intracellular compartment and further guarantee its protection against degradation. These systems should combine adequate intracellular delivery and permit lung delivery either by aerosol or dry powders.

The first obstacle to such a delivery is the resistance by respiratory mucus and alveolar fluids such as lung surfactant (Table I). Indeed, in the large airways, a continuously renewed mucus layer constitutes a barrier to assure the defence against inhaled materials [28, 29]. Mucus is composed mainly of water and mucins, long flexible highly glycosylated proteins that constitute around 1-5 % of the total weight of the whole mucus [30, 31]. Mucus traps the inhaled materials which are then effectively removed from the respiratory tract toward the upper end of the tracheal tube via the mucociliary clearance process [31]. This complex mechanism, which guarantees lung integrity in physiological conditions, can undergo important changes associated with pathological diseases or in the case of inhalation of various toxic compounds. Chronic disorders of the respiratory tract, such as asthma and cystic fibrosis

as well as exposure to cigarette smoke, pollutants and urban particular matter, are associated with impaired barrier function and changes in the composition of the mucus layer [32-36].

Table I - Tissue and cellular barriers for lung delivery of siRNA

	Barriers to siRNA delivery to the lung	Consequences	SiRNA delivery strategies
Tissue level	Aerodynamic properties	Modulate the biodistribution in the different regions of the lung	Aerosol formulation Liquid droplets (nebulization) Dry powders (spray-drying)
	Muco-ciliary clearance	Limits the period of time the carrier has to cross the mucus barrier and reach the epithelial cells	
	Stability in the bronchoalveolar fluids	Degradation of the carrier or the siRNA	
Cellular Level	Intracellular penetration	Insufficient amount of siRNA internalized	Nanocarrier formulation Lipid-based Polymer-based Virus-like vectors
	Intracellular stability	Quick endo-lysosomal degradation of siRNA, reduction of siRNA amount in the cytoplasm	
	Subcellular distribution	SiRNA must be delivered to the cytoplasm in order to be active	

One other barrier is the size of the inhaled material [37]. For lung delivery, the geometric diameter, particle shape and density are taken into account resulting in the so called aerodynamic diameter (AD). The AD of the particles affects the magnitude of forces acting on them. While inertial and gravitational effects increase with increasing particle size, diffusion produces larger displacement as particle size decreases (Figure 2). Large particles (> 5 μm AD) usually impact on airway wall at bifurcations. They are usually deposited higher up in the airway such as the back of the throat or pharynx [38]. When the AD of particles ranges from 1 to 5 μm , they are subject to sedimentation by gravitational force that occurs in smaller airways and respiratory bronchioles (Figure 2). The optimal particle size for efficient

deposition at the lower respiratory tract is considered to be between 1 and 3 μm [39, 40] (Figure 2). The movement of smaller particles ($< 1 \mu\text{m}$ aerodynamic diameter) is controlled by Brownian motion. And as the particle size further decreases, deposition in the lung increases again due to the increasing mobility through diffusion [37]. However, only nanoparticles that are less than 100 nm appear to settle effectively to the alveolar region with a fractional deposition of around 50 % [41, 42]. When the diameter gets larger in the nanoscale range, a high proportion, up to 80 %, can be exhaled [43, 44].

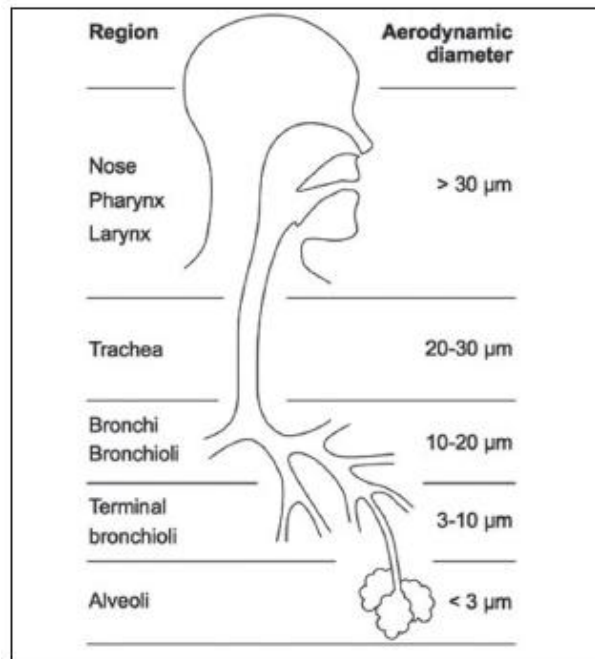


Figure 2. Particle deposition along the pulmonary tract as a function of the aerodynamic diameter.

III. Lung delivery of siRNA by nanoscale delivery systems

In the effort to enhance gene silencing, various non-viral nanoscale delivery systems have been developed for siRNA delivery, and a large part, summarized in Table II, are based on liposomal or polymeric delivery systems [3, 4, 45, 46]. Most systems developed for this purpose have a size of one to several hundreds of nanometers, and should thus be termed “sub-micron particles” rather than “nanoparticles” according to the latest European Commission recommendation of 18 October 2011 on the definition of nanomaterials.

1. Lipid-based delivery systems

Several commercially available cationic lipids, including Lipofectamine2000, DOTAP (N-[1-(2,3-dioleoyloxy)propyl]-N,N,N-trimethylammonium methylsulfate) and DOTMA(N-[1-(2,3-dioleoyloxy)propyl]-N,N,N-trimethylammonium chloride), have been selected and applied to the delivery of nucleic acids from all types: plasmid, antisense oligonucleotides and siRNA [47]. At the same time, researchers are still designing and synthesizing new lipids [48, 49] mostly to reduce the adverse effects described for the first cationic lipids [50, 51]. Cationic lipids added in excess to nucleic acids form positively charged lipoplexes which strongly interact with the negatively charged cell membrane facilitating their endocytosis and further cytoplasmic delivery [52]. Dioleylphosphatidylethanolamine (DOPE), a lipid helper, is generally associated with cationic lipids since it participates on the formation of the complexes with nucleic acids [53] and facilitates endosomal membrane disruption by forming hexagonal phases at the acidic pH of the endosomes [54]. Strategies involving the covalent attachment of a targeting ligand at the extremity of poly(ethylene glycol) (PEG) chains grafted onto liposomes have also been explored. Ligands specifically promote intracellular accumulation of the nucleic acid-containing lipid particle into the target cells and further lead to improved gene silencing [55]. Regarding lung delivery, cationic liposomes carrying siRNA have the ability to be aerosolized [56] and they have shown, *in vitro*, to deliver intracellularly siRNA in the human lung cancer cell lines A549 and H661 [57], human bronchial epithelial cells [58] or type II rat alveolar epithelial cells [59].

Table II: *In vitro* and *in vivo* intranasal or intratracheal delivery of siRNA by nanoscale organic and non viral carriers

Target	Delivery Technology	Model	Biological action (<i>in vivo</i> or <i>in vitro</i>)	Reference
In vitro experiments				
Human telomerase reverse transcriptase	Hyaluronic acid-bearing DOTAP/DOPE liposomes	A549 lung cancer cells	Transfection of siRNA cells was markedly improved with HA-modified liposomes targeting the CD44 receptor. Telomerase activity was successfully inhibited after a treatment with lipoplexes prepared with antiTERT siRNA.	[64]
BCL-2	Antagonist G-bearing DOTAP/HSPC/CHOL/DSPE-PEG	Human variant small cell lung cancer (SCLC) cell	Increased internalization in SCLC. No enhanced down regulation of Bcl-2.	[69]
Cyclin B1	Linear Polyethyleneimine (PEI)	H460 lung cancer cell line	Higher apoptotic effect	[105]
Enhanced green fluorescence protein (EGFP)	Poly(b-amino ester)s (PAEs), composed of low molecular weight PEI and poly(ethylene glycol) (PEG)	A549 lung cancer cells	79% silencing is obtained by PAE	[106]
Enhanced green fluorescence protein (EGFP) and Protein kinase B (Akt1)	Chitosan-graft-polyethylenimine copolymer composed of chitosan and low molecular weight polyethylenimine	A549 lung cancer cells	Silencing of EGFP expression is approximately 2.5 folds more than that of PEI25K	[107]
Enhanced green fluorescence protein (EGFP)	Chitosan nanoparticles	H1299 human lung carcinoma cells	Silencing up to 80% is obtained	[115]

Enhanced green fluorescent protein (EGFP) and TNF- α (tumour necrosis factor)	Freeze-dried chitosan/siRNA nanoparticles	H1299 human lung carcinoma cell line expressing EGFP and TNF- α expressing RAW murine macrophage cell line	EGFP knockdown efficiency increases with the siRNA concentration and depends on the presence of sucrose as lyoprotectant. Chitosan particles yielded more specific TNF- α knockdown than particles formed with lipid.	[116]
Luciferase	pHPMA-MPPM (poly((2-hydroxypropyl) methacrylamide 1-methyl-2-piperidine methanol)) TMC (O-methyl-free N,N,N-trimethylated chitosan)	Human lung cancer cells (H1299)	Luciferase expression was silenced by 30–40% increasing up to 70–80% in the presence of an endosomolytic peptide or a photochemical internalizing agent	[122]
Luciferase	PVA/PLGA nanoparticles	human lung cancer H1299 luc cells	Luciferase knockdown of 80–90% with minor to no cytotoxicity	[118]
<i>In vivo</i> experiments				
BCL-2	Cationic DOTAP lipid	Mice Intratracheal	Higher peak concentrations and longer retention of siRNA in the lungs when compared with systemic administration	[75]
B-galactosidase	Cationic lipid Genzyme (GL) 67	Mice Intratracheal	Reduced β gal mRNA levels in the airway epithelium but no protein expression	[76]
SPARC (matricellular protein)	Cationic lipid Dharma-FECT™	Mice-induced fibrosis Intratracheal	SPARC siRNA reduced gene and protein expression of collagen type 1 in fibroblasts Lung fibrosis induced by bleomycin is reduced with SPARC siRNA and was accompanied by an inhibition of connective tissue growth factor expression in these same tissues	[77]

Highly conserved regions of the nucleoprotein or acidic polymerase in Influenza viruses	Cationic lipid oligofectamine (Invitrogen)	Mice Intravenous followed by Intranasal	Delivery of the siRNAs reduced lung virus titers in infected mice. Protection is specific and not mediated by an antiviral IFN response	[78]
Respiratory syncytial virus (RSV)-P protein and parainfluenza virus (PIV) type 3 (HPIV3) P protein	TransIT-TKO™ (Mirus Bio Corp)	Mice Intranasal	Specific reduction of pulmonary RSV and PIV titer. SiRNAs free of transfection reagent, also inhibited pulmonary viral titers.	[79]
Severe acute respiratory syndrome (SARS) coronavirus	Infasurf® (calfactant) Extract of natural surfactant from calf lungs which includes phospholipids, neutral lipids, and hydrophobic surfactant-associated proteins B and C	Mice Intranasal	The siRNAs provided relief from SCV infection–induced fever, diminished SCV viral levels and reduced acute diffuse alveoli damage	[80]
GAPDH protein	Infasurf® (calfactant) Extract of natural surfactant from calf lungs which includes phospholipids, neutral lipids, and hydrophobic surfactant-associated	Mice Intranasal	Reduction of lung concentration of GAPDH protein 50% at 24 h and 67% at 7 days.	[81]
Protein kinase B (Akt1)	Poly(ester amine)	Mice	Silencing of Akt1 in the lungs without affecting Akt2 and Akt3 or affecting the protein expression of Akt1 in other organs	[109]

Nevertheless, liposome-based carriers still face some challenges for optimal siRNA delivery. These particles may be inadequate as they are associated after systemic administration with an intrinsic problem of non-specific interactions with blood components [51]. Some improvements were tested, such as the inclusion of anionic charges in PEG, which gives a greater colloidal stability in presence of serum [60]. However, when covering lipoplexes with PEG to reduce aggregation, a decrease of transfection efficiency is observed *in vitro* [61, 62]. Therefore it is important to find other ways to achieve targeting of lung cells. We have designed hyaluronic acid (HA)-coated lipoplexes for the targeted delivery to cancer cells that overexpress the HA binding receptor CD44 [63, 64]. This approach is based on the properties of HA, that, besides being an endogenous polymer, fulfills important mechanical or structural functions [65], interacting with its principal cell surface receptor CD44. The latter plays an important role on cell-cell/cell-matrix interaction, cell adhesion and migration and signal transduction from the extracellular to the intracellular compartment [66-68]. SiRNA transfection was improved with HA-modified liposomes, in CD44 positive A549 cells but not in Calu-3 cells that do not display the receptor. Santos et al. [69] have designed lipoplexes bearing as targeting ligand antagonist G, a substance P analogue that competitively inhibits basal and neuropeptide-stimulated growth of different small-cell lung cancer (SCLC) [70]. The targeted vesicles showed increased internalization in SCLC, as well as in other tumor cells and HMEC-1 microvascular endothelial cells, but the improved cellular association did not correlate with enhanced downregulation of the targeted Bcl-2. This absence of Bcl-2 downregulation was due to an inadequate release of the nucleic acids from the endocytic pathway, because of the presence of 10 mol% of PEG incorporated in the SLP formulation and/or to the absence of membrane destabilizing/fusogenic lipids.

To improve siRNA delivery, Chen et al. [71] developed a promising novel non-glycerol based cationic lipid, DSGLA (N,N-distearyl- N-methyl-N-2[N'-(N2-guanidino-L-lysiny)] aminoethyl ammonium chloride) that was formulated in lipid-polycation-DNA (LPD) nanoparticles containing DOTAP and targeted with PEG tethered with anisamide (AA). This new lipid contained both guanidinium and lysine residues as a cationic head group, that were chosen due to the fact that guanidinium groups are capable of forming hydrogen bonds with nucleic acid bases, thus further enhancing the capacity to deliver plasmid siRNA [71]. The lysine groups were selected for decreasing the cytotoxicity observed with the commercial lipid DOTAP contained in the LPD nanoparticles previously described by the authors [72, 73]. The presence of 10 μ M DSGLA in AA-bearing LPD was found to decrease extracellular signal-regulated kinases (ERK1/2) activation in H460 cells. The lipids without guanidine group did not cause the inhibition of ERK1/2 activation, and on the contrary, due to the antiapoptotic effect of DOTAP, an increased ERK1/2 activation was observed.

Among all lipid systems developed for treating lung cancer or other pulmonary diseases only a few have been administered in animal models by local administration, either intranasally or intratracheally. Garbuzenko et al. [74, 75] compared intratracheal v/s intravenous delivery of DOTAP-siRNA lipoplexes in mice. Intratracheal administration led to higher siRNA peak concentrations and a much longer retention of liposome-siRNA in the lungs when compared with systemic administration. In another experiment, GL67, a cationic lipid from Genzyme, mediated the uptake of siRNAs into airway epithelium *in vivo* in mice. siRNAs were complexed to GL67 and the resulting suspension was placed as a single bolus into the nasal cavity and rapidly sniffed into the lungs [76]. Following *in vivo* lung transfection, siRNAs were visible only in alveolar macrophages. siRNAs targeted to β -galactosidase reduced β gal mRNA levels in the airway epithelium of K18-lacZ mice by 30 % as shown by RT-PCR. However, this was insufficient to reduce protein expression [76]. In another experiment, C57BL/6 mice were induced for skin and lung fibrosis by bleomycin and followed by SPARC siRNA treatment through subcutaneous injection and intratracheal instillation, respectively using DharmaFECT 1 as transfection reagent. SPARC (secreted protein, acidic and rich in cysteine), is a component of the extracellular matrix which has been reported as a bio-marker for fibrosis in interstitial pulmonary fibrosis. After treatment, it was shown that lung fibrosis induced by bleomycin was markedly reduced by treatment with SPARC siRNA. The anti-fibrotic effect of SPARC siRNA *in vivo* was accompanied by an inhibition of connective growth factor (CTGF) expression in these same tissues. The lung distribution of intratracheally injected fluorescent siRNA showed that intense fluorescence was distributed within epithelial cells of bronchi and bronchioles, and only weak fluorescence was detected in the parenchyma [77]. It is unclear so far why such a difference of lung distribution was observed in both studies. Physico-chemical properties of complexes such as size, charge or other surface properties might play an important role in their distribution.

Complexes comprised of Oligofectamine and a siRNA specific for highly conserved regions of the nucleoprotein or acidic polymerase were found to inhibit influenza A virus replication *in vivo* after intranasal administration to mice [78]. The same inhibition was obtained on respiratory syncytial virus (RSV) and parainfluenza virus (PIV) using siRNAs against viral genes, instilled intranasally in mouse, associated or not with the transfection reagents TransIT-TKO. [79]. Finally, suspensions of siRNAs, with or without the transfection reagent Lipofectamine were administered intranasally in an *in vivo* murine model of Equine Herpes Virus Type 1 (EHV-1) infection using an EHV-1-specific siRNA. Although the administration of free siRNA induced protection against clinical signs like weight loss, no significant difference could be observed between the effectiveness of siRNA complexed with the transfection reagent Lipofectamine or with buffer (PBS). This agrees with some reports where the activity of intranasally administered free siRNA in various animal models has been clearly

demonstrated, and was in some cases superior to that of lipoplexes [80, 81]. Finally, a more recent study has demonstrated the inflammatory properties of lipoplexes carrying siRNA [82].

2. Polymeric nanoparticles

Nanoparticles are among the various siRNA delivery systems considered for pulmonary application [4, 83-85]. These nanoscale carriers present several advantages for the treatment of respiratory diseases, such as prolonged drug release, cell specific targeted drug delivery or modified biological distribution of the therapeutic agent, both at the cellular and organ level [86]. Nanoparticles composed of polymers show assurance in fulfilling the stringent requirements placed on these delivery systems, such as targeting of specific sites or cell populations in the lung, release of the drug in a predetermined manner, and degradation within an acceptable period of time [87]. Moreover, studies using inhaled nanoparticles dispersed in aqueous droplets suggest that the mucus clearance can be overcome by nanoparticles, and the drug efficiently transported to the respiratory epithelium [88].

2.1. Association of siRNA to cationic polymer systems by complexation

Several polymer nanoparticle systems have been developed to enhance intracellular delivery of nucleic acids [3, 4, 89]. As for cationic lipids, at physiological pH, siRNA can electrostatically interact with cationic charges from polymers to form polyplexes simply by mixing the components in optimal conditions. The positive charges can either come from soluble cationic polymers or cationic nanoparticles. As the complex generally possesses a global positive surface charge, they get easily attached to the negatively charged cell surface and subsequently undergo endocytosis [90].

One of the main polymers used is polyethyleneimine (PEI), a branched polymer with high cationic potential. The complexes formed between nucleic acids and PEI are usually stable, dispersible, non-covalent and have a net positive charge, which allows interaction with negatively charged cell membranes, followed by internalization by endocytosis [4]. The delivery of the nucleic acid to the cytoplasm occurs by the “proton sponge effect” [91], in which the protonation of the numerous amino groups in the polymer causes osmotic rupture of the endosome and a cytosolic release of the nucleic acid [92-95]. Additionally, after complexation, siRNA is efficiently protected from degradation both *in vitro* in the presence of RNase and *in vivo* in the presence of serum nucleases [99]. Consequently, PEI has been employed in several studies for efficient siRNA delivery *in vitro* and *in vivo* [4, 100]. Lin et al. [105] tested linear PEIs forming cationic complex with siRNA to target Cyclin B1, an indispensable protein for cell mitosis. After treatment with siRNA alone, lung cancer cells

population in the G2/M phase of the cell cycle increased to around 5 % (compared with control) whereas cells treated with PEI-siRNA complex had a significant increase to around 13 %, indicating better arrest of the cell mitosis in the G2/M phase of cell cycles by treatment with the complex. Bolcato-Bellemin et al. [110] used linear PEI for the formation of complexes, and modified the siRNA structure adding short complementary A5-8/T5-8 overhangs to make the siRNA bind to each other, forming a large “gene-like” structure. With these new sticky overhangs, the PEI-siRNA complex showed increased stability and improved RNase protection and gene silencing in lung cancer cells. While linear PEI is capable of providing a high efficiency of systemic gene delivery to the lungs, branched PEI has been associated with higher levels of acute toxicity [101]. Indeed, higher molecular weight PEIs are related to increased cytotoxicity, due to aggregation of the polymer on the outer cell membrane, which thereby induces necrosis [102]. Also, PEI toxicity might be caused by the rapid adsorption of plasma proteins onto the positively charged polymers, which can lead to aggregation. Regarding siRNA, Beyerle et al. [103] showed that the toxicity is also dependant on cell type, and Thomas et al. [104] found that linear fully deacylated PEI of 25 kDa and 87 kDa were the most effective for lung delivery. Cytotoxicity and transfection efficiency of PEI are directly proportional to its molecular weight [96]. Efforts to reduce the toxicity or improve stability of the polyplexes have been made by synthesis of PEI with graft copolymers such as linear PEG [97, 98]. A modified PEI system, poly (β -amino ester) (PAE) composed of low molecular weight PEI and PEG was complexed with siRNA [106]. The complex was shown to transfect A549 lung cancer cells with a siRNA targeting the enhanced green fluorescence protein (EGFP) achieving 79 % silencing, higher than the standard 25 kDa PEI complex. In a subsequent study, the authors combined the advantages of chitosan (another cationic polymer: for more details see below) and of a modified PEI system. They synthesized a chitosan-graft-PEI (CHI-g-PEI) copolymer, composed of chitosan and low molecular weight PEI [107]. The CHI-g-PEI carrier complexed with siRNA silenced EGFP expression approximately 2.5 times more than that of 25kDa PEI in A549 cells. The carrier was also used to study the silencing of Akt1 protein expression. Such protein has a vital role in lung cancer, since its overexpression is related to the mechanisms of cancer cell survival, proliferation, and metastasis [108, 109]. Efficient knockdown of Akt1 mRNA as well as the decrease in Akt1 protein expression was observed using the new carrier. Also the addition of peptides such as HIV-TAT to cationic PEG-PEI copolymers has been studied to enhance transfection efficiency in bronchial cells *in vitro* [111]. Recently, non-invasive aerosolized siRNA delivery systems were developed for lung cancer treatment. A degradable PEI-PEG copolymer was synthesized by reaction of low-molecular weight PEI with PEG diacrylate [112]. An aerosol of poly(ester amine)/Akt1-targeting siRNA complex was delivered into mice with urethane-induced lung cancer through a nose-only inhalation system. Following aerosol delivery twice weekly for 4 weeks, Akt1 siRNA delivered in complexes with

poly(ester amine) showed down-regulation of Akt related signals and inhibited the progression of tumors in the lung cancer model of K-rasLA1 mice [109].

Beside PEI, chitosan is a natural polysaccharide both mucoadhesive and mucopermeable, two qualities that are advantageous for targeted delivery of siRNA to the respiratory tract [113, 114]. Additionally, it is well tolerated, biodegradable, and forms cationic complexes with nucleic acids. Chitosan has been effective for siRNA delivery and gene silencing with low toxicity [22, 113]. In an interesting study, the high degree of deacetylation and high chitosan molecular weight were identified by Liu et al. [115] as important parameters for efficient siRNA-mediated knockdown, thus highlighting the importance of polymer chemical properties for the optimization of gene silencing using chitosan/siRNA nanoparticles. Andersen et al. [116, 117] delivered chitosan/siRNA nanoparticles targeting the enhanced green fluorescent protein (EGFP). They found that EGFP knockdown efficiency increased with siRNA concentration and that it could be achieved using freeze-dried nanoparticles, lyophilized directly within the cell culture dishes or onto surfaces, and used later by simply adding the cell suspension directly. At low siRNA concentration (< 25 nM) the highest knockdown was obtained at relatively high sucrose concentrations used as cryoprotectant (60 % knockdown at 10 % sucrose) whereas, at high siRNA concentration (50 nM), 5 % sucrose was sufficient to reach maximum knock down efficiency (70 %). Compared with lipoplexes using (TransIT-TKO), freeze-dried TransIT-TKO/siRNA were more effective than chitosan/siRNA at all concentrations tested, although chitosan particles yielded more specific TNF- α knockdown than particles formed with lipid, which also exhibited significantly lower viability of approximately 60 %, compared to 90-100 % of the chitosan/siRNA nanoparticles.

Other cationic polymers have been used. Nguyen et al. [118] designed a branched biodegradable polyester consisting of tertiary-amine-modified PLA backbones grafted to PLGA. This polymer was previously found to show high transfection efficiency [119], superior biocompatibility compared to PEI [120], rapid degradation rates [120] and low acute toxicity and inflammatory response after pulmonary application [121]. Nguyen et al. [118] found that small siRNA dosages (of 5 and 10 pmol) were necessary to achieve the aimed luciferase knockdown of 80-90 % in H1299 human lung carcinoma cell with minor to no cytotoxicity. Also, at a polymer ratio of 10:1 the nebulized nanoparticles displayed comparable knockdown efficiency to the non-nebulized samples. Varkouhi et al. [122] evaluated the gene-silencing activity of two enzymatically-degradable designed polymers: trimethylated chitosan (TMC) and pHPMA-MPPM (poly((2-hydroxypropyl) methacrylamide 1-methyl-2-piperidine methanol)). Both compounds showed a rather important silencing effect (higher than current surfactants) with less toxicity, reaching 30 to 40 %. These values increased up to 70-80 % in the presence of an endosomolytic peptide or a photochemical internalizing agent.

2.2. Encapsulation of siRNA within polymer nanocapsules

Another established approach for lung delivery of siRNA involves poly (lactic-co-glycolic acid) (PLGA) nanoparticles. PLGA is approved for human use by the Food and Drug Administration (FDA), and several PLGA-based formulations have received worldwide marketing approval [123]. This synthetic biodegradable polymer was shown to be useful for drug delivery formulations with good biocompatibility, cellular uptake and controlled release characteristics [124-126], but also a high stability during nebulization [127]. According to Campolongo and Luo [128], PLGA nanoparticles have attracted much attention since they are assumed to meet the criteria required for successful siRNA delivery: i) they are sufficiently small for efficient tissue penetration and cellular uptake, ii) the siRNA can be entrapped into the PLGA matrix, which offers physical protection against RNase activity as well as a favorable colloidal stability of the system, and iii) the PLGA particles generally possess an excellent controllable and alterable degradation profile, allowing drug release to span from days to years depending on the molecular weight, the composition of the block copolymer and the structure of the nanoparticles [129]. Even though, regarding nucleotide encapsulation, formulation of PLGA nanoparticles also presents some challenges. One of them is that it is difficult to load smaller nucleic acid molecules like siRNA into PLGA nanoparticles and obtain a high loading and encapsulation efficiency with the use of classical preparation methods. As other low molecular weight compounds, siRNA easily leaks from the inner water phase into the outer water phase during preparation due to its relatively low molecular weight, its hydrophilic character and the electrostatic repulsion forces present between the phosphate groups in the siRNA backbone and the anionic acid groups in the PLGA polymer [118]. Also, the degradation of PLGA leads to the formation of acidic products, lactic and glycolic acid, which can cause DNA degradation and damage [130].

The optimal parameters for preparation of siRNA-loaded PLGA nanoparticles by the double emulsion solvent evaporation method were studied by Cun et al. [129]. The formulation and preparation process parameters were rationally optimized by an understanding of the effect of the parameters: i) the volume ratio between the inner water phase and the oil phase, ii) the PLGA concentration, iii) the sonication time for the primary emulsification, iv) the siRNA load and v) the amount of acetylated bovine serum albumin (Ac-BSA) added to the inner water phase to stabilize the primary emulsion. PLGA concentration and the volume ratio were the only significant main effects. Surprisingly, siRNA load was found not to contribute significantly to the encapsulation efficiency. The suggested explanations for the individual effects were that the increased PLGA concentration resulted in a further stabilization of the primary emulsion and limited the diffusion of siRNA through and out of the organic phase due to the increased viscosity of the organic phase, and that a higher inner water phase volume reduced the concentration gradient between the inner and the outer water phase.

2.3. Mineral nanoparticles

Calcium phosphate (CaP) nanoparticles have also been studied to improve nucleotide transfection [131-136]. CaP is a well used non-viral vector for *in vitro* transfection due to the fact that it is rapidly dissolved in the cytoplasm's acidic pH, and that it presents little cell toxicity [134, 135, 137]. Recently, Li et al. [138] combined the advantages of a core/shell nanoparticle structure and CaP nanoparticle to achieve a prolonged circulation time and an elevated endosome release mechanism. The authors studied nanoparticles with a CaP core and PEG-phospholipid coating to target luciferase in human lung cancer H460 cells, and an improvement in the gene-silencing effect was observed. CaP dissolved at a low pH, causing nanoparticle de-assembly, the dissolved calcium and phosphate ions increased the osmotic pressure and caused endosome swelling to release the encapsulated siRNA.

2.4. Viral-like synthetic vectors

Lastly, virus-like synthetic vectors as influenza virus envelopes [139] or virosomes have been applied to deliver siRNA *in vitro*. The use of virosomes has some advantages for antiviral siRNA delivery in the lung, such as the fact that they are expected to be taken up by the cells infected with the virus [140] and their relatively high efficiency. For certain types of viral vectors, a relatively long duration of gene expression can also be achieved [101]. However, progress in virosome research is hampered by the difficulty in manufacturing viral envelopes [140], inefficiency, impossibility of repeated administration and severe complications associated with their immunogenicity and oncogenic potential [101, 114, 141-143]. The well-documented case of the death of Jesse Gelsinger due to complications associated with an adenoviral vector highlights this problem [144].

IV. Means to deliver nanoscale carriers as dry powders

The study of the nanoparticle delivery into the respiratory system is also important, whether they are administered as aerosol droplets or dry powders. As mentioned earlier in this review, the study of the aerodynamic diameter of the particles containing nanoparticles is crucial to an optimized delivery to the lower respiratory tract. Also, the characteristics of the liquid media or solid excipients that surround the nanoparticles will influence their release kinetics after deposition in the airways, and thus the time it will take until the nanoparticles themselves are in contact with epithelial cells or macrophages.

Our group has designed multistage or “trojan” delivery system that combines the advantages of microspheres (i.e, long term release) and polyplexes (i.e., enhanced nucleic acid intracellular penetration) [145-148]. Indeed, solid nanoparticulate complexes made of PEI and nucleic acids were encapsulated into a polymer matrix [146, 148]. ODN complexation with PEI improved the encapsulation efficiency probably by an electrostatic interaction between the cationic ODN/ PEI complex and the anionic PLGA [145, 146, 148]. Release rate was shown to be dependent on the porosity of the microparticles: the higher the porosity, the faster the release. Low porous particles were shown to delivery constantly the nanoparticles with the consequence of improving the intracellular penetration once reaching the target. Microparticles consisting of aggregates of PLGA nanoparticles surrounding a hollow core were developed using non-biodegradable [39] and biodegradable PLGA polymers [149] because of their high aerodynamic properties, these particles seem very promising for lung delivery of nanoparticles.

Conclusion

Although lung delivery of siRNA represents an important field for therapeutic applications, the need of nanoscale carriers is essential to allow their delivery. A variety of systems have shown efficiency *in vitro*, as the systems based on cationic lipids. Other cationic polymers were able to complex siRNA, and biodegradable polymers were able to encapsulate siRNA, and they can be further surface-modified and functionalized to enhance targeting properties. Nevertheless, *in vivo* delivery also requires the control of aerosol formulation of the nanoparticles. And despite some successful experiments reported here, the studies carried out *in vivo* do not all show a real benefit of lung inhaled nanoparticulate systems. Further research is needed in order to better understand the distribution of such particles after lung administration.

References

1. Devi G.R.- siRNA-based approaches in cancer therapy.- *Cancer Gene Ther.*, 13, 819-829, 2006.
2. Aagaard L., Rossi J.J. - RNAi therapeutics: principles, prospects and challenges. - *Adv. Drug Deliv Rev.*, 59, 75-86, 2007.
3. Fattal E., Bochot A. - State of the art and perspectives for the delivery of antisense oligonucleotides and siRNA by polymeric nanocarriers. - *Int. J. Pharm.*, 364, 237-248, 2008.
4. Fattal E., Barratt G. - Nanotechnologies and controlled release systems for the delivery of antisense oligonucleotides and small interfering RNA. - *Br. J. Pharm.*, 157, 179-194, 2009.
5. Fire A., Xu S., Montgomery M.K., Kostas S.A., Driver S.E., Mello C.C.- Potent and specific genetic interference by double-stranded RNA in *Caenorhabditis elegans*. - *Nature*, 391, 806-811, 1998.
6. Elbashir S.M., Harborth J., Lendeckel W., Yalcin A., Weber K., Tuschl T. - Duplexes of 21-nucleotide RNAs mediate RNA interference in cultured mammalian cells. - *Nature*, 411, 494-498, 2001.
7. Vaucheret H., Fagard M. - Transcriptional gene silencing in plants: targets, inducers and regulators. - *Trends Genet.*, 17, 29-35, 2001.
8. Kennerdell J.R., Yamaguchi S., Carthew R.W. - RNAi is activated during *Drosophila* oocyte maturation in a manner dependent on aubergine and spindle-E. - *Genes Dev.*, 16, 1884-1889, 2002.
9. Timmons L., Fire A. - Specific interference by ingested dsRNA. - *Nature*, 395, 854, 1998.
10. Ketting R.F., Fischer S.E., Bernstein E., Sijen T., Hannon G.J., Plasterk R.H. - Dicer functions in RNA interference and in synthesis of small RNA involved in developmental timing in *C. elegans*. - *Genes Dev.*, 15, 2654-2659, 2001.
11. Hannon G.J., Rossi J.J. - Unlocking the potential of the human genome with RNA interference. - *Nature*, 431, 371-378, 2004.
12. Meister G., Tuschl T. - Mechanisms of gene silencing by double-stranded RNA. - *Nature*, 431, 343-349, 2004.
13. Nykanen A., Haley B., Zamore P.D. - ATP requirements and small interfering RNA structure in the RNA interference pathway. - *Cell*, 107, 309-321, 2001.
14. Martinez J., Patkaniowska A., Urlaub H., Lührmann R., Tuschl T. - Single-stranded antisense siRNAs guide target RNA cleavage in RNAi. - *Cell*, 110, 565-574, 2002.
15. Zamore P.D., Tuschl T., Sharp P.A., Bartel D.P. - RNAi: double-stranded RNA directs the ATP-dependent cleavage of mRNA at 21 to 23 nucleotide intervals. - *Cell*, 101, 25-33, 2000.
16. Leung R.K., Whittaker P.A. - RNA interference: from gene silencing to gene-specific therapeutics. - *Pharmacol. Ther.*, 107, 222-239, 2005.
17. Lee R.C., Feinbaum R.L., Ambros V. - The *C. elegans* heterochronic gene *lin-4* encodes small RNAs with antisense complementarity to *lin-14*. - *Cell*, 75, 843-854, 1993.
18. Hutvagner G., McLachlan J., Pasquinelli A.E., Balint E., Tuschl T., Zamore P.D. - A cellular function for the RNA-interference enzyme Dicer in the maturation of the *let-7* small temporal RNA. - *Science*, 293, 834-838, 2001.
19. Jana S., Chakraborty C., Nandi S., Deb J.K. - RNA interference: potential therapeutic targets. - *Appl. Microbiol. Biotechnol.*, 65, 649-657, 2004.
20. Sontheimer E.J., Carthew R.W.- Silence from within: endogenous siRNAs and miRNAs. - *Cell*, 122, 9-12, 2005.
21. Chu C., Rana T.M. - Translation repression in human cells by microRNA-induced gene silencing requires RCK/p54. - *PLoS Biol.*, 4, e210, 2006.
22. de Fougerolles A., Novobrantseva T. - siRNA and the lung: research tool or therapeutic drug? - *Curr. Opin. Pharmacol.*, 8, 280-285, 2008.

23. Koshkina N.V., Agoulnik I.Y., Melton S.L., Densmore C.L., Knight V. - Biodistribution and pharmacokinetics of aerosol and intravenously administered DNA-polyethyleneimine complexes: optimization of pulmonary delivery and retention. - *Molecular Therapy*, 8, 249-254, 2003.
24. Sham J.O.H., Zhang Y., Finlay W.H., Roa W.H., Lobenberg R. - Formulation and characterization of spray-dried powders containing nanoparticles for aerosol delivery to the lung. - *Int. J. Pharm.*, 269, 457-467, 2004.
25. Zou Y., Tornos C., Qiu X., Lia M., Perez-Soler R. - p53 aerosol formulation with low toxicity and high efficiency for early lung cancer treatment. - *Clinical Cancer Res.*, 13, 4900-4908, 2007.
26. Soutschek J., Akinc A., Bramlage B., Charisse K., Constien R., Donoghue M., Elbashir S., Geick A., Hadwiger P., Harborth J., John M., Kesavan V., Lavine G., Pandey R.K., Racie T., Rajeev K.G., Rohl I., Toudjarska I., Wang G., Wuschko S., Bumcrot D., Koteliansky V., Limmer S., Manoharan M., Vornlocher H.P. - Therapeutic silencing of an endogenous gene by systemic administration of modified siRNAs. - *Nature*, 432, 173-178, 2004.
27. Dykxhoorn D.M., Lieberman J. - Knocking down disease with siRNAs. - *Cell*, 126, 231-235, 2006.
28. Knowles M.R., Hohneker K.W., Zhou Z., Olsen J.C., Noah T.L., Hu P.C., Leigh M.W., Engelhardt J.F., Edwards L.J., Jones K.R., Grossman M., Wilson J.M., Johnson L.G., Boucher R.C. - A controlled study of adenoviral-vector-mediated gene transfer in the nasal epithelium of patients with cystic fibrosis. - *N. Engl. J. Med.*, 333, 823-831, 1995.
29. Cone R.A. - Barrier properties of mucus. - *Adv. Drug Del. Rev.*, 61, 75-85, 2009.
30. Quraishi M.S., Jones N.S., Mason J. - The rheology of nasal mucus: a review. - *Clin. Otolaryngol. Allied Sci.*, 23, 403-413, 1998.
31. Samet J.M., Cheng P.W. - The role of airway mucus in pulmonary toxicology. - *Environ. Health Perspect.*, 102, Suppl. 2, 89-103, 1994.
32. Evans C.M., Koo J.S. - Airway mucus: the good, the bad, the sticky. - *Pharmacol. Ther.*, 121, 332-348, 2009.
33. Jany B., Gallup M., Tsuda T., Basbaum C. - Mucin gene expression in rat airways following infection and irritation. - *Biochem. Biophys. Res. Commun.*, 181, 1-8, 1991.
34. Ling S.H., van Eeden S.F. - Particulate matter air pollution exposure: role in the development and exacerbation of chronic obstructive pulmonary disease. - *Int. J. Chronic Obstructive Pulmonary Disease*, 4, 233-243, 2009.
35. Ahn M.H., Kang C.M., Park C.S., Park S.J., Rhim T., Yoon P.O., Chang H.S., Kim S.H., Kyono H., Kim K.C. - Titanium dioxide particle-induced goblet cell hyperplasia: association with mast cells and IL-13. - *Respiratory Research*, 6, 34, 2005.
36. Haswell L.E., Hewitt K., Thorne D., Richter A., Gaca M.D. - Cigarette smoke total particulate matter increases mucous secreting cell numbers *in vitro*: a potential model of goblet cell hyperplasia. - *Toxicol In vitro*, 24, 981-987, 2010.
37. Yang W., Peters J.I., Williams R.O., 3rd - Inhaled nanoparticles, a current review. - *Int. J. Pharm.*, 356, 239-247, 2008.
38. Suarez S., Hickey A.J. - Drug properties affecting aerosol behavior. - *Respir. Care*, 45, 652-666, 2000.
39. Tsapis N., Bennett D., Jackson B., Weitz D.A., Edwards D.A. - Trojan particles: large porous carriers of nanoparticles for drug delivery. - *Proc. Natl. Acad. Sci. USA*, 99, 12001-12005, 2002.
40. Sakagami M. - *In vivo*, *in vitro* and *ex vivo* models to assess pulmonary absorption and disposition of inhaled therapeutics for systemic delivery. - *Adv. Drug Deliv. Rev.*, 58, 1030-1060, 2006.
41. Patton J.S., Byron P.R. - Inhaling medicines: delivering drugs to the body through the lungs. - *Nat. Rev. Drug Discov.*, 6, 67-74, 2007.
42. Byron P.R. - Prediction of drug residence times in regions of the human respiratory-tract following aerosol inhalation. - *J. Pharm. Sci.*, 75, 433-438, 1986.

43. Heyder J., Rudolf G.- Mathematical-models of particle deposition in the human respiratory-tract. - *J. Aerosol. Sci.*, 15, 697-707, 1984.
44. Heyder J., Gebhart J., Rudolf G., Schiller C.F., Stahlhofen W. - Deposition of particles in the human respiratory-tract in the size range 0.005-16-Mu-M. - *J. Aerosol. Sci.*, 17, 811-825, 1986.
45. Gilmore I.R., Fox S.P., Hollins A.J., Akhtar S. - Delivery strate- gies for siRNA-mediated gene silencing. - *Curr. Drug Deliv.*, 3, 147-145, 2006.
46. Li W., Szoka F.C., Jr. - Lipid-based nanoparticles for nucleic acid delivery. - *Pharm. Res.*, 24, 438-449, 2007.
47. Fattal E., Delattre J., Dubernet C., Couvreur P. - Liposomes for the delivery of nucleotides and oligonucleotides. - *STP Pharma Sci.*, 9, 383-390, 1999.
48. Han S.E., Kang H., Shim G.Y., Suh M.S., Kim S.J., Kim J.S., Oh Y.K. - Novel cationic cholesterol derivative-based liposomes for serum-enhanced delivery of siRNA. - *Int. J. Pharm.*, 2007.
49. De Rosa G., De Stefano D., Laguardia V., Arpicco S., Simeon V., Carnuccio R., Fattal E. - Novel cationic liposome formulation for the delivery of an oligonucleotide decoy to NF-kappaB into activated macrophages. - *Eur. J. Pharm. Biopharm.*, 70, 7-18, 2008.
50. Plank C., Mechtler K., Szoka F.C., Jr., Wagner E. - Activation of the complement system by synthetic DNA complexes: a potential barrier for intravenous gene delivery. - *Hum. Gene Ther.*, 7, 1437-1446, 1996.
51. Lambert G., Fattal E., Brehier A., Feger J., Couvreur P. - Ef- fect of polyisobutylcyanoacrylate nanoparticles and lipofectin loaded with oligonucleotides on cell viability and PKC alpha neosynthesis in HepG2 cells. - *Biochimie*, 80, 969-976, 1998.
52. Lavigne C., Thierry A.R. - Specific subcellular localization of siRNAs delivered by lipoplex in MCF-7 breast cancer cells. - *Biochimie*, 89, 1245-1251, 2007.
53. De Oliveira M.C., Fattal E., Couvreur P., Lesieur P., Bourgaux C., Ollivon M., Dubernet C. - pH-sensitive liposomes as a carrier for oligonucleotides: a physico-chemical study of the interaction between DOPE and a 15-mer oligonucleotide in quasi-anhydrous samples. - *Biochim. Biophys. Acta*, 1372, 301-310, 1998.
54. Fattal E., Couvreur P., Dubernet C.- "Smart" delivery of antisense oligonucleotides by anionic pH-sensitive liposomes. - *Adv. Drug Deliv. Rev.*, 56, 931-946, 2004.
55. Cardoso A., Trabulo S., Moreira J.N., Duzgunes N., de Lima M.C. - Targeted lipoplexes for siRNA delivery. - *Methods Enzy- mol.*, 465, 267-287, 2009.
56. Gautam A., Waldrep J.C., Densmore C.L. - Aerosol gene therapy. - *Mol. Biotechnol.*, 23, 51-60, 2003.
57. Toulany M., Minjgee M., Kehlbach R., Chen J., Baumann M., Rodemann H.P. - ErbB2 expression through heterodimerization with erbB1 is necessary for ionizing radiation- but not EGF- induced activation of Akt survival pathway. - *Radiother. Oncol.*, 97, 338-345, 2010.
58. Han S.W., Roman J. - Fibronectin induces cell proliferation and inhibits apoptosis in human bronchial epithelial cells: pro-oncogenic effects mediated by PI3-kinase and NF-kappa B. - *Oncogene*, 25, 4341-4349, 2006.
59. Ma X., Xu D., Ai Y., Ming G., Zhao S. - Fas inhibition attenuates lipopolysaccharide-induced apoptosis and cytokine release of rat type II alveolar epithelial cells. - *Mol. Biol. Rep.*, 37, 3051- 3056, 2010.
60. Nicolazzi C., Mignet N., de la Figuera N., Cadet M., Ibad R.T., Seguin J., Scherman D., Bessodes M. - Anionic polyethyleneg- lycol lipids added to cationic lipoplexes increase their plasmatic circulation time. - *J. Control. Release*, 88, 429-443, 2003.
61. Bally M.B., Harvie P., Wong F.M., Kong S., Wasan E.K., Reimer D.L. - Biological barriers to cellular delivery of lipid-based DNA carriers. - *Adv. Drug Deliv. Rev.*, 38, 291-315, 1999.
62. Shi F., Wasungu L., Nomden A., Stuart M.C., Polushkin E., Engberts J.B., Hoekstra D. - Interference of poly(ethylene glycol)-lipid analogues with cationic-lipid-mediated delivery of oligonucleotides; role of lipid exchangeability and non-lamellar transitions. - *Biochem J.*, 366, 333-341, 2002.

63. Surace C., Arpicco S., Dufay-Wojcicki A., Marsaud V., Bouclier C., Clay D., Cattel L., Renoir J.M., Fattal E. - Lipoplexes targeting the CD44 hyaluronic acid receptor for efficient transfection of breast cancer cells. - *Molecular Pharmaceutics*, 6, 1062-1073, 2009.
64. Taetz S., Bochot A., Surace C., Arpicco S., Renoir J.M., Schaefer U.F., Marsaud V., Kerdine-Roemer S., Lehr C.M., Fattal E. - Hy- aluronic acid-modified DOTAP/DOPE liposomes for the targeted delivery of anti-telomerase siRNA to CD44-expressing lung cancer cells. - *Oligonucleotides*, 19, 103-115, 2009.
65. Bastow E.R., Byers S., Golub S.B., Clarkin C.E., Pitsillides A.A., Fosang A.J. - Hyaluronan synthesis and degradation in cartilage and bone. - *Cell. Mol. Life Sci.*, 65, 395-413, 2008.
66. Turley E.A. - Extracellular matrix remodeling: multiple paradigms in vascular disease. - *Circ. Res.*, 88, 2-4, 2001.
67. Jothy S. - CD44 and its partners in metastasis. - *Clin. Exp. Metastasis*, 20, 195-201, 2003.
68. Ponta H., Sherman L., Herrlich P.A. - CD44: from adhesion molecules to signalling regulators. - *Nat. Rev. Mol. Cell Biol.*, 4, 33-45, 2003.
69. Santos A.O., da Silva L.C., Bimbo L.M., de Lima M.C., Simoes S., Moreira J.N. - Design of peptide-targeted liposomes containing nucleic acids. - *Biochim. Biophys. Acta*, 1798, 433-441, 2010.
70. Clive S., Webb D.J., MacLellan A., Young A., Byrne B., Robson L., Smyth J.F., Jodrell D.I. - Forearm blood flow and local responses to peptide vasodilators: a novel pharmacodynamic measure in the phase I trial of antagonist G, a neuropeptide growth factor antagonist. - *Clin. Cancer Res.*, 7, 3071-3078, 2001.
71. Chen Y., Sen J., Bathula S.R., Yang Q., Fittipaldi R., Huang L. - Novel cationic lipid that delivers siRNA and enhances therapeutic effect in lung cancer cells. - *Mol. Pharm.*, 6, 696-705, 2009.
72. Li S.D., Huang L. - Surface-modified LPD nanoparticles for tumor targeting. - *Ann NY Acad. Sci.*, 1082, 1-8, 2006.
73. Li S.D., Chen Y.C., Hackett M.J., Huang L. - Tumor-targeted delivery of siRNA by self-assembled nanoparticles. - *Mol. Ther.*, 16, 163-169, 2008.
74. Garbuzenko O.B., Saad M., Pozharov V.P., Reuhl K.R., Mainelis G., Minko T. - Inhibition of lung tumor growth by complex pulmonary delivery of drugs with oligonucleotides as suppressors of cellular resistance. - *Proc. Natl. Acad. Sci. USA*, 107, 10737- 10742, 2010.
75. Garbuzenko O.B., Saad M., Betigeri S., Zhang M., Vetcher A.A., Soldatenkov V.A., Reimer D.C., Pozharov V.P., Minko T. - Intratracheal versus intravenous liposomal delivery of siRNA, antisense oligonucleotides and anticancer drug. - *Pharm. Res.*, 26, 382-394, 2009.
76. Griesenbach U., Kitson C., Escudero Garcia S., Farley R., Singh C., Somerton L., Painter H., Smith R.L., Gill D.R., Hyde S.C., Chow Y.H., Hu J., Gray M., Edbrooke M., Ogilvie V., MacGregor G., Scheule R.K., Cheng S.H., Caplen N.J., Alton E.W. - Inefficient cationic lipid-mediated siRNA and antisense oligonucleotide transfer to airway epithelial cells *in vivo*. - *Respir. Res.*, 7, 26, 2006.
77. Wang J.C., Lai S., Guo X., Zhang X., de Crombrugghe B., Sonnyal S., Arnett F.C., Zhou X. - Attenuation of fibrosis *in vitro* and *in vivo* with SPARC siRNA. - *Arthritis Res. Ther.*, 12, R60, 2010.
78. Tompkins S.M., Lo C.Y., Tumpey T.M., Epstein S.L. - Protection against lethal influenza virus challenge by RNA interference *in vivo*. - *Proc. Natl. Acad. Sci. USA*, 101, 8682-8686, 2004.
79. Bitko V., Musiyenko A., Shulyayeva O., Barik S. - Inhibition of respiratory viruses by nasally administered siRNA. - *Nat. Med.*, 11, 50-55, 2005.
80. Li B.J., Tang Q., Cheng D., Qin C., Xie F.Y., Wei Q., Xu J., Liu Y., Zheng B.J., Woodle M.C., Zhong N., Lu P.Y. - Using siRNA in prophylactic and therapeutic regimens against SARS coronavirus in Rhesus macaque. - *Nat. Med.*, 11, 944-951, 2005.
81. Massaro D., Massaro G.D., Clerch L.B. - Noninvasive delivery of small inhibitory RNA and other reagents to pulmonary alveoli in mice. - *Am. J. Physiol. Lung Cell Mol. Physiol.*, 287, L1066- 1070, 2004.

82. Gutbier B., Kube S.M., Reppe K., Santel A., Lange C., Kaufmann J., Suttorp N., Witzenrath M. - RNAi-mediated suppression of constitutive pulmonary gene expression by small interfering RNA in mice. - *Pulm. Pharmacol. Ther.*, 23, 334-344, 2010.
83. Toub N., Malvy C., Fattal E., Couvreur P. - Innovative nanotechnologies for the delivery of oligonucleotides and siRNA. - *Biomed. Pharmacother.*, 60, 607-620, 2006.
84. Fattal E., Bochot A. - Ocular delivery of nucleic acids: antisense oligonucleotides, aptamers and siRNA. - *Adv. Drug Deliv. Rev.*, 58, 1203-1223, 2006.
85. Reischl D., Zimmer A. - Drug delivery of siRNA therapeutics: potentials and limits of nanosystems. - *Nanomedicine*, 5, 8-20, 2009.
86. Beck-Broichsitter M., Gauss J., Packhaeuser C.B., Lahnstein K., Schmehl T., Seeger W., Kissel T., Gessler T. - Pulmonary drug delivery with aerosolizable nanoparticles in an ex vivo lung model. - *Int. J. Pharm.*, 367, 169-178, 2009.
87. Rytting E., Nguyen J., Wang X., Kissel T. - Biodegradable polymeric nanocarriers for pulmonary drug delivery. - *Expert Opin. Drug Deliv.*, 5, 629-639, 2008.
88. Schurch S., Gehr P., Im Hof V., Geiser M., Green F. - Surfactant displaces particles toward the epithelium in airways and alveoli. - *Respir. Physiol.*, 80, 17-32, 1990.
89. Fattal E., Vauthier C., Aynie I., Nakada Y., Lambert G., Malvy C., Couvreur P. - Biodegradable polyalkylcyanoacrylate nanoparticles for the delivery of oligonucleotides. - *J. Control. Release*, 53, 137-143, 1998.
90. Gomes dos Santos A.L., Bochot A., Tsapis N., Artzner F., Bejjani R.A., Thillaye-Goldenberg B., de Kozak Y., Fattal E., Behar-Cohen F. - Oligonucleotide-polyethylenimine complexes targeting retinal cells: structural analysis and application to anti-TGFbeta-2 therapy. - *Pharm. Res.*, 23, 770-781, 2006.
91. Behr J.P. - The proton sponge: a trick to enter cells the viruses did not exploit. - *Chimia*, 51, 34-36, 1997.
92. Boussif O., Zanta M.A., Behr J.P. - Optimized galenics improve *in vitro* gene transfer with cationic molecules up to 1000-fold. - *Gene Ther.*, 3, 1074-1080, 1996.
93. Zuber G., Dauty E., Nothisen M., Belguise P., Behr J.P. - Towards synthetic viruses. - *Adv. Drug Deliv. Rev.*, 52, 245-253, 2001.
94. Akinc A., Thomas M., Klibanov A.M., Langer R. - Exploring polyethylenimine-mediated DNA transfection and the proton sponge hypothesis. - *J. Gene Med.*, 7, 657-663, 2005.
95. Werth S., Urban-Klein B., Dai L., Hobel S., Grzelinski M., Bakowsky U., Czubayko F., Aigner A. - A low molecular weight fraction of polyethylenimine (PEI) displays increased transfection efficiency of DNA and siRNA in fresh or lyophilized complexes. - *J. Control. Release*, 112, 257-270, 2006.
96. Godbey W.T., Mikos A.G. - Recent progress in gene delivery using non-viral transfer complexes. - *J. Control. Release*, 72, 115-125, 2001.
97. Vinogradov S.V., Bronich T.K., Kabanov A.V. - Self-assembly of polyamine-poly(ethylene glycol) copolymers with phosphorothioate oligonucleotides. - *Bioconjug. Chem.*, 9, 805-812, 1998.
98. Petersen H., Fechner P., Fischer D., Kissel T. - Synthesis, characterization, and biocompatibility of polyethylenimine-graft-poly(ethylene glycol) block copolymers. - *Macromolecules*, 35, 6867-6874, 2002.
99. Urban-Klein B., Werth S., Abuharbeid S., Czubayko F., Aigner A. - RNAi-mediated gene-targeting through systemic application of polyethylenimine (PEI)-complexed siRNA *in vivo*. - *Gene Ther.*, 12, 461-466, 2005.
100. Malek A., Merkel O., Fink L., Czubayko F., Kissel T., Aigner A. - *In vivo* pharmacokinetics, tissue distribution and underlying mechanisms of various PEI(-PEG)/siRNA complexes. - *Toxicol. Appl. Pharmacol.*, 236, 97-108, 2009.
101. Kuruba R., Wilson A., Gao X., Li S. - Targeted delivery of nucleic acid-based therapeutics to the pulmonary circulation. - *AAPS J.*, 11, 23-30, 2009.

102. Fischer D., Bieber T., Li Y., Elsasser H.P., Kissel T. - A novel non-viral vector for DNA delivery based on low molecular weight, branched polyethylenimine: effect of molecular weight on transfection efficiency and cytotoxicity. - *Pharm. Res.*, 16, 1273-1279, 1999.
103. Beyerle A., Hobel S., Czubayko F., Schulz H., Kissel T., Aigner A., Stoeger T. - *In vitro* cytotoxic and immunomodulatory profiling of low molecular weight polyethylenimines for pulmonary application. - *Toxicol. In vitro*, 23, 500-508, 2009.
104. Thomas M., Lu J.J., Ge Q., Zhang C., Chen J., Klibanov A.M. - Full deacylation of polyethylenimine dramatically boosts its gene delivery efficiency and specificity to mouse lung. - *Proc. Natl. Acad. Sci. USA*, 102, 5679-5684, 2005.
105. Lin S.Y., Lin F.S., Chen M.K., Tsai L.R., Jao Y.C., Lin H.Y., Wang C.L., Hwu Y.K., Yang C.S. - One-pot synthesis of linear-like and photoluminescent polyethylenimines for intracellular imaging and siRNA delivery. - *Chem. Commun. (Camb.)*, 46, 5554-5556, 2010.
106. Jere D., Xu C.X., Arote R., Yun C.H., Cho M.H., Cho C.S. - Poly(beta-amino ester) as a carrier for si/shRNA delivery in lung cancer cells. - *Biomaterials*, 29, 2535-2547, 2008.
107. Jere D., Jiang H.L., Kim Y.K., Arote R., Choi Y.J., Yun C.H., Cho M.H., Cho C.S. - Chitosan-graft-polyethylenimine for Akt1 siRNA delivery to lung cancer cells. - *Int. J. Pharm.*, 378, 194-200, 2009.
108. Brognard J., Clark A.S., Ni Y., Dennis P.A. - Akt/protein kinase B is constitutively active in non-small cell lung cancer cells and promotes cellular survival and resistance to chemotherapy and radiation. - *Cancer Res.*, 61, 3986-3997, 2001.
109. Xu C.X., Jere D., Jin H., Chang S.H., Chung Y.S., Shin J.Y., Kim J.E., Park S.J., Lee Y.H., Chae C.H., Lee K.H., Beck G.R., Jr., Cho C.S., Cho M.H. - Poly(ester amine)-mediated, aerosol-delivered Akt1 small interfering RNA suppresses lung tumorigenesis. - *Am. J. Respir. Crit. Care Med.*, 178, 60-73, 2008.
110. Bolcato-Bellemin A.L., Bonnet M.E., Creusat G., Erbacher P., Behr J.P. - Sticky overhangs enhance siRNA-mediated gene silencing. - *Proc. Natl. Acad. Sci. USA*, 104, 16050-16055, 2007.
111. Kleemann E., Neu M., Jekel N., Fink L., Schmehl T., Gessler T., Seeger W., Kissel T. - Nanocarriers for DNA delivery to the lung based upon a TAT-derived peptide covalently coupled to PEG-PEI. - *J. Control. Release*, 109, 299-316, 2005.
112. Park M.R., Han K.O., Han I.K., Cho M.H., Nah J.W., Choi Y.J., Cho C.S. - Degradable polyethylenimine-alt-poly(ethylene glycol) copolymers as novel gene carriers. - *J. Control. Release*, 105, 367-380, 2005.
113. Howard K.A., Rahbek U.L., Liu X., Damgaard C.K., Glud S.Z., Andersen M.O., Hovgaard M.B., Schmitz A., Nyengaard J.R., Besenbacher F., Kjems J. - RNA interference *in vitro* and *in vivo* using a novel chitosan/siRNA nanoparticle system. - *Mol. Ther.*, 14, 476-484, 2006.
114. Durcan N., Murphy C., Cryan S.A. - Inhalable siRNA: potential as a therapeutic agent in the lungs. - *Mol. Pharm.*, 5, 559-566, 2008.
115. Liu X., Howard K.A., Dong M., Andersen M.O., Rahbek U.L., Johnsen M.G., Hansen O.C., Besenbacher F., Kjems J. - The influence of polymeric properties on chitosan/siRNA nanoparticle formulation and gene silencing. - *Biomaterials*, 28, 1280-1288, 2007.
116. Andersen M.O., Howard K.A., Paludan S.R., Besenbacher F., Kjems J. - Delivery of siRNA from lyophilized polymeric surfaces. - *Biomaterials*, 29, 506-512, 2008.
117. Andersen M.O., Howard K.A., Kjems J. - RNAi using a chitosan/ siRNA nanoparticle system: *in vitro* and *in vivo* applications. - *Methods Mol. Biol.*, 555, 77-86, 2009.
118. Nguyen J., Steele T.W., Merkel O., Reul R., Kissel T. - Fast degrading polyesters as siRNA nanocarriers for pulmonary gene therapy. - *J. Control. Release*, 132, 243-251, 2008.
119. Oster C.G., Wittmar M., Unger F., Barbu-Tudoran L., Schaper A.K., Kissel T. - Design of amine-modified graft polyesters for effective gene delivery using DNA-loaded nanoparticles. - *Pharm. Res.*, 21, 927-931, 2004.

120. Unger F., Wittmar M., Kissel T. - Branched polyesters based on poly[vinyl-3-(dialkylamino)alkylcarbamate-co-vinyl acetate-co-vinyl alcohol]-graft-poly(d,l-lactide-co-glycolide): effects of polymer structure on cytotoxicity. - *Biomaterials*, 28, 1610-1619, 2007.
121. Dailey L.A., Jekel N., Fink L., Gessler T., Schmehl T., Wittmar M., Kissel T., Seeger W. - Investigation of the proinflammatory potential of biodegradable nanoparticle drug delivery systems in the lung. - *Toxicol. Appl. Pharmacol.*, 215, 100-108, 2006.
122. Varkouhi A.K., Lammers T., Schiffelers R.M., Van Steenbergen M.J., Hennink W.E., Storm G. - Gene silencing activity of siRNA polyplexes based on biodegradable polymers. - *Eur. J. Pharm. Biopharm.*, 2011.
123. Jain R.A. - The manufacturing techniques of various drug loaded biodegradable poly(lactide-co-glycolide) (PLGA) devices. - *Bio-materials*, 21, 2475-2490, 2000.
124. Cartiera M.S., Johnson K.M., Rajendran V., Caplan M.J., Saltzman W.M. - The uptake and intracellular fate of PLGA nanoparticles in epithelial cells. - *Biomaterials*, 30, 2790-2798, 2009.
125. Nie H., Ho M.L., Wang C.K., Wang C.H., FuY.C. - BMP-2 plasmid loaded PLGA/HAp composite scaffolds for treatment of bone defects in nude mice. - *Biomaterials*, 30, 892-901, 2009.
126. Mura S., Hillaireau H., Nicolas J., Le Droumaguet B., Gueutin C., Zanna S., Tsapis N., Fattal E. - Influence of surface charge on the potential toxicity of PLGA nanoparticles towards Calu-3 cells. - *International Journal of Nanomedicine*, (in press), 2011.
127. Manca M.L., Mourtas S., Dracopoulos V., Fadda A.M., Antimi-siaris S.G. - PLGA, chitosan or chitosan-coated PLGA micro-particles for alveolar delivery? A comparative study of particle stability during nebulization. - *Colloids Surf. B Biointerfaces*, 62, 220-231, 2008.
128. Campolongo M.J., Luo D. - Drug delivery: old polymer learns new tracts. - *Nat. Mater.*, 8, 447-448, 2009.
129. Cun D., Jensen D.K., Maltesen M.J., Bunker M., Whiteside P., Scurr D., Foged C., Nielsen H.M. - High loading efficiency and sustained release of siRNA encapsulated in PLGA nanoparticles: quality by design optimization and characterization. - *Eur. J. Pharm. Biopharm.*, 77, 26-35, 2011.
130. Walter E., Moelling K., Pavlovic J., Merkle H.P. - Microencapsulation of DNA using poly(DL-lactide-co-glycolide): stability issues and release characteristics. - *J. Control. Release*, 61, 361-374, 1999.
131. Roy I., Mitra S., Maitra A., Mozumdar S. - Calcium phosphate nanoparticles as novel non-viral vectors for targeted gene delivery. - *Int. J. Pharm.*, 250, 25-33, 2003.
132. Welzel T., Radtke I., Meyer-Zaika W., Heumann R., Epple M. - Transfection of cells with custom-made calcium phosphate nanoparticles coated with DNA. - *J. Mater. Chem.*, 14, 2213-2217, 2004.
133. Maitra A. - Calcium phosphate nanoparticles: second-generation nonviral vectors in gene therapy. - *Expert Review of Molecular Diagnostics*, 5, 893-905, 2005.
134. Sokolova V., Kovtun A., Prymak O., Meyer-Zaika W., Kubareva E.A., Romanova E.A., Oretskaya T.S., Heumann R., Epple M. - Functionalisation of calcium phosphate nanoparticles by oligonucleotides and their application for gene silencing. - *J. Mater. Chem.*, 17, 721-727, 2006.
135. Sokolova V.V., Radtke I., Heumann R., Epple M. - Effective transfection of cells with multi-shell calcium phosphate-DNA nanoparticles. - *Biomaterials*, 27, 3147-3153, 2006.
136. Olton D., Li J., Wilson M.E., Rogers T., Close J., Huang L., Kumta P.N., Sfeir C. - Nanostructured calcium phosphates (NanoCaPs) for non-viral gene delivery: Influence of the synthesis parameters on transfection efficiency. - *Biomaterials*, 28, 1267-1279, 2007.
137. Bisht S., Bhakta G., Mitra S., Maitra A. - pDNA loaded calcium phosphate nanoparticles: highly efficient non-viral vector for gene delivery. - *Int. J. Pharm.*, 288, 157-168, 2005.
138. Li J., Chen Y.C., Tseng Y.C., Mozumdar S., Huang L. - Biodegradable calcium phosphate nanoparticle with lipid coating for systemic siRNA delivery. - *J. Control. Release*, 142, 416-421, 2010.

139. de Jonge J., Holtrop M., Wilschut J., Huckriede A. - Reconstituted influenza virus envelopes as an efficient carrier system for cellular delivery of small-interfering RNAs. - *Gene Therapy*, 13, 400-411, 2005.
140. de Fougerolles A., Novobrantseva T. - siRNA and the lung: research tool or therapeutic drug? - *Current Opinion in Pharmacology*, 8, 280-285, 2008.
141. Lehrman S. - Virus treatment questioned after gene therapy death. - *Nature*, 401, 517-518, 1999.
142. Cavazzana-Calvo M., Fischer A. - Gene therapy for severe combined immunodeficiency: are we there yet? - *J. Clin. Invest.*, 117, 1456, 2007.
143. Di Gioia S., Conese M. - Polyethylenimine-mediated gene delivery to the lung and therapeutic applications. - *Drug Design, Development and Therapy*, 2, 163, 2008.
144. Zallen D. - US gene therapy in crisis. - *Trends in Genetics*, 16, 272-275, 2000.
145. De Rosa G., Quaglia F., La Rotonda M.I., Appel M., Alphandary H., Fattal E. - Poly(lactide-co-glycolide) microspheres for the controlled release of oligonucleotide/polyethylenimine complexes. - *J. Pharm. Sci.*, 91, 790-799, 2002.
146. De Rosa G., Bochot A., Quaglia F., Besnard M., Fattal E. - A new delivery system for antisense therapy: PLGA microspheres encapsulating oligonucleotide/polyethyleneimine solid complexes. - *Int. J. Pharm.*, 254, 89-93, 2003.
147. De Rosa G., Quaglia F., Bochot A., Ungaro F., Fattal E. - Long-term release and improved intracellular penetration of oligonucleotide-polyethylenimine complexes entrapped in biodegradable microspheres. - *Biomacromolecules*, 4, 529-536, 2003.
148. Gomes dos Santos A.L., Bochot A., Doyle A., Tsapis N., Siepmann J., Siepmann F., Schmalzer J., Besnard M., Behar-Cohen F., Fattal E. - Sustained release of nanosized complexes of polyethylenimine and anti-TGF-beta 2 oligonucleotide improves the outcome of glaucoma surgery. - *J. Control. Release*, 112, 369-381, 2006.
149. Gomez-Gaete C., Fattal E., Silva L., Besnard M., Tsapis N. - Dexamethasone acetate encapsulation into Trojan particles. - *J. Control. Release*, 128, 41-49, 2008.

Travaux antérieurs

**Chapitre 2 - Lipid based nanosystems for CD44 targeting in cancer treatment:
recent significant advances, ongoing challenges and unmet needs**

Travaux antérieurs - Chapitre 2

Lipid based nanosystems for CD44 targeting in cancer treatment: recent significant advances, ongoing challenges and unmet needs**Résumé**

De nombreuses preuves expérimentales obtenues dans des modèles cellulaires et animaux démontrent l'importance de l'interaction entre l'acide hyaluronique (HA) et le récepteur CD44 dans la prolifération et la migration cellulaire, l'inflammation et la croissance des tumeurs. Afin de tirer profit de cette interaction, la conception de nanomédicaments modifiés par l'HA a été exploitée au cours de la dernière décennie pour le ciblage de cellules surexprimant les récepteurs CD44, dans le but de transporter des médicaments aux cellules cancéreuses ou inflammatoires. La modification des particules par l'HA offre la possibilité de cibler sélectivement ces cellules et améliorer ainsi l'efficacité des médicaments. L'efficacité de ce ciblage est cependant influencée par plusieurs facteurs, dont le poids moléculaire de l'HA, sa conformation et disponibilité sur la surface des nanoparticules, la densité de son recouvrement ainsi que la charge et taille de ces nanomédicaments. Dans ce chapitre, nous nous concentrons sur l'impact de la modification par l'HA de nanomédicaments à base de lipides sur ces caractéristiques. Nous discutons comment cette modification influence les propriétés physicochimiques de ces systèmes, leur activité biologique, l'interaction avec des récepteurs CD44, les voies d'internalisation cellulaire, leur toxicité, l'activation du système complément et des macrophages et leur pharmacocinétique.

*Chapitre rédigé sous forme d'article de review pour publication dans Nanomedicine en 2015.
Auteurs: Thais Leite Nascimento, Hervé Hillaireau, Elias Fattal.*

Literature review – Chapter 2

Lipid based nanosystems for CD44 targeting in cancer treatment: recent significant advances, ongoing challenges and unmet needs**Abstract**

Extensive experimental evidence in cells and animal models demonstrate the important role of hyaluronic acid (HA)-CD44 interaction in cell proliferation and migration, inflammation and tumor growth. Taking advantage of this interaction, the design of HA-modified nanocarriers has been investigated in the past decade for the targeting of CD44-overexpressing cells with the purpose of delivering drugs to cancer or inflammatory cells. Particle modification with HA offers the possibility of selectively targeting those cells and improving drug efficacy. The effect of such a modification on targeting efficacy is however influenced by several factors, including HA molecular weight (MW), conformation and availability on the surface of the carriers, grafting density and particle charge and size. In this review, we focus on the impact of HA-modification of lipid-based nanoparticles on their characteristics. We discuss how modification of their structure induced by HA influences particle physicochemical properties, biological activity, interaction with CD44 receptors, intracellular trafficking pathways, toxicity, complement/macrophage activation and pharmacokinetics. Our aim is to give an overview on how to control nanocarrier functionalization by HA to design more efficient CD44-targeting lipid nanocarriers.

Chapter written in review article form and submitted for publication to the journal Nanomedicine in 2015. Authors: Thais Leite Nascimento, Hervé Hillaireau, Elias Fattal.

Introduction

Much effort has been devoted over the past few decades to improve the treatment of cancer, and advances in nanotechnology and tumor biology have enabled the development of efficient nanocarriers to deliver therapeutic agents to the tumor tissue [1-4]. These nanocarriers have offered unique possibilities to overcome cellular barriers in order to improve the delivery of various drugs and drug candidates, including promising therapeutic biomacromolecules (i.e., nucleic acids, proteins) [5]. In this context, one of the main adhesion/homing molecules involved in tumor progression and metastasis, CD44, has attracted much attention. Targeting these molecules is a promising approach in the treatment of cancer. These receptors are expressed on many types of tumors and accumulate numerous functions, such as supporting cell migration and transmitting survival signals through interactions with its numerous ligands [6-8].

The main ligand of CD44 receptors is hyaluronic acid (HA, hyaluronate, hyaluronan). The interaction between these two molecules is influenced by several factors. The conformation and availability of the ligands on the surface of nanoparticles, HA molecular weight, grafting density, particle charge and size, and the stability of the nanocarrier in physiological environment are examples of factors that should be considered when studying the targeting of CD44 receptors by HA-containing nanocarriers.

In this review, based on the design of lipid-based nanosystems, we have addressed these important issues, which are crucial for the rational design and optimization of CD44-targeted, hyaluronan-based nanotherapeutics for improved intracellular delivery. The influence of these modifications on their structure and physicochemical properties is discussed, as well as in their biological activity, including interaction with CD44 receptors, intracellular trafficking pathways, toxicity and complement/macrophage activation as well as the pharmacokinetics changes. Our aim is to give an overview on how to control the HA-particle modification to help designing more efficient CD44-targeting lipid nanocarriers.

CD44: structure and role

The cluster of differentiation 44 (CD44) is a single chain glycoprotein encoded by a gene located on the short arm of chromosome 11 [9]. This gene is composed of 20 exons, and alternate splicing of the 10 central exons [10] and post-translational modifications are responsible for the existence of variant isoforms (CD44v). Molecular mass of the different CD44 isoforms range from ~80 kDa to ~250 kDa

[6]. The most abundant isoform of human CD44 protein, CD44s, is the smallest one and lacks any variant exons. CD44E, a large isoform, is also abundant and expressed mainly in epithelial cells [11], while other CD44 isoforms are rarely present on normal tissues. In particular, CD44s is abundantly expressed by both normal and cancer cells, whereas the variant CD44 isoforms are expressed mostly by cancer cells [12].

CD44 belongs to the cell adhesion molecules family (CAM), together with integrins, selectins and cadherins. These molecules are involved in the contact between cells and between cells and the extracellular matrix. They are critical to the maintenance of tissue integrity, regulating growth, survival, differentiation and cell migration. Under pathological disorder, CD44 is involved in the tumor progression as well as the metastatic process [13]. An increasing number of studies [14-17] have evidenced that a small population of tumor cells (less than 0.1%) exhibit an indefinite proliferation potential, and are responsible for maintaining the tumor and, possibly, for the formation of new tumors at metastatic loci. These are referred to as cancer stem cells or cancer-initiating cells, in which CD44 has been identified as an important marker due to its interaction with different growth factor receptors [18].

Several types of tumors overexpress CD44 receptors, such as lung [19], ovarian [20], pancreatic [21], colon [22], prostate [23] and acute leukemia [24]. The level of expression depends on the cell type and the differentiation degree. The CD44 extracellular domain can interact with innumerable components of the extracellular matrix, including collagen, fibronectin, fibrinogen and laminin [25,26], and its principal ligand is hyaluronic acid (HA, hyaluronate, hyaluronan) (Figure 1).

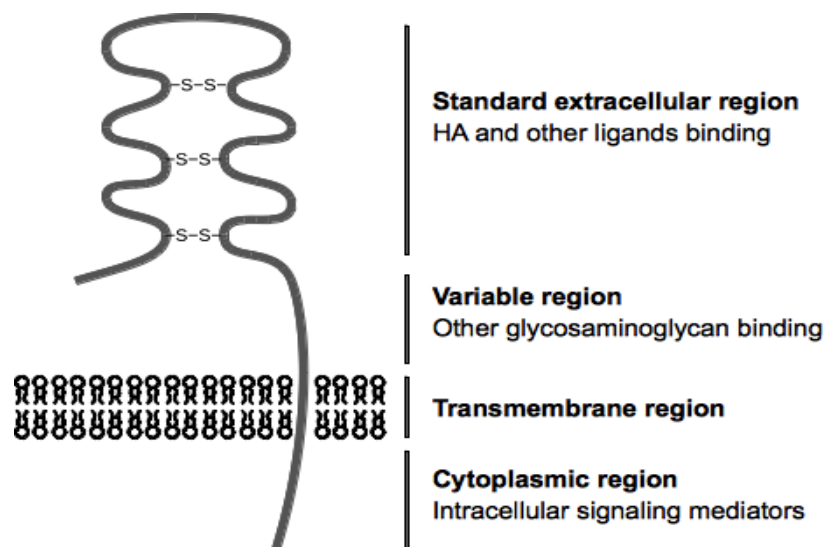


Figure 1: Structure of the CD44 receptor

Hyaluronic acid: a natural ligand of CD44

HA is a negatively charged hydrophilic linear polymer composed of repeating disaccharide units of D-glucuronic acid and N-acetyl-D-glucosamine linked by alternating β -1,4 and β -1,3 glycosidic bonds. It is biocompatible, being the major component of the extracellular matrix. In the matrix, HA plays a structural role, which depends on its hydrodynamic properties as well as on its interaction with other components of the matrix. HA influences intracellular signaling mainly by binding to its main cell-surface receptors CD44 and RHAMM (receptor for hyaluronan-mediated motility), but it also interacts with other cell surface receptors such as ICAM-1 (intracellular adhesion molecule-1), TLR-4 (toll-like receptor-4), HARE (HA receptor for endocytosis), and LYVE-1 (lymphatic vessel endocytic receptor) [27].

Since it is also concentrated in regions of high cell division and invasion (during embryonic morphogenesis, inflammation, wound repair, and cancer) [28], HA is involved in tumorigenesis. Its biological properties are dependent on its molecular weight [29]. Native high molecular weight (HMW) HA has been shown to be non-toxic and non-immunogenic [30]. It also does not induce expression of genes involved in proliferation or inflammation [31] and counteracts proangiogenic effects of the HA oligomers [32]. When HA fragments from 2 to 100 kDa (about 4 to 250 disaccharide units) bind to CD44, they induce angiogenic effects that have been described *in vitro*, contributing to tumor growth [33,34].

HA-CD44 binding affinity is dependent on the size of the polysaccharide. The specific binding domain of CD44 to HA comprises 160 amino acid residues. Hexamers and decamers are considered the shortest length able to bind CD44, and larger oligomers (over 20) have more affinity for the receptors because they have the ability to bind several CD44 at the same time [35]. CD44 proteins exist in three states with respect to HA binding: nonbinding; nonbinding unless activated by physiological stimuli; and constitutively binding [18]. To date, receptor mediated endocytosis of HA and macropinocytosis of bulk phase HA have been reported (Figure 2). CD44-mediated endocytosis can occur via lipid rafts or by the clathrin-coated pit pathway. Receptors for HA endocytosis may be recycled to the cell surface or turned-over. HA saccharides are further digested to HA oligosaccharides by hyaluronidases (HAses) in the endosome into fragments that could have several biological functions [36]. Different signaling pathways can be triggered after HA-CD44 interaction occurs, depending on cell type and HA molecular weight. The participation of HA in CD44 signaling for different cell activities including proliferation, migration, and inflammation in normal tissues and in organ pathology illustrates the important and complex role of HA in modulating cell behavior [37].

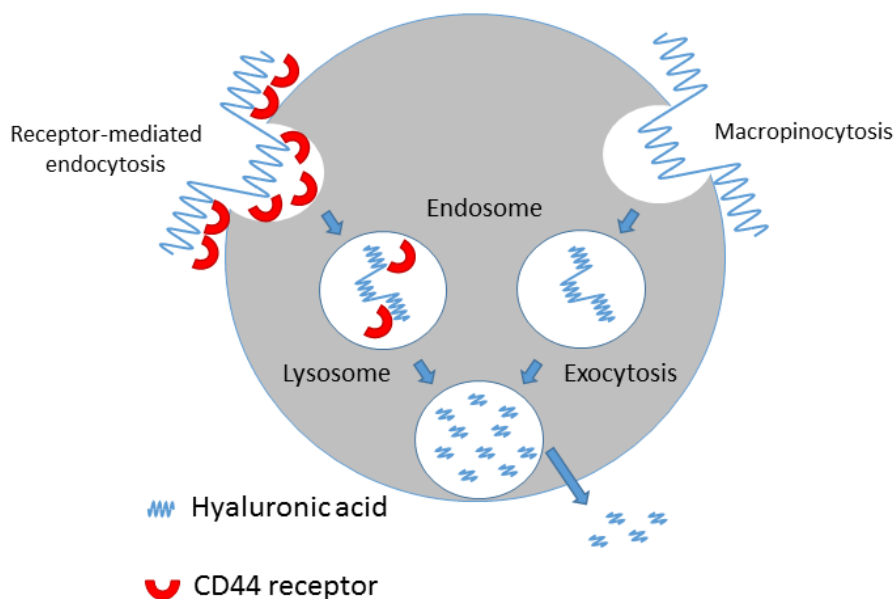


Figure 2: Mechanism of cellular internalization of hyaluronic acid.

Lipid-based CD44-targeting nanocarriers

Lipid-based nanocarriers have attracted increasing scientific and commercial attention in the context of drug delivery for *in vivo* applications due to their overall low toxicity [41]. Presently, many lipid-based colloids are approved and commercialized for clinical use. Shortcomings frequently encountered with active compounds, such as poor solubility, normal tissue toxicity, poor specificity and stability are expected to be overcome through the use of lipid-based nanocarriers. Surface-modification of these carriers offers moreover the possibility to overcome biological barriers so that they will preferentially accumulate in disease target cells [42]. The present review focuses on the surface modification of solid lipid nanoparticles, nanostructured lipid carriers and liposomes with HA for CD44 targeting. After a short description of the nanocarriers, the influence of these modifications on their activity will be discussed.

Solid lipid nanoparticles

Solid lipid nanoparticles (SLN) are nanocarriers made from lipids that are solid at room temperature [43]. They have been introduced in the 1990's as an alternative to polymeric nanoparticles and have been explored since then due to their low toxicity [44] and relatively simple and cost-effective large scale production using high pressure homogenization, for instance [45]. The major driving force for

SLN drug carriers is the perception that these particles may have superior *in vitro* and *in vivo* stability compared to other colloidal carrier systems [46]. Surface modification of SLN has been used to improve the cell penetrating capacity of these particles. Namely, protamine [47,48], cell penetrating peptides [49,50], among others, have been investigated. HA-modified SLN have been recently used by Apaolaza et al. [51] for the targeted delivery of DNA to overexpressing ARPE-19 compared to HEK-293 cells. Complexes prepared with HA of either 150, 500 or 1630 kDa, protamine and DNA were obtained by electrostatic interactions with SLN. The incorporation of HA in these SLN formulations induced a 7-fold increase in the transfection capacity of SLNs on ARPE-19 cells, regardless of the amount and molecular weight of HA. CD44 inhibition studies suggested the participation of the CD44 receptors in the internalization of the vectors. Besides increasing transfection efficiency, modification of the vectors with HA also increased cell viability after treatment, compared to the plain SLN. SLN coated with HA by electrostatic interactions were also tested by Tran et al. [52] (Figure 3A). In their study, 3 kDa HA-decorated SLNs were used for the tumor-targeted delivery of vorinostat, a histone deacetylase inhibitor. Surface modification of SLNs increased cellular uptake of these vectors in CD44 overexpressing A549 and SCC-7 cells. Moreover, competitive binding assays with a pretreatment with HA confirmed the receptor-mediated internalization of the particles. The coating by HA also increased SLN cytotoxicity compared to the free drug and the non-modified SLNs. These nanocarriers increased the circulation time of vorinostat and reduced its clearance in rats, resulting in higher plasma concentration than the free drug.

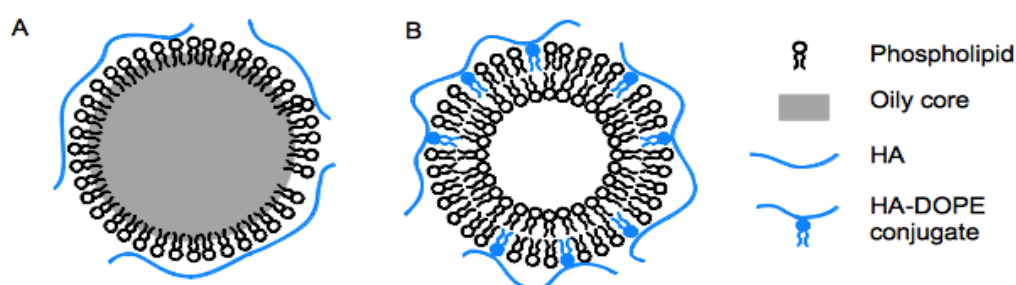


Figure 3: Association of hyaluronic acid A) by adsorption to solid lipid nanoparticles or nanostructured lipid carriers; B) by association to a phospholipid inserted in phospholipid bilayer of liposomes.

Nanostructured lipid carriers

Nanostructured lipid carriers (NLC) consist in a new generation of lipid NPs that were introduced in the late 1990's. These nanocarriers are characterized by a core consisting of a mixture of solid and liquid lipids, where the resulting matrix has a lower melting point than the original solid lipid, while still solid at body temperature [53,54]. Compared to SLN, NLC have the advantage of offering

increased drug loading and decreased drug leakage, although the drug loading capacity for hydrophilic drugs of both type of particles is still low compared, for example, to liposomes. They have been mostly used for chemotherapeutic drug delivery, and surface modification has been carried with biotin [55], anti-VEGFR-2 antibody [56] and transferrin [57] in order to improve the *in vitro* and *in vivo* efficacy of these carriers. HA-modified nanostructured lipid carriers loaded with paclitaxel were studied by Yang et al. [58] for the treatment of tumors overexpressing CD44. In their report, the authors described a more prolonged paclitaxel release from HA-coated particles, attributed to the increase in the diffusion distance of the drug from the nanocarriers due to the HA coating on the surface of NLC. HA-coating also promoted an increase in cell cytotoxicity of NLC compared to commercially available Taxol® against B16 murine melanoma cells, CT26 mouse colon cancer cells and HCT116 human colon cancer cell lines. *In vivo*, HA-NLC showed an increased antitumor activity and were better tolerated than Taxol by B16-bearing Kunming mice, as observed by animals' weight loss. HA-coated NLC also prolonged paclitaxel plasma circulation time, and increased its accumulation in the tumor.

Liposomes

Liposomes have been studied for decades as drug delivery carriers to diseased cells, and great advances in cancer treatment and other diseases were achieved. For example, Doxil® improved therapeutic efficacy of doxorubicin in cancer treatment by enhancing selective drug accumulation in tumors [59,60] and led to breakthrough developments in the area. Another very successful case is AmBisome®, which improved the treatment of fungal infections in immunocompromised patients [61-63]. Presently, a number of liposome-based products are on the market for the treatment of Kaposi sarcoma [64], breast cancer [65], aspergillosis [66,67], meningitis [68] and leukemia [69], and many more are in clinical testing [70].

The popularity of liposomes is explained by several advantages offered by these nanocarriers as drug-delivery systems. They are able to encapsulate both lipophilic compounds, in the lipid bilayer, and hydrophilic compounds, in their aqueous core. They usually have good biocompatibility, low toxicity and immunogenicity, and are biodegradable [71]. Besides, they are very versatile vesicles, and their structure can be modified to adjust their *in vivo* fate. The choice of specific lipids can for example control the release of the encapsulated drug in the targeted tissue by overheating [72-74]. Using cationic lipids in the liposome formulation allows the complexation of nucleotides by ionic interactions, a strategy that has been extensively used for nucleotide delivery and gene therapy [75,76]. Ligands, such as antibodies [77,78], folate [79], aptamers [80-84] or peptides [85] can be

attached to liposome surface to bind specific receptors on the cell surface. Particularly, liposomes modified with HA have been largely explored for the drug targeting to CD44-expressing cells. Ongoing work on modification of liposomes with HA has focused mainly on specifically delivering antitumor drugs (small or large molecules) to CD44-overexpressing tumor cells. HA-liposomes were proven as effective carriers of miR-34a, a prognostic biomarker, to MDA-MB-231 breast tumors overexpressing hyaluronan receptors [86]. They were also used by Qhattal et al. [87,88] to target these cells *in vitro* and *in vivo*. In these studies, it was observed that the cellular targeting efficiency of HA-liposomes depended strongly upon HA MW, grafting density, and cell-surface CD44 density. A liposome formulation coated with HA was also developed for MDA-MB-231 targeted delivery of an anticancer agent and MR imaging of breast cancer [89]. In this study, HA-modification reduced the toxicity of liposomes, increased serum stability and promoted tumor-accumulation of these vesicles. In our investigations on HA-liposomes carrying either DNA or siRNA, higher transfection efficiencies of CD44-overexpressing MDA-MB-231 [90] and A549-luc cells [91,92] were also observed. These HA-modified lipoplexes presented good biocompatibility and low complement activation [90]. Landesman-Milo et al. [93] also used HA-coated liposomes prepared with neutral phospholipids and cholesterol to target A549 CD44-overexpressing cells. The authors observed specific binding and internalization of HA-modified particles. Liposomes were shown to be non-toxic and efficient in delivering siRNAs to the targeted cells [93]. Dalla Pozza et al. [94] and Arpicco et al. [95] designed HA-liposomes prepared with low MW HA to target highly CD44-expressing MiaPaCa2 pancreatic adenocarcinoma cells. In the first study, the authors demonstrated a selective uptake of HA-liposomes by MiaPaCa2 cells compared to CD44-non expressing VIT1 cells. In the second study, the cellular uptake ability and the *in vitro* and *in vivo* anti-tumoral activity of HA-liposomes carrying gemcitabine (GEM) were investigated. An increased cellular internalization of liposomes covered with HA and increased *in vitro* and *in vivo* sensitivity towards GEM-containing HA-liposomes were observed. Dual-function liposomes with HA targeting and pH-responsive cell-penetrating peptide were prepared by Jiang et al. [96] for tumor-targeted drug delivery to hepatocellular carcinoma cells. HA was utilized to decrease liposomes interaction with plasma proteins, and once at the tumor site, its degradation by HAses exposed the R6H4 peptide. These paclitaxel-containing liposomes presented stronger cytotoxicity, efficient intracellular trafficking and preferential tumor accumulation.

HA-modified liposomes have also been used to target macrophages, in the context of the treatment of inflammatory diseases. Glucksam-Galnoy et al. [97] investigated the interactions between non-modified and HA-modified unilamellar (HA-ULV) and multilamellar (HA-MLV) liposomes and macrophages, and describe a substantially favored binding of the MLV species over the ULV species.

Internalization of exclusively non-modified MLV was observed in this study, and the authors suggested that small HA-ULV provide stealth properties and are suitable for delivering anti-inflammatory drugs to the macrophage surface, while HA-MLV would be suitable for delivering anti-inflammatory drugs inside macrophages and reducing inflammation cell-signaling TNF- α production.

Gan et al. [77] used HA-modification for the treatment of retinal inflammation, a common process of posterior ocular diseases that can lead to severe vision loss. The authors developed core-shell lipid nanoparticles, consisting of chitosan nanoparticles covered with a lipid layer modified with HA, to target retinal pigment epithelium (RPE) cells, generally considered as the therapeutic target of inflammation pathogenesis. As commonly described for liposomes after intravitreal administration [98] these vesicles had a longer residence time *in vivo* and in addition could efficiently pass through the vitreous barrier being preferentially internalized by the CD44-expressing RPE cells.

The reports about HA-liposomes for drug delivery to CD44 positive cells clearly established their advantages over the non-targeted liposomes. The characteristics of the nanocarriers related to the density and size of HA influence directly their ability to interact with the receptors on the targeted cells, and therefore impact on their biological activity. Taking into consideration the large amount of studies related to liposomes compared to all other types of nanocarriers, we discuss below how their modification with HA influences their physicochemical characteristics and their efficacy *in vitro* and *in vivo*.

Functionalization of liposomes with HA

Basically, two different preparation methods are used for inserting HA within the liposomal membrane. In one of them, HA is linked to the surface of preformed liposomes by a covalent conjugation. In this method, first described by Yerushalmi and Margalit in 1998 [99], carboxylic residues of HA are pre-activated by incubation with the condensing agent ethyl-dimethyl-aminopropyl-carbodiimide (EDC) in aqueous acid medium. The activated HA is then added to the nanocarrier suspension at basic pH, where an amidic bond will be formed with the lipids amine groups. This method seems to yield coating efficiencies that allow efficient CD44-binding [12,77,86-88,93,97,100], which is desirable since a minimal amount of HA is necessary to target the receptors [101]. The inconvenience of this technique is that post-conjugation must be made for every preparation of liposomes, which is time consuming since the reaction lasts for more than 24 h [99]. In the second approach, liposomes are prepared in the presence of HA conjugated to a lipid anchor (Figure 3B). Low molecular weight (LMW) HA can be linked to an aminated lipid such as phosphatidylethanolamine (PE) [102], dipalmitoyl phosphatidylethanolamine (DPPE) [94],

diphytanoyl glycerophosphatidylethanolamine (DiPhPE) [103] by reductive amination, using a sodium borohydride as reducing agent, providing a conjugate in which only one lipid molecule is linked to HA which will interact with other lipid within the bilayer structure (Figure 4A). HMWHA can be coupled to 1,2-dioleoyl-sn-glycero-3-phosphoethanolamine (DOPE) by means of an amidation reaction in which the amino group is randomly linked to the carboxylic residues of the polymer and then introduced into liposomes bilayer [90,92] (Figure 4B). Using this approach allows a faster preparation of HA-vesicles, since the HA-lipid conjugate can be synthesized previously and stored to be used for multiple formulations. It also yields coating efficiencies that allow efficient CD44-binding [89,90,92,95,103]. Unfortunately, association efficiency of HA to liposomes is not systematically quantified, which renders the comparison of these two methods rather difficult. Nevertheless, chemical conjugation of HA has been proved to be more efficient than the functionalization of liposomes with unconjugated HA [92,104], since in this case, HA is not anchored on the liposome structure but merely attached to liposomes by electrostatic interactions. Instead of being conjugated to phospholipids, HA has been also chemically coupled to other lipids such as ceramide [89] or sterarylamine [104]. In both cases, liposomes were efficiently targeting CD44 positive cells.

Since many aspects related to the presence of HA on vesicle surface are important in determining their biological effect, a better comprehension of particle structure after modification with HA is an important step of the formulation characterization. For instance, the arrangement of HA on liposome surface will have an important influence on their biological activity. In principle, linear HA polymer can behave just like polyethylene glycol (PEG), another hydrophilic polymer frequently used for the modification of liposome surface. This means that depending on the HA molecular weight and grafting density, HA chains grafted on the lipid bilayers can show brush, mushroom, or pancake conformation [87]. Also, because HA is linked with several anchors, the conformation of the HA around the liposomes might be different from these conformations [92] and therefore, each conformation will have its own thickness of hydration layer, steric hindrance and disposition of binding moieties [105].

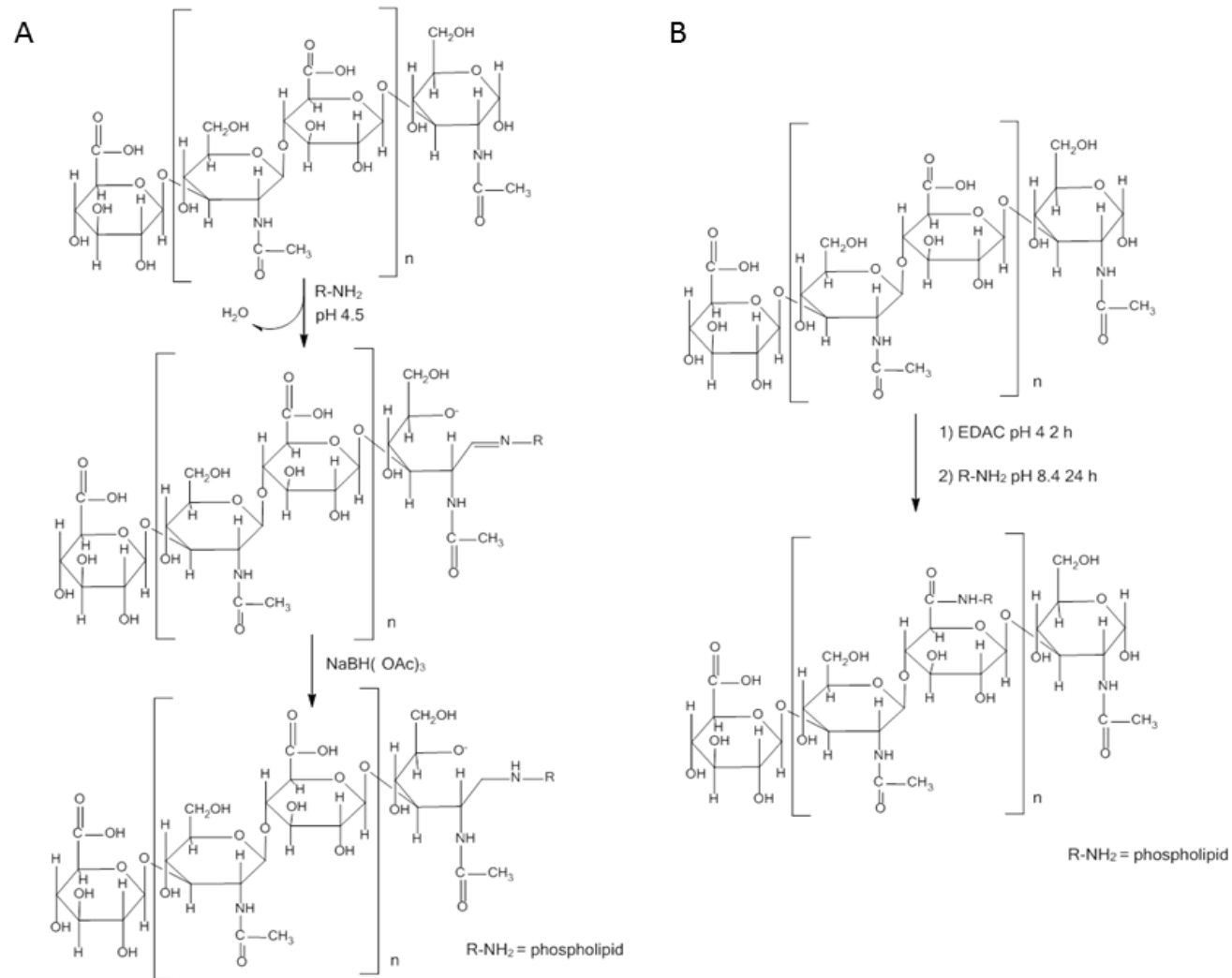


Figure 4: Coupling reaction of aminated phospholipids to HA by (A) by reductive amination on the extremity of LMW-HA or (B) amidation on carboxylic residues of HMW-HA.

Effect of HA molecular weight and grafting density on nanoparticle physicochemical properties

The most common route of administration of nanocarrier suspensions is the intravenous one. This administration pathway allows a maximum amount of particles to circulate and find their cell targets immediately after administration. Cells are able to internalize nanocarriers by either phagocytosis or receptor-mediated endocytosis, meaning that particle size may affect internalization depending on cell type. However, the diameter of capillaries is the most limiting factor for nanocarriers size when administered through the intravenous route. A size of 200 nm is considered as optimal for nanocarriers to circulate in the narrowest vessels avoiding embolization [5,106]. Therefore, liposomes of around 100 nm are usually preferred. Since HA is a hydrophilic polymer, its placement on nanoparticle surface increases nanoparticle mean hydrodynamic diameter. This increase is generally used to characterize particle coverage and reflects the presence of HA on their surface. Several authors have demonstrated that particle size progressively increases with HA MW [87,95,107]. For example, in one of the above-mentioned studies [95], HA-liposomes had a mean diameter of 160 ± 5 and 208 ± 7 nm when prepared with HA of molecular weights of 80 and 1000 kDa, respectively. A progressive increase in particle diameter with increasing concentrations of grafted polymer chain units is also commonly observed.

Besides the measurement of hydrodynamic diameter, microscopy can be used to give extra information on the structure of the particles. For instance, Arpicco et al. [95] demonstrate that hyaluronated liposomes revealed a particulate surface coating, which was absent in plain liposomes, and were decorated by fluffy dark structures, confirming that HA molecules were exposed on liposome surface. Gan et al. [77] described similar observations, where the analysis of HA-liposomes (named liponanoparticles) by transmission electron microscope (TEM) exhibited black spots surrounded by gray rims, confirming the core-shell structure of the particles. Tiantian et al. [107] used TEM to describe the change in liposome shape caused by the presence of HA, and reported the formation of more spherical structures than for non-coated liposomes.

Exploring nanoparticle surface charge modification by measuring the zeta potential can be used to describe surface coating of nanoparticles by HA. Whether the initial liposomes display a neutral [97,108], negative [95,107] or positive charge [90-92], a clear change in the zeta potential is systematically observed after insertion of HA on these structures. Since HA is an anionic polymer, when present on the surface of the vesicles, it causes a decrease in zeta potential, and for this reason, HA-modified lipid vesicles are usually neutral or negative. This is beneficial when stability in serum and vesicle toxicity are considered, since HA decreases particle interaction with serum proteins and masks the surface charge of cationic particles as discussed in more details below.

Another important aspect of the physicochemical characterization of nanoparticles is the evaluation of their stability under conditions that resemble the *in vivo* environment. Particle stability is a complex function of nanoparticle surface characteristics and components of surrounding medium [109]. In physiological conditions, nanoparticles may interact with biological components, which leads to the formation of a protein corona [110]. Coating with proteins may induce conformational changes [111-113] or modification in size and zeta potential [114-116]. These changes can dramatically affect particles' stability, interaction with membrane and cells, and clearance [117]. For liposomes, as for many other particle types, immediate aggregation can occur when particles interact with blood components [117-119]. However, when particles are modified with HA, the decreased charge and additional steric hindrance caused by the hydrophilic coating can improve their stability [40,120]. For instance, Park et al. [89] describe that, while conventional liposomes formed large aggregates immediately after incubation in 50% FBS, particle size of the HA-coated liposomes was maintained for at least 24 h. We have also observed that the presence of HA results in an improvement of lipoplexes stability in the presence of serum. The diameter of lipoplexes (lipids:DNA ratio of 2) did not differ significantly in the serum-containing cell culture media, while non-modified lipoplexes aggregated immediately upon dilution [92]. These observations support the idea that HA-modification, while improving *in vivo* stability, could potentially ameliorate the pharmacokinetic performance of HA-modified particles [89].

Alteration of encapsulation efficiency after modification of lipid vesicles with HA has not been frequently described. Modification of the entrapment of drugs in the hydrophilic core or in the lipophilic bilayers of liposomes is unlikely, assuming that the addition of HA does not alter in a great extent, for example, the liposome structure or the fluidity of the lipid bilayers. On the other hand, when active drug encapsulation depends on the interaction with the lipids for their association, it is plausible to imagine that steric hindrance or the negative charge of HA could represent barriers for this association. This is the case for complexation of nucleic acids to liposome surface during the formation of lipoplexes. A possible competition between the negative charges of DNA and RNA molecules with the ones of HA for the binding to cationic lipid could take place. This competition can be influenced by the binding strength of each component with the cationic lipids. HA molecules may also represent a barrier to the binding of the nucleic acids. This steric hindrance has been observed for DNA lipoplexes that presented PEG on their surface [121]. Similar observations have however not been reported for HA-modified liposomes. In our recent studies with HA-modified lipoplexes, even for preparations using HA of 1,600 kDa [90,92], its presence did not prevent nucleic acid association but reduced the amount of HA that was initially attached on liposomes surface before lipoplex formation [92].

Although alterations in the encapsulation efficiency properties of liposomes have not been reported, authors described changes in the drug release properties from vesicles caused by the insertion of HA in

their structure. Tiantian et al. [107] observed, for example, that the release profile of docetaxel was prolonged after liposome coating with HA. This observation was not related to the molecular weight of HA, but rather to the decrease of the bilayer fluidity upon association of HA [122]. Moreover, drug release from HA-liposomes can be altered due to different degradation ratios of HA occurring at different pH. Park et al. [89] observed an increase in doxorubicin release from liposomes with decreasing pH values. Kim also observed an accelerated release of miRNA from liposomes at acidic compared to neutral pH. This pH-dependent release from HA liposomes reflects the physiological breakdown of HA. The degradation of HA in aqueous solution is caused by hydrolysis attributed to the random scission of its polymer chains, and its degradation rate strongly depends on pH. HA is indeed more labile in acidic than neutral conditions [123,124]. Jiang et al. [96] used this characteristic to design pH-responsive HA/cell-penetrating peptide decorated-liposomes for tumor-targeted paclitaxel delivery. Indeed, it was shown that the degradation of HA by HAase-rich tumor microenvironment allowed exposure of the cell penetrating peptide and cell internalization [96].

Effect of HA molecular weight and density on the interaction with CD44 receptors

Overall, the previous observations confirm that it is important to understand the physicochemical characteristics of the formulated HA-liposomes. It is however not enough to have HA on the surface of liposomes since HA moieties should also be available for interaction with the CD44 receptors. Affinity of liposomes for CD44 receptors strongly depends on the molecular weight of the HA oligomers, hexamers and decamers being the smallest sequences of HA that can interact with CD44 receptors. As they have the ability to bind simultaneously to several CD44 units, HMW HA has more affinity to these receptors than LMW HA [35].

The measurement of CD44-HA interaction is often related to chemical techniques such as NMR [125] or biological techniques such as SDS-PAGE, Western blot, immunostaining, or finally cellular localization by techniques adjacent to cell culture such as flow cytometry or fluorescence microscopy [25,126,127]. Particularly, the importance of the interaction between free HA or HA-functionalized liposomes with CD44 receptors is often determined using surface plasmon resonance (SPR). In this technique, the extracellular moieties of CD44, CD44-Fc, are attached to a gold surface, and HA molecules of different molecular weights, non-modified or HA-particles are put in contact with the receptors. The amount of ligands that interact with the surface is then measured in real time, since this experiment is performed in a continuous flow. Mizrahy et al. [100] evaluated the correlation between the lengths of HA oligomers and their binding affinity to CD44 receptors using SPR. The authors analyzed the interaction with CD44 receptors of HA of 6.4, 31, 132, 700 and 1500 kDa, and confirmed the interaction with multiple receptors for HA with MW of 132 kDa and higher. A small

library of liposomes distinguished only by the MW of their surface anchored HA was then prepared, and it was observed that the affinity towards CD44 was controlled solely by adjusting the HA MW on the surface of NP. The results from these experiments showed the same trend observed in the experiments with free HA, clearly indicating stronger binding of HMW HA to the receptor. Controlling the molecular weight of HA attached on the surface of liposomes can be used as an approach to selectively target the right receptors. Ruhela et al. [103] used this strategy to optimize CD44 receptor targeting and reduce liposome interaction with the HARE receptor in the liver. The authors assumed that HA oligomers of 10–20 units are long enough to bind to the CD44 receptor but shorter than the HA length required to tightly bind to the HARE receptor of liver endothelial cells. Indeed, HA oligomers of 10–18 monosaccharides were used to prepare the diphytanoyl glycerophosphatidylethanolamine (DiPhPE)-HA conjugates inserted into liposomes and were shown to strongly bind to COS7 cells overexpressing CD44.

Cellular binding, uptake and trafficking pathways

Competitive binding assays are performed *in vitro* to observe CD44-mediated internalization and to understand the intracellular trafficking pathways involved in the uptake of HA-particles. A simple method to test the binding of these particles to the receptors is pre-treating cells with an excess of free HA or anti-CD44 antibody. For example, upon blocking of CD44 receptors with free HA, Kim et al. [86] observed a complete uptake suppression in MCF-7 and MDA-MB-231 cell lines. Gan et al. [77] also observed that ligand pretreatment did not change the cellular uptake of plain and lipid nanoparticles prepared with LMW HA, while the cellular uptake of particles prepared with HMW HA was significantly reduced in CD44-expressing ARPE-19 cells. In the work of Arpicco et al. [95], MiaPaCa2 cells were pre-incubated with a saturable amount of free HMW HA (51 kDa) before treatment to validate the specificity of HA-liposome uptake through the CD44 receptor. A 75% reduction of the uptake, in comparison with the control (without incubation with free HMW HA), was observed in cells treated with liposome-bearing HMW HA (2000 kDa) at 24 h [95]. Dalla Pozza et al. [94] reported that the ability of MiaPaCa2 cells (CD44⁺) to incorporate both 4.8 or 12 kDa HA-liposome formulations was significantly higher than that of VIT1 cells (CD44⁻), suggesting that liposome internalization in MiaPaCa2 cells was mainly mediated by HA. Surace et al. [90] observed that the transfection of DNA HA-lipoplexes on the CD44-expressing MDA-MB-231 cells was highly inhibited by anti-CD44 Hermes-1 antibody [128] but not by the nonspecific anti-ErbB2 antibody. Meanwhile, the transfection of MCF-7 cells was not altered whether they were transfected in the presence of Hermes-1 antibody or not. A concentration-dependent activity was observed, with a maximum gene inhibition efficiency reaching 70% in comparison with the control when cells were treated with 1 µg/mL of anti-CD44 Hermes-1

before transfection. In another experiment, Dufay-Wojcicki et al. [92] tested the intracellular pathway for green fluorescent protein (GFP)-expressing DNA-cationic lipoplexes modified by HA. Cells were pre-treated with HA to saturate CD44, or HA was blocked using CD44 antibody, and in both cases a decrease of 40% in GFP expression was observed [92]. The incubation of HA-liposomes with cells at 4 °C, a temperature which inhibits all the active energy-mediated processes, significantly reduced the uptake in MiaPaCa2 cells, suggesting that HA-liposomes entered cells via an endocytic pathway. These results were also confirmed by confocal laser scanner microscopy. In these experiments, MiaPaCa2 cells treated with fluorescein-labeled HA-liposomes for 1 h at 37 °C were strongly fluorescent and VIT1 cells showed in contrast a very low signal, as well as MiaPaCa2 cells treated with non-targeted liposomes or at 4 °C. In one study [129], the authors also analyzed the effect of temperature on HA-liposome uptake by incubating the A549 cells with HA-liposomes for 2 h at 4 °C. As expected, the incubation of HA-liposomes with cells at 4 °C inhibited the active energy-mediated processes, reducing uptake of 5-8 kDa and 175-350 kDa HA-liposomes by 68% and 53%, respectively, compared to uptake at 37 °C. This finding confirms that HA-liposomes are taken up inside the cells via an energy-dependent endocytosis pathway.

The endocytic pathways involved in the internalization of nanoparticles are clathrin-mediated, caveolae-mediated, macropinocytosis and other clathrin- and caveolae-independent process [5]. The cellular uptake of liposomes, like for other types of particles, will depend on their surface charge, size, cell type and the molecular composition of the cell surface [130]. It is difficult to describe a consistent profile of liposomes matching each of these endocytic pathways. Indeed, unlike phagocytosis occurring primarily in professional phagocytes, other endocytic mechanisms may take place in virtually all types of cells and vary accordingly; differences will also occur between the apical and basolateral membranes of a polarized cell. Moreover, several endocytic mechanisms often take place simultaneously [5]. The study of the influence of these characteristics on the internalization of particles has an important impact in the drug delivery field. For instance, nanocarriers may be tailored in order to be metabolized into the lysosomes and release their content intracellularly as a consequence of lysosomal biodegradation after clathrin-mediated endocytosis [5]. They can also be designed to by-pass the lysosomal degradation pathway and reach the cytoplasm by caveolae-mediated endocytosis when the carried cargo is highly sensitive to enzymes [5,131,132].

Qhattal et al. examined the effects of several membrane entry inhibitors on the uptake of HA-liposomes by preincubating A549 cells with the inhibitors before treatment with HA-liposomes. Chlorpromazine was used to inhibit the assembly and disassembly of clathrin [133] and test the clathrin-mediated endocytosis. Amiloride was used as a specific inhibitor of the Na⁺/H⁺ exchange required for macropinocytosis. Filipin III and nystatin were used to inhibit caveolae-mediated uptake by partitioning into membranes and sequestering sterols [134]. None of these inhibitors showed any

effect on the uptake of HA-liposomes. When blocking lipid rafts (cell membrane microdomains rich in cholesterol, sphingolipids and cell surface receptors [129]) using methyl- β -cyclodextrin, the uptake of HA-liposomes was reduced by nearly 45% compared to untreated cells, suggesting that HA-liposomes are taken up into the cells via the lipid raft-mediated endocytosis which is cholesterol-dependent [133]. In a similar study, Dalla Pozza et al. [94] pre-treated MiaPaCa2 cells with increasing amounts of individual membrane entry inhibitors before incubation with 4.8 or 12 kDa HA-liposome formulations. The flow cytometry analysis also revealed that methyl- β -cyclodextrin (M β CD) strongly decreased the HA-liposome uptake, in a concentration dependent manner, while treatment with chlorpromazine, nystatin and amiloride (inhibitors of clathrin- or caveolae-mediated uptake or macropinocytosis, respectively), did not alter the fluorescence of the cells compared to controls. Incubation with caveolae-inhibitor filipin reduced by 60% the transfection efficiency of HMW hyaluronic acid-bearing DNA lipoplexes (using a plasmid coding for the GFP) in A549 cells. Moreover, when genistein, another inhibitor of this internalization pathway was used, GFP expression was lowered by 90% [92]. In contrast, using the clathrin-mediated endocytosis inhibitor chlorpromazine, transfection levels were not changed. Nevertheless, transfection efficiency was also blocked by an excess of HA or CD44 antibody. Both caveolin [135] and CD44 [10] are present in lipid rafts domains, it is therefore likely that the inhibition of CD44 by an excess of HA or CD44 antibody is blocking one of the pathways for caveolin phosphorylation, which is necessary to start the caveolae-dependent endocytosis [136].

In vitro and in vivo toxicity and inflammation of HA-liposomes

An important concern regarding the use of nanoparticles for targeted delivery of active substances *in vivo* is the risk that they can cause adverse effects in the body. This is one of the key aspects in the development of nanocarriers for *in vivo* application, and although no conclusive guidelines have been made for preparing low immuno-stimulatory nanomedicines, all nanocarriers need to go through rigorous toxicology studies before regulatory approval [137].

As previously discussed, it is well accepted that HA of different MW causes different effects on cellular functions after binding to CD44 receptors. HMW HA is present under homeostatic conditions, and plays a key role in the structural integrity of tissues. It is therefore considered to be biocompatible or bio-inert [138]. Under certain pathological inflammatory conditions, such as cancers, fragments of LMW HA are produced due to a reduction of the activity of HA synthases [139] and an increased activity of hyaluronidases [139]. These small fragments (from 2 to 100 kDa, about 4 to 250 disaccharide units) have been shown to have an angiogenic effect *in vitro*, contributing to tumor growth [140]. It has also been described that LMW HA provoke immuno-stimulatory [141] and proinflammatory effects upon binding to CD44 [142]. Nevertheless, not all literature reports are

consistent [100], and a more complex behavior is observed when the toxicity of HA-modified liposomes particles is studied. Similarly as for the other aspects of nanoparticle activity, their interaction with the immune system will be controlled not only by HA MW, but also by particle size, shape, surface and composition.

In the study designed by Mizhary et al. [100], where liposomes with different MW HA were prepared, the authors report that none of the vesicles showed any apparent effect on the proliferation of highly CD44-expressing NCI/ADR-RES (for adriamycin-resistant cell line), TK-1 and RAW 264.7 cells. No macrophage activation or complement activation caused by these nanocarriers were detected. Additionally, no cytokine induction was observed regardless of the HA MW anchored to the surface of nanoparticles. These results were compared to a previous study where significantly higher amounts of free LMW HA but not HMW HA induced inflammatory gene expression in peritoneal and alveolar macrophages [143], providing a good example that toxicity is a dose-relative notion [144]. The authors discuss that covalently attaching HA to the surface of liposomes hinders processing by cells, and may account for the lack of macrophage activation. HA-liposomes prepared by Kim et al. [86] with 1000 kDa HA also showed high biocompatibility on CD44-expressing (98.8%) MDA-MB-231 cells compared to low CD44-expressing (3.6%) MCF-7 cells. Similarly, uni- and multilamellar HA-liposomes prepared by Glucksam-Galnoy et al. [97] with 1500 kDa HA did not elicit any TNF- α response. The secretion level of three different inflammatory interleukins was tested by Landesman-Milo et al. [93] using IL-6 and TNF- α as a model for the innate immune response and IL-10 as a model for the late immune response. In this study, where liposomes were coated with 700 kDa HA, neither the HA-modified nor the uncoated particles caused an elevated secretion of both innate and late cytokines response.

An improvement of liposome biocompatibility by coating lipid bilayers with HA was even observed by Gan et al. [77], who described that HA-liposomes did not show cytotoxicity on CD44-expressing human retinal pigment epithelial (ARPE-19) cells, compared to the non-modified liposomes. Similarly, Park et al. [89] described a recovery of cell viability from around 40% to 100% upon coating the outer surface of liposomes with HA. The authors attributed this effect to a protection of HA against the disruption of cellular membrane by the liposome itself, which reduced cytotoxicity versus the plain liposomes.

These results are not unexpected, not only considering HA MW, but also the type of nanoparticles. Liposomes are generally considered to be safe and non-immunogenic, since the lipids used in the formulation are quite often ubiquitous to the cellular composition. For cationic liposomes, though, it has been described that alterations of the net charge of cell membranes and adverse effects on the activity of ion channels, membrane receptors and enzymes can occur [145]. These alterations depend on the cationic nature of the lipid head group and its ratio with neutral lipid [144], and raise a concern about the safety of these vesicles. In our studies with cationic liposomes [90-92], lipoplexes presented good biocompatibility. DNA lipoplexes prepared with increasing lipids:DNA ratios (2, 4, and 6) and non-

modified and HA-modified liposomes for the targeting of CD44-overexpressing A549 cells [92] showed low activation of the complement, as measured by the activation of the protein C3 that is also considered as a good indicator of the capacity of macrophages of the mononuclear phagocyte system (MPS) to phagocyte the drug carrier.

Effect of HA-modification on liposome pharmacokinetics

Almost immediately after entering the organism through the intravenous route, liposomes are recognized by opsonins. These specific serum proteins, mainly IgG and IgM immunoglobulins and complement components (C3, C4, C5) [146-148], adsorb onto particle surface inducing their recognition and binding by specific receptors present on the surface of cells from the MPS [149]. These cells will capture liposomes by endocytosis and remove them from the circulation [150]. Components that inhibit the phagocytosis of pathogens or particles, referred to as dysopsonins, are also present in the serum. Human serum albumin and IgA, for example, possess dysopsonic properties and their presence on particle surface has been shown to reduce recognition and phagocytosis [151]. The balance between blood opsonic proteins and suppressive proteins regulates therefore the extent and rate of liposome clearance, which will depend on particle size and surface properties [109,151].

When it comes to regular liposomes, phagocytosis is enhanced for larger and multilamellar particles [5,152,153], as well as for charged or hydrophobic surfaces [154-156]. HA being a hydrophilic molecule, its presence on the surface of liposomes will increase vesicle stealth properties, resulting in longer circulation time. Tumor targeting can also be expected by modifying particles with HA, further improving accumulation of the nanocarrier in the tumor region and leading to improved activity *in vivo* [89].

Park et al. [89] observed an improved *in vivo* behavior of doxorubicin-encapsulating liposomes modified with the insertion of a HA-ceramide conjugate. While plain liposomes immediately aggregated in the presence of 50% FBS, the *in vitro* stability of HA-liposomes was maintained during 24 h. However, the most important effect of HA insertion was tumor targeting. The *in vivo* diagnostic and tumor treatment capabilities of the formulation was evaluated in a MDA-MB-231 tumor-xenografted mouse model. Fluorescence signal on the tumor region, corresponding to the presence of the particles, was 2.6-fold higher than that of plain liposomes, and increased up to 89% 2 h after injection compared to the free drug distribution. The authors attributed the accumulation of the nanocarrier in the tumor region to the serum stability of the particles and more importantly to its slow clearance *in vivo* and prolonged circulation in the blood stream. Dalla Pozza et al. [94], comparing HA-liposomes prepared with LMW HA of 12 and 4.8 kDa, observed that the volume of tumors in mice treated with 12 kDa HA-liposomes increased at a significant lower extent than that in mice treated with 4.8 kDa HA

liposomes or non-targeted liposomes. At the end of the treatment, free GEM did not inhibit the tumor growth in the drug-resistant pancreatic cancer xenograft model used, while liposome formulations displayed different levels of efficacy. 12kDa HA-liposomes determined a reduction in the mean tumor mass of about 50% compared to 4.8 kDa HA liposomes or non-targeted liposomes and about 65% compared to control or free GEM treatment. Kim et al. [86] used HA-coated liposomes to target breast cancer cells over expressing CD44, and achieved enhanced intracellular delivery and optical imaging of miR-34a beacons. The coating with HMW HA promoted a tumor-specific delivery of the imaging probe. 1 h after the intravenous injection of non-modified and HA-liposomes, injection of the latest provided strong fluorescence signal in CD44-positive tumor bearing mice, while non-modified and blocking groups using excess HA as controls showed significantly reduced fluorescence signals. Using these nanocarriers, the authors achieved targeted optical imaging of miR-34a expression levels.

These results suggest that modifying liposome surface with HA provides a hydrophilic shield that will reduce interaction with plasma proteins and increase particle circulation time. This has led to the proposition of HA as an alternative to PEG, when reduced opsonisation and MPS uptake combined with the targeting properties of HA are desired [108,157]. Qhattal et al. [88] tested this hypothesis with a systematic study of the pharmacokinetics of HA-liposomes with three different HA polymer lengths (5-8, 50-60 and 175-350 kDa) and compared with that of PEGylated liposomes. It was shown that the clearance of HA-liposomes was dependent on HA length. Indeed, the addition of HMW HA to the surface of liposomes accelerated the clearance of the particles from the blood compared to low MW HA. This finding was related to the high affinity of the particles for other HA receptors such as HARE and LYVE-1, which are abundantly expressed in normal sinusoidal endothelial cells of the liver, spleen, and activated tissue macrophages [88,158,159], that are responsible for active clearance of liposomes from the circulation.

Changes in pharmacokinetics by HA are not strictly limited to intravenous administration. Gan et al. [77] described an increase in residence time after coating lipid-chitosan nanoparticles with 10-100 and 200-400 kDa HA and administration by the intravitreal route. The authors observed that 7 days after injection, approximately one-third of the total fluorescence related to the non-coated particles was cleared from the targeted vitreous region, while for the 200-400 kDa HA-coated liposomes, approximately 75% of the fluorescence still remained in the retinal pigment epithelium/choroid. An improved penetration on the targeted site of action was also described after the *in vivo* treatment. While both non-coated and HA-particles passed through the vitreous barrier and reached the inner limiting membrane, red fluorescence of HA-liposomes was found in the RPE layer in the inflamed eyes, which was not observed in the non-coated group.

Conclusion and future perspective

Modifying the surface of lipid-based nanoparticles with HA offers the possibility of targeting CD44-overexpressing cells and takes advantage of the biological relevance of CD44-HA interaction on tumor growth and progression. HA-modification of nanoparticles can indeed change physicochemical properties, alter stability, toxicity, and influence particle distribution and efficiency *in vitro* and *in vivo*. The complexity of the structure of lipid-based nanocarriers displaying HA on their surface implicates that a thorough characterization of the nanocarrier is necessary to understand its activity.

Although many studies conclude that LMW HA are more effective for inducing long circulating properties in lipid nanocarriers than HMW, the question is still opened regarding the angiogenic effect of these fragments. Furthermore, studies are still needed to better understand how the modification by HA influences *in vivo* distribution and tissue accumulation of these nanocarriers particularly in the case of cancer. Whether the improved efficacy is only due to pharmacokinetic modifications of the carriers added to an enhanced penetration and retention effect with or without targeting CD44 on tumor cells is still an open question. Within the tumor it would be important to determine what is the subpopulation of cells that is interacting with the carriers and whether these cells are cancer stem cells. Future perspectives include a comparison of the hyaluronic acid-coating strategy with more recent others that combine nanocarriers and aptamers or antibodies as ligands for CD44.

Table 1: Different types of liposomes associated to hyaluronic acid for targeting CD44

Carrier	Drug	target	HA MW	Method of HA insertion on the formulation	Reference
HA-multilamellar liposomes		NCI/ADR-RES ovarian adenocarcinoma, RAW 264.7 macrophages and TK-1T cell lymphoma cells	6.4, 31, 132, 700 and 1500 kDa	HA conjugated on preformed liposomes (by carbodiimide conjugation chemistry)	[100]
HA-liposomes		Mice liver endothelial cells	500-700 kDa	Electrostatic attraction (incubation of preformed liposomes with HA-stearylamine conjugate)	[104]
HA-liposomes	miR-34a (miRNA)	MCF-7 and MDA-MB-231 breast cancer cells	1000 kDa	HA conjugated on DSPE-PEG2000 amine on the surface of preformed liposomes	[86]
HA-liposomes (uni and multilamellar)		RAW264.7 macrophages	1500 kDa	HA conjugated on preformed liposomes (by carbodiimide conjugation chemistry)	[97]
HA-liposomes	Gemcitabine	PaCa44, PaCa3, Panc1, CFPAC1, PT45P1, T3M4, Suit-2, Mia-PaCa2, PC1J, HPAF II, and PSN1 pancreatic adenocarcinoma cell lines	4.8 and 12 kDa	HA-DPPE conjugates inserted upon liposome preparation (thin lipid film hydration)	[95]
HA-modified core shell liponanoparticles		ARPE-19 retinal pigment epithelial cells	10-100 and 200-400 kDa	HA conjugated on preformed liposomes (by carbodiimide conjugation chemistry)	[77]

HA-coated lipid-based-nanoparticles	siRNA	NCI/ADR-RES ovarian tumor and A549 lung carcinoma cells	700 kDa	HA conjugated on preformed liposomes (by carbodiimide conjugation chemistry)	[93]
HA-liposomes	Docetaxel	(model drug) / lymphatic system	80 and 1000 kDa	Electrostatic attraction (thermostat titration of preformed liposomes on HA solution)	[107]
HA-liposomes		A549 lung carcinoma, MDA-MB-231 and MCF7 breast cancer cells	5-8, 10-12, 175-350 and 1600 kDa	HA conjugated on preformed liposomes (by carbodiimide conjugation chemistry)	[87]
HA-liposomes with or without PEG		MDA-MB-231 breast cancer cells	5-8, 50-60 and 175-350 kDa	HA conjugated on preformed liposomes (by carbodiimide conjugation chemistry)	[88]
HA-liposomes	Paclitaxel	HepG2 hepatocarcinoma cells	210 kDa	Electrostatic attraction (incubation of preformed liposomes with HA solution)	[96]
HA-liposomes		COS-7 kidney fibroblast cells	HA oligomers (10-20 monosaccharides)	HA-DiPhPE conjugates inserted upon liposome preparation	[103]
HA-liposomes	Gadopentetate dimeglumine doxorubicin	MDA-MB-231 breast cancer cells	4.7 kDa	HA-ceramide conjugates inserted upon liposome preparation (thin lipid film formation)	[89]
HA-liposomes	Gemcitabine	Mia-Paca pancreatic carcinoma cells	4.8 and 12 kDa	HA-DPPE conjugates inserted upon liposome preparation (thin lipid film hydration)	[94]

HA-liposomes	DNA	MDA-MB-231 and MCF-7 breast cancer cells	1500 kDa	HA-DOPE conjugates inserted upon liposome preparation (thin lipid film hydration)	[90]
HA-liposomes	siRNA	A549 lung carcinoma cells	1500 kDa	HA-DOPE conjugates inserted upon liposome preparation (thin lipid film hydration)	[91]
HA-liposomes	DNA	A549 lung carcinoma cells	1600 kDa	HA-DOPE conjugates inserted upon liposome preparation (thin lipid film hydration)	[92]
HA-solid lipid nanoparticles	DNA	/ ARPE-19 and HEK-293 cells	150, 500 and 1630 kDa	Electrostatic interactions (HA-protamine-DNA complexes incubated with preformed SLN)	[51]
HA-solid lipid nanoparticles	Vorinostat	/ SCC-7 squamous cell carcinoma, MCF-7 human breast adenocarcinoma, A549 human epithelial lung adenocarcinoma	3 kDa	Electrostatic interactions (HA incubated with preformed SLN)	[52]
HA-nanostructured lipid carriers	Paclitaxel	/ B16 murine melanoma cells, CT26 mouse colon cancer cells and HCT116 human colon cancer cells	300 kDa	Electrostatic interactions (HA incubated with preformed NLC)	[58]

References

1. Farokhzad OC, Langer R. Nanomedicine: Developing smarter therapeutic and diagnostic modalities. *Advanced Drug Delivery Reviews*, 58(14), 1456-1459 (2006).
2. Peer D, Karp JM, Hong S, Farokhzad OC, Margalit R, Langer R. Nanocarriers as an emerging platform for cancer therapy. *Nat Nano*, 2(12), 751-760 (2007).
3. Choi KY, Saravanakumar G, Park JH, Park K. Hyaluronic acid-based nanocarriers for intracellular targeting: Interfacial interactions with proteins in cancer. *Colloids and Surfaces B-Biointerfaces*, 99, 82-94 (2012).
4. Torchilin VP. Multifunctional nanocarriers. *Advanced Drug Delivery Reviews*, 64, Supplement(0), 302-315 (2012).
5. Hillaireau H, Couvreur P. Nanocarriers' entry into the cell: relevance to drug delivery. *Cellular and Molecular Life Sciences*, 66(17), 2873-2896 (2009).
6. Naor D, Wallach-Dayana SB, Zahalka MA, Sionov RV. Involvement of CD44, a molecule with a thousand faces, in cancer dissemination. *Seminars in Cancer Biology*, 18(4), 260-267 (2008).
7. Bourguignon LYW, Shiina M, Li J-J. Chapter Ten - Hyaluronan-CD44 Interaction Promotes Oncogenic Signaling, microRNA Functions, Chemoresistance, and Radiation Resistance in Cancer Stem Cells Leading to Tumor Progression. In: *Advances in Cancer Research*. Melanie, AS, Paraskevi, H (Eds.) (Academic Press, 2014) 255-275.
8. Skandalis SS, Gialeli C, Theocharis AD, Karamanos NK. Advances and Advantages of Nanomedicine in the Pharmacological Targeting of Hyaluronan-CD44 Interactions and Signaling in Cancer. *Advances in cancer research*, 123, 277-317 (2013).
9. Goodfellow PN, Banting G, Wiles MV *et al*. The gene, MIC4, which controls expression of the antigen defined by monoclonal-antibody F10.44.2, is on human chromosome-1. *European Journal of Immunology*, 12(8), 659-663 (1982).
10. Ponta H, Sherman L, Herrlich PA. CD44: From adhesion molecules to signalling regulators. *Nature Reviews Molecular Cell Biology*, 4(1), 33-45 (2003).
11. Iida N, Bourguignon LY. New CD44 splice variants associated with human breast cancers. *Journal of cellular physiology*, 162(1), 127-133 (1995).
12. Arpicco S, De Rosa G, Fattal E. Lipid-based nanovectors for targeting of CD44-overexpressing tumor cells. *Journal of drug delivery*, 2013 (2013).
13. Orian-Rousseau V. CD44, a therapeutic target for metastasising tumours. *European Journal of Cancer*, 46(7), 1271-1277 (2010).
14. Reya T, Morrison SJ, Clarke MF, Weissman IL. Stem cells, cancer, and cancer stem cells. *Nature*, 414(6859), 105-111 (2001).
15. Al-Hajj M, Wicha MS, Benito-Hernandez A, Morrison SJ, Clarke MF. Prospective identification of tumorigenic breast cancer cells. *Proc Natl Acad Sci U S A*, 100(7), 3983-3988 (2003).
16. Simeone DM. Pancreatic cancer stem cells: implications for the treatment of pancreatic cancer. *Clin Cancer Res*, 14(18), 5646-5648 (2008).
17. Du L, Wang H, He L *et al*. CD44 is of Functional Importance for Colorectal Cancer Stem Cells. *Clinical Cancer Research*, 14(21), 6751-6760 (2008).
18. Misra S, Heldin P, Hascall VC *et al*. Hyaluronan-CD44 interactions as potential targets for cancer therapy. *FEBS Journal*, 278(9), 1429-1443 (2011).
19. O'Flaherty JD, Barr M, Fennell D *et al*. The Cancer Stem-Cell Hypothesis Its Emerging Role in Lung Cancer Biology and Its Relevance for Future Therapy. *Journal of Thoracic Oncology*, 7(12), 1880-1890 (2012).
20. Ween MP, Oehler MK, Ricciardelli C. Role of Versican, Hyaluronan and CD44 in Ovarian Cancer Metastasis. *International journal of molecular sciences*, 12(2), 1009-1029 (2011).
21. Lee CJ, Dosch J, Simeone DM. Pancreatic cancer stem cells. *Journal of Clinical Oncology*, 26(17), 2806-2812 (2008).
22. Kozovska Z, Gabrisova V, Kucerova L. Colon cancer: Cancer stem cells markers, drug resistance and treatment. *Biomedicine & Pharmacotherapy*, 68(8), 911-916 (2014).

23. Iczkowski KA. Cell adhesion molecule CD44: its functional roles in prostate cancer. *American journal of translational research*, 3(1), 1-7 (2010).
24. Konopleva MY, Jordan CT. Leukemia stem cells and microenvironment: biology and therapeutic targeting. *Journal of Clinical Oncology*, 29(5), 591-599 (2011).
25. Sebban LE, Ronen D, Levartovsky D *et al.* The involvement of CD44 and its novel ligand galectin-8 in apoptotic regulation of autoimmune inflammation. *Journal of Immunology*, 179(2), 1225-1235 (2007).
26. Aruffo A, Stamenkovic I, Melnick M, Underhill CB, Seed B. CD44 is the principal cell-surface receptor for hyaluronate. *Cell*, 61(7), 1303-1313 (1990).
27. Jiang D, Liang J, Noble PW. Hyaluronan as an immune regulator in human diseases. *Physiological reviews*, 91(1), 221-264 (2011).
28. Menzel EJ, Farr C. Hyaluronidase and its substrate hyaluronan: biochemistry, biological activities and therapeutic uses. *Cancer Letters*, 131(1), 3-11 (1998).
29. Lu H-D, Zhao H-Q, Wang K, Lv L-L. Novel hyaluronic acid–chitosan nanoparticles as non-viral gene delivery vectors targeting osteoarthritis. *International Journal of Pharmaceutics*, 420(2), 358-365 (2011).
30. Laurent TC, Fraser J. Hyaluronan. *The FASEB Journal*, 6(7), 2397-2404 (1992).
31. Noble PW. Hyaluronan and its catabolic products in tissue injury and repair. *Matrix Biology*, 21(1), 25-29 (2002).
32. Deed R, Rooney P, Kumar P *et al.* Early-response gene signalling is induced by angiogenic oligosaccharides of hyaluronan in endothelial cells. Inhibition by non-angiogenic, high-molecular-weight hyaluronan. *Int J Cancer*, 71(2), 251-256 (1997).
33. West DC, Hampson IN, Arnold F, Kumar S. ANGIOGENESIS INDUCED BY DEGRADATION PRODUCTS OF HYALURONIC-ACID. *Science*, 228(4705), 1324-1326 (1985).
34. Stern R. Hyaluronidases in cancer biology. *Seminars in Cancer Biology*, 18(4), 275-280 (2008).
35. Jaracz S, Chen J, Kuznetsova LV, Ojima L. Recent advances in tumor-targeting anticancer drug conjugates. *Bioorganic & Medicinal Chemistry*, 13(17), 5043-5054 (2005).
36. Roden L, Campbell P, Fraser JR, Laurent TC, Pertoft H, Thompson JN. Enzymic pathways of hyaluronan catabolism. *Ciba Found Symp*, 143, 60-76; discussion 76-86, 281-285 (1989).
37. Vigetti D, Karousou E, Viola M, Deleonibus S, De Luca G, Passi A. Hyaluronan: biosynthesis and signaling. *Biochim Biophys Acta*, 1840(8), 2452-2459 (2014).
38. Chen B, Miller RJ, Dhal PK. Hyaluronic Acid-Based Drug Conjugates: State-of-the-Art and Perspectives. *Journal of Biomedical Nanotechnology*, 10(1), 4-16 (2014).
39. Skandalis SS, Gialeli C, Theocharis AD, Karamanos NK. Advances and Advantages of Nanomedicine in the Pharmacological Targeting of Hyaluronan-CD44 Interactions and Signaling in Cancer. In: *Hyaluronan Signaling and Turnover*. Simpson, MA, Heldin, P (Eds.) (2014) 277-317.
40. Oh EJ, Park K, Kim KS *et al.* Target specific and long-acting delivery of protein, peptide, and nucleotide therapeutics using hyaluronic acid derivatives. *Journal of controlled release*, 141(1), 2-12 (2010).
41. Puri A, Loomis K, Smith B *et al.* Lipid-based nanoparticles as pharmaceutical drug carriers: from concepts to clinic. *Crit Rev Ther Drug Carrier Syst*, 26(6), 523-580 (2009).
42. Miller AD. Lipid-Based Nanoparticles in Cancer Diagnosis and Therapy. *Journal of Drug Delivery*, 2013, 9 (2013).
43. Battaglia L, Gallarate M. Lipid nanoparticles: state of the art, new preparation methods and challenges in drug delivery. *Expert opinion on drug delivery*, 9(5), 497-508 (2012).
44. Lasa-Saracibar B, Estella-Hermoso de Mendoza A, Guada M, Dios-Vieitez C, Blanco-Prieto MJ. Lipid nanoparticles for cancer therapy: state of the art and future prospects. *Expert opinion on drug delivery*, 9(10), 1245-1261 (2012).
45. Muller RH, Mader K, Gohla S. Solid lipid nanoparticles (SLN) for controlled drug delivery - a review of the state of the art. *European Journal of Pharmaceutics and Biopharmaceutics*, 50(1), 161-177 (2000).

46. Freitas C, Muller RH. Stability determination of solid lipid nanoparticles (SLN) in aqueous dispersion after addition of electrolyte. *Journal of microencapsulation*, 16(1), 59-71 (1999).
47. Delgado D, del Pozo-Rodríguez A, Solinis MA *et al.* Dextran and Protamine-Based Solid Lipid Nanoparticles as Potential Vectors for the Treatment of X-Linked Juvenile Retinoschisis. *Human Gene Therapy*, 23(4), 345-355 (2012).
48. He SN, Li YL, Yan JJ *et al.* Ternary nanoparticles composed of cationic solid lipid nanoparticles, protamine, and DNA for gene delivery. *International Journal of Nanomedicine*, 8, 2859-2869 (2013).
49. Zhang YL, Zhang ZH, Jiang TY *et al.* Cell uptake of paclitaxel solid lipid nanoparticles modified by cell-penetrating peptides in A549 cells. *Pharmazie*, 68(1), 47-53 (2013).
50. Fan T, Chen C, Guo H *et al.* Design and evaluation of solid lipid nanoparticles modified with peptide ligand for oral delivery of protein drugs. *European Journal of Pharmaceutics and Biopharmaceutics*, 88(2), 518-528 (2014).
51. Apaolaza PS, Delgado D, Pozo-Rodríguez Ad, Gascón AR, Solinís M^Á. A novel gene therapy vector based on hyaluronic acid and solid lipid nanoparticles for ocular diseases. *International Journal of Pharmaceutics*, 465(1–2), 413-426 (2014).
52. Tran TH, Choi JY, Ramasamy T *et al.* Hyaluronic acid-coated solid lipid nanoparticles for targeted delivery of vorinostat to CD44 overexpressing cancer cells. *Carbohydr Polym*, 114, 407-415 (2014).
53. Gastaldi L, Battaglia L, Peira E *et al.* Solid lipid nanoparticles as vehicles of drugs to the brain: Current state of the art. *European Journal of Pharmaceutics and Biopharmaceutics*, 87(3), 433-444 (2014).
54. Liu D, Liu Z, Wang L, Zhang C, Zhang N. Nanostructured lipid carriers as novel carrier for parenteral delivery of docetaxel. *Colloids and Surfaces B: Biointerfaces*, 85(2), 262-269 (2011).
55. Zhou X, Zhang X, Ye Y *et al.* Nanostructured lipid carriers used for oral delivery of oridonin: An effect of ligand modification on absorption. *International Journal of Pharmaceutics*, 479(2), 391-398 (2015).
56. Liu D, Liu F, Liu Z, Wang L, Zhang N. Tumor specific delivery and therapy by double-targeted nanostructured lipid carriers with anti-VEGFR-2 antibody. *Molecular pharmaceutics*, 8(6), 2291-2301 (2011).
57. Han YQ, Zhang Y, Li DN, Chen YY, Sun JP, Kong FS. Transferrin-modified nanostructured lipid carriers as multifunctional nanomedicine for codelivery of DNA and doxorubicin. *International Journal of Nanomedicine*, 9, 4107-4115 (2014).
58. Yang X-y, Li Y-x, Li M, Zhang L, Feng L-x, Zhang N. Hyaluronic acid-coated nanostructured lipid carriers for targeting paclitaxel to cancer. *Cancer Letters*, 334(2), 338-345 (2013).
59. Gabizon A, Catane R, Uziely B *et al.* Prolonged circulation time and enhanced accumulation in malignant exudates of doxorubicin encapsulated in polyethylene-glycol coated liposomes. *Cancer Res*, 54(4), 987-992 (1994).
60. Barenholz Y. Doxil[®] — The first FDA-approved nano-drug: Lessons learned. *Journal of Controlled Release*, 160(2), 117-134 (2012).
61. Moen MD, Lyseng-Williamson KA, Scott LJ. Liposomal Amphotericin B A Review of its Use as Empirical Therapy in Febrile Neutropenia and in the Treatment of Invasive Fungal Infections. *Drugs*, 69(3), 361-392 (2009).
62. Ringden O, Meunier F, Tollemar J *et al.* Efficacy of Amphotericin-B encapsulated in liposomes (Ambisome) in the treatment of invasive fungal-infections in immunocompromised patients. *Journal of Antimicrobial Chemotherapy*, 28, 73-82 (1991).
63. Leenders A, Reiss P, Portegies P *et al.* Liposomal amphotericin B (AmBisome) compared with amphotericin B both followed by oral fluconazole in the treatment of AIDS-associated cryptococcal meningitis. *Aids*, 11(12), 1463-1471 (1997).
64. Petre CE, Dittmer DP. Liposomal daunorubicin as treatment for Kaposi's sarcoma. *International Journal of Nanomedicine*, 2(3), 277-288 (2007).

65. Batist G, Ramakrishnan G, Rao CS *et al.* Reduced cardiotoxicity and preserved antitumor efficacy of liposome-encapsulated doxorubicin and cyclophosphamide compared with conventional doxorubicin and cyclophosphamide in a randomized, multicenter trial of metastatic breast cancer. *Journal of Clinical Oncology*, 19(5), 1444-1454 (2001).
66. Walsh TJ, Hiemenz JW, Seibel NL *et al.* Amphotericin B lipid complex for invasive fungal infections: analysis of safety and efficacy in 556 cases. *Clinical Infectious Diseases*, 26(6), 1383-1396 (1998).
67. Bowden R, Chandrasekar P, White MH *et al.* A double-blind, randomized, controlled trial of amphotericin B colloidal dispersion versus amphotericin B for treatment of invasive aspergillosis in immunocompromised patients. *Clinical Infectious Diseases*, 35(4), 359-366 (2002).
68. Glantz MJ, Jaeckle KA, Chamberlain MC *et al.* A randomized controlled trial comparing intrathecal sustained-release cytarabine (DepoCyt) to intrathecal methotrexate in patients with neoplastic meningitis from solid tumors. *Clinical cancer research*, 5(11), 3394-3402 (1999).
69. Rodriguez M, Pytlík R, Kozak T *et al.* Vincristine sulfate liposomes injection (Marqibo) in heavily pretreated patients with refractory aggressive non-Hodgkin lymphoma. *Cancer*, 115(15), 3475-3482 (2009).
70. Allen TM, Cullis PR. Liposomal drug delivery systems: From concept to clinical applications. *Advanced Drug Delivery Reviews*, 65(1), 36-48 (2013).
71. Deshpande PP, Biswas S, Torchilin VP. Current trends in the use of liposomes for tumor targeting. *Nanomedicine*, 8(9), 1509-1528 (2013).
72. Alaouie AM, Sofou S. Liposomes with Triggered Content Release for Cancer Therapy. *Journal of Biomedical Nanotechnology*, 4(3), 234-244 (2008).
73. Grüll H, Langereis S. Hyperthermia-triggered drug delivery from temperature-sensitive liposomes using MRI-guided high intensity focused ultrasound. *Journal of Controlled Release*, 161(2), 317-327 (2012).
74. May JP, Li SD. Hyperthermia-induced drug targeting. *Expert Opinion on Drug Delivery*, 10(4), 511-527 (2013).
75. Li W, Szoka FC, Jr. Lipid-based nanoparticles for nucleic acid delivery. *Pharm Res*, 24(3), 438-449 (2007).
76. Lin QY, Chen J, Zhang ZH, Zheng G. Lipid-based nanoparticles in the systemic delivery of siRNA. *Nanomedicine*, 9(1), 105-120 (2014).
77. Gan L, Wang J, Zhao Y *et al.* Hyaluronan-modified core-shell liponanoparticles targeting CD44-positive retinal pigment epithelium cells via intravitreal injection. *Biomaterials*, 34(24), 5978-5987 (2013).
78. Loureiro JA, Gomes B, Coelho MAN, Pereira MD, Rocha S. Targeting nanoparticles across the blood-brain barrier with monoclonal antibodies. *Nanomedicine*, 9(5), 709-722 (2014).
79. Mattheolabakis G, Rigas B, Constantinides PP. Nanodelivery strategies in cancer chemotherapy: biological rationale and pharmaceutical perspectives. *Nanomedicine*, 7(10), 1577-1590 (2012).
80. Yu B, Tai HC, Xue WM, Lee LJ, Lee RJ. Receptor-targeted nanocarriers for therapeutic delivery to cancer. *Molecular Membrane Biology*, 27(7), 286-298 (2010).
81. Yang L, Zhang XB, Ye M *et al.* Aptamer-conjugated nanomaterials and their applications. *Advanced Drug Delivery Reviews*, 63(14-15), 1361-1370 (2011).
82. Ababneh N, Alshaer W, Allozi O *et al.* In vitro selection of modified RNA aptamers against CD44 cancer stem cell marker. *Nucleic Acid Ther*, 23(6), 401-407 (2013).
83. Alshaer W, Hillaireau H, Vergnaud J, Ismail S, Fattal E. Functionalizing Liposomes with anti-CD44 Aptamer for Selective Targeting of Cancer Cells. *Bioconjug Chem*, (2014).
84. Liu B, Zhang JN, Liao J *et al.* Aptamer-Functionalized Nanoparticles for Drug Delivery. *Journal of Biomedical Nanotechnology*, 10(11), 3189-3203 (2014).

85. Du AW, Stenzel MH. Drug Carriers for the Delivery of Therapeutic Peptides. *Biomacromolecules*, 15(4), 1097-1114 (2014).
86. Kim E, Yang J, Park J *et al.* Consecutive Targetable Smart Nanoprobe for Molecular Recognition of Cytoplasmic microRNA in Metastatic Breast Cancer. *ACS Nano*, 6(10), 8525-8535 (2012).
87. Qhattal HSS, Liu X. Characterization of CD44-Mediated Cancer Cell Uptake and Intracellular Distribution of Hyaluronan-Grafted Liposomes. *Molecular Pharmaceutics*, 8(4), 1233-1246 (2011).
88. Qhattal HSS, Hye T, Alali A, Liu X. Hyaluronan Polymer Length, Grafting Density, and Surface Poly(ethylene glycol) Coating Influence in Vivo Circulation and Tumor Targeting of Hyaluronan-Grafted Liposomes. *ACS Nano*, 8(6), 5423-5440 (2014).
89. Park J-H, Cho H-J, Yoon HY *et al.* Hyaluronic acid derivative-coated nanohybrid liposomes for cancer imaging and drug delivery. *Journal of Controlled Release*, 174, 98-108 (2014).
90. Surace C, Arpicco S, Dufay-Wojcicki A *et al.* Lipoplexes Targeting the CD44 Hyaluronic Acid Receptor for Efficient Transfection of Breast Cancer Cells. *Molecular Pharmaceutics*, 6(4), 1062-1073 (2009).
91. Taetz S, Bochot A, Surace C *et al.* Hyaluronic Acid-Modified DOTAP/DOPE Liposomes for the Targeted Delivery of Anti-Telomerase siRNA to CD44-Expressing Lung Cancer Cells. *Oligonucleotides*, 19(2), 103-115 (2009).
92. Wojcicki AD, Hillaireau H, Nascimento TL *et al.* Hyaluronic acid-bearing lipoplexes: Physico-chemical characterization and in vitro targeting of the CD44 receptor. *Journal of Controlled Release*, (2012).
93. Landesman-Milo D, Goldsmith M, Leviatan Ben-Arye S *et al.* Hyaluronan grafted lipid-based nanoparticles as RNAi carriers for cancer cells. *Cancer Letters*, 334(2), 221-227 (2013).
94. Dalla Pozza E, Lerda C, Costanzo C *et al.* Targeting gemcitabine containing liposomes to CD44 expressing pancreatic adenocarcinoma cells causes an increase in the antitumoral activity. *Biochimica et Biophysica Acta (BBA)-Biomembranes*, 1828(5), 1396-1404 (2013).
95. Arpicco S, Lerda C, Dalla Pozza E *et al.* Hyaluronic acid-coated liposomes for active targeting of gemcitabine. *European Journal of Pharmaceutics and Biopharmaceutics*, 85(3), 373-380 (2013).
96. Jiang T, Zhang Z, Zhang Y *et al.* Dual-functional liposomes based on pH-responsive cell-penetrating peptide and hyaluronic acid for tumor-targeted anticancer drug delivery. *Biomaterials*, 33(36), 9246-9258 (2012).
97. Glucksam-Galnoy Y, Zor T, Margalit R. Hyaluronan-modified and regular multilamellar liposomes provide sub-cellular targeting to macrophages, without eliciting a pro-inflammatory response. *Journal of Controlled Release*, 160(2), 388-393 (2012).
98. Bochot A, Fattal E. Liposomes for intravitreal drug delivery: a state of the art. *Journal of controlled release : official journal of the Controlled Release Society*, 161(2), 628-634 (2012).
99. Yerushalmi N, Margalit R. Hyaluronic acid-modified bioadhesive liposomes as local drug depots: effects of cellular and fluid dynamics on liposome retention at target sites. *Arch Biochem Biophys*, 349(1), 21-26 (1998).
100. Mizrahy S, Raz SR, Hasgaard M *et al.* Hyaluronan-coated nanoparticles: the influence of the molecular weight on CD44-hyaluronan interactions and on the immune response. *Journal of Controlled Release*, 156(2), 231-238 (2011).
101. Lesley J, Hascall VC, Tammi M, Hyman R. Hyaluronan binding by cell surface CD44. *Journal of Biological Chemistry*, 275(35), 26967-26975 (2000).
102. Eliaz RE, Szoka FC, Jr. Liposome-encapsulated doxorubicin targeted to CD44: a strategy to kill CD44-overexpressing tumor cells. *Cancer Res*, 61(6), 2592-2601 (2001).
103. Ruhela D, Kivimäe S, Szoka FC. Chemoenzymatic Synthesis of Oligohyaluronan-Lipid Conjugates. *Bioconjugate Chemistry*, 25(4), 718-723 (2014).
104. Toriyabe N, Hayashi Y, Hyodo M, Harashima H. Synthesis and Evaluation of Stearylated Hyaluronic Acid for the Active Delivery of Liposomes to Liver Endothelial Cells. *Biological & Pharmaceutical Bulletin*, 34(7), 1084-1089 (2011).
105. Lasic DD. Novel applications of liposomes. *Trends in Biotechnology*, 16(7), 307-321 (1998).

106. Schäfer V, von Briesen H, Andreesen R *et al.* Phagocytosis of nanoparticles by human immunodeficiency virus (HIV)-infected macrophages: a possibility for antiviral drug targeting. *Pharmaceutical Research*, 9(4), 541-546 (1992).
107. Tiantian Y, Wenji Z, Mingshuang S *et al.* Study on intralymphatic-targeted hyaluronic acid-modified nanoliposome: Influence of formulation factors on the lymphatic targeting. *International Journal of Pharmaceutics*, 471(1–2), 245-257 (2014).
108. Peer D, Margalit R. Loading mitomycin C inside long circulating hyaluronan targeted nanoliposomes increases its antitumor activity in three mice tumor models. *Int J Cancer*, 108(5), 780-789 (2004).
109. Ishida T, Harashima H, Kiwada H. Liposome clearance. *Bioscience reports*, 22, 197-224 (2002).
110. Nel AE, Mädler L, Velegol D *et al.* Understanding biophysicochemical interactions at the nanobio interface. *Nature materials*, 8(7), 543-557 (2009).
111. Cedervall T, Lynch I, Lindman S *et al.* Understanding the nanoparticle–protein corona using methods to quantify exchange rates and affinities of proteins for nanoparticles. *Proceedings of the National Academy of Sciences*, 104(7), 2050-2055 (2007).
112. Lundqvist M, Stigler J, Elia G, Lynch I, Cedervall T, Dawson KA. Nanoparticle size and surface properties determine the protein corona with possible implications for biological impacts. *Proceedings of the National Academy of Sciences*, 105(38), 14265-14270 (2008).
113. Lynch I, Dawson KA. Protein-nanoparticle interactions. *Nano Today*, 3(1), 40-47 (2008).
114. Dutta D, Sundaram SK, Teegarden JG *et al.* Adsorbed proteins influence the biological activity and molecular targeting of nanomaterials. *Toxicological Sciences*, 100(1), 303-315 (2007).
115. Chithrani BD, Ghazani AA, Chan WC. Determining the size and shape dependence of gold nanoparticle uptake into mammalian cells. *Nano letters*, 6(4), 662-668 (2006).
116. Moghimi SM, Hunter AC, Murray JC. Long-circulating and target-specific nanoparticles: theory to practice. *Pharmacol Rev*, 53(2), 283-318 (2001).
117. Pavlin M, Bregar VB. Stability of nanoparticle suspensions in different biologically relevant media. *Dig J Nanomater Bios*, 7(4), 1389-1400 (2012).
118. Allouni ZE, Cimpan MR, Høl PJ, Skodvin T, Gjerdet NR. Agglomeration and sedimentation of TiO₂ nanoparticles in cell culture medium. *Colloids and Surfaces B: Biointerfaces*, 68(1), 83-87 (2009).
119. Ji Z, Jin X, George S *et al.* Dispersion and stability optimization of TiO₂ nanoparticles in cell culture media. *Environmental science & technology*, 44(19), 7309-7314 (2010).
120. Choi KY, Min KH, Na JH *et al.* Self-assembled hyaluronic acid nanoparticles as a potential drug carrier for cancer therapy: synthesis, characterization, and in vivo biodistribution. *Journal of Materials Chemistry*, 19(24), 4102-4107 (2009).
121. Suk JS, Kim AJ, Trehan K *et al.* Lung gene therapy with highly compacted DNA nanoparticles that overcome the mucus barrier. *Journal of Controlled Release*, 178, 8-17 (2014).
122. Volodkin D, Mohwald H, Voegel J-C, Ball V. Coating of negatively charged liposomes by polylysine: Drug release study. *Journal of Controlled Release*, 117(1), 111-120 (2007).
123. Tokita Y, Okamoto A. Hydrolytic degradation of hyaluronic acid. *Polymer Degradation and Stability*, 48(2), 269-273 (1995).
124. Gura E, Hüchel M, Müller P-J. Specific degradation of hyaluronic acid and its rheological properties. *Polymer Degradation and Stability*, 59(1), 297-302 (1998).
125. Takeda M, Terasawa H, Sakakura M *et al.* Hyaluronan recognition mode of CD44 revealed by cross-saturation and chemical shift perturbation experiments. *Journal of Biological Chemistry*, 278(44), 43550-43555 (2003).
126. Lesley J, Gal I, Mahoney DJ *et al.* TSG-6 modulates the interaction between hyaluronan and cell surface CD44. *Journal of Biological Chemistry*, 279(24), 25745-25754 (2004).
127. Alves CS, Yakovlev S, Medved L, Konstantopoulos K. Biomolecular characterization of CD44-fibrin(ogen) binding: distinct molecular requirements mediate binding of standard and variant isoforms of CD44 to immobilized fibrin(ogen). *J Biol Chem*, 284(2), 1177-1189 (2009).

128. Li L, Heldin C-H, Heldin P. Inhibition of platelet-derived growth factor-BB-induced receptor activation and fibroblast migration by hyaluronan activation of CD44. *Journal of Biological Chemistry*, 281(36), 26512-26519 (2006).
129. Simons K, Gerl MJ. Revitalizing membrane rafts: new tools and insights. *Nature Reviews Molecular Cell Biology*, 11(10), 688-699 (2010).
130. Rejman J, Bragonzi A, Conese M. Role of Clathrin- and Caveolae-Mediated Endocytosis in Gene Transfer Mediated by Lipo- and Polyplexes. *Mol Ther*, 12(3), 468-474 (2005).
131. Bareford LM, Swaan PW. Endocytic mechanisms for targeted drug delivery. *Advanced Drug Delivery Reviews*, 59(8), 748-758 (2007).
132. Conner SD, Schmid SL. Regulated portals of entry into the cell. *Nature*, 422(6927), 37-44 (2003).
133. Wang LH, Rothberg KG, Anderson RGW. MIS-ASSEMBLY OF CLATHRIN LATTICES ON ENDOSOMES REVEALS A REGULATORY SWITCH FOR COATED PIT FORMATION. *Journal of Cell Biology*, 123(5), 1107-1117 (1993).
134. Brown DA. Lipid rafts, detergent-resistant membranes, and raft targeting signals. *Physiology*, 21, 430-439 (2006).
135. Hooper NM. Detergent-insoluble glycosphingolipid/cholesterol-rich membrane domains, lipid rafts and caveolae (review). *Molecular Membrane Biology*, 16(2), 145-156 (1999).
136. Long M, Huang S-H, Wu C-H, Shackelford GM, Jong A. Lipid raft/caveolae signaling is required for *Cryptococcus neoformans* invasion into human brain microvascular endothelial cells. *Journal of Biomedical Science*, 19 (2012).
137. Chen WC, May JP, Li S-D. Immune responses of therapeutic lipid nanoparticles. *Nanotechnology Reviews*, 2(2), 201-213 (2013).
138. Pardue EL, Ibrahim S, Ramamurthi A. Role of hyaluronan in angiogenesis and its utility to angiogenic tissue engineering. *Organogenesis*, 4(4), 203-214 (2008).
139. Ormiston ML, Slaughter GR, Deng Y, Stewart DJ, Courtman DW. The enzymatic degradation of hyaluronan is associated with disease progression in experimental pulmonary hypertension. *American journal of physiology. Lung cellular and molecular physiology*, 298(2), L148-157 (2010).
140. Stern R. Hyaluronan catabolism: a new metabolic pathway. *European journal of cell biology*, 83(7), 317-325 (2004).
141. Stern R, Asari AA, Sugahara KN. Hyaluronan fragments: an information-rich system. *European journal of cell biology*, 85(8), 699-715 (2006).
142. Bollyky PL, Falk BA, Wu RP, Buckner JH, Wight TN, Nepom GT. Intact extracellular matrix and the maintenance of immune tolerance: high molecular weight hyaluronan promotes persistence of induced CD4+ CD25+ regulatory T cells. *Journal of leukocyte biology*, 86(3), 567-572 (2009).
143. Scheibner KA, Lutz MA, Boodoo S, Fenton MJ, Powell JD, Horton MR. Hyaluronan fragments act as an endogenous danger signal by engaging TLR2. *The Journal of Immunology*, 177(2), 1272-1281 (2006).
144. Lv H, Zhang S, Wang B, Cui S, Yan J. Toxicity of cationic lipids and cationic polymers in gene delivery. *Journal of Controlled Release*, 114(1), 100-109 (2006).
145. Felgner JH, Kumar R, Sridhar C *et al.* Enhanced gene delivery and mechanism studies with a novel series of cationic lipid formulations. *Journal of Biological Chemistry*, 269(4), 2550-2561 (1994).
146. Vonarbourg A, Passirani C, Saulnier P, Benoit JP. Parameters influencing the stealthiness of colloidal drug delivery systems. *Biomaterials*, 27(24), 4356-4373 (2006).
147. Patel H. Serum opsonins and liposomes: Their interaction and opsonophagocytosis. *Critical reviews in therapeutic drug carrier systems*, 9(1), 39-90 (1991).
148. Harashima H, Sakata K, Funato K, Kiwada H. Enhanced hepatic uptake of liposomes through complement activation depending on the size of liposomes. *Pharmaceutical research*, 11(3), 402-406 (1994).

149. Thiele L, Diederichs JE, Reszka R, Merkle HP, Walter E. Competitive adsorption of serum proteins at microparticles affects phagocytosis by dendritic cells. *Biomaterials*, 24(8), 1409-1418 (2003).
150. Patel LN, Zaro JL, Shen W-C. Cell penetrating peptides: intracellular pathways and pharmaceutical perspectives. *Pharm Res-Dord*, 24(11), 1977-1992 (2007).
151. Bimbo LM, Peltonen L, Hirvonen J, Santos HA. Toxicological Profile of Therapeutic Nanodelivery Systems. *Current drug metabolism*, 13(8), 1068-1086 (2012).
152. Raz A, Bucana C, Fogler WE, Poste G, Fidler IJ. Biochemical, morphological, and ultrastructural studies on the uptake of liposomes by murine macrophages. *Cancer Research*, 41(2), 487-494 (1981).
153. Nardin A, Lefebvre ML, Labroquere K, Faure O, Abastado JP. Liposomal muramyl tripeptide phosphatidylethanolamine: Targeting and activating macrophages for adjuvant treatment of osteosarcoma. *Current cancer drug targets*, 6(2), 123-133 (2006).
154. Ahsan FL, Rivas IP, Khan MA, Suarez AIT. Targeting to macrophages: role of physicochemical properties of particulate carriers-liposomes and microspheres-on the phagocytosis by macrophages. *Journal of Controlled Release*, 79(1-3), 29-40 (2002).
155. Thiele L, Rothen-Rutishauser B, Jilek S, Wunderli-Allenspach H, Merkle HP, Walter E. Evaluation of particle uptake in human blood monocyte-derived cells in vitro. Does phagocytosis activity of dendritic cells measure up with macrophages? *Journal of Controlled Release*, 76(1-2), 59-71 (2001).
156. Bradley AJ, Devine DV, Ansell SM, Janzen J, Brooks DE. Inhibition of liposome-induced complement activation by incorporated poly(ethylene glycol) lipids. *Archives of biochemistry and biophysics*, 357(2), 185-194 (1998).
157. Peer D, Margalit R. Tumor-targeted hyaluronan nanoliposomes increase the antitumor activity of liposomal Doxorubicin in syngeneic and human xenograft mouse tumor models. *Neoplasia*, 6(4), 343-353 (2004).
158. Wrobel T, Dziegiel P, Mazur G, Zabel M, Kuliczowski K, Szuba A. LYVE-1 expression on high endothelial venules (HEVs) of lymph nodes. *Lymphology*, 38(3), 107-110 (2005).
159. Harris EN, Kyosseva SV, Weigel JA, Weigel PH. Expression, processing, and glycosaminoglycan binding activity of the recombinant human 315-kDa hyaluronic acid receptor for endocytosis (HARE). *J Biol Chem*, 282(5), 2785-2797 (2007).

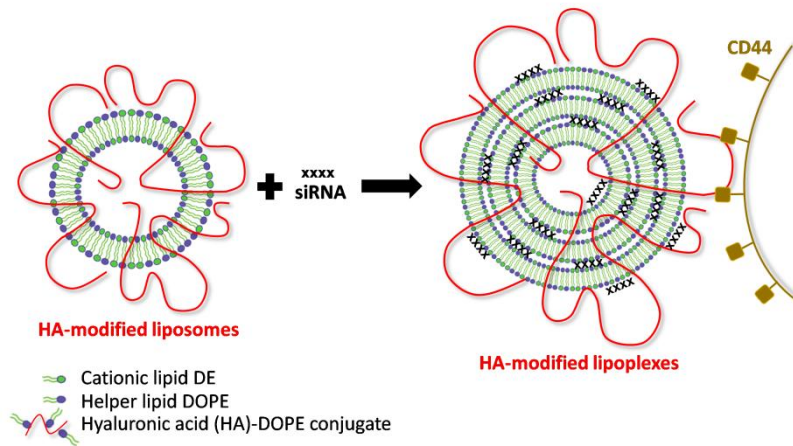
Travaux expérimentaux

Travaux expérimentaux

Chapitre 1 - Supramolecular organization and siRNA binding of hyaluronic acid-modified lipoplexes for targeted delivery to CD44 receptor

Travaux expérimentaux - Chapitre 1**Supramolecular organization and siRNA binding of hyaluronic acid-modified lipoplexes for targeted delivery to CD44 receptor****Résumé**

La stabilité, la toxicité, les interactions avec les composants biologiques et l'efficacité *in vitro* et *in vivo* des lipoplexes sont directement influencés par leur structure. Dans ce chapitre, la formation de lipoplexes de siRNA obtenus par la complexation de liposomes modifiés avec de l'acide hyaluronique (HA) à des siRNA a été étudiée, ainsi que les paramètres influençant leur organisation supramoléculaire. L'insertion de l'HA dans la structure du liposome au moment de la formation des vésicules a entraîné une augmentation de la taille des liposomes en fonction de la concentration d'HA. Leur complexation avec les siRNA a encore augmenté la taille des particules obtenues. Ces lipoplexes présentent un diamètre autour de 110 nm lorsque le siRNA a été associé à des ratios de charge (+/-) de 266 à 50, et autour de 230 nm à ratios +/- de 4 à 1. Les potentiels zeta des lipoplexes modifiés par HA sont de l'ordre de + 50 mV à des ratios +/- de 266 à 50, et une diminution à des valeurs négatives de -30 à -45 mV à des ratios +/- de 4 à 1 a été observée. L'ajout du conjugué HA-DOPE n'a pas compromis l'association du siRNA à des liposomes, bien que l'ajout des acides nucléiques lors de la formation des lipoplexes ait provoqué un déplacement d'une partie du conjugué HA-DOPE de la structure des lipoplexes, comme montré par électrophorèse capillaire. La titration calorimétrique isotherme et les études de diffraction des rayons X ont démontré que, sous l'effet des interactions électrostatiques avec les siRNA, un réarrangement des bicouches lipidiques a lieu, conduisant à la formation de vésicules oligolamellaires. Ce phénomène est dépendant de la quantité de molécules de siRNA et du degré de modification par l'HA, comme observé par analyse de la diffraction des rayons-X et confirmé visuellement par cryo-microscopie. Ces images ont révélé la coexistence de vésicules sphériques unilamellaires et oligolamellaires dans la population de liposomes, et a confirmé la réorganisation des bicouches lipidiques et la formation de structures oligolamellaires denses. Enfin, le positionnement convenable de l'HA sur la surface des lipoplexes et sa capacité de se lier spécifiquement aux récepteurs de CD44 de manière concentration-dépendante ont été démontrés par la technique de résonance plasmonique de surface.



Chapitre rédigé sous forme d'article et soumis pour publication à Langmuir. Auteurs : Thais Leite Nascimento, Hervé Hillaireau, Magali Noiray, Claudie Bourgaux, Silvia Arpicco, Gérard Pehau-Arnaudet, Myriam Taverna, Nicolas Tsapis, Elias Fattal.

Experimental work – Chapter 1**Supramolecular organization and siRNA binding of hyaluronic acid-modified lipoplexes for targeted delivery to CD44 receptor****Abstract**

Lipoplexes stability, toxicity, interaction with biological components and efficiency *in vitro* and *in vivo* are directly influenced by their structure. In this work, the formation of siRNA lipoplexes from hyaluronic acid (HA)-modified liposomes and siRNA was studied, as well as the parameters influencing their supramolecular organization. The Insertion of HA in the liposome structure at the moment of vesicle formation increased liposome size, depending on HA concentration. Subsequent complexation with siRNA further increased the size of the resulting lipoplexes, reaching around 110 nm when siRNA was associated at charge ratios (+/-) from 266 to 50, and around 230 nm at +/- ratios from 4 to 1. HA-modified lipoplexes' zeta potentials were around + 50 mV at +/- ratios from 266 to 50, and decreased to negative values from -30 to -45 mV at +/- ratios from 4 to 1. The addition of the HA-DOPE conjugate did not compromise siRNA binding to liposomes, although the addition of nucleic acids upon lipoplex formation accounted for a displacement of part of the HA-DOPE conjugate from the lipoplex structure, as shown by capillary electrophoresis. Isothermal titration calorimetry and X-ray diffraction studies demonstrated that following electrostatic interactions with siRNA, a rearrangement of the lipid bilayers takes place resulting in the formation of condensed oligolamellar vesicles. This phenomenon is dependent on the amount of siRNA molecules and the degree of modification with HA, as observed by X-ray diffraction analysis and confirmed visually by cryo-TEM microscopy. These images revealed the coexistence of spherical unilamellar and oligolamellar vesicles on liposomes population, and confirmed the reorganization of the lipid bilayers and the formation of dense oligolamellar structures. Finally, the suitable positioning of HA on the lipoplex surface and HA ability to specifically bind to the CD44 receptors in a concentration-dependent manner was demonstrated by surface plasmon resonance analysis.

Introduction

Downregulation of gene expression using small interfering RNA (siRNA) has raised a broad interest for medical applications. siRNAs are short double-stranded RNA molecules of 19-21 nucleotides in length, that besides being highly efficient and selective, offer the possibility of a long-lasting therapeutic effect for gene-related diseases. One of the strands is entitled the guide, which is complementary to the coding region of the target mRNA, while the other is known as the passenger strand. Once in the cytoplasm, the guide strand binds to the target RNA molecule, which promotes the enzymatic cleavage of the mRNA and prevents the synthesis of the protein of interest. These molecules however face some impediments to a successful application, similarly to other nucleotide-based therapeutics like plasmid DNA or antisense oligonucleotides¹. As a result of their small size, they are rapidly eliminated by the kidneys and show circulating half-lives of seconds to minutes². They are also susceptible to degradation by nucleases in the plasma. Within the tissues, they do not cross cell membranes readily because of their negative charge, hydrophilicity and molecular size. Also, siRNAs are taken up by most mammalian cells in a way that does not preserve their activity³. Therefore, the future of this therapeutic approach heavily depends on the development of delivery systems able to carry these molecules from their administration site to their intracellular pharmacological target⁴.

Complexes formed by electrostatic interactions between cationic liposomes and siRNA, called lipoplexes, are considered as the most suitable carriers for intracellular delivery of nucleic acids and particularly for siRNA^{5, 6}. In addition, they are versatile systems, whose surface can be modified to increase their circulation time and improve their interaction with the target⁷. One of the key factors influencing siRNA delivery is the macromolecular shape of the lipoplexes^{8, 9}. Their final structure has a significant impact on particle stability, interaction with biological components, cytotoxicity^{9, 10} and intracellular trafficking^{11, 12}, and will therefore determine their efficiency *in vitro* and *in vivo*¹³. It is therefore important to consider an accurate and detailed understanding of lipoplex structure and physicochemical characteristics.

Hyaluronic acid (HA) is a glycosaminoglycan polymer composed of disaccharide units of *N*-acetylglucosamine and D-glucuronic acid linked together through alternating β -1,3 and β -1,4 glycosidic bonds¹⁴. It is biocompatible, being the major component of the extracellular matrix. The native high molecular weight HA is non-toxic and non-immunogenic¹⁵. It does not induce expression of genes involved in proliferation or inflammation¹⁶ and counteracts proangiogenic effects of the HA oligomers^{17, 18}. Surface modification of cationic liposomes with high molecular weight HA can improve their efficacy by mediating active CD44 targeting in tumors and can also increase their circulation time, due to a possible dysopsonization effect due to the hydrophilic coating effect of HA^{19, 20, 21, 22}.

In this study, we describe the design and physicochemical characterization of novel HA-lipoplexes entrapping siRNA. The lipoplex composition is based on the cationic lipid 2-(2-3-didodecyloxypropyl)hydroxyethyl] ammonium bromide (DE), which has shown promising transfection efficiency in different cell lines compared to the cationic lipids currently available on the market²³. To achieve the targeting of CD44 receptors, lipoplexes were surface-coated using a conjugate of HA and L-alpha-dioleylethanolamine (DOPE)²⁴. In previous studies, modification of lipoplexes with HA-DOPE conjugate demonstrated increased transfection of CD44-expressing cells using plasmid DNA^{18, 25} and siRNA²⁴. The supramolecular organization and formation of these lipoplexes, however, remained an open question. Here, a study of the formation of these nanocarriers and the aspects influencing the organization of the lipid bilayers was performed using a combination of dynamic light scattering, capillary electrophoresis, cryo-TEM microscopy, surface plasmon resonance and small angle X-ray scattering techniques.

Materials and Methods

Materials

The cationic lipid [2-(2-3-didodecyloxypropyl)hydroxyethyl] ammonium bromide (DE) was synthesized as described previously²³. L-alpha-dioleylethanolamine (DOPE) and phosphatidylethanolamine conjugated to rhodamine (PE-rhodamine) were purchased from Avanti Polar Lipids distributed by Sigma Aldrich (Saint Quentin Fallavier, France). High molecular weight HA (sodium salt, 1600 kDa, purity of 95%) was provided by Acros organics (Geel, Belgium). SiRNA (19 bp) was purchased from Eurogentec (Angers, France) and diluted in RNase-free water before use. The HA-DOPE conjugate was synthesized as described previously²⁵. In the following, water refers to ultrapurified MilliQ[®] water (Millipore, France) with a resistivity ≥ 18 M Ω ·cm.

Liposomes and lipoplexes preparation

Liposomes of DOPE/DE at 1:1 w/w ratio (equivalent to a molar ratio of 0.78:1) were prepared in water by the ethanol injection method^{24, 26}. Separate solutions of DE and DOPE, stored in chloroform under nitrogen at -20°C, were dried under pressure in a rotary evaporator. The dried lipids were then dissolved in absolute ethanol at a concentration of 10 mg/mL. For liposome preparation, 0.06 to 0.9 mL of the ethanolic lipid solution were rapidly injected into RNase free water under magnetic stirring.

HA-liposomes were prepared by diluting an aqueous stock solution of the HA-DOPE conjugate (1 mg/mL) to different concentrations in RNase free water before injection. Each conjugate have 3 µg of DOPE/mg of HA. The HA-DOPE content of liposomes is expressed as mass ratio of HA-DOPE to other lipids (DE + DOPE) (10% refers to 1:10 w/w). Liposome suspensions were dialyzed against 1 L of MilliQ water overnight in Spectra/Por CE dialysis tubes with a molecular weight cutoff of 50 kDa (Spectrum Laboratories, Breda, Netherlands) to eliminate ethanol. Lipoplexes were then prepared at different charge ratios (+/- ratios) by adding one volume of the 3 mM liposome suspension into two volumes of siRNA solution at different concentrations (0.11, 0.16, 0.22, 0.44, 5.52, 7.36, 11.05 and 22.10 µM for +/- ratios of 200, 134, 100, 50, 4, 3, 2 and 1) in an Eppendorf tube, and gently homogenizing by pipetting up and down. Suspensions of 15 µL – 2.5 mL of lipoplexes were usually prepared and incubated for 1 hour at room temperature before use.

Hydrodynamic diameter and zeta potential measurement

The mean hydrodynamic diameter, polydispersity index (Pdl) and zeta potential were determined with a Zetasizer Nano Zs (Malvern Instruments Ltd, Malvern, UK). Before each measurement, liposomes and lipoplexes were diluted in 1 mM NaCl. Measurements were carried out in triplicate at 25 °C for at least three independent preparations.

Colloidal stability of lipoplexes in isotonic media

Non-coated, 10% HA-liposomes and HA-lipoplexes at various charge ratios were prepared as described above and diluted down to 66 µg/mL of lipids with 0.9% w/v NaCl or 5% w/v glucose. Changes in hydrodynamic diameter upon dilution were monitored at 25°C. The accuracy of measurements was verified by mixing each suspension thoroughly before each measurement. All experiments were performed at least in duplicate.

Lipoplexes siRNA content

siRNAs were labeled at the 5'-end with γ -³³P-ATP (Perkin-Elmer Life Sciences, Courtaboeuf, France) catalyzed by T4 polynucleotide kinase (New England Biolabs, Frankfurt am Main, Germany) according to the manufacturer's protocol. Lipoplexes were prepared with radiolabeled siRNA at various +/- ratios (2-134) from non-coated or 10% HA-liposomes. Suspensions were placed in the upper chamber of Amicon Ultra-0.5 ml filters (cutoff value 100 kDa; Millipore). After adding 200 µL of RNase-free water, samples were centrifuged (14,000 g, 30 min, 4°C). This procedure was repeated five times.

Binding efficiencies were determined by comparing the sum of specific radioactivity of the washings to the radioactivity of the siRNA solution used for the lipoplexes preparation. Experiments were performed in triplicate.

Capillary electrophoresis

A Beckman P/ACE System 5500 was used with an uncoated fused silica capillary of 57 cm of effective length and an internal diameter of 75 μm . Electrophoresis conditions to analyze HA-DOPE conjugate were derived from Grimshaw et al.²⁷ for the assay of HA. The capillary was first conditioned by four successive rinsing steps of 5 min each with water, 1 M NaOH, 0.1 M NaOH and back to water. Before each analysis, the capillary was washed at 20 psi with water for 2 min, 0.1 M NaOH for 3 min and finally equilibrated with the background electrolyte for 5 min. The separation buffer was 65 mM sodium tetraborate containing 20mM of sodium dodecyl sulfate (SDS) with pH 9.0. Sample injection was carried out at 0.5 psi for 5 s. All samples were adjusted to a concentration of 1 mg/mL of HA or HA-DOPE by evaporation under vacuum using an Eppendorf Concentrator® at 30 °C. This step was validated after verification by dynamic light scattering that no modification of the diameter and zeta potential occurred during the concentration. The free fraction of conjugate was determined using a HA-DOPE 1mg/ml solution as an internal standard. Samples containing 1 mg/mL HA-DOPE + HA-DOPE solutions at 0.25, 0.5, 1 and 2.5 mg/mL were analyzed and the peak areas obtained were used to form calibration curves. The peak areas found by extrapolation of the sample curves to the point [HA-DOPE]=0 were used in the HA-DOPE calibration curve to determine the free amount of conjugate. Detection wavelength was 200 nm and the voltage applied was +25 kV. The capillary was maintained at 25 °C during electrophoresis. Experiments were performed at least in duplicate.

Isothermal titration calorimetry

The thermodynamics of the interaction between siRNA and the cationic liposomes, coated or not with HA, was evaluated by isothermal titration calorimetry (ITC) (Microcal Inc., USA). Aliquots of 10 μL of aqueous siRNA solution (19.7 μM) filled into a 283 μL syringe were used to titrate the aqueous suspension of liposomes (98 μM of total lipids) into the calorimetric sample cell accurately thermostated at 25°C. Agitation speed was 307 rpm and intervals between injections was 500 s. Background of titration consisted in injecting the siRNA solution in MilliQ® water. The heats of dilution were insignificant compared with the binding interaction heats.

Cryo-transmission electron microscopy

10% HA-liposomes and HA-lipoplexes containing siRNA at +/- ratios of 2 and 134 were observed using cryo-transmission electron microscopy (cryo-TEM). The preparation of liposome samples was performed as follows. 4 μL of liposome concentrated aqueous suspension were placed on Quantifoil R2/2 grids (Quantifoil, Germany). The samples were cryofixed in liquid ethane (-180°C) using the Leica EMGP (Leica, Austria). For lipoplex samples, grids were pre-treated with 1 mM CaCl_2 for 1 min. Grids were transferred using a cryo-holder (626 DH Gatan) for observation on a Tecnai F20 electron microscope (FEI, USA). Images were recorded under low electron dose conditions at 200 kV on a camera Gatan Ultrascan 4000 with Digital Micrograph (Gatan, USA) version 1.83.842. Doses were previously quantified using a faraday cup.

Small angle X-ray scattering (SAXS)

Suspensions of liposomes and lipoplexes were loaded into quartz capillaries (diameter 1.5 mm, Glas-Müller, Berlin, Germany). The top of the capillaries was sealed with a drop of paraffin to prevent water evaporation. Small-angle X-ray scattering experiments were performed on the SWING beamline at the SOLEIL synchrotron. The energy was set to 11 keV. The scattering intensity was reported as a function of scattering vector $q = 4\pi/\lambda \sin \theta$, where 2θ is the scattering angle and λ is the wavelength of the incident beam. Calibration of the q -range ($0.008 \text{ \AA}^{-1} - 0.4 \text{ \AA}^{-1}$) was carried out with silver behenate as standard. Data were collected with a two-dimensional CCD detector. The acquisition time was 50 s. Intensity values were normalized to account for beam intensity, acquisition time, and sample transmission. Each scattering pattern was then integrated circularly to yield the intensity as a function of q . The scattered intensity from a capillary filled with water was subtracted from the sample scattering curves.

HA-lipoplex CD44 receptor affinity by surface plasmon resonance spectroscopy

Interaction of non-coated and HA-lipoplexes with CD44 receptors was monitored by surface plasmon resonance (SPR) spectroscopy using a BIAcore T100 (GE Healthcare Life Sciences, Vélizy, France) instrument. Human recombinant CD44-Fc receptors were immobilized on a carboxymethylated dextran sensor chip (series S CM3, GE Healthcare) using amine coupling. Carboxylic groups were activated by a mixture of EDC/NHS during 7 min at 10 $\mu\text{L}/\text{min}$ followed by an injection of 17 $\mu\text{g}/\text{mL}$ CD44-Fc in a 10 mM acetate buffer at pH 4.4 during 5 min at 10 $\mu\text{L}/\text{min}$. The remaining groups were

blocked by an injection of ethanolamine. A flow channel blocked by ethanolamine was used as a reference surface. The specific interaction of HA-lipoplexes (at the concentrations 0.3, 0.6, 1.2, 2.4 and 4.8 μM of lipids) with the immobilized CD44-Fc was assessed. All the experiments were conducted at a flow rate of 50 $\mu\text{L}/\text{min}$ in 150 mM NaCl, with a contact time of 360 s. The surface was washed for 640 s and regenerated with a 34 mM octyl-glucoside solution for 30 s at 50 $\mu\text{L}/\text{min}$ and 10 mM NaOH for 30 s at 100 $\mu\text{L}/\text{min}$ after each sample analysis. Free 1600 kDa HA solution was systematically passed through the channel to verify the integrity of CD44-Fc receptors. The analyses were performed in triplicate using BIAcore T100 evaluation software, version 2.0.2 (GE Healthcare).

Results and discussion

In this study, siRNA-loaded lipoplexes coated with hyaluronic acid (HA) were formulated and characterized to investigate their structure and affinity to CD44 receptors, with a view to develop effective gene silencing nanomedicines targeting this receptor, a key marker of cancer metastasis. We have chosen to coat the lipoplexes with a large molecular weight HA since we have already shown that, an increased internalization of siRNA binding these HA-lipoplexes was obtained in CD44 expressing cells²⁴. siRNA HA-lipoplexes were here characterized using a combination of light-scattering technique, radioactive labeling, diameter and surface charge analyses, capillary electrophoresis, cryo-TEM microscopy, SAXS and surface plasmon resonance.

To insert HA on the lipoplex structure, a HA-DOPE conjugate was prepared by a condensation reaction between the carboxylic residues of HA and amino groups of DOPE lipids. DOPE within the conjugate was used as a lipid anchor. The absence of free DOPE on the conjugate was confirmed by thin layer chromatography, and the amount of lipids was quantified as $1.1 \pm 0.5\%$ w/w using the Stewart assay²⁸. Non-coated liposomes obtained by the ethanol injection method were of 88 ± 8 nm in size (Figure 1). The effect of HA-DOPE insertion on the diameter and zeta potential was studied by adding 0, 5, 10 and 15% (w/w) of conjugate when preparing the liposomes. A gradual increase in diameter with increasing HA-DOPE content was observed (Figure 1) indicating the insertion of HA on the liposome structure. Liposomes with 15% HA-DOPE reached diameters of 142 ± 19 nm, and higher amounts of conjugate resulted in the formation of agglomerates, probably due to bridging interaction between HA molecules on lipoplex surface. Non-coated and HA-liposomes maintained their size for at least 4 months when stored at 4°C. The absence of vesicles or micelles formed by the HA-DOPE conjugate itself was confirmed using light scattering measurements. Zeta potential values were positive in the range of +55 to +30 mV for liposome preparations due to the presence of amino groups of the cationic lipid DE,

gradually decreasing with increasing amounts of HA-DOPE conjugate, again confirming the presence of HA on the surface of the particles.

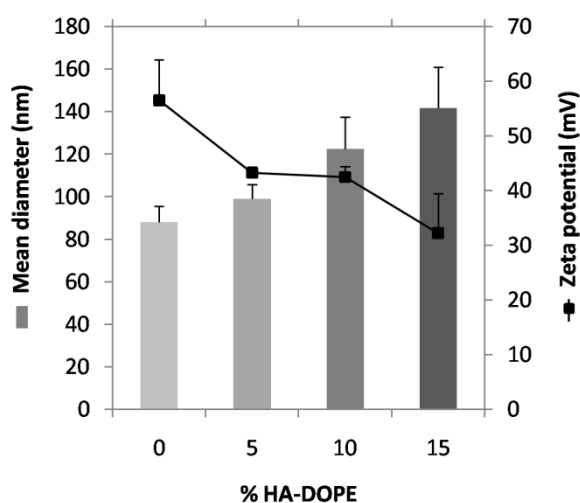


Figure 1. Mean hydrodynamic diameter and zeta potential of cationic liposomes prepared without or with 5, 10 or 15% of HA-DOPE (n=3). Data = mean \pm SD.

Ten percent of HA-DOPE was chosen for the preparation of lipoplexes. This amount was previously shown to be optimal amount for transfection of MDA-MB231 and A549 cancer cells expressing CD44^{18, 25}. Complexation of liposomes with siRNA at low concentrations (+/- ratios of 200, 100 and 50) resulted in lipoplexes with diameters comparable to those of liposomes, around 90 nm for the non-coated and 120 nm for the HA-liposomes (Figure 2).

When higher amounts of siRNA were complexed (at ratios 4, 3, 2 and 1), the diameter of non-coated and HA-liposome increased to around 140 and 230 nm, respectively (Figure 2). The size distribution in these samples was quite large. The Pdl of HA-liposomes and HA-lipoplexes was however below 0.23 for all lipoplex formulations. The zeta potential measurements of lipoplexes clearly confirmed differences in the degree of surface modification. Between ratios 200 and 50, all formulations were positively charged, with a slight reduction of the zeta potential being observed for the HA-lipoplexes, when compared to the non-coated lipoplexes (Figure 2). At lower +/- ratios, a decrease in zeta potential was observed for all lipoplexes formulations (Figure 2). The shift from positive to negative surface charges for the non-coated liposomes was observed between +/- ratios 2 and 1, which demonstrated that the neutralization of surface charges occurs when there is an equimolarity of positive and negative charges on the lipoplex structure. Interestingly, this turning point from positive to negative surface charge is shifted for the HA-lipoplexes. In this case, the amount of siRNA molecules needed to achieve neutrality is smaller, confirming the presence of the negatively charged HA

molecules on the liposome structure. The effect of dilution of HA- liposomes/lipoplexes in physiological media was studied. Both HA-liposomes and HA-lipoplexes (+/- ratio of 2) maintained their size and surface charge when diluted in 0.9% w/v NaCl and 5% w/v glucose (Figure S1). These data demonstrate previous results confirming that the HA-lipoplexes are rather stable in different medium even in the presence of serum¹⁸.

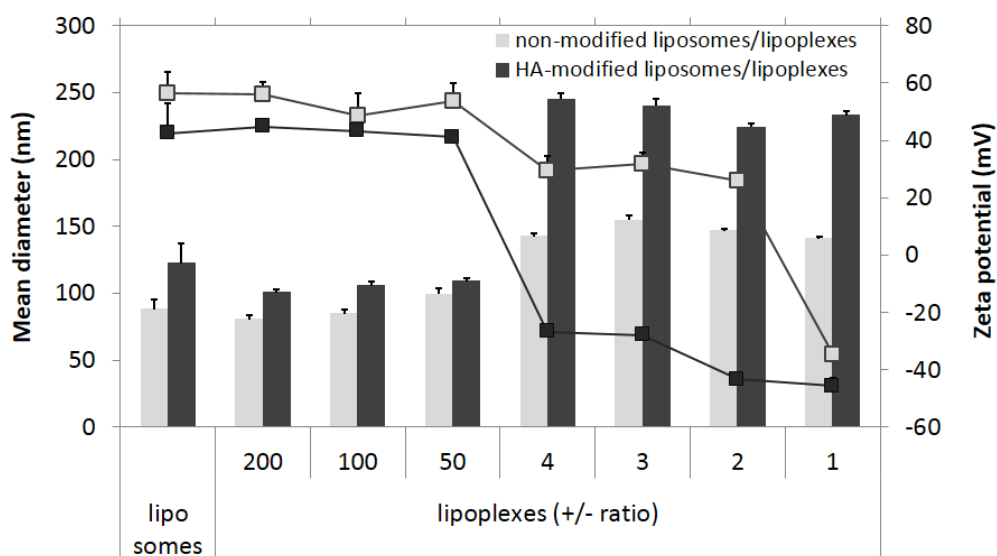


Figure 2. Mean hydrodynamic diameter (bars) and zeta potential (lines) of cationic liposomes and lipoplexes prepared without (grey) or with 10% HA-DOPE (black) at different +/- ratios (200, 100, 50, 4, 3, 2, 1). Data = mean \pm SD.

The effect of liposome modification by HA-DOPE on the association rate between liposomes and siRNA to form lipoplexes was measured after radioactive labeling of siRNA. Interestingly, the presence of HA on liposome surface did not compromise the association to the siRNA molecules (Figure 3 A and B). More than 90% of the added siRNA was bound to the liposomes for +/- ratios as low as 2 (Figure 3 A) while the amount of siRNA bound to lipoplexes increased progressively reaching approximately 300 μ g/mg of lipids (Figure 3 B). Maximum entrapment efficiency of nucleotides is commonly described for lipoplex-like structures^{29, 30, 31, 32}. The strong interactions between the negative phosphate groups on nucleotides and the positive charges of amino groups on cationic lipids leads to such high association efficiency^{33, 34, 35}. However, this binding decreased to 60-70% at a +/- ratio of 1, indicating a possible saturation of the available positively charged binding sites on the liposomes occurring between +/- ratios of 1 and 2 (Figure 3 A). Lipoplexes at +/- ratio 2 (negative zeta potential) were chosen for further experiments while in some cases and to understand lipoplex formation higher +/- ratio were used (positively charged close to the initial liposome characteristics). Non-coated liposomes and their respective lipoplexes were used for comparison.

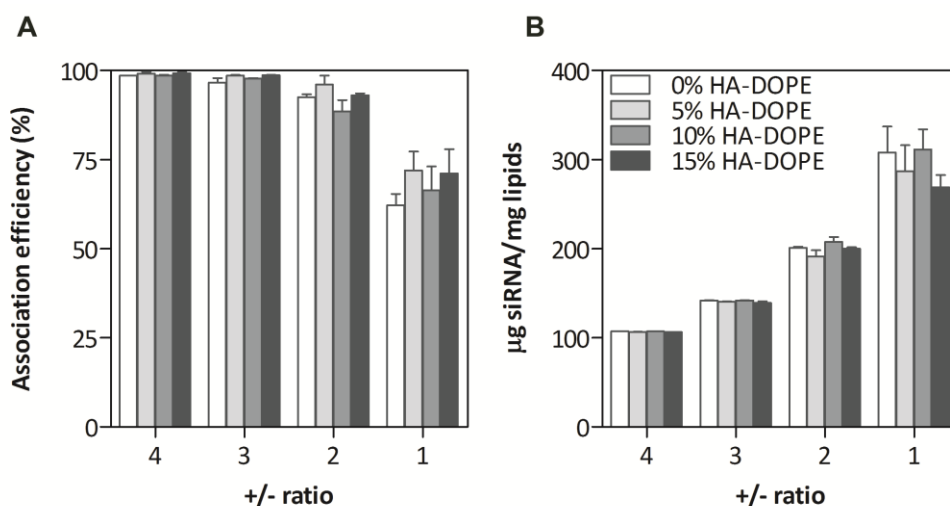


Figure 3. (A) siRNA association efficiency (%) to liposomes and (B) siRNA loading ($\mu\text{g}_{\text{siRNA}}/\text{mg}_{\text{lipids}}$) of lipoplexes as a function of the +/- ratio and the HA-DOPE content of the parent liposomes. Data = mean \pm SD.

The heat exchanged during the interaction between DE/DOPE liposomes and siRNA was analyzed by isothermal titration calorimetry. Figure 4 shows the cumulative heat curves plotted against the siRNA/DE molar ratios for each liposome type, with the raw ITC data processed and fitted to obtain the thermodynamic parameters of the interaction. A first negative enthalpy change occurs in the interaction of both non-coated and HA-liposomes with siRNA molecules. This exothermic reaction represents the interaction between DE lipid molecules and siRNA, and the fact that it occurs almost identically for both samples confirms the previous observation that the presence of HA does not prevent the interaction between siRNA and DE.

The exothermic binding of siRNA molecules to liposomes was observed until all of the binding sites in the liposomes were occupied at +/- ratio 1, corresponding to a molar ratio of siRNA/DE of 0.025, as evidenced by radioactivity measurements. The monotonous decrease of the amount of heat produced after each injection suggested that there is only one type of binding site in the liposomes³⁶. These observations are in agreement with reports from the literature on thermodynamic studies of DNA lipoplexes containing DOPE in their composition^{37, 19, 39}. They are related to the fact that DOPE amine groups ($\text{p}K_a = 9.5$) are unprotonated before binding due to the high surface pH usually measured in cationic liposomes (around 11) whereas proton uptake occurs upon lipoplex formation³⁹. Since DOPE protonation is an exothermic process, it is suggested, as shown in DOTAP:DOPE-containing lipoplex³⁷, that changes in the protonation state of DOPE account for the exothermic nature of complex formation with these lipids.

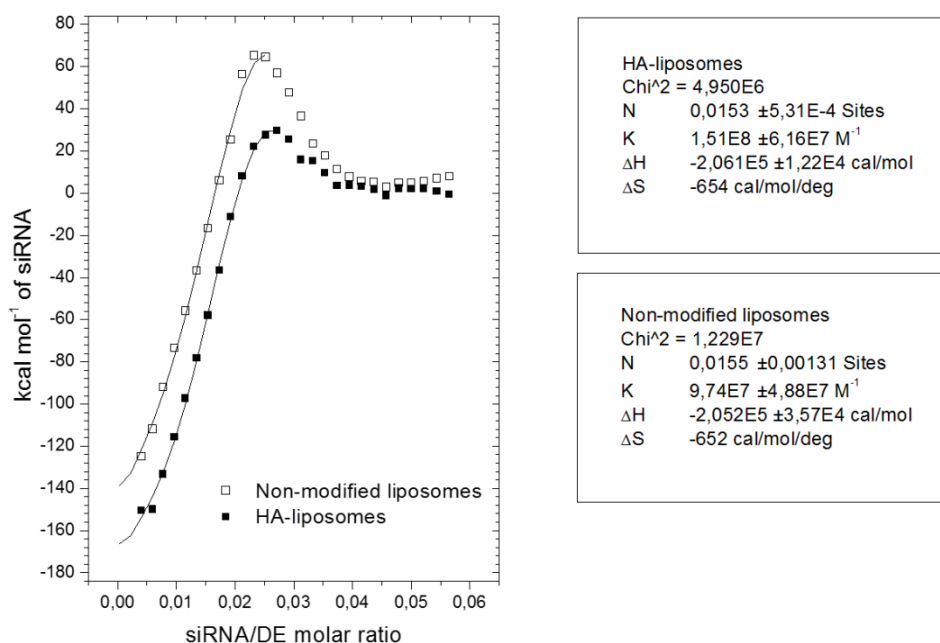


Figure 4. Cumulative heat curves and thermodynamic parameters obtained from calorimetric titration of siRNA solution at 19.7 μM (10 μl /injection) into non-coated or HA-liposomes suspension at 98 μM .

Assessment of the HA-DOPE conjugate purity and determination of the HA-DOPE fraction bound to liposomes and lipoplexes were carried out by capillary electrophoresis. HA-DOPE migration time was 5 min and the electrophoretic profile of the conjugate did not display the characteristic peak of unconjugated HA expected at 8 min, demonstrating the absence of free HA in the conjugate (Figure S2). Large amounts of the HA-DOPE conjugate added to the formulations were found associated to the liposomes and lipoplexes +/- ratio 134 (66 and 78%, respectively) (Table 1). A decrease of HA-conjugate associated to lipoplexes at +/- ratio 2, reaching 36% was observed (Table 1). A similar phenomenon was previously observed for lipoplexes prepared using plasmid DNA¹⁸. As discussed above, the association of nucleotide molecules to cationic lipids is known to be strong, and commonly yields stable lipoplexes with high association efficiencies^{33, 40}. We hypothesized that the large and concentrated amount of negative charges on the siRNA molecules leads to a competition with the negative charges of HA for interaction with the positive charges of cationic lipids, causing some displacement of HA-DOPE conjugate molecules from the liposome structure. This implies that HA-DOPE insertion in the lipoplexes does not only occur through the DOPE moiety but also via electrostatic interactions.

Table 1. HA-DOPE conjugate association efficiency to liposomes and lipoplexes prepared at +/- ratios 134 and 2.

Preparation	% HA-DOPE associated
Liposomes DE:DOPE:DOPE-HA	66.5 ± 3.9
Lipoplexes DE:DOPE:DOPE-HA:siRNA (+/- 134)	78.8 ± 9.8
Lipoplexes DE:DOPE:DOPE-HA:siRNA (+/- 2)	36.3 ± 3.9

Cryo-TEM images of cationic liposomes revealed the coexistence of spherical unilamellar and oligolamellar vesicles (Figure 5). The diameters observed were in the range of the hydrodynamic diameters measured, with some degree of heterogeneity correlated to a measured polydispersity index of 0.22. A modification of this morphology was observed after addition of siRNA to liposomes. At a +/- ratio of 134, lipoplexes shape was less spherical and homogeneous than the liposomes (Figure 5A and B). At a +/- ratio of 2, the structural changes were even more pronounced (Figure 5C). All liposomes/lipoplexes appeared as dense multilamellar structures, suggesting a reorganization of lipids in presence of siRNA. In particular, the intralamellar distances appeared smaller than those observed on the parent oligolamellar liposomes. These observed lipoplexes can be compared to the well-known “sandwich” structures^{41, 42, 43, 29}, suggesting the presence of electron-dense siRNA molecules intercalated between the cationic lipidic membranes⁶. The deformation and rearrangement of the liposomal membranes are a result of the strong electrostatic interaction between cationic lipid head groups and siRNA phosphate groups^{43, 29}. This structural modification is beneficial as far as siRNA stability is concerned. Indeed, the bilayer packing around each other promotes the protection of the siRNA molecules from degradation better than an exclusive surface-association, in which they would be more susceptible to degradation by serum nucleases^{29, 45}.

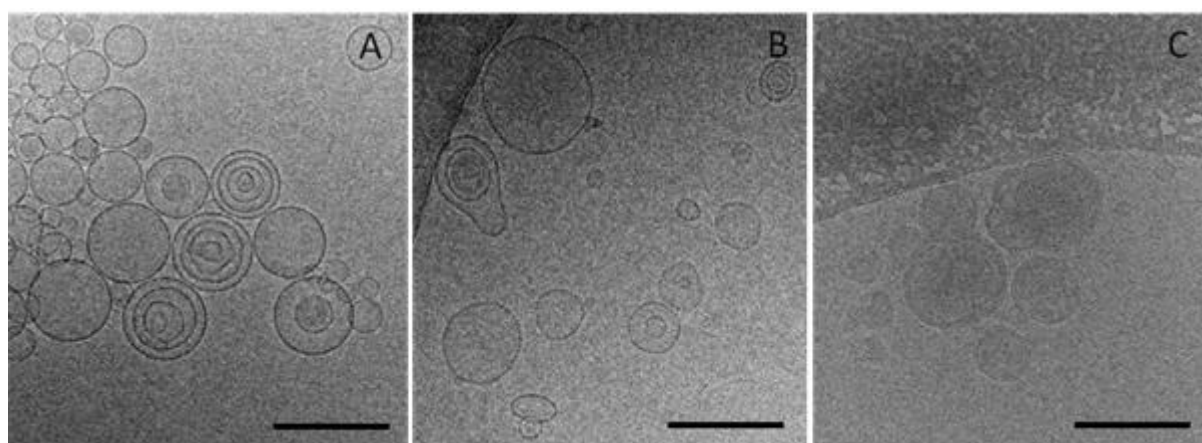


Figure 5. Cryo-TEM images of HA-modified (A) liposomes, (B) lipoplexes at a +/- ratio of 134 and (C) lipoplexes at a +/- ratio of 2. Scale bars = 200 nm.

Evidences of the siRNA localization were provided by cryo-TEM analysis. When the particles were submitted to the electron beam for acquisition of images, the formation of “bubbles” was observed (Figure 6). Micrographs were recorded at approximately 3 electrons/Å² per exposure, with intervals of 10 s between exposures. Bubbling started on the second exposure with the appearance of several small bubbles, which merge to give fewer and larger ones later in the exposure sequence. This occurred for all of the +/- 2 lipoplexes, a few of the +/- 134 lipoplexes and none on the liposomes structures, indicating that this event occurred only when siRNA was present. The pattern of the bubbles formation inside the vesicles is shown in Figure 6. We hypothesize that bubbling is due to the degradation of water molecules associated to the siRNAs, since the pattern of the bubble formation observed is characteristic of the formation of hydrogen gas upon electron radiation of samples^{46, 47}. Bubblegram imaging has been previously used for structural localization of proteins in vitrified specimens and DNA-viruses internal structure investigation^{48, 49, 50}. We report here for the first time bubble formation evidencing siRNA localization within the lipoplexes. The uniform localization of the bubbles confirms the distribution of siRNA molecules within the lipoplexes, intercalated with the lipid membranes.

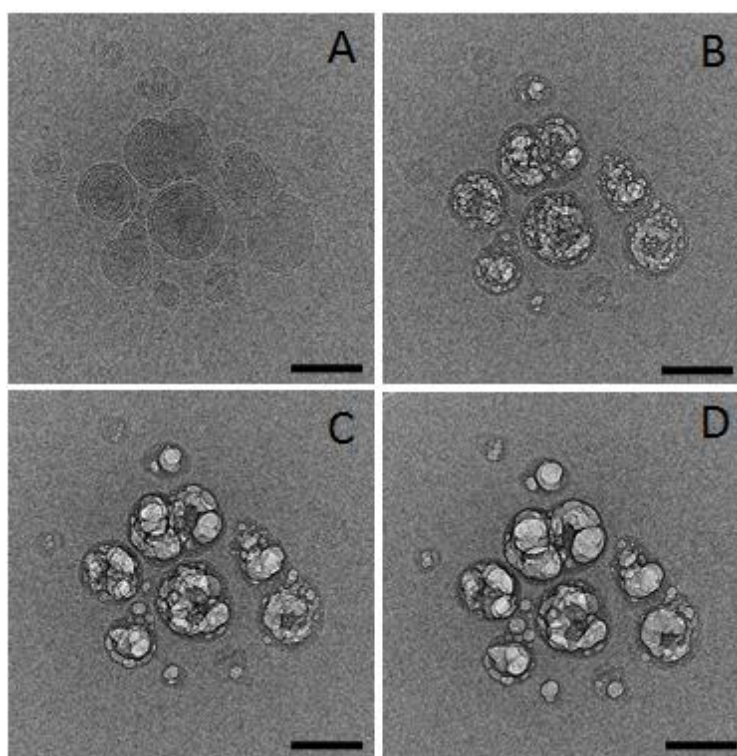


Figure 6. Cryo-TEM images of HA-modified lipoplexes at a +/- ratio of 2 after exposure to approximately (A) 3, (B) 6, (C) 9 and (D) 12 electrons/Å², evidencing the formation of bubbles where siRNA is present. Scale bars = 200 nm.

The structure of non-coated and HA-liposomes with 5, 10 and 15% HA-DOPE was further investigated using synchrotron small-angle X-ray scattering (SAXS). The pattern of the non-coated liposome suspension exhibits a broad bump, consistent with the bilayer form factor of unilamellar vesicles⁵¹ (Figure 7A).

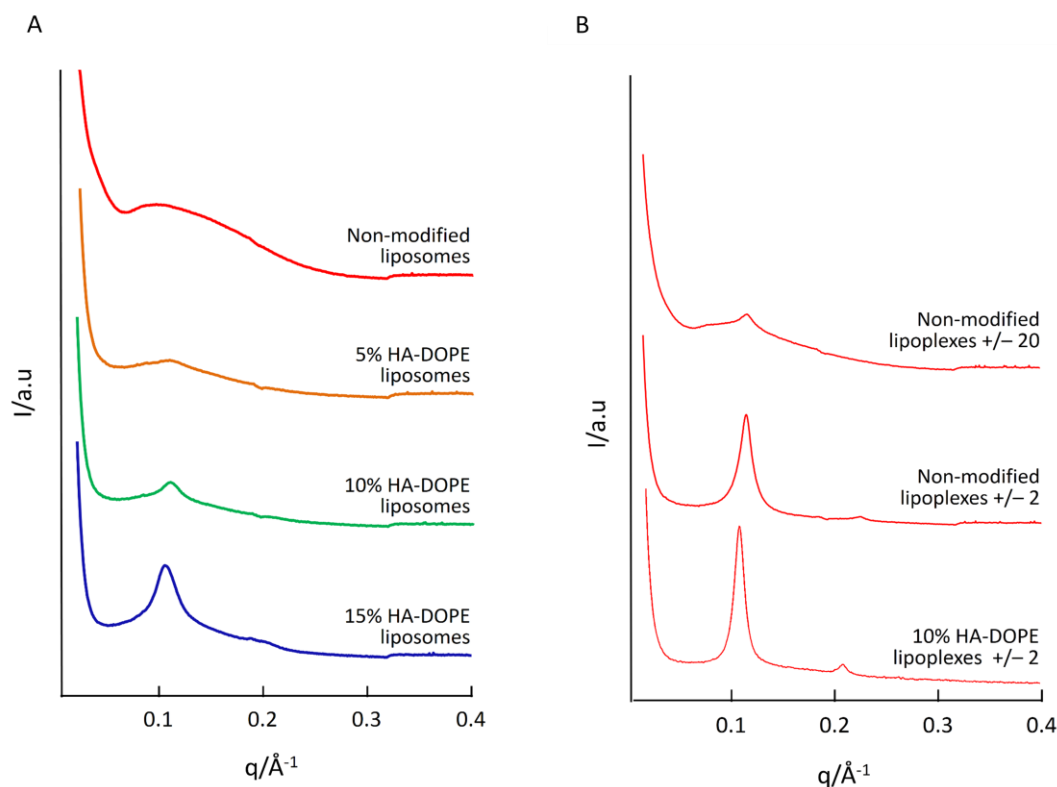


Figure 7. (A) Small-angle X-ray diffraction patterns recorded at room temperature for cationic liposomes, either non-coated or prepared with 5, 10 or 15% HA-DOPE. The gradual increase in diffraction peak intensity suggests a gradual reorganization of the unilamellar liposomes into oligolamellar structures (a.u. = arbitrary units). (B) Small-angle X-ray diffraction patterns recorded at room temperature for non-coated and HA-lipoplexes prepared at +/- ratio 2 and 20. The well-defined Bragg peaks suggest the formation of DOPE/DE-siRNA or HA-DOPE/DE-siRNA complexes, with siRNA confined between regularly stacked lipid bilayers.

The SAXS curves of HA-liposomes reveal the gradual increase of the diffraction peak intensities when increasing amounts of HA were added to the formulation, indicating the formation of increasingly dense multilamellar structures⁵². This interestingly shined a light on liposome organization in the presence of hyaluronic acid. In our method for liposome preparation, HA is present at the moment the vesicles are formed. We may therefore assume that a portion of the multiple DOPE units bound to each HA molecule intercalates within the DOPE and DE bilayers upon liposome preparation^{25, 53}. The correlation between regularly spaced bilayers gives rise to a Bragg peak. A tiny peak is barely detected

in 5% HA-DOPE liposome curve. As HA-DOPE content in the formulation increases, the intensity of the Bragg peak increases while its full width at half-maximum decreases, indicative of a higher number of bilayers in vesicles and/or of multilamellar vesicles in the preparation. However, the lack of a second-order peak until 15% of HA-DOPE suggests weakly ordered stacks of bilayers. The characteristic repeat spacing (d-spacing), corresponding to the sum of the bilayer thickness and water thickness, is deduced from the position of the Bragg peak ($d = 2\pi/q$). A small increase in d is observed, from $d = 60.4 \text{ \AA}$ ($q = 0.104 \text{ \AA}^{-1}$) to $d = 63.4 \text{ \AA}$ ($q = 0.099 \text{ \AA}^{-1}$) when the HA-DOPE amount increases from 10 to 15%, likely reflecting a higher hydration of the lamellar phase and a more important steric repulsion. The structural differences between the non-coated and HA-liposomes could be tentatively related to the differences of net surface charge between bilayers. Indeed, a net surface charge induces electrostatic repulsion between bilayers so that they can swell in excess water. The spontaneous formation of unilamellar vesicles in DOPE/DE system may be explained by electrostatic repulsion overwhelming van der Waals attraction between bilayers. Addition of HA-DOPE leads to a progressive decrease in the bilayer surface charge, and consequently in repulsive forces between bilayers, so that a multilamellar structure is formed. Furthermore, negatively charged HA could bridge positively charged lipid bilayers. As previously reported, siRNA interacts with cationic DOPE/DE liposomes. The SAXS patterns of non-coated lipoplexes evidence the reorganization of unilamellar liposomes into oligolamellar vesicles in the presence of siRNA, at low +/- ratios. Indeed, at +/- 20 ratio, only a small correlation peak appears at $q = 0.116 \text{ \AA}^{-1}$ ($d = 54.1 \text{ \AA}$), suggesting that unilamellar liposomes with siRNA adsorbed on their surface coexist with a few oligolamellar vesicles. In contrast, at +/- ratio 2 a sharp Bragg peak at $q = 0.112 \text{ \AA}^{-1}$ and a faint second order, indicative of a lamellar phase with d-spacing 56.1 \AA are observed (Figure 7B). When HA-liposomes are used for the preparation of lipoplexes (+/- 2 ratio), a sharper Bragg peak at $q = 0.102 \text{ \AA}^{-1}$ and a stronger second order are observed, reflecting a more ordered lamellar phase with d-spacing 61.4 \AA . This suggests that siRNA is confined between ordered lipid bilayers. A similar behavior was observed for HA-lipoplexes. These findings are consistent with the existing schematic models of lipoplex formation^{42, 54} and with the evolution of nanoparticle sizes upon complexation. This gradual modification of vesicle morphology after interaction between siRNA and cationic liposomes measured by SAXS was confirmed by cryo-TEM microscopy as shown above.

The binding affinity to CD44 receptors of non-coated and 10% HA-lipoplexes prepared at a +/- ratio of 2 was determined using surface plasmon resonance (SPR). CD44-Fc were immobilized in a stable and suitably oriented manner on the surface, as confirmed by an analysis of the interaction of the receptors with HA solution. HA did not show any binding when exposed to the reference surface, indicating that binding to the receptors was specific. The immobilization protocol allowed the binding of 100-150 RU, corresponding to $0.1\text{-}0.15 \text{ ng}\cdot\text{mm}^{-2}$ of CD44-Fc per channel. Sensorgrams obtained by interaction of different concentrations of HA-lipoplexes and plain lipoplexes with the CD44-Fc-

immobilized sensor chip were used to analyze the binding affinity. Representative sensorgrams obtained in this experiment are shown in Figure 8.

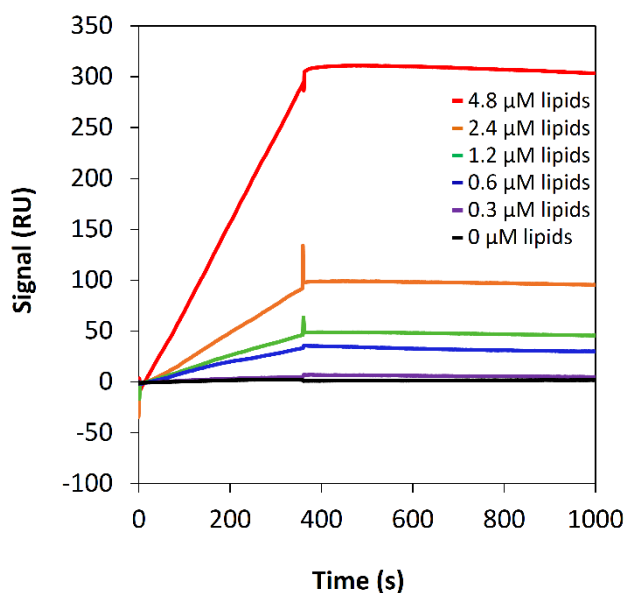


Figure 8. SPR sensorgrams obtained by injection of 10% HA-lipoplexes +/- ratio 2 on CD44-Fc-immobilized sensor chips. Samples were diluted in NaCl 150 mM to 4.8, 2.4, 1.2, 0.6 and 0.3 μM of lipids. Signals of HA-lipoplexes were normalized using signals from non-modified lipoplexes at the same concentrations, to eliminate non-specific interactions signals.

Signals of HA-lipoplexes were normalized using signals from non-modified lipoplexes at the same concentrations, to eliminate non-specific interactions signals. Considering the molecular weight of the CD44-Fc used for these experiments (48.6 kDa), we estimate that 12.3-18.5 receptors were immobilized per nm^2 . The difference between the obtained signals reveals a concentration-dependent and preferential affinity of HA-lipoplexes compared to the non-modified lipoplexes (Figure 8), thereby confirming both the suitable positioning of HA on the lipoplexes surface and HA ability to specifically bind to the CD44 receptors. The CD44-Fc immobilization combined with the surface rinsing protocol after HA interactions represent a significant improvement on the SPR techniques to analyze HA binding to CD44. First, the low sensor surface capacity was suitable for the interaction studies⁵⁵. Previously reported SPR data on HA-CD44 interaction are based on interaction studies on highly loaded sensor surfaces^{56, 57, 58}, which complicates data analysis and may misrepresent the interaction between HA and CD44⁵⁹. Second, the rinsing protocol promoted the detachment of HA-lipoplexes from the CD44-Fc surface after each analysis without damaging the receptors. This was an experimental hurdle due to the multivalent aspect of this interaction, and required many optimization steps. Little or no desorption upon rinsing high molecular weight HA molecules after interaction with its receptors have

been described until now^{60, 59}. The kinetic model that best fitted the data obtained was the “heterogeneity model” with 4 independent binding sites. Nevertheless, we believe that due to the presence of multiple binding sites on each HA, the complexity of the HA-lipoplex structure and re-binding events during dissociation, a precise kinetic characterization of the HA-lipoplexes-CD44 interaction cannot be properly resolved.

Conclusion

Lipoplexes are promising siRNA delivery systems that have been studied for gene expression inhibition. An accurate and detailed comprehension of their structure and physicochemical characteristics is crucial because of their influence *in vitro* and *in vivo* efficiency of these nanocarriers. Here, we developed and investigated in detail the structure of novel HA-lipoplexes for the delivery of siRNA. With the combination of radioactive labeling, diameter and surface charge analyses, capillary electrophoresis, cryo-TEM microscopy, SAXS and surface plasmon resonance, the influence of the components of the formulation on lipoplex morphology was determined. We demonstrated an improvement on SPR method for CD44-HA binding studies and described for the first time evidencing of siRNA localization using cryo-TEM microscopy. We provided additional information showing the interest of lipoplexes containing the HA-DOPE conjugate, which associated large amounts of siRNA, improved stability in physiological media and provided increasing affinity to CD44 receptors with increasing HA content. These outputs contribute to the improvement of the siRNA lipoplexes development and characterization methods, and give future research directions for the characterization of these nanocarriers for successful use in gene delivery.

Supporting Information

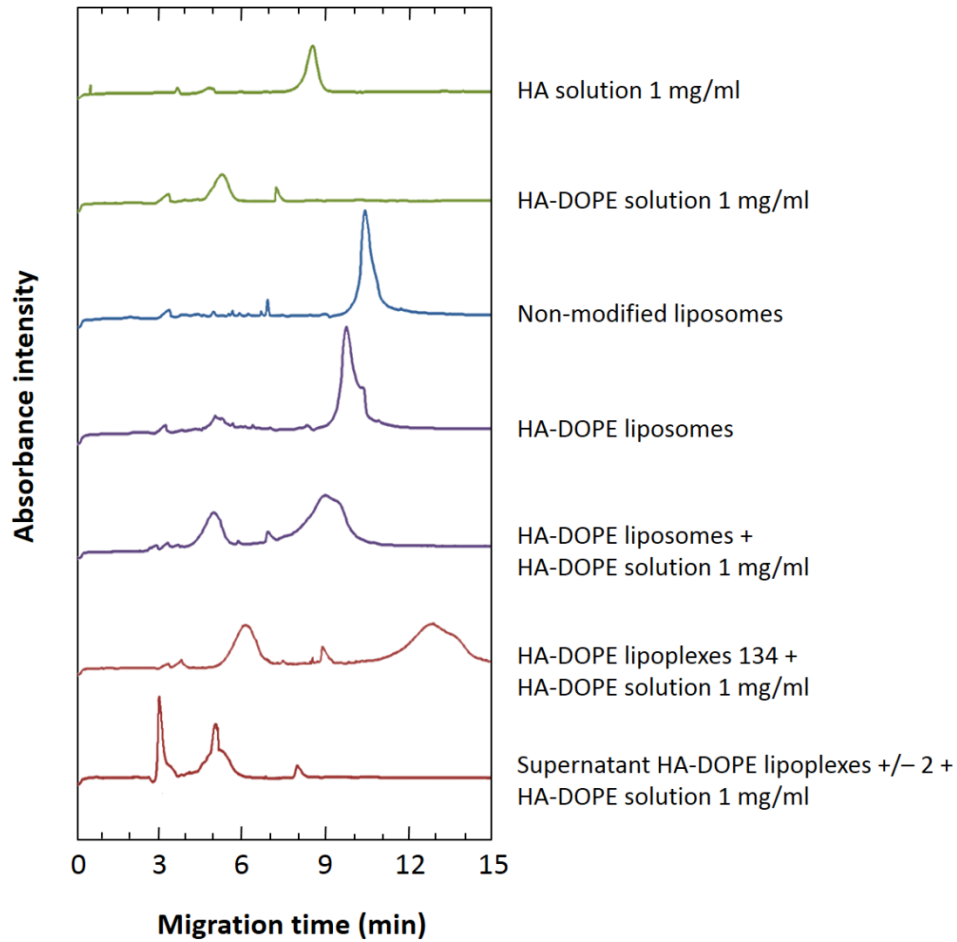


Figure 1. Electropherograms obtained by capillary electrophoresis analysis of samples containing HA or HA-DOPE at 1 mg/mL: HA solution, HA-DOPE solution, non-modified liposomes, liposomes modified with 10% HA-DOPE, liposomes modified with 10% HA-DOPE + internal standard (HA-DOPE solution 1 mg/mL), lipoplexes +/- ratio 134 modified with 10% HA-DOPE + internal standard (HA-DOPE solution 1 mg/mL) and lipoplexes modified with 10% HA-DOPE +/- ratio 2 + internal standard (HA-DOPE solution 1 mg/mL).

References

1. Nascimento, T.; Hillaireau, H.; Fattal, E. Nanoscale particles for lung delivery of siRNA. *Journal of drug delivery science and technology* **2012**, *22* (1), 99-108.
2. Soutschek, J.; Akinc, A.; Bramlage, B.; Charisse, K.; Constien, R.; Donoghue, M.; Elbashir, S.; Geick, A.; Hadwiger, P.; Harborth, J.; John, M.; Kesavan, V.; Lavine, G.; Pandey, R. K.; Racie, T.; Rajeev, K. G.; Rohl, I.; Toudjarska, I.; Wang, G.; Wuschko, S.; Bumcrot, D.; Koteliansky, V.; Limmer, S.; Manoharan, M.; Vornlocher, H. P. Therapeutic silencing of an endogenous gene by systemic administration of modified siRNAs. *Nature* **2004**, *432* (7014), 173-8.
3. Aagaard, L.; Rossi, J. J. RNAi therapeutics: Principles, prospects and challenges. *Adv Drug Deliv Rev* **2007**, *59* (2-3), 75-86.
4. Oh, Y.-K.; Park, T. G. siRNA delivery systems for cancer treatment. *Advanced Drug Delivery Reviews* **2009**, *61* (10), 850-862.
5. Barros, S. A.; Gollob, J. A. Safety profile of RNAi nanomedicines. *Advanced Drug Delivery Reviews* **2012**, *64* (15), 1730-1737.
6. Belletti, D.; Tonelli, M.; Forni, F.; Tosi, G.; Vandelli, M. A.; Ruozi, B. AFM and TEM characterization of siRNAs lipoplexes: A combinatory tools to predict the efficacy of complexation. *Colloids and Surfaces A: Physicochemical and Engineering Aspects* **2013**, *436*, 459-466.
7. Kanasty, R. L.; Whitehead, K. A.; Vegas, A. J.; Anderson, D. G. Action and Reaction: The Biological Response to siRNA and Its Delivery Vehicles. *Mol Ther* **2012**, *20* (3), 513-524.
8. Gershon, H.; Ghirlando, R.; Guttman, S. B.; Minsky, A. Mode of formation and structural features of DNA-cationic liposome complexes used for transfection. *Biochemistry* **1993**, *32* (28), 7143-7151.
9. Parvizi, P.; Jubeli, E.; Raju, L.; Khalique, N. A.; Almeer, A.; Allam, H.; Manaa, M. A.; Larsen, H.; Nicholson, D.; Pungente, M. D.; Fyles, T. M. Aspects of nonviral gene therapy: Correlation of molecular parameters with lipoplex structure and transfection efficacy in pyridinium-based cationic lipids. *International Journal of Pharmaceutics* **2014**, *461* (1–2), 145-156.
10. Putnam, D. Polymers for gene delivery across length scales. *Nat Mater* **2006**, *5* (6), 439-451.
11. Ma, B.; Zhang, S.; Jiang, H.; Zhao, B.; Lv, H. Lipoplex morphologies and their influences on transfection efficiency in gene delivery. *Journal of Controlled Release* **2007**, *123* (3), 184-194.
12. Gratton, S. E.; Ropp, P. A.; Pohlhaus, P. D.; Luft, J. C.; Madden, V. J.; Napier, M. E.; DeSimone, J. M. The effect of particle design on cellular internalization pathways. *Proceedings of the National Academy of Sciences* **2008**, *105* (33), 11613-11618.
13. Mahato, R. I. Water insoluble and soluble lipids for gene delivery. *Advanced Drug Delivery Reviews* **2005**, *57* (5), 699-712.
14. Arpicco, S.; De Rosa, G.; Fattal, E. Lipid-based nanovectors for targeting of CD44-overexpressing tumor cells. *Journal of drug delivery* **2013**, *2013*.
15. Laurent, T. C.; Fraser, J. Hyaluronan. *The FASEB Journal* **1992**, *6* (7), 2397-2404.
16. Noble, P. W. Hyaluronan and its catabolic products in tissue injury and repair. *Matrix Biol* **2002**, *21* (1), 25-9.
17. Deed, R.; Rooney, P.; Kumar, P.; Norton, J. D.; Smith, J.; Freemont, A. J.; Kumar, S. Early-response gene signalling is induced by angiogenic oligosaccharides of hyaluronan in endothelial cells. Inhibition by non-angiogenic, high-molecular-weight hyaluronan. *Int J Cancer* **1997**, *71* (2), 251-6.
18. Wojcicki, A. D.; Hillaireau, H.; Nascimento, T. L.; Arpicco, S.; Taverna, M.; Ribes, S.; Bourge, M.; Nicolas, V.; Bochot, A.; Vauthier, C. Hyaluronic Acid-Bearing Lipoplexes: Physico-Chemical Characterization And In Vitro Targeting Of The CD44 Receptor. *Journal of Controlled Release* **2012**.
19. Eliaz, R. E.; Szoka, F. C., Jr. Liposome-encapsulated doxorubicin targeted to CD44: a strategy to kill CD44-overexpressing tumor cells. *Cancer Res* **2001**, *61* (6), 2592-601.

20. Peer, D.; Florentin, A.; Margalit, R. Hyaluronan is a key component in cryoprotection and formulation of targeted unilamellar liposomes. *Biochimica et Biophysica Acta (BBA) - Biomembranes* **2003**, *1612* (1), 76-82.
21. Peer, D.; Margalit, R. Loading mitomycin C inside long circulating hyaluronan targeted nanoparticles increases its antitumor activity in three mice tumor models. *Int J Cancer* **2004**, *108* (5), 780-9.
22. Qhattal, H. S. S.; Liu, X. Characterization of CD44-Mediated Cancer Cell Uptake and Intracellular Distribution of Hyaluronan-Grafted Liposomes. *Molecular Pharmaceutics* **2011**, *8* (4), 1233-1246.
23. Arpicco, S.; Canevari, S.; Ceruti, M.; Galmozzi, E.; Rocco, F.; Cattel, L. Synthesis, characterization and transfection activity of new saturated and unsaturated cationic lipids. *Farmaco* **2004**, *59* (11), 869-78.
24. Taetz, S.; Bochot, A.; Surace, C.; Arpicco, S.; Renoir, J. M.; Schaefer, U. F.; Marsaud, V.; Kerdine-Roemer, S.; Lehr, C. M.; Fattal, E. Hyaluronic Acid-Modified DOTAP/DOPE Liposomes for the Targeted Delivery of Anti-Telomerase siRNA to CD44-Expressing Lung Cancer Cells. *Oligonucleotides* **2009**, *19* (2), 103-115.
25. Surace, C.; Arpicco, S.; Dufay-Wojcicki, A.; Marsaud, V.; Bouclier, C.; Clay, D.; Cattel, L.; Renoir, J. M.; Fattal, E. Lipoplexes Targeting the CD44 Hyaluronic Acid Receptor for Efficient Transfection of Breast Cancer Cells. *Molecular Pharmaceutics* **2009**, *6* (4), 1062-1073.
26. Batzri, S.; Korn, E. D. Single bilayer liposomes prepared without sonication. *Biochim. Biophys. Acta* **1973**, *298*, 1015-1019.
27. Grimshaw, J.; Trocha-Grimshaw, J.; Fisher, W.; Rice, A.; Smith, S.; Spedding, P.; Duffy, J.; Mollan, R. Quantitative analysis of hyaluronan in human synovial fluid using capillary electrophoresis. *Electrophoresis* **1996**, *17* (2), 396-400.
28. Stewart, J. C. M. COLORIMETRIC DETERMINATION OF PHOSPHOLIPIDS WITH AMMONIUM FERROTHIOCYANATE. *Analytical biochemistry* **1980**, *104* (1), 10-14.
29. Li, W.; Szoka Jr, F. C. Lipid-based nanoparticles for nucleic acid delivery. *Pharmaceutical Research* **2007**, *24* (3), 438-449.
30. Kesharwani, P.; Gajbhiye, V.; Jain, N. K. A review of nanocarriers for the delivery of small interfering RNA. *Biomaterials* **2012**, *33* (29), 7138-7150.
31. Wu, S. Y.; Putral, L. N.; Liang, M.; Chang, H.-I.; Davies, N. M.; McMillan, N. A. Development of a novel method for formulating stable siRNA-loaded lipid particles for in vivo use. *Pharmaceutical Research* **2009**, *26* (3), 512-522.
32. Kapoor, M.; Burgess, D. J. Efficient and safe delivery of siRNA using anionic lipids: formulation optimization studies. *International Journal of Pharmaceutics* **2012**, *432* (1), 80-90.
33. Lu, H.-D.; Zhao, H.-Q.; Wang, K.; Lv, L.-L. Novel hyaluronic acid-chitosan nanoparticles as non-viral gene delivery vectors targeting osteoarthritis. *International Journal of Pharmaceutics* **2011**, *420* (2), 358-365.
34. Kim, A. J.; Boylan, N. J.; Suk, J. S.; Lai, S. K.; Hanes, J. Non-degradative intracellular trafficking of highly compacted polymeric DNA nanoparticles. *Journal of Controlled Release* **2012**, *158* (1), 102-107.
35. Landesman-Milo, D.; Goldsmith, M.; Leviatan Ben-Arye, S.; Witenberg, B.; Brown, E.; Leibovitch, S.; Azriel, S.; Tabak, S.; Morad, V.; Peer, D. Hyaluronan grafted lipid-based nanoparticles as RNAi carriers for cancer cells. *Cancer Letters* **2013**, *334* (2), 221-227.
36. Ikonen, M.; Murtomäki, L.; Kontturi, K. Microcalorimetric and zeta potential study on binding of drugs on liposomes. *Colloids and Surfaces B: Biointerfaces* **2010**, *78* (2), 275-282.
37. Pozharski, E.; MacDonald, R. C. Thermodynamics of Cationic Lipid-DNA Complex Formation as Studied by Isothermal Titration Calorimetry. *Biophysical Journal* **2002**, *83* (1), 556-565.
39. Lobo, B. A.; Koe, G. S.; Koe, J. G.; Middaugh, C. R. Thermodynamic analysis of binding and protonation in DOTAP/DOPE (1 : 1): DNA complexes using isothermal titration calorimetry. *Biophysical chemistry* **2003**, *104* (1), 67-78.

40. De Rosa, G.; De Stefano, D.; Laguardia, V.; Arpicco, S.; Simeon, V.; Carnuccio, R.; Fattal, E. Novel cationic liposome formulation for the delivery of an oligonucleotide decoy to NF-kappaB into activated macrophages. *Eur J Pharm Biopharm* **2008**, *70* (1), 7-18.
41. Gustafsson, J.; Arvidson, G.; Karlsson, G.; Almgren, M. Complexes between cationic liposomes and DNA visualized by cryo-TEM. *Biochimica et Biophysica Acta (BBA)-Biomembranes* **1995**, *1235* (2), 305-312.
42. Huebner, S.; Battersby, B. J.; Grimm, R.; Cevc, G. Lipid-DNA complex formation: reorganization and rupture of lipid vesicles in the presence of DNA as observed by cryoelectron microscopy. *Biophys J* **1999**, *76* (6), 3158-66.
43. Xu, Y.; Hui, S.-W.; Frederik, P.; Szoka Jr, F. C. Physicochemical Characterization and Purification of Cationic Lipoplexes. *Biophysical Journal* **1999**, *77* (1), 341-353.
45. Peer, D.; Lieberman, J. Special delivery: targeted therapy with small RNAs. *Gene therapy* **2011**, *18* (12), 1127-1133.
46. Leapman, R. D.; Sun, S. Cryo-electron energy loss spectroscopy: observations on vitrified hydrated specimens and radiation damage. *Ultramicroscopy* **1995**, *59* (1), 71-79.
47. Meents, A.; Gutmann, S.; Wagner, A.; Schulze-Briese, C. Origin and temperature dependence of radiation damage in biological samples at cryogenic temperatures. *Proceedings of the National Academy of Sciences* **2010**, *107* (3), 1094-1099.
48. Black, L. W.; Thomas, J. A. Condensed genome structure. In *Viral molecular machines*; Springer, 2012, pp 469-487.
49. Wu, W.; Thomas, J. A.; Cheng, N.; Black, L. W.; Steven, A. C. Bubblegrams reveal the inner body of bacteriophage ϕ KZ. *Science* **2012**, *335* (6065), 182-182.
50. Cheng, N.; Wu, W.; Watts, N. R.; Steven, A. C. Exploiting radiation damage to map proteins in nucleoprotein complexes: The internal structure of bacteriophage T7. *Journal of structural biology* **2014**, *185* (3), 250-256.
51. Bouwstra, J. A.; Gooris, G. S.; Bras, W.; Talsma, H. SMALL-ANGLE X-RAY-SCATTERING - POSSIBILITIES AND LIMITATIONS IN CHARACTERIZATION OF VESICLES. *Chemistry and physics of lipids* **1993**, *64* (1-3), 83-98.
52. Battersby, B. J.; Grimm, R.; Huebner, S.; Cevc, G. Evidence for three-dimensional interlayer correlations in cationic lipid-DNA complexes as observed by cryo-electron microscopy. *Biochimica et Biophysica Acta (BBA)-Biomembranes* **1998**, *1372* (2), 379-383.
53. Arpicco, S.; Lerda, C.; Dalla Pozza, E.; Costanzo, C.; Tsapis, N.; Stella, B.; Donadelli, M.; Dando, I.; Fattal, E.; Cattel, L. Hyaluronic acid-coated liposomes for active targeting of gemcitabine. *European Journal of Pharmaceutics and Biopharmaceutics* **2013**, *85* (3), 373-380.
54. Weisman, S.; Hirsch-Lerner, D.; Barenholz, Y.; Talmon, Y. Nanostructure of cationic lipid-oligonucleotide complexes. *Biophysical Journal* **2004**, *87* (1), 609-614.
55. Myszka, D. G. Improving biosensor analysis. *Journal of Molecular Recognition* **1999**, *12* (5), 279-284.
56. Ogino, S.; Nishida, N.; Umemoto, R.; Suzuki, M.; Takeda, M.; Terasawa, H.; Kitayama, J.; Matsumoto, M.; Hayasaka, H.; Miyasaka, M. Two-state conformations in the hyaluronan-binding domain regulate CD44 adhesiveness under flow condition. *Structure* **2010**, *18* (5), 649-656.
57. Sebban, L. E.; Ronen, D.; Levartovsky, D.; Elkayam, O.; Caspi, D.; Aamar, S.; Amital, H.; Rubinow, A.; Golan, I.; Naor, D. The involvement of CD44 and its novel ligand galectin-8 in apoptotic regulation of autoimmune inflammation. *The Journal of Immunology* **2007**, *179* (2), 1225-1235.
58. Banerji, S.; Hide, B. R.; James, J. R.; Noble, M. E.; Jackson, D. G. Distinctive properties of the hyaluronan-binding domain in the lymphatic endothelial receptor Lyve-1 and their implications for receptor function. *Journal of Biological Chemistry* **2010**, *285* (14), 10724-10735.
59. Mizrahy, S.; Raz, S. R.; Hasgaard, M.; Liu, H.; Soffer-Tsur, N.; Cohen, K.; Dvash, R.; Landsman-Milo, D.; Bremer, M. G. E. G.; Moghimi, S. M. Hyaluronan-coated nanoparticles: The influence

- of the molecular weight on CD44-hyaluronan interactions and on the immune response. *Journal of Controlled Release* **2011**, *156* (2), 231-238.
60. Wolny, P. M.; Banerji, S.; Gounou, C.; Brisson, A. R.; Day, A. J.; Jackson, D. G.; Richter, R. P. Analysis of cd44-hyaluronan interactions in an artificial membrane system insights into the distinct binding properties of high and low molecular weight hyaluronan. *Journal of Biological Chemistry* **2010**, *285* (39), 30170-30180.

Travaux expérimentaux

**Chapitre 2 - Efficient delivery of siRNA by hyaluronic acid-modified lipoplexes
targeting CD44 receptors**

Travaux expérimentaux - Chapitre 2**Efficient delivery of siRNA by hyaluronic acid-modified lipoplexes targeting CD44 receptors****Résumé**

L'utilisation des nanovecteurs modifiés par de l'acide hyaluronique (HA) est une approche prometteuse pour les thérapies ciblant les tumeurs surexpriment des récepteurs CD44. Dans ce chapitre, nous avons examiné l'impact de la modification par l'HA sur la capacité de ciblage des lipoplexes vecteurs de siRNA. La capture cellulaire et localisation intracellulaire des lipoplexes-HA ont été évalués par cytométrie en flux et microscopie de fluorescence, et ont montré que les lipoplexes modifiés par l'HA sont internalisés plus rapidement que les lipoplexes non modifiés, et une fois dans des cellules, ils sont localisés principalement à l'intérieur des endosomes. La capacité des lipoplexes à transporter des molécules de siRNA intactes au cytoplasme a été évaluée en testant l'inhibition d'expression génique *in vitro* et *in vivo* sur la lignée cellulaire de cancer du poumon A549-luc. 81 % d'inhibition d'expression de luciférase ont été obtenus *in vitro* avec lipoplexes-HA à un ratio +/- de 2. *In vivo*, le traitement avec les lipoplexes-HA transportant un siRNA anti-luciférase a mené à une diminution statistiquement significative de l'expression de luciférase en comparaison au traitement avec du NaCl 0.9 %, ce qui a été confirmé par la réduction de l'expression d'ARNm de la luciférase dans le poumon des animaux traités avec les lipoplexes-HA. L'analyse de la distribution des lipoplexes dans les poumons a montré que les lipoplexes modifiés par l'HA sont distribués de façon plus importante et plus homogène dans le tissu pulmonaire que les lipoplexes non modifiés. Ces résultats confirment le potentiel des lipoplexes-HA dans le transport ciblé de siRNA via les récepteurs CD44.

Chapitre rédigé sous forme d'article à être soumis pour publication à Nanomedicine. Auteurs : Thais Leite Nascimento, Hervé Hillaireau, Melania Rivano, Claudine Deloménie, Delphine Courilleau, Silvia Arpicco, Justin Hanes, Elias Fattal.

Experimental work – Chapter 2

Efficient delivery of siRNA by hyaluronic acid-modified lipoplexes targeting CD44 receptors**Abstract**

The use of hyaluronic acid (HA)-modified nanocarriers is a promising approach for CD44-overexpressing tumor targeting therapies. In the present study, we investigated the impact of HA-modification on the targeting capacity of siRNA lipoplexes. Cellular uptake and intracellular localization of HA-lipoplexes were evaluated by flow cytometry and fluorescence microscopy, and showed that HA-modified lipoplexes are internalized more rapidly than non-modified ones, and once within cells, they are localized primarily in endosomes. The ability of the lipoplexes to carry intact siRNA to the cytoplasm was assessed by testing gene expression inhibition on the A549-luc lung cancer cell line in vitro and in vivo. 81% of luciferase gene expression inhibition was obtained in vitro with HA-lipoplexes at +/- ratio 2. In vivo, treatment with HA-lipoplexes carrying luc siRNA led to a statistically significant decrease of luciferase expression in comparison with treatment with 0.9% NaCl, which was confirmed by the reduction of the expression of luciferase mRNA in the lung of animals treated with HA-lipoplexes. Analysis of the lipoplexes distribution in the lungs showed that HA-modified lipoplexes are largely and more homogeneously distributed in the lung tissue after in vivo administration. These results support the role of HA-lipoplexes in CD44-targeting siRNA delivery.

Chapter written in the form of a research article to be submitted for publication to Nanomedicine. Authors: Thais Leite Nascimento, Hervé Hillaireau, Melania Rivano, Claudine Deloménie, Delphine Courilleau, Silvia Arpicco, Justin Hanes, Elias Fattal.

Introduction

Downregulation of gene expression is a promising strategy that meets different applications in therapeutics. Small interfering RNA (siRNA) molecules present the inherent advantage of nucleic acid therapies consisting in the almost unrestricted choice of targets[1]. They also offer a high efficiency and selectivity compared to other antisense strategies such as antisense DNA oligonucleotides and ribozymes[2]. SiRNA has shown potentialities for the treatment of lung diseases including the treatment of inflammatory, immune and infectious diseases, cystic fibrosis (CF) and cancer[3]. However, their clinical use, even for lung diseases, is still limited due to the same obstacles faced by other nucleotide-based therapeutics. Indeed, siRNA are rapidly degraded by nucleases showing half-lives in biological fluids of the order of seconds to minutes[4]. Moreover, siRNA lacks selectivity for the targeted tissue[1, 3, 5-7]. Within the tissues, they do not cross cell membranes readily because of their negative charge, hydrophilicity and molecular size[8, 9]. To overcome these limitations and enable siRNA delivery to their site of action, different nanocarriers systems have been investigated, including the biocompatible lipid-based liposomes, or lipoplexes.

Hyaluronic acid (HA) has been extensively used as ligand particularly to design HA-lipid-based nanoparticles targeting the CD44 receptor[16][17]. HA is a glycosaminoglycan polymer composed of disaccharide units of *N*-acetylglucosamine and D-glucuronic acid linked together through alternating β -1,3 and β -1,4 glycosidic bonds[17]. It is biocompatible, being the major component of the extracellular matrix. The native high molecular weight HA is non-toxic and non-immunogenic[18]. It does not induce expression of genes involved in proliferation or inflammation[19] and counteracts proangiogenic effects of the HA oligomers[20, 21]. At last but not least, HA can be utilized as an addressing molecule due to the expression of its membrane receptor, CD44, on tumor initiating cells[22].

It was shown that surface modification of cationic liposomes with high molecular weight HA can improve their efficacy by mediating active CD44 targeting in tumors[16, 23-28]. HA can also increase liposome circulation time due to possible dysopsonisation effects[24, 29, 30]. In our group, we have studied the HA-modification of lipoplexes by the synthesis of a HA-DOPE conjugate and its insertion in the DNA lipoplex structure[21, 31, 32]. An improved and receptor-mediated transfection efficiency of breast and lung cancer cells overexpressing CD44 receptors was reported[21, 31]. In a preliminary report, it was also shown that siRNA lipoplexes covered with hyaluronic acid could enter at a larger extent into A549 CD44⁺ cells than Calu-3 CD44⁻ cells[32].

In the present study, HA-DOPE modified cationic siRNA lipoplexes were designed using a non-commercialized cationic lipid that has demonstrated promising transfection efficiency in different cell

lines[33, 34], the [2-(2-3didodecyloxypropyl)hydroxyethyl] ammonium bromide (DE). The presence of HA on lipoplex surface, and the effects of this modification on cell internalization were evaluated. Also, the ability of the lipoplexes to carry intact siRNA to the cytoplasm was assessed by testing gene expression inhibition on the A549-luc lung cancer cell line *in vitro* and *in vivo*.

Material and methods

Materials

The cationic lipid [2-(2-3didodecyloxypropyl)hydroxyethyl] ammonium bromide (DE) was synthesized as described[33]. L-alpha-dioleoylphosphatidylethanolamine (DOPE) and phosphatidylethanolamine conjugated to rhodamine (PE-rhodamine) were purchased from Avanti Polar Lipids distributed by Sigma Aldrich (Saint Quentin Fallavier, France). High molecular weight hyaluronic acid (HA) (sodium salt, 1600 kDa, purity of 95%) was provided by Acros organics (Geel, Belgium). pGL3 luciferase (firefly) and control siRNA (19bp) were purchased from Eurogentec (Angers, France). The HA-DOPE conjugate was synthesized as described previously[31].

Liposomes and lipoplexes preparation

Liposomes of DOPE/DE at 1:1 w/w ratio were prepared in water by the ethanol injection method[32, 35]. Separate solutions of DE and DOPE were prepared in chloroform, and then mixed and evaporated to dryness under reduced pressure in a rotary evaporator. Following evaporation, the lipid films were re-dissolved in absolute ethanol at a concentration of 10 mg/mL. For liposome preparation, the ethanolic lipid solution was rapidly injected into RNase free water under magnetic stirring. HA-modified liposomes were prepared by diluting an aqueous stock solution of the HA-DOPE conjugate (1 mg/mL) to different concentrations in RNase free water before injection. The HA-DOPE content of liposomes is expressed as mass ratio of HA-DOPE to other lipids (DE + DOPE) (10% refers to 1:10 w/w). Liposome suspensions were dialyzed against MilliQ water overnight in Spectra/Por CE dialysis tubes with a molecular weight cutoff of 50kDa (Spectrum Laboratories, Breda, Netherlands) to eliminate ethanol. Lipoplexes were then prepared at charge ratios (+/- ratios) of 2 and 134 by adding one volume of the 3 mM liposome suspension into two volumes of siRNA solution at 11.05 or 0.16 μ M, respectively, in an Eppendorf tube, and gently homogenizing by pipetting up and down. Suspensions of 15 μ l – 2.5 ml of lipoplexes were usually prepared and incubated for 1 hour at room temperature before use.

Diameter and zeta potential measurement

Mean diameter and zeta potential were determined with a Zetasizer NanoZs (Malvern Instruments Ltd, Malvern, UK). Before each measurement, liposomes and lipoplexes were diluted in 1 mM NaCl. Measurements were carried out in triplicate at 25 °C on at least three independent preparations.

Lipoplexes stability in the presence of serum

Non-modified HA-liposomes and lipoplexes at +/- ratios 134 and 2 were prepared as described earlier and diluted to 66 µg/mL of lipids with cell culture medium with or without 10% serum. Samples were incubated at 37 °C and changes in mean diameter were measured at 0, 35 and 70 min. The accuracy of measurements was verified by mixing each suspension thoroughly before each measurement. Experiments were performed in triplicate.

Cell culture

A549-luc-C8 Bioware Cell Line, a luciferase-expressing cell line derived from A549 adenocarcinomic human alveolar epithelial cells, was purchased from Caliper Life Sciences (Hopkinton, USA). The cells were cultured using RPMI-1640 medium supplemented with 10% FBS, 50 units/mL penicillin and 50 units/mL streptomycin. Cells were maintained at 37°C in a humidified atmosphere with 5% CO₂. To improve homogeneity of luciferase expression and increase luminescence signals, a protocol for selection pressure was optimized. Before each experiment, cells were cultured for 12 days using the RPMI medium described previously with addition of 75 µg/ml Geneticin®G418 antibiotic (Gibco, Paisley, Scotland).

CD44 expression

A549, A549-luc and G418-selected A549-luc cells were rinsed with PBS FCS 1% and incubated 25 min at 4 °C with CD44-labeled FITC antibody (Beckman Coulter, Fullerton, USA) according to manufacturer's instructions. Cells were then washed twice in PBS-FCS 1% before being recovered in RPMI-FCS 1%. Cell suspensions were analyzed by flow cytometry (Accuri C6, BD Biosciences, Le Pont de Claix, France), and mean fluorescence intensities were collected on channel FL-2. Analyses were performed in duplicate with 10,000 cells measured in each sample. FITC mouse IgG1 antibody was used as isotype control. Results are given as a percentage of cells above fluorescence threshold.

Cell viability

Cellular mitochondrial activity was evaluated after incubation with liposomes and lipoplexes using the 3-[4,5-dimethylthiazol-2-yl]-3,5-diphenyl tetrazolium bromide (MTT) test. Cells were seeded in 96-well plates at a density of 70,000 cells/mL and allowed to adhere. After 24 h, cells were rinsed with PBS and fresh serum-free medium was added to the wells. Liposomes and lipoplexes were diluted in RPMI serum-free medium and added to the wells at various lipid concentrations (0.3-272 μ M). Six hours after incubation, serum was added to the wells at 10% v/v, and cells were incubated for 48 h. Then, 20 μ L of a 5 mg/mL MTT solution was added to each well. After 2 h of incubation at 37°C, the medium was discarded and 100 μ L of DMSO was added to lyse the cells and solubilize the formazan crystals. The absorbance was measured with a micro-plate reader at 540nm. Each liposome or lipoplex concentration was evaluated in triplicate, and the experiment was performed at least three times. Cell viability was expressed as the percentage of mitochondrial activity relative to the non-treated cells.

Lipoplexes uptake

Cells were seeded on 12-well plates at a density of 72,000 cells/mL and allowed to adhere. After 24 h, cells were rinsed with PBS, and fresh serum-free medium was added to the wells. Rhodamine-labeled liposomes and lipoplexes at +/- ratios 2 and 134 were diluted in RPMI serum-free medium and added into the wells at a final lipid concentration of 100 μ M (67 nM of siRNA for lipoplexes at +/- ratio 2 and 1 nM of siRNA for lipoplexes 134), and incubated at 37 °C. After 2, 5, 24 or 48 h, supernatants were discarded, and cells rinsed twice with PBS and harvested by 1 \times trypsin. Cell suspensions were analyzed by flow cytometry, and mean fluorescence intensities (MFI) were collected on channel FL-2. Results were expressed as the ratio of the MFI of each sample to the MFI of non-treated cells. All measurements were performed in triplicate.

Subcellular localization of lipoplexes

The intracellular trafficking of lipoplexes +/- ratios 2 and 134 was investigated on A549 cells using confocal laser scanning microscopy. A549 cells were seeded at a density of 150,000 cells/mL on coverslips and allowed to adhere at 37 °C, 5% CO₂. After 24 h, cells were rinsed with PBS and fresh serum-free medium was added to the wells. Cells were then treated with rhodamine-labeled lipoplexes at a final lipid concentration of 100 μ M. After 2 h, 6 h or 24 h of incubation, cells were rinsed with PBS and fixed by addition of 800 μ L of 4% paraformaldehyde in PBS (w/v) during 20 min. After washing with PBS, 10 μ L of Vectashield® mounting medium for fluorescence (Vector

Laboratories, Inc., Burlingame, USA) was used to prepare the slides. Fluorescence experiments were performed with a confocal laser scanning microscope LSM 510-Meta (Zeiss, Germany) using a 63×/1.4 plan-Apochromat objective lens, a helium neon laser (excitation wavelength 543 nm) and a long pass emission filter LP 560 nm. The pinhole was set at 1.0 Airy unit (0.8 µm optical slice thickness). Twelve bit numerical images were acquired with LSM 510 software version 3.2.

***In vitro* luciferase inhibition**

The ability of lipoplexes to inhibit luciferase gene expression on A549-luc cells was carried out. For that, cells were seeded on 96-well plates at a density of 30,000 cells/mL and allowed to adhere. After 24 h, cells were rinsed with PBS, and fresh serum-free medium without red phenol was added to the wells. Lipoplexes were prepared with control and anti-luciferase siRNA at +/- ratios 134 and 2, with non-modified or HA-liposomes. Lipoplexes were diluted in serum-free medium and added into the wells at a final lipid concentration of 100 µM. Six hours after incubation, serum was added to the wells at 10% v/v and cells were incubated for 48 h. Fifty microliters of BriteLite (Perkin-Elmer Life Sciences, Courtaboeuf, France), containing both lysis buffer and luciferin substrate were then added to the wells. Plates were vortexed for 3 minutes and luciferase enzyme activity was quantified using the Envision Xcite luminometer (Perkin ElmerLife Sciences, Courtaboeuf, France) at ultrasensible mode, with measurement time of 0,1 sec/well. Measurements were performed in 8 replicates for each sample of lipoplexes. Luciferase activity of untreated cells was measured simultaneously as a baseline for comparison. Controls of non-targeting siRNA lipoplexes were used to observe the effect of the formulations on luciferase activity.

Distribution of lipoplexes in mouse lung

To investigate the distribution of lipoplexes in the mouse lung, healthy CF mice (female, 6–8 weeks) were treated with a single i.v. injection of rhodamine-labeled non-modified or HA-lipoplexes containing 20 µg of siRNA. Thirty minutes later, mice were euthanized using an excess of isoflurane. Lungs were dissected and flash-frozen with liquid nitrogen in Tissue-Tek O.C.T. Compound. Transverse sections of 10 µm of thickness were obtained at various points along the length of the tissue using a Leica CM-3050-S cryostat. The sections were stained with ProLong® Gold antifade reagent with DAPI (Molecular Probes, Eugene, OR) and images were captured with an inverted epifluorescence microscope (Zeiss Axio Observer).

A549 intravenous experimental lung metastatic model

Animal studies were carried out in strict accordance to the recommendations in the Guide for the Care and Use of Laboratory Animals of the National Institutes of Health. Five-week-old female athymic nude mice (Foxn1nu) were purchased from Harlan Laboratories (Gannat, France) and maintained in specific pathogen-free conditions throughout the experiment. Animals were kept in sterile cages (maximum of four mice/cage) bedded with sterilized soft wood granulate at a 12 h light/dark cycle, and supplied with chow and autoclaved water. All manipulations were performed under a laminar flow hood. A459-luc cells at 80% confluence were harvested, washed 3 times and suspended in PBS. Mice were injected in the tail vein with 1.5 million cells suspended in 200 µl of PBS, and tumor growth in the lungs was monitored weekly by bioluminescence imaging.

Bioluminescence imaging (BLI)

Bioluminescence from luciferase expressing A549 cells (A549-luc) was measured using IVIS® Lumina Series III LT (Perkin Elmer, USA). Firefly luciferin (Perkin Elmer, USA) was injected intraperitoneally 6 minutes before imaging at a concentration of 100 mg/kg. Mice were then anesthetized using 4% isoflurane and placed on a warmed stage inside the light-tight camera box with continuous exposure to 2.5% isoflurane. Images were made from ventral and dorsal views from 6 to 15 min after luciferin injection. Data were analyzed based on total photon emission (photons/sec) in the region of interest over the thoracic space.

***In vivo* luciferase inhibition**

The *in vivo* delivery of luciferase siRNA was tested in female athymic nude mice bearing the A549-luc metastatic cancer. Bioluminescence measurements were made before treatment. Each group (8 animals) was then treated once a day for 3 days by i.v. injection of either NaCl 0.9%, luciferase-siRNA solution, HA-lipoplexes prepared with nonspecific control siRNA, HA-lipoplexes prepared with luciferase siRNA or non-modified lipoplexes prepared with luciferase siRNA. Total siRNA amount injected was 60 µg/mouse. At 24 h post treatment, bioluminescence was quantified, mice were euthanized and lungs were removed for siRNA quantification by qPCR. Efficiency of gene expression inhibition *in vivo* was quantified by the comparison of luminescence signals before and after treatment.

RNA extraction from lung tissues

The lungs from 4 siRNA lipoplex-treated and 3 vehicle-treated mice were frozen in situ with liquid nitrogen, and tissue was stored at $-80\text{ }^{\circ}\text{C}$ until used for molecular studies. The whole lung tissue from each animal was homogenized with ceramic beads in a Precellys[®]24 (Bertin, France) before extraction of total RNA using Trizol[®] RNA isolation reagent (Life Technologies, France) according to the manufacturer's instructions. RNA purity and quantity was assessed by UV measurement using a BioMate[®]3S spectrophotometer (Thermo Scientific, France). RNA integrity was evaluated by capillary electrophoresis using RNA 6000 Nano chips and the Bioanalyzer 2100 (Agilent Technologies, USA).

Quantification of luciferase mRNA expression by RT-qPCR

For quantification of mRNA expression, cDNAs were first synthesized by reverse-transcription from 1 μg of total RNA, with random hexamers and oligo-dT priming using the iSCRIPT enzyme (Bio-Rad Laboratories, USA), according to the manufacturer's instructions. PCR primer pairs specific to the target and reference genes (Table 1, Supplementary Information) were designed using Primer3Plus software. cDNA synthesized from 4 ng of total RNA was amplified in a CFX96 real time thermal cycler (Bio-Rad) using the SSoADV Univer SYBR Green Supermix (Bio-Rad) reagent, with 500 nM final concentrations of each primer, in duplicates of 10 μl reactions, by 45 two-step cycles (95 $^{\circ}\text{C}$ 5 s ; 60 $^{\circ}\text{C}$ 30 s). 'No RT' controls were amplified on all genes to verify genomic DNA contamination, and melting curve analysis was performed to assess the purity of the PCR products. PCR efficiencies, calculated for each gene from the slopes of calibration curves generated from the pool of all cDNA samples, were above 95%. GeNorm in qBase Plus tool[36] was used to select r18S, HPRT, TBP and ACTB genes as references for normalization of mRNA expression results. The normalized relative expression of target genes in samples was determined using the C_q method with correction for PCR efficiencies, where $\text{NRQ} = E_{\text{Target}}^{\Delta C_q \text{ Target}} / E_{\text{Ref}}^{\Delta C_q \text{ Ref}}$ and $\Delta C_q = C_{q \text{ sample}} - C_{q \text{ calibrator}}$ [37]. Final results were expressed as the n-fold differences in target gene expression in lipoplex-treated vs vehicle-treated mice.

Statistical analysis

Statistical analysis of data was performed by analysis of variance (ANOVA) followed by Bonferroni or Mann-Whitney's (for qPCR) tests. Differences were considered to be statistically significant at a level of $P < 0.05$.

Results

Lipoplexes preparation and stability

The mean diameter, polydispersity index (Pdl), zeta potential and amount of siRNA associated to the obtained non-modified and HA-modified liposomes and lipoplexes are reported on Table 1. Insertion of the HA-DOPE conjugate in the liposome structure caused an increase in liposome mean diameter, from 90 ± 12 nm for non-modified liposomes to 108 ± 3 nm for HA-liposomes. Surface charge of liposomes was positive, as expected due to the presence of the cationic amino groups of the DE lipid. The localization of HA moieties on liposome surface was confirmed by the reduction of the surface charge compared to the non-modified liposomes. Further decrease in the surface charge upon addition of siRNA and formation of lipoplexes confirmed the association of the densely charged siRNA molecules. When diluted in cell culture medium a difference between non-modified and HA-lipoplexes was observed (Figure 1, Supplementary Information). In the presence of serum proteins, HA-modified liposomes and lipoplexes had a lesser tendency to aggregation compared to their non-modified counterparts.

Table 1. Mean diameter, polydispersity index (Pdl), zeta potential and % of siRNA associated measurements for non-modified and HA-liposomes and lipoplexes prepared at ratios +/- 134 and 2.

Composition	Diameter (nm)	Pdl	Zeta Potential (mV)	% siRNA associated
DE:DOPE	90.4 ± 12.3	0.243 ± 0.06	57 ± 2.2	–
DE:DOPE:DOPE-HA	108.6 ± 3.1	0.216 ± 0.04	35.4 ± 0.8	–
DE:DOPE:siRNA (134)	76.43 ± 7.3	0.268 ± 0.04	46.5 ± 1.3	99.2 ± 0.7
DE:DOPE:DOPE-HA:siRNA (134)	93.4 ± 5.1	0.307 ± 0.02	30.1 ± 1.7	99.0 ± 0.4
DE:DOPE:siRNA (2)	161.7 ± 15.6	0.171 ± 0.06	28 ± 1.9	93.0 ± 0.6
DE:DOPE:DOPE-HA:siRNA (2)	233.5 ± 12.6	0.151 ± 0.03	-42.7 ± 3.4	96.0 ± 2.6

CD44 expression by A549-luc cells

The presence of CD44 receptors on the surface of A549-luc cells was evaluated by flow cytometry before and after cell selection with G418, to confirm that this selection, necessary to improve homogeneity of luciferase expression and increase luminescence signals, did not alter cellular expression of the receptor. The results show that almost 100% of the cells expressed CD44 receptors on their surface, and that the amount of receptors did not change after treatment with G418 (Table 2). Figure 1 shows representative histograms of flow cytometry analysis of CD44 in A549, A549-luc and G418-selected A549-luc cells.

Table 2. Expression of CD44 receptor on A549, A549-luc and A549-luc selected by G418 cell lines reported as RMFI (Relative Median Fluorescence Intensity) and % of analyzed cells (n = 3).

Cell line	RMFI	% of analyzed cells
A549	1081197 ± 3614	99,28%
A549-luc	1155851 ± 1945	99,86%
A549-luc sel	1089800 ± 10968	99,24%

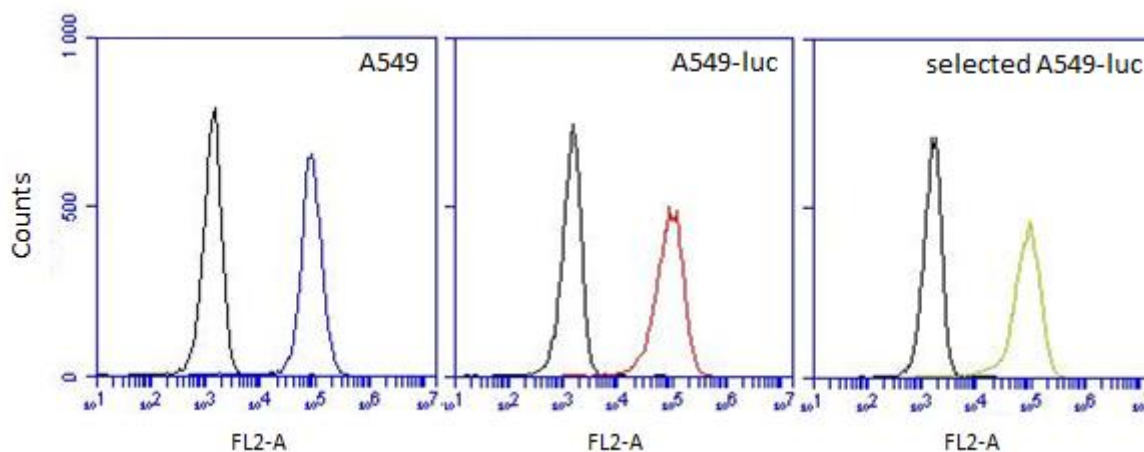


Figure 1. Flow cytometry analysis of CD44 expression on human cancer cell lines A549 (A), A549-luc (B) and A549-luc selected by G418 (C). Cells were incubated with IgG1-FITC isotype control (black) and CD44-FITC antibody (blue, red and green), and the mean fluorescence intensity (MFI) was measured.

Cytotoxicity

As a first step for in vitro experiments, a comparative cytotoxicity test was performed on A549-luc cells using non-modified and HA-modified liposomes and lipoplexes at +/- ratios of 2 and 134. Cells were incubated for 48 h with liposomes/lipoplexes formulations at concentrations ranging from 0.1 to 300 μM lipids. The results show that the modification by HA and the presence of siRNA in the samples did not alter their toxicity profiles (Figure 2). To ensure a cell viability above 80%, the lipid concentration was maintained at 10 μM for further in vitro experiments.

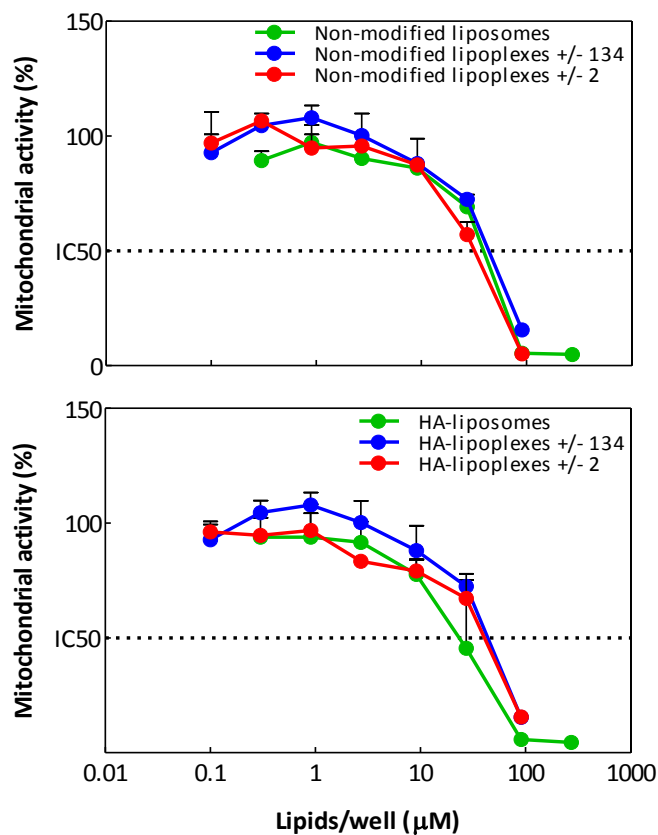


Figure 2. A549-luc mitochondrial activity as a function of lipid concentration, determined by MTT test after incubation with liposomes and lipoplexes. Cells were incubated for 48 h with non-modified and HA-liposomes and lipoplexes at +/- ratios 2 and 134, at concentrations from 0.1 to 300 μM lipids/well (n=3).

Lipoplexes uptake and intracellular distribution

The uptake of liposomes/lipoplexes by A549-luc cells was investigated using fluorescently labeled, non-modified and HA-modified liposomes and lipoplexes at +/- ratios of 134 and 2. The uptake was quantified by flow cytometry as the cell-associated fluorescence after extensive washing of the cell layer (Figure 3). A progressively increasing uptake from 2 to 48 h was observed for liposomes and lipoplexes (ratio 134). At all analyzed times, uptake of liposomes and lipoplexes ratio 134 containing the HA-DOPE conjugate was higher compared to the non-modified particles, which demonstrated a weak cellular uptake. HA-lipoplexes at a ratio of 2 were internalized more rapidly compared to all other analyzed particles. At 2 h, a plateau of the uptake of these lipoplexes was already observed, and high cellular fluorescence intensity was observed until 48 h, demonstrating the importance of HA-modification of particle surface when internalization by CD44-expressing cells is desired.

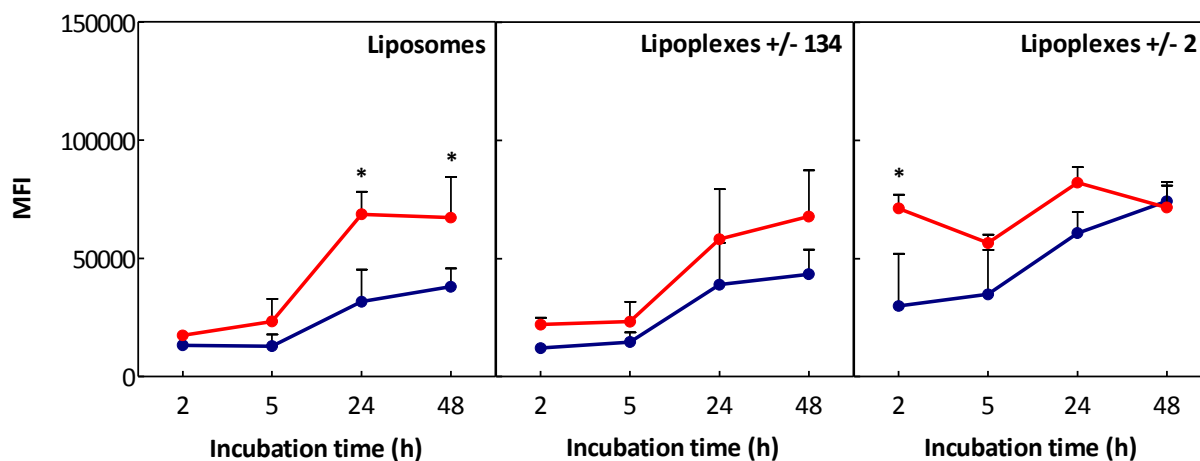


Figure 3. Uptake kinetics of rhodamine-labeled non-modified (blue) and HA-modified (red) liposomes and lipoplexes by A549-luc cells, quantified by flow cytometry as the mean fluorescence intensity (MFI). Cells were incubated for 48 h with particles at a lipid concentration of 100 μ M ($n = 3$).

The intracellular distribution of lipoplexes in A549-luc cells was assessed by confocal laser microscopy. Non-modified and HA-rhodamine-labeled lipoplexes were prepared at +/- ratios 134 and 2 with fluorescently-labeled siRNA. The diffuse fluorescence observed in ortho-images confirmed lipoplex localization in the cell cytoplasm, rather than merely bound to the cell membrane (Figure 2, Supplementary Information). Images from 2, 6 and 24 h after incubation (Figure 4) show a progressive internalization of lipoplexes, as observed by the augmentation of global lipid fluorescence from 2 to 6 h, after which the fluorescence plateaued.

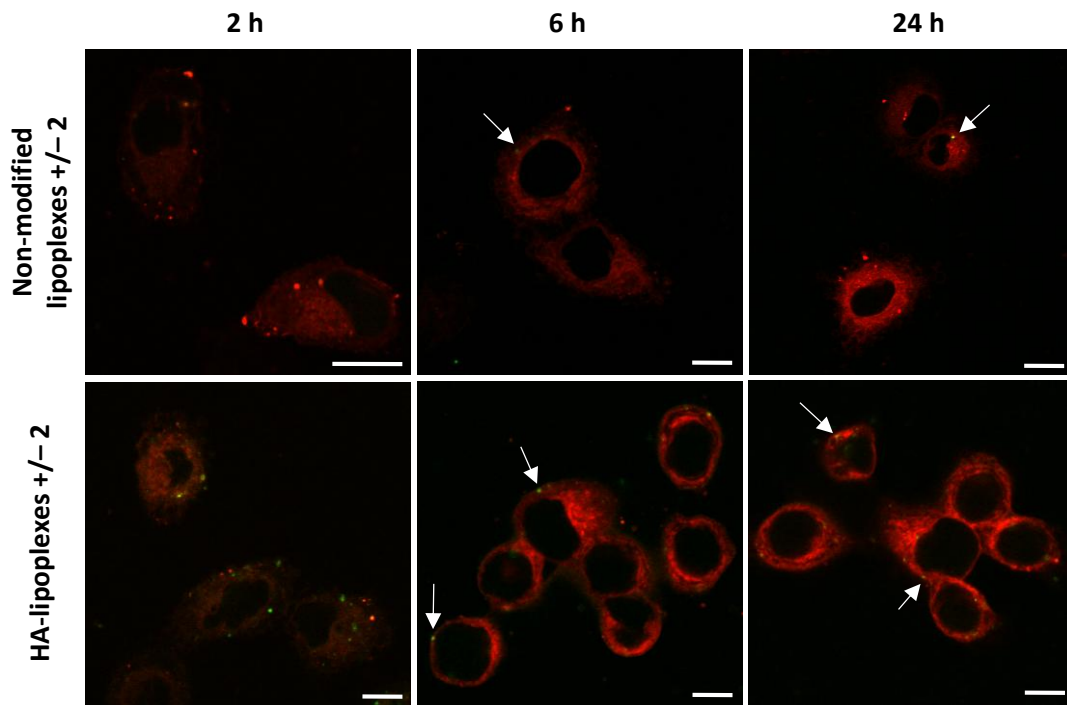


Figure 4. Localization and intracellular distribution of unmodified and HA-DOPE modified lipoplexes prepared at +/- ratio 2 with rhodamine-labeled liposomes and FAM-labeled siRNA (arrows). Confocal laser microscopy images were obtained after 2, 6 and 24 h (37 °C) incubation. Scale bars = 10 μ m.

***In vitro* luciferase gene expression inhibition**

The ability of lipoplexes to carry siRNA into the cell cytoplasm was then evaluated by measuring the inhibition of luciferase activity in A549-luc cells. Differences between non-modified and HA-DOPE lipoplexes were studied with lipoplexes at +/- ratios 134 and 2 prepared using luciferase-specific siRNA and non-specific control siRNA. The results in Figure 5 show that specific inhibition by luciferase siRNA was observed compared to control (scramble) siRNA. For a +/- ratio 134, *ca.* 63% luciferase inhibition was observed after incubation with lipoplexes modified by the HA-DOPE conjugate, compared to *ca.* 23% for the non-modified lipoplexes. The highest luciferase inhibitions were obtained with lipoplexes at +/- ratio 2, with *ca.* 70% for the non-modified and *ca.* 81% for the HA-modified vesicles.

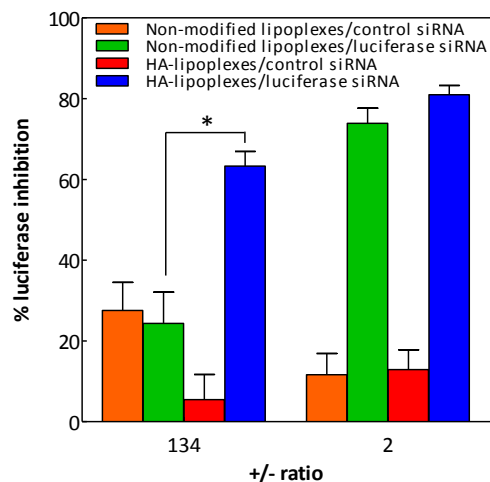


Figure 5. Luciferase expression inhibition in A549-luc cells by siRNA lipoplexes at +/- ratios 134 and 2 prepared with non-modified or HA-liposomes. Cells were incubated with lipoplexes for 48h before luminescence measurements (n=8).

Lung distribution of lipoplexes

To visualize the influence of HA surface modification of lipoplexes on their distribution in the lungs following intravenous administration to mice, fluorescently labeled lipoplexes were prepared at +/- ratio 2, HA-modified or not. After i.v. injection to CF mice, particle distribution was observed using fluorescence microscopy. Figure 6 shows representative images of the lipoplexes distribution in the lungs. A large difference in tissue distribution was observed between these two types of particles 30 min following administration. The fluorescence related to HA-lipoplexes was homogeneously distributed throughout the lungs. Meanwhile, weak fluorescence spots were observed for the non-modified lipoplexes, evidencing the sparse distribution and the formation of aggregates. This indicated that the modification of the lipoplex structure with HA promotes a better distribution in the lung tissue.

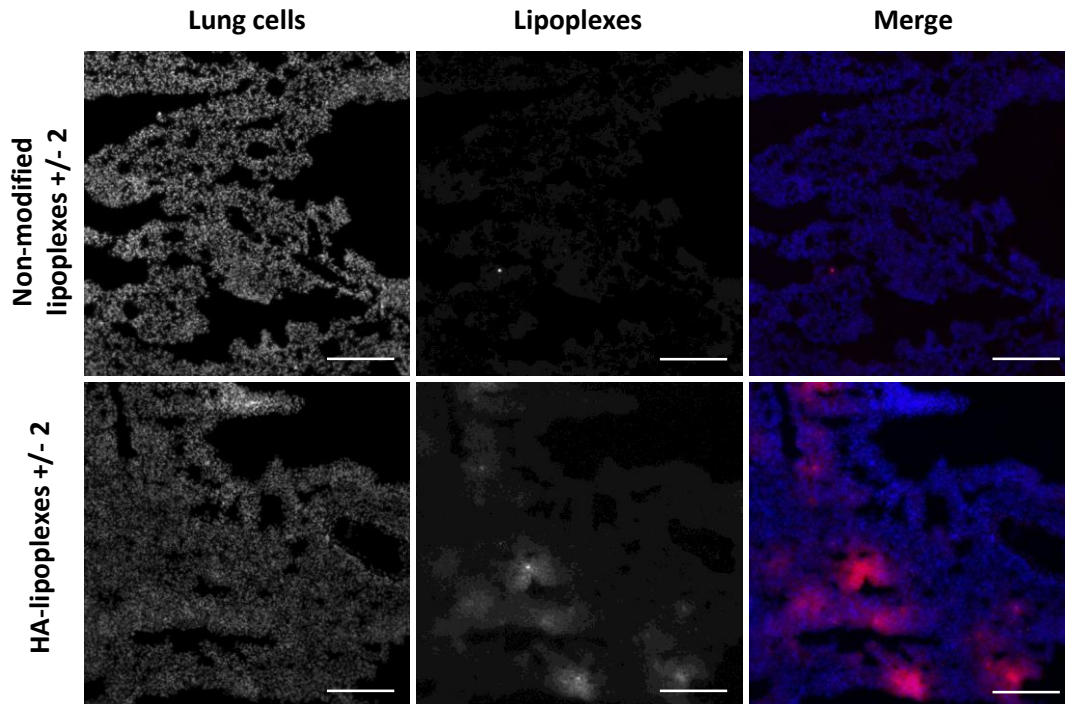


Figure 6. Representative image of the lipoplexes distribution in the lungs of mice. Pictures were taken with a 10x magnification. From left to right, first frame: image taken using the filter for DAPI staining (cells), second frame: image taken using the filter for rhodamine staining (lipoplexes), third frame: merge, showing lungs cells in blue and lipoplexes in red. Non-modified lipoplexes +/- ratio 2 and HA-lipoplexes +/- ratio 2 were administered by intravenous injection. Animals were euthanized and lungs were dissected and flash-frozen 30 minutes after treatment. Scale bars = 100 μ m.

Tumor growth and *in vivo* luciferase inhibition

To test the ability of HA-lipoplexes to silence gene expression *in vivo*, we developed a metastatic tumor model using the luciferase-expressing A549-luc cells. 1.5 million cells suspended in 200 μ L of PBS were injected in the tail vein of athymic nude mice, and tumor growth was monitored weekly by bioluminescence imaging. A steady progression of lung tumor growth was measured over the period of 40 days, which correlated to the finding of tumor nodules on the macroscopic analysis of lungs. No changes in the body weight of mice were observed throughout the study. Figure 7 shows tumor growth measured by BLI imaging, typical time-dependent ventral images of a mouse with average bioluminescence demonstrating lung colonization over time, and a representative image of lungs dissected 40 days after cell injection.

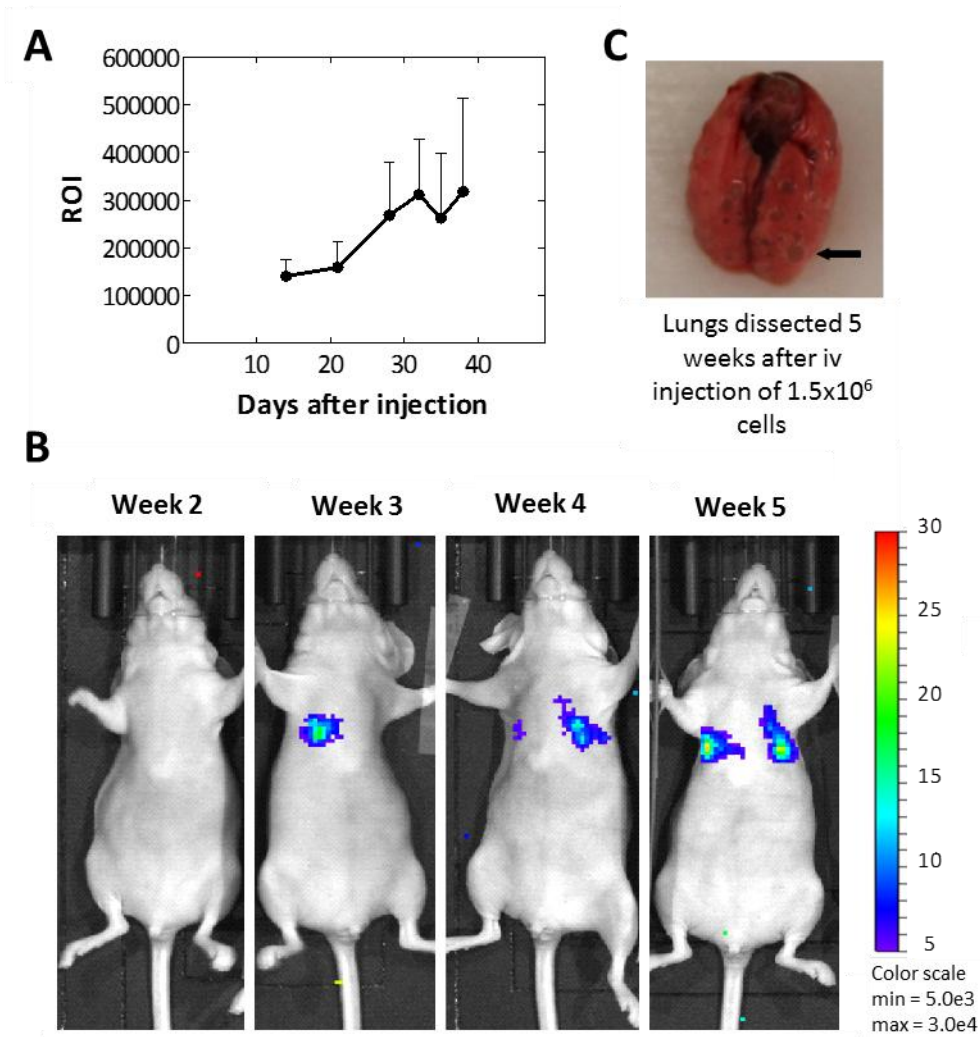


Figure 7. A. Tumor growth monitored for 40 days by BLI after intravenous injection of 1.5 million A549-luc cells in athymic nude mice (n=50). B. Representative time-dependent ventral images of a mouse with average bioluminescence demonstrating lung colonization over time. C. Representative image of a lung dissected after 40 days following intravenous injection of 1.5 million A549-luc cells. The arrow indicates the tumor metastasis.

The tumor targeting potential and the ability of lipoplex formulations to knockdown luciferase mRNA were then investigated on the developed metastatic model of human lung A549 non-small cell lung carcinoma. Mice were randomized in 5 groups and treated once a day for 3 days by intravenous injections of either NaCl 0.9%, luciferase-siRNA solution, HA-lipoplexes prepared with nonspecific control siRNA, HA-lipoplexes prepared with luciferase siRNA or non-modified lipoplexes prepared with luciferase siRNA. Tumor growth, calculated as the bioluminescence on the thoracic region after treatment relative to the bioluminescence before treatment, is shown in Figure 8. Treatment with HA-lipoplexes carrying luc siRNA led to a statistically significant decrease of luciferase expression in

comparison with controls and non-modified lipoplexes. While tumor luminescence increased to $120 \pm 13\%$ after treatment with vehicle and to $133 \pm 27\%$ after treatment with non-modified lipoplexes, it decreased to $83 \pm 27\%$ after treatment with HA-lipoplexes.

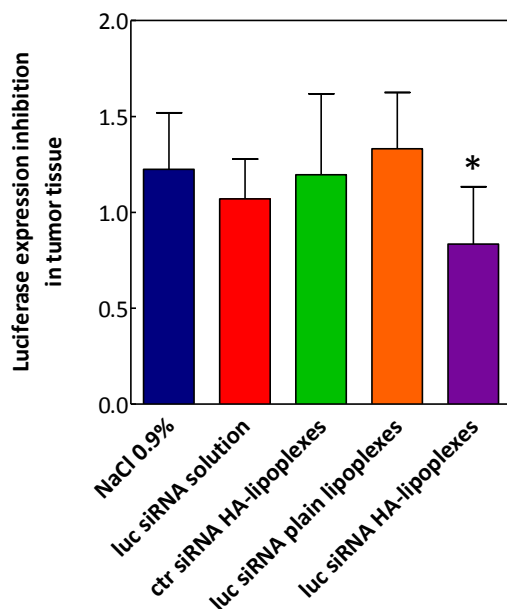


Figure 8. Luciferase expression inhibition in nude athymic mice, calculated as the bioluminescence on the thoracic region after treatment compared to the bioluminescence before treatment. Mice were inoculated intravenously with 1,5 million A549-luc cells. After 4 weeks, animals were treated once a day for 3 days by intravenous injections of NaCl 0.9%, luciferase-siRNA solution, HA-lipoplexes prepared with nonspecific control siRNA, HA-lipoplexes prepared with luciferase siRNA or non-modified lipoplexes prepared with luciferase siRNA. Data represent the mean \pm SD ($n \geq 6$). *, $P < 0.05$ versus vehicle.

Quantification of luciferase mRNA expression by RT-qPCR

The objective of the real-time PCR assays was to determine if the observed decrease in tumor luminescence could be identified as the inhibition of luciferase mRNA expression in the lung tissues. The transcriptional expression analysis showed a 54% reduction of the expression of PGL3-luc transcript in the lung of animals treated with HA-lipoplexes compared to animals treated with NaCl 0.9% (Figure 9). This result is not statistically significant ($p=0.16$) considering the number of lungs analyzed, and should be confirmed on a higher number of animals. However, combined with the results from the luminescence measurements, it confirms the inhibitory activity of siRNA lipoplexes upon the expression of PGL3-luc in our model.

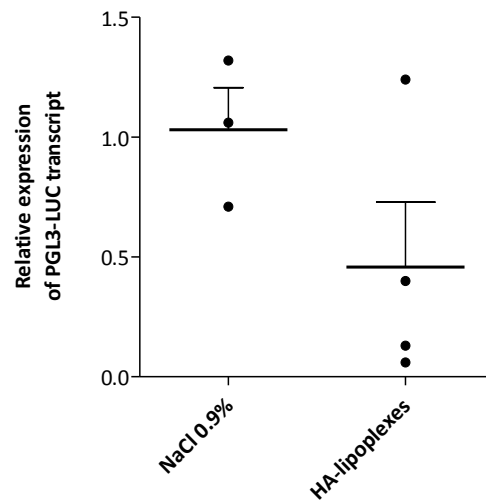


Figure 9. Relative expression of PGL3-LUC mRNA transcript in nude athymic mice, calculated using r18S, HPRT, TBP and ACTB genes as references for normalization of mRNA expression. Results are expressed as the n-fold differences in target gene expression in HA-lipoplex-treated vs NaCl 0.9%-treated mice. Data represent the mean \pm SD (n=3;4).

Discussion

The aim of this study was to characterize in vitro and in vivo the potential of HA-modified lipoplexes for the targeted delivery of siRNA to CD44-expressing A549 lung cancer cells. As we have previously observed that this amount was optimal for the transfection of MDA-MB231 and A549 cancer cells expressing CD44[21, 31], 10% (wHA/wtotal lipids) of HA-DOPE conjugate [31] was used to prepare HA-modified liposomes and lipoplexes, namely HA-liposomes and HA-lipoplexes, in which the DOPE lipid served as an anchor for the insertion of HA on the vesicle structure.

Lipoplexes showed increased diameter with the modification by the conjugate insertion and the addition of siRNA, reaching 230 nm for the HA-lipoplexes at \pm ratio 2, that presented the highest amounts of siRNA associated to the vesicles. This is frequently described for the modification of lipid vesicles with HA[39-41], since HA is a hydrophilic polymer and its placement on nanoparticle surface increases nanoparticles mean hydrodynamic diameter. The oligolamellar characteristic of the lipoplexes permitted a siRNA entrapment efficacy of $96.0 \pm 2.6\%$. HA lipoplexes were more stable than their counterparts with no HA due to a stabilization mechanism being the repulsion between negative charges of HA and serum proteins, minimizing their nonspecific interactions and causing a stabilization of the particles.

The biological activity of HA-lipoplexes was evaluated using the A549-luc human lung carcinoma cell line, which proved to be a suitable model for CD44 targeting since the totality of the cell population exhibited the CD44 membrane receptor. Measurement of cellular mitochondrial activity of cells exposed to liposomes/lipoplexes showed that the modification by HA did not change lipoplex toxicity. This biocompatibility is consistent with the ubiquitous and nontoxic characteristics of HA[39], and is in agreement with previous studies in which the modification of neutral[23, 27], negatively[39, 43] or positively charged[31] liposomes with HA revealed no apparent effect on cellular proliferation of CD44-overexpressing cells. Park and co-workers[44] even observed an increase in MDA-MB-231 cell viability from 40 to 106% after incubation with HA-liposomes for 72 h, attributed to the coating of the lipid bilayer by HA and its protection against the disruption of cellular membrane caused by the plain liposomes. Similar results were described for solid lipid nanoparticles and nanostructured lipid carriers [45] and [46], where higher cytotoxicity of non-modified particles is observed when compared with their HA-coated counterparts. This difference was explained by the presence of the cationic lipids didecyldimethyl ammonium bromide[45] and hexadecyltrimethyl ammonium bromide[46] on the surface of the nanoparticles, resulting in destruction of the cell membrane, which was prevented by coating with HA. The cytotoxicity of cationic lipids and polymers has been investigated in several studies, especially due to the increasing interest in these compounds for their ability of forming lipoplexes upon incubation with negatively charged nucleic acids[47-49]. When present on nanoparticles, these cationic compounds upon binding to the cell surface, may be recognized as a signal of danger for cells (inducing pro-apoptotic or pro-inflammatory reactions) or contribute to activate cascades that are classically activated by endogenous cationic compounds[50]. This toxicity depends though on several factors besides the particle surface charge, such as the lipid type, amount and charge[44], and its ratio in combination with helper lipids[48]. Our results suggest that the cytotoxicity profile of HA-lipoplexes is not related to the changes in particle surface charge, since cells responded similarly when incubated with all formulations, and that cytotoxicity was observed only after incubation with high concentration of vesicles.

Quantification of lipid-related fluorescence by flow cytometry showed higher internalization in A549 CD44-overexpressing cells of samples that contained the conjugate, confirming the crucial role of the receptor in the endocytosis process, as shown previously by our group and others[29, 32, 38, 51-53]. Despite that the higher fluorescence associated to the uptake of the plain lipoplexes +/- ratio 2 at 48h masked the effect of HA presence on the internalization of these lipoplexes, cell fluorescence intensity was clearly higher for HA-lipoplexes in all other time points.

After delivery into the target cells, efficient siRNA vectors must escape endosomes and release siRNA into the cytoplasm, allowing the interaction of siRNA with the endogenous RISC[55, 56]. Confocal images of cellular uptake and intracellular distribution of lipoplexes confirmed their progressive

internalization, with a plateau reached at 6 h. The diffuse cytoplasmic fluorescence observed from 6 h, as opposed to a more punctuated fluorescence consistent with the presence of endocytic vesicles containing lipoplexes at 2 h[57, 58], indicates that lipoplexes were able to escape endosomes and reach the cytosol.

The efficiency of anti-luc siRNA lipoplexes in promoting gene expression inhibition was tested *in vitro* by measuring the inhibition of the luciferase activity on A549-luc cells. The observed reduction of luciferase expression was attributed to the inhibition caused by siRNA that reached cytoplasm after being transported into the cells by the lipoplexes. More than 80% luciferase inhibition was achieved with HA-lipoplexes at +/- ratio 2 and 65% with HA-DOPE lipoplexes at +/- ratio 134. This corresponds to 67 nM and 1 nM siRNA/well, and demonstrates the high siRNA delivery efficiency of the lipoplexes. High luc-siRNA specificity was observed by luciferase inhibition after treatment with non-modified lipoplexes +/- 2. The luciferase expression inhibition of 70% compared to the cells treated with control siRNA showed that even the transport of small amounts of siRNA to the cytoplasm (as shown by uptake studies), strong luciferase inhibition can be obtained. This is in agreement with the lipoplexes uptake studies. Although higher cellular internalization was observed for all HA-modified particles until 24 h, after 48 h of incubation the preferential uptake and thus gene expression inhibition effect of the HA-lipoplexes +/- ratio 2 is masked by the continuous internalization of the non-modified oligolamellar lipoplexes +/- ratio 2. Taken together, these results confirm that CD44 receptor mediated endocytosis plays a role on the uptake of HA-lipoplexes, and that these particles are able to efficiently release siRNA within the cell cytoplasm. This is promising when *in vivo* administration is considered, where small amounts of the particle actually reach the targeted cells.

The modification of nanoparticles with HA has been explored mainly for its ability to specifically bind to various cells that overexpress CD44, a common marker for tumor initiating cells-cancer stem cells (CSC) in human carcinomas. Since a variety of cells, including breast, ovarian, colon, stomach, and lung carcinomas[59] overexpress these receptors, the formulation of HA-modified particles is a promising strategy to promote receptor-mediated cellular entry. This strategy has been proved largely efficient *in vitro*[60]. When *in vivo* activity is tested, though, results are less outstanding. Most of the currently developed nanosystems, including the actively targeted ones, exhibit a discrepancy between targetability *in vitro* and *in vivo*[61]. Long blood circulation is critical for active tumor targeting, and to reach the targeted cells after intravenous injection, nanoparticles first have to resist clearance from the circulation by the RES. This is not the case for all HA-modified nanoparticles. Even though HA has been successfully used as a hydrophilic coating and even proposed as an alternative to PEG to increase blood circulation of nanoparticles [23, 24, 43, 61], [62] exemplified that depending on the polymer length of HA and on their negative surface charge, HA-liposomes may even suffer a faster clearance. Therefore, a case-by-case analysis of the *in vivo* fate of HA-particles is necessary. To test the

hypothesis that HA-lipoplexes can transport siRNA into the cytoplasm of CD44-overexpressing cells *in vivo*, we developed a model of human lung A549 non-small cell lung carcinoma. The bioluminescence images and appearance of lung nodules confirmed lung metastasis. Lipoplexes were then administered by bolus intravenous injection, at a volume of 0.1 mL per 10 g of body weight, which is normally acceptable in human therapy. Results confirmed the advantage of HA-lipoplexes over non-modified lipoplexes on the inhibition of luciferase expression by decrease in luminescence and PGL3-LUC transcript in the tumors. Tissue analysis after administration of rhodamine-labeled HA-lipoplexes revealed diffuse fluorescence corresponding to the HA-lipoplexes in the mouse lung, which was not the case with non-modified lipoplexes. Taken together, these results indicate that our HA-lipoplexes are able to carry the siRNA molecules to the cytoplasm of CD44-overexpressing cells. These HA-modified carriers benefit from the EPR effect, as consequence of the increase in hydrophilicity and longer circulation time caused by the presence of HA on the surface of the particles, and of the CD44-targeting promoted by HA moieties[44].

Conclusion

The results presented here show the potentialities of HA-lipoplexes as siRNA carriers to CD44-overexpressing cells. Lipoplexes are stable in the presence of serum, and their structural modification with the HA-DOPE conjugate improves cellular internalization mediated by the CD44 receptor. After uptake, lipoplexes are distributed in the cytoplasm, where the carried siRNA promotes highly efficient gene expression inhibition. The HA-lipoplexes are able to transport *in vivo* a dose of intact siRNA for uptake and ultimately intracellular function, and are thus a promising tool for anticancer therapeutic gene expression inhibition.

Supplementary Information

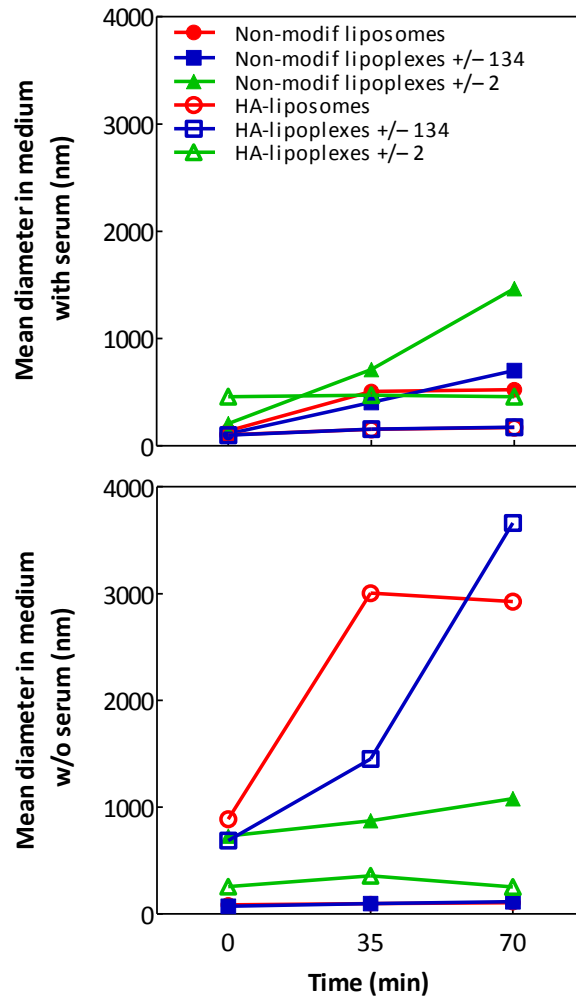


Figure 1. Colloidal stability of non-modified and HA-modified liposomes and lipoplexes at +/- ratios of 134 and 2 in cell culture medium without serum and containing 10% serum measured over 70 min by dynamic light scattering (n = 3).

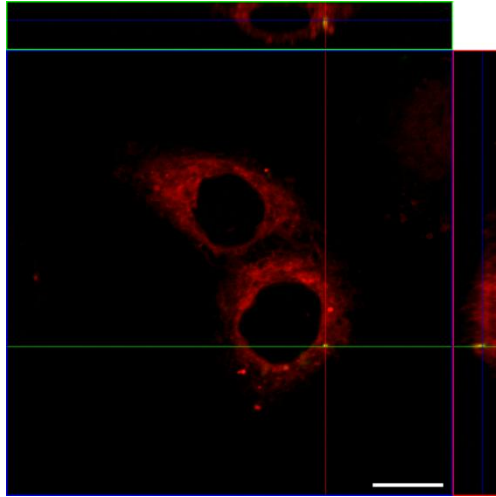


Figure 2. Confocal microscopic ortho-image of cells incubated for 6 h with HA-DOPE lipoplexes +/- ratio 2, illustrating siRNA present on the cell cytoplasm. The upper stripe shows the ortho-image along the green line and the stripe on the right shows the ortho-image along the red line. Scale bars = 10 μm .

Table 1. Primers used for qPCR.

Gene name	Accession	Primer	Sequence (5'-3')	Amplicon size (bp)
PGL3-LUC	U47296	Forward	GGAGTTGTGTTTGTGGAC	75
		Reverse	GAGGATCTCTCTGATTTTTC	
R18S	NR_003278	Forward	TCATAAGCTTGC GTTGAT	70
		Reverse	ACCATCCAATCGGTAGTAG	
ACTB	NM_007393	Forward	AGAGGGAAATCGTGCGTGAC	139
		Reverse	CAATAGTGATGACCTGGCCGT	
HPRT1	NM_013556	Forward	AGCTACTGTAATGATCAGTCAACG	200
		Reverse	AGAGGTCCTTTTCACCAGCA	
TBP	NM_013684	Forward	ACTTAGCTGGGAAGCCCAAC	129
		Reverse	ACGGACA ACTGCGTTGATTTT	

References

1. Aagaard, L. and J.J. Rossi, *RNAi therapeutics: Principles, prospects and challenges*. Adv Drug Deliv Rev, 2007. **59**(2-3): p. 75-86.
2. Bertrand, J.R., et al., *Comparison of antisense oligonucleotides and siRNAs in cell culture and in vivo*. Biochem Biophys Res Commun, 2002. **296**(4): p. 1000-4.
3. Nascimento, T.L., H. Hillaireau, and E. Fattal, *Nanoscale particles for lung delivery of siRNA*. Journal of Drug Delivery Science and Technology, 2012. **22**(1): p. 99-108.
4. Soutschek, J., et al., *Therapeutic silencing of an endogenous gene by systemic administration of modified siRNAs*. Nature, 2004. **432**(7014): p. 173-8.
5. Devi, G.R., *siRNA-based approaches in cancer therapy*. Cancer Gene Ther, 2006. **13**(9): p. 819-29.
6. Fattal, E. and A. Bochot, *State of the art and perspectives for the delivery of antisense oligonucleotides and siRNA by polymeric nanocarriers*. International journal of pharmaceutics, 2008. **364**(2): p. 237-248.
7. Fattal, E. and G. Barratt, *Nanotechnologies and controlled release systems for the delivery of antisense oligonucleotides and small interfering RNA*. British Journal of Pharmacology, 2009. **157**(2): p. 179-194.
8. Dykxhoorn, D.M. and J. Lieberman, *Knocking down disease with siRNAs*. Cell, 2006. **126**(2): p. 231-5.
9. Fattal, E., et al., *Lipoplexes Targeting the CD44 Hyaluronic Acid Receptor for Efficient Transfection of Breast Cancer Cell*. Human Gene Therapy, 2009. **20**(6): p. 682-682.
10. Kanazawa, T., et al., *Delivery of siRNA to the brain using a combination of nose-to-brain delivery and cell-penetrating peptide-modified nano-micelles*. Biomaterials, 2013. **34**(36): p. 9220-9226.
11. Jiang, G., et al., *Hyaluronic acid–polyethyleneimine conjugate for target specific intracellular delivery of siRNA*. Biopolymers, 2008. **89**(7): p. 635-642.
12. Jere, D., et al., *Poly(beta-amino ester) as a carrier for si/shRNA delivery in lung cancer cells*. Biomaterials, 2008. **29**(16): p. 2535-47.
13. Jere, D., et al., *Chitosan-graft-polyethylenimine for Akt1 siRNA delivery to lung cancer cells*. Int J Pharm, 2009. **378**(1-2): p. 194-200.
14. Andersen, M.O., et al., *Delivery of siRNA from lyophilized polymeric surfaces*. Biomaterials, 2008. **29**(4): p. 506-12.
15. Nguyen, J., et al., *Fast degrading polyesters as siRNA nano-carriers for pulmonary gene therapy*. J Control Release, 2008. **132**(3): p. 243-51.
16. Landesman-Milo, D., et al., *Hyaluronan grafted lipid-based nanoparticles as RNAi carriers for cancer cells*. Cancer Letters, 2013. **334**(2): p. 221-227.
17. Fattal, E., *Lipid-Based Nanovectors for Targeting of CD44-Overexpressing Tumor Cells*. Journal of drug delivery, 2013. **2013**.
18. Laurent, T.C. and J. Fraser, *Hyaluronan*. The FASEB Journal, 1992. **6**(7): p. 2397-2404.
19. Noble, P.W., *Hyaluronan and its catabolic products in tissue injury and repair*. Matrix Biology, 2002. **21**(1): p. 25-29.
20. Deed, R., et al., *Early-response gene signalling is induced by angiogenic oligosaccharides of hyaluronan in endothelial cells. Inhibition by non-angiogenic, high-molecular-weight hyaluronan*. Int J Cancer, 1997. **71**(2): p. 251-6.
21. Wojcicki, A.D., et al., *Hyaluronic acid-bearing lipoplexes: Physico-chemical characterization and in vitro targeting of the CD44 receptor*. Journal of Controlled Release, 2012. **162**(3): p. 545-552.
22. Al-Hajj, M., et al., *Prospective identification of tumorigenic breast cancer cells*. Proc Natl Acad Sci U S A, 2003. **100**(7): p. 3983-8.

23. Peer, D. and R. Margalit, *Loading mitomycin C inside long circulating hyaluronan targeted nano-liposomes increases its antitumor activity in three mice tumor models*. *Int J Cancer*, 2004. **108**(5): p. 780-9.
24. Peer, D. and R. Margalit, *Tumor-targeted hyaluronan nanoliposomes increase the antitumor activity of liposomal Doxorubicin in syngeneic and human xenograft mouse tumor models*. *Neoplasia*, 2004. **6**(4): p. 343-53.
25. Rivkin, I., et al., *Paclitaxel-clusters coated with hyaluronan as selective tumor-targeted nanovectors*. *Biomaterials*, 2010. **31**(27): p. 7106-7114.
26. Yang, X.-y., et al., *Hyaluronic acid-coated nanostructured lipid carriers for targeting paclitaxel to cancer*. *Cancer Letters*, 2012.
27. Glucksam-Galnoy, Y., T. Zor, and R. Margalit, *Hyaluronan-modified and regular multilamellar liposomes provide sub-cellular targeting to macrophages, without eliciting a pro-inflammatory response*. *Journal of Controlled Release*, 2012. **160**(2): p. 388-393.
28. Ruhela, D., S. Kivimäe, and F.C. Szoka, *Chemoenzymatic Synthesis of Oligohyaluronan–Lipid Conjugates*. *Bioconjugate Chemistry*, 2014. **25**(4): p. 718-723.
29. Qhattal, H.S.S. and X.L. Liu, *Characterization of CD44-Mediated Cancer Cell Uptake and Intracellular Distribution of Hyaluronan-Grafted Liposomes*. *Molecular Pharmaceutics*, 2011. **8**(4): p. 1233-1246.
30. Peer, D., A. Florentin, and R. Margalit, *Hyaluronan is a key component in cryoprotection and formulation of targeted unilamellar liposomes*. *Biochimica et Biophysica Acta (BBA) - Biomembranes*, 2003. **1612**(1): p. 76-82.
31. Surace, C., et al., *Lipoplexes Targeting the CD44 Hyaluronic Acid Receptor for Efficient Transfection of Breast Cancer Cells*. *Molecular Pharmaceutics*, 2009. **6**(4): p. 1062-1073.
32. Taetz, S., et al., *Hyaluronic Acid-Modified DOTAP/DOPE Liposomes for the Targeted Delivery of Anti-Telomerase siRNA to CD44-Expressing Lung Cancer Cells*. *Oligonucleotides*, 2009. **19**(2): p. 103-115.
33. Arpicco, S., et al., *Synthesis, characterization and transfection activity of new saturated and unsaturated cationic lipids*. *Farmaco*, 2004. **59**(11): p. 869-78.
34. De Rosa, G., et al., *Novel cationic liposome formulation for the delivery of an oligonucleotide decoy to NF-kappaB into activated macrophages*. *Eur J Pharm Biopharm*, 2008. **70**(1): p. 7-18.
35. Batzri, S. and E.D. Korn, *Single bilayer liposomes prepared without sonication*. *Biochim. Biophys. Acta*, 1973. **298**: p. 1015-1019.
36. Vandesompele, J., et al., *Accurate normalization of real-time quantitative RT-PCR data by geometric averaging of multiple internal control genes*. *Genome Biology*, 2002. **3**(7): p. 12.
37. Hellemans, J., et al., *qBase relative quantification framework and software for management and automated analysis of real-time quantitative PCR data*. *Genome Biology*, 2007. **8**(2): p. 14.
38. Wojcicki, A.D., et al., *Hyaluronic Acid-Bearing Lipoplexes: Physico-Chemical Characterization And In Vitro Targeting Of The CD44 Receptor*. *Journal of Controlled Release*, 2012.
39. Arpicco, S., et al., *Hyaluronic acid-coated liposomes for active targeting of gemcitabine*. *European Journal of Pharmaceutics and Biopharmaceutics*, 2013. **85**(3): p. 373-380.
40. Gan, L., et al., *Hyaluronan-modified core-shell liponanoparticles targeting CD44-positive retinal pigment epithelium cells via intravitreal injection*. *Biomaterials*, 2013. **34**(24): p. 5978-5987.
41. Tiantian, Y., et al., *Study on intralymphatic-targeted hyaluronic acid-modified nanoliposome: Influence of formulation factors on the lymphatic targeting*. *International Journal of Pharmaceutics*, 2014. **471**(1–2): p. 245-257.
42. Surace, C., et al., *Lipoplexes targeting the CD44 hyaluronic acid receptor for efficient transfection of breast cancer cells*. *Molecular Pharmaceutics*, 2009. **6**(4): p. 1062-1073.
43. Mizrahy, S., et al., *Hyaluronan-coated nanoparticles: the influence of the molecular weight on CD44-hyaluronan interactions and on the immune response*. *Journal of Controlled Release*, 2011. **156**(2): p. 231-238.
44. Park, J.-H., et al., *Hyaluronic acid derivative-coated nanohybrid liposomes for cancer imaging and drug delivery*. *Journal of Controlled Release*, 2014. **174**: p. 98-108.

45. Tran, T.H., et al., *Hyaluronic acid-coated solid lipid nanoparticles for targeted delivery of vorinostat to CD44 overexpressing cancer cells*. Carbohydrate Polymers, 2014. **114**: p. 407-15.
46. Yang, X.-y., et al., *Hyaluronic acid-coated nanostructured lipid carriers for targeting paclitaxel to cancer*. Cancer Letters, 2013. **334**(2): p. 338-345.
47. Lv, H., et al., *Toxicity of cationic lipids and cationic polymers in gene delivery*. Journal of Controlled Release, 2006. **114**(1): p. 100-109.
48. Morille, M., et al., *Progress in developing cationic vectors for non-viral systemic gene therapy against cancer*. Biomaterials, 2008. **29**(24–25): p. 3477-3496.
49. Zhang, S., et al., *Cationic compounds used in lipoplexes and polyplexes for gene delivery*. Journal of Controlled Release, 2004. **100**(2): p. 165-180.
50. Lonez, C., M. Vandenbranden, and J.-M. Ruyschaert, *Cationic lipids activate intracellular signaling pathways*. Advanced Drug Delivery Reviews, 2012. **64**(15): p. 1749-1758.
51. Mizrahy, S., et al., *Hyaluronan-coated nanoparticles: The influence of the molecular weight on CD44-hyaluronan interactions and on the immune response*. Journal of Controlled Release, 2011. **156**(2): p. 231-238.
52. Dalla Pozza, E., et al., *Targeting gemcitabine containing liposomes to CD44 expressing pancreatic adenocarcinoma cells causes an increase in the antitumoral activity*. Biochimica et Biophysica Acta (BBA)-Biomembranes, 2013. **1828**(5): p. 1396-1404.
53. Ganesh, S., et al., *Hyaluronic acid based self-assembling nanosystems for CD44 target mediated siRNA delivery to solid tumors*. Biomaterials, 2013.
54. Rehman, Z.u., I.S. Zuhorn, and D. Hoekstra, *How cationic lipids transfer nucleic acids into cells and across cellular membranes: Recent advances*. Journal of Controlled Release, 2013. **166**(1): p. 46-56.
55. Nascimento, T., H. Hillaireau, and E. Fattal, *Nanoscale particles for lung delivery of siRNA*. Journal of drug delivery science and technology, 2012. **22**(1): p. 99-108.
56. Oh, Y.-K. and T.G. Park, *siRNA delivery systems for cancer treatment*. Advanced Drug Delivery Reviews, 2009. **61**(10): p. 850-862.
57. Damiani, M.T., et al., *Rab coupling protein associates with phagosomes and regulates recycling from the phagosomal compartment*. Traffic, 2004. **5**(10): p. 785-797.
58. Oliveira, S., et al., *Photochemical internalization enhances silencing of epidermal growth factor receptor through improved endosomal escape of siRNA*. Biochimica et Biophysica Acta (BBA)-Biomembranes, 2007. **1768**(5): p. 1211-1217.
59. Day, A.J. and G.D. Prestwich, *Hyaluronan-binding proteins: tying up the giant*. Journal of Biological Chemistry, 2002. **277**(7): p. 4585-4588.
60. Arpicco, S., G. De Rosa, and E. Fattal, *Lipid-based nanovectors for targeting of CD44-overexpressing tumor cells*. Journal of drug delivery, 2013. **2013**.
61. Jiang, T., et al., *Dual-functional liposomes based on pH-responsive cell-penetrating peptide and hyaluronic acid for tumor-targeted anticancer drug delivery*. Biomaterials, 2012. **33**(36): p. 9246-9258.
62. Qhattal, H.S.S., et al., *Hyaluronan Polymer Length, Grafting Density, and Surface Poly(ethylene glycol) Coating Influence in Vivo Circulation and Tumor Targeting of Hyaluronan-Grafted Liposomes*. ACS Nano, 2014. **8**(6): p. 5423-5440.

Travaux expérimentaux

Chapitre 3 - Study of the diffusion in respiratory mucus, lung distribution and *in vivo* gene silencing after intrapulmonary administration of hyaluronic acid-modified siRNA cationic lipoplexes

Travaux expérimentaux - Chapitre 3

Study of the diffusion in respiratory mucus, lung distribution and *in vivo* gene silencing after intrapulmonary administration of hyaluronic acid-modified siRNA cationic lipoplexes**Résumé**

L'administration locale de composés thérapeutiques aux poumons offre la possibilité d'améliorer le traitement de maladies pulmonaires grâce à un accès instantané, de fortes concentrations locales et donc moins de risques de la toxicité. Dans ce travail, nous avons étudié la diffusion des lipoplexes-HA de siRNA dans le mucus, afin d'évaluer la faisabilité de l'administration pulmonaire fr ces particules. Des liposomes cationiques ont été préparés par la méthode d'injection d'éthanol et les lipoplexes ont été obtenus en mélangeant la dispersion de liposomes avec la solution de siRNA. Les études utilisant la technique de « multiple particle tracking (MPT) » ont montré que la présence d'HA combinée à l'ajout de siRNA ont permis l'obtention de deux formulations de lipoplexes présentant un pénétration efficace dans le mucus, les lipoplexes-HA and les lipoplexes-PEG/HA. Ces particules ont présenté des déplacements moyens quadratiques (mean squared displacement, MSD) seulement 3.5 et 2.4 fois plus petits que les particules contrôle de polystyrène, et des fractions importantes des populations ont rapidement pénétré dans le mucus respiratoire. Après administration pulmonaire chez la souris, les lipoplexes modifiées par l'HA ont été distribués de façon plus importante dans les poumons, comparé aux lipoplexes non modifiés, tandis que les lipoplexes-PEG/HA ont montré des distributions plulmonaires les plus intenses et uniformes parmi les formulations testées. L'inhibition de l'expression de luciferase après administration intrapulmonaire a aussi été testée utilisant le modèle métastatique A549-luc, mais aucun effet du traitement avec lipoplexes n'a été observé, probablement en raison de la différente localisation des cellules tumorales et des lipoplexes dans les poumons. Des études plus approfondies de l'administration locale des lipoplexes-HA et lipoplexes-PEG/HA devront être effectuées, afin de tirer profit des capacités mucopénétrantes de ces vecteurs de siRNA.

Chapitre rédigé sous forme d'article à être soumis pour publication. Auteurs : Thais Leite Nascimento, Gregg Duncan, Hervé Hillaireau, Jung Soo Suk, Justin Hanes, Elias Fattal.

Experimental work - Chapter 3**Study of the diffusion in respiratory mucus, lung distribution and *in vivo* gene silencing after intrapulmonary administration of hyaluronic acid-modified siRNA cationic lipoplexes****Abstract**

Local administration of therapeutic compounds to the lungs offers the possibility to improve the treatment of lung diseases by means of instant access, high local concentrations and therefore less risk of toxicity. In this work, we studied the mucus diffusion of hyaluronic acid (HA)-modified siRNA lipoplexes in order to evaluate the feasibility of pulmonary administration of these particles to treat lung diseases. Cationic liposomes were prepared by the ethanol injection method and lipoplexes were prepared by mixing the liposome dispersion with siRNA solution. Multiple particle tracking (MPT) technique studies showed that the presence of HA together with the addition of siRNA allowed the preparation of two efficient mucus-penetrating lipoplexes formulations, HA-lipoplexes and PEG/HA-lipoplexes. These particles presented mean squared displacements only 3.5 and 2.4-fold smaller than the mucus-penetrating polystyrene control nanoparticles, and high fractions of population that rapidly penetrated respiratory mucus. After intrapulmonary administration, HA-modified siRNA lipoplexes were largely distributed in the lungs of mice, compared to the non-modified lipoplexes, while PEG/HA-lipoplexes showed the most intense and uniform distribution of the samples analyzed. *In vivo* luciferase expression inhibition after intrapulmonary administration was also tested using an A549-luc lung metastatic model, but no effect of the treatment with lipoplexes was observed, probably due to the different localization of tumor cells and lipoplexes in the lungs. Further investigation of local administration of HA and PEG/HA-modified lipoplexes should be carried out, since these siRNA carriers showed a promising mucus penetrating ability.

The work described in this chapter was performed in collaboration with the laboratory of Prof. Justin Hanes, at the Center for Nanomedicine of the Department of Ophthalmology at the Johns Hopkins Hospital, in Baltimore, Maryland, United States. It is written in the form of a research article to be submitted for publication. Authors: Thais Leite Nascimento, Gregg Duncan, Hervé Hillaireau, Jung Soo Suk, Justin Hanes, Elias Fattal.

Introduction

Small interfering RNAs (siRNAs) are potent molecules able to block gene expression after entering cell cytoplasm. The possibility of controlling disease-associated genes makes RNA interference an attractive choice for future therapeutics against cancer, autoimmune diseases, dominant genetic disorders and viral infections [1, 2].

Administration of siRNA targeting the lungs has been studied for the down-regulation of a variety of targets including heme-oxygenase [3, 4], interleukin-5 [5], Fas [6], macrophage inflammatory protein (MIP)-2 [7] and p38 MAP kinase [8]. The utility of siRNA for treating respiratory viral infections has been also explored [9, 10]. In most of these cases, siRNA has been administered using delivery vectors including polymeric nanoparticles, liposomes and chitosan nanoparticles. For lung cancer therapy, increasing efforts have focused on the development of local administration of gene therapy because it has mainly two advantages: instant access and a high ratio of the gene deposited non-invasively within the lung [11]. Local delivery directly to the lungs could increase siRNA transport efficiency and therefore improve the treatment of lung diseases [12, 13]. Local administration offers also the advantage of achieving higher pulmonary concentrations of the therapeutic agent with a total dose considerably lower than that required for systemic administration, resulting in less risk of toxicity and adverse effects [14, 15]. Moreover, the lungs possess a great absorption surface area (100 m²), extensive vascularization, thin alveolar epithelium (0,1 – 0,2 µm) and a small air-blood exchange passage distance [16], which facilitates the local and systemic treatment of diseases.

Despite the great potential applications for targeted local delivery, siRNAs still face pharmacokinetic and cell penetration limitations. As a result of their small size, they are rapidly eliminated by the kidneys and show circulating half-lives of the order of seconds to minutes [17]. They are also susceptible to degradation by nucleases in the plasma, and tend to accumulate mainly in the liver and kidney and to a lesser extent in the heart, spleen and lungs [18]. Within the tissues, they do not cross cell membranes readily because of their negative charge, hydrophilicity and molecular size. Also, siRNAs are not taken up by most mammalian cells in a way that preserves their activity [1]. Therefore, an effective delivery system is considered almost as a prerequisite for effective siRNA-mediated gene silencing [19, 20].

The potential of hyaluronic acid (HA)-modified cationic liposomes as siRNA carriers and their targeting to CD44-overexpressing cells were explored during the PhD thesis in which this chapter is included. Cationic liposomes of L-alpha-dioleylphosphatidyl ethanolamine (DOPE) and the cationic lipid [2-(2-3-didodecyloxypropyl)hydroxyethyl] ammonium bromide (DE) [21] containing different amounts of hyaluronic acid were obtained and their interaction with siRNA, forming lipoplexes, was characterized. Specific interaction of HA-modified lipoplexes with CD44 receptors was observed using the Surface

Plasmon Resonance technique. *In vitro* studies were performed using the A549-luc lung cancer cell model, with which luciferase expression inhibition was demonstrated using an anti-luciferase specific siRNA. Preferential internalization of HA-lipoplexes was observed, as well as cytoplasm localization. Also, effective luciferase inhibition was observed on an A549 experimental lung metastatic model in mice after administration by intravenous administration of HA-modified lipoplexes.

The work presented in this chapter aimed at studying the mucus diffusion of HA and PEG-modified siRNA lipoplexes in order to evaluate the viability of administering these particles by the pulmonary route to treat lung diseases. This study was motivated by the hydrophilic and “bioinert” characteristics of high-molecular weight HA [22], and the fact that coating particles with hydrophilic polymers (e.g., PEG, pluronic) is the strategy used to develop “mucus-penetrating particles” (MPP). Interestingly, HA has been proposed as an alternative to PEG for the preparation of targeted liposomes encapsulating small molecules [23, 24] or lipoplexes [25, 26]. Cationic liposomes were prepared by the ethanol injection method and lipoplexes were prepared by mixing the liposome dispersion with siRNA solution. The diffusion of lipoplexes in mucus was studied using the multiple particle tracking (MPT) technique, and distribution of HA-modified siRNA lipoplexes in the mouse lung after pulmonary administration was analyzed. *In vivo* gene expression inhibition after intrapulmonary administration was also tested using the tumor model described in Chapter 2.

Materials and Methods

Materials

The cationic lipid [2-(2-3didodecyloxypropyl)hydroxyethyl] ammonium bromide (DE) was synthesized as described previously [21]. L- α -dioleoylphosphatidylethanolamine (DOPE), phosphatidylethanolamine conjugated to rhodamine (PE-rhodamine) and N-(carbonyl-methoxypolyethyleneglycol 2000)-1,2-dipalmitoyl-sn-glycero-3-phosphoethanolamine (DPPE-PEG2000) were purchased from Avanti Polar Lipids distributed by Sigma Aldrich (Saint Quentin Fallavier, France). High molecular weight hyaluronic acid (HA) (sodium salt, 1600 kDa, purity of 95%) was provided by Acros organics (Geel, Belgium). Control siRNA (19 bp) was purchased from Eurogentec (Angers, France). The DOPE-HA conjugate was synthesized and characterized as described previously [25].

Liposomes and lipoplexes preparation

Liposomes of DOPE/DE at 1:1 w/w ratio were prepared in water by the ethanol injection method [27, 28]. Separate solutions of DE and DOPE were prepared in chloroform, and then mixed and evaporated to dryness under reduced pressure in a rotary evaporator. Following evaporation, the lipid films were re-dissolved in absolute ethanol at a concentration of 10 mg/mL. For liposome preparation, the ethanolic lipid solution was rapidly injected into RNase free water under magnetic stirring. HA and PEG-modified liposomes were prepared by diluting an aqueous stock solution of the HA-DOPE conjugate (1 mg/mL) and PEG to different concentrations in RNase free water before injection. The HA-DOPE/PEG content of liposomes is expressed as mass ratio of HA-DOPE/PEG to other lipids (DE + DOPE) (10% refers to 1:10 w/w). Liposome suspensions were dialyzed against 1 L of MilliQ water overnight in Spectra/Por CE dialysis tubes with a molecular weight cutoff of 50kDa (Spectrum Laboratories, Breda, Netherlands) to eliminate ethanol. Fluorescent rhodamine-labeled liposomes were prepared by substituting 1% of DOPE lipid by phosphatidylethanolamine conjugated to rhodamine (PE-rhodamine) in the formulations. Lipoplexes were then prepared at different charge ratios (+/- ratios) by adding one volume of the 3 mM liposome suspension into two volumes of siRNA solution at different concentrations (0.11, 0.16, 0.22, 0.44, 5.52, 7.36, 11.05 and 22.10 μ M for +/- ratios of 200, 134, 100, 50, 4, 3, 2 and 1 respectively) in an Eppendorf tube, and gently homogenizing by pipetting up and down. Suspensions of 15 μ L – 2.5 mL of lipoplexes were usually prepared and incubated for 1 hour at room temperature before use.

Diameter and zeta potential measurement

Diameter and zeta potential were determined with a Zetasizer Nano Zs (Malvern Instruments Ltd, Malvern, UK). Before each measurement, liposomes and lipoplexes were diluted in 1 mM NaCl. Measurements were carried out in triplicate at 25 °C.

siRNA labeling with Cy3

siRNA was labeled using the Mirus Label-IT Cy3 labeling kit (Fisher Scientific) according to the manufacturer's protocol. Cy3-labeled lipoplexes were prepared by mixing 2 volumes of siRNA solution with 1 volume of liposome suspension. Lipoplexes at +/- ratios 2 and 8 were used for the experiments.

Mucus sample collection

The method used in this section was described by Schuster *et al* [29]. Human airway mucus samples were collected in accordance with a protocol approved by the Johns Hopkins Medicine Institutional Review Board (study number NA_00038606). Patients who required intubation as part of general anesthesia for elective, non-cardiothoracic surgery at the Johns Hopkins Hospital were identified. Only patients with no cardiopulmonary or respiratory comorbidities and no smoking history were included in this study. At the end of surgery, the endotracheal tube was removed from the patient, and the distal 10 cm portion, including the balloon cuff, was cut and placed in a 50 mL centrifuge tube. The specimens were then spun at 1000 rpm ($220 \times g$) for 30 s, yielding an average mucus volume of 0.5 mL. Mucus with visible blood contamination was not included in the analysis. Mucus samples were stored at 4 °C and analyzed within 24 h of collection.

Multiple particle tracking (MPT) of lipoplexes

Cy3-labeled lipoplexes were added in custom-made 30 μ L microwells to 30 μ L (3% dilution) of water or lung mucus, and equilibrated for 1 h prior to microscopy. Twenty second movies at 66.7 ms temporal resolution were acquired via Evolve 512 EMCCD camera (Photometrics, Tucson, AZ) equipped on an inverted epifluorescence microscope (Axio Observer D1, Zeiss; Thornwood, NY) with a 100 \times /1.4NA objective. Movies were analyzed with Metamorph software (Universal Imaging, Glendale, WI) to extract x, y-coordinates of lipoplexes centroids over time. Time-averaged mean square displacement (MSD) for individual gene carriers were calculated as a function of time scale(τ) [32]. Bulk transport properties were calculated by geometric ensemble-averaging of individual MSD. Exposure time of 66.7 ms was used to capture fluorescent snapshots of lipoplexes, and MSD values are presented at a time scale of 1 s [30].

Distribution of lipoplexes in mouse lung

Female CF-1 mice of 6-8 weeks (CF-1 mice, strain code 023, Charles River Laboratories, Wilmington, MA) were anesthetized using 2,2,2-tribromoethanol (Sigma-Aldrich) diluted with PBS (1:80 v/v). 600 μ L of the anesthetic were injected intraperitoneally and mice were monitored until the loss of pedal reflex. Cy3 and rhodamine-labeled liposomes and lipoplexes were then administered in the lungs using a microsyringe (PennCentury). Thirty minutes later, mice were euthanized using an excess of isoflurane. Lungs were dissected and flash-frozen with liquid nitrogen in Tissue-Tek O.C.T. Compound. Transverse sections of 10 μ m of thickness were obtained at various points along the length of the

tissue using a Leica CM-3050-S cryostat. The sections were stained with ProLong® Gold antifade reagent with DAPI (Molecular Probes, Eugene, OR) and images were captured with an inverted epifluorescence microscope (Zeiss Axio Observer). HA-liposomes, HA-lipoplexes at a +/- ratio of 2, non-modified lipoplexes at a +/- ratio of 2, PEG/HA-lipoplexes at a +/- ratio of 8, HA-lipoplexes at a +/- ratio of 2 and non-modified lipoplexes at a +/- ratio of 2 were analyzed. Each animal was treated with a single dose of lipoplexes containing 20 µg of siRNA. Lipoplexes were concentrated to final volumes of 50 µL/mouse for pulmonary administration.

A549 intravenous experimental lung metastatic model

Animal studies were carried out in strict accordance to the recommendations in the Guide for the Care and Use of Laboratory Animals of the National Institutes of Health. Five-week-old female athymic nude mice (Foxn1nu) were purchased from Harlan Laboratories (Gannat, France) and maintained in specific pathogen-free conditions throughout the experiment. Animals were kept in sterile cages (maximum of four mice/cage) bedded with sterilized soft wood granulate at a 12 h light/dark cycle, and supplied with chow and autoclaved water. All manipulations were performed under a laminar flow hood. A459-luc cells at 80% confluence were harvested, washed 3 times and suspended in PBS. Mice were injected in the tail vein with 1.5 million cells suspended in 150 µL of PBS, and tumor growth in the lungs was monitored weekly by bioluminescence imaging.

Bioluminescence imaging (BLI)

Bioluminescence from luciferase expressing A549 cells (A549luc) was measured using IVIS® Lumina Series III LT (Perkin Elmer, USA). Firefly luciferin (Perkin Elmer, USA) was injected intraperitoneally 6 minutes before imaging at a concentration of 100 mg/kg. Mice were then anesthetized using 4% isoflurane and placed on a warmed stage inside the light-tight camera box with continuous exposure to 2.5% isoflurane. Images were made from ventral and dorsal views from 6 to 15 min after luciferin injection. Data were analyzed based on total photon emission (photons/sec) in the region of interest over the thoracic space.

***In vivo* luciferase inhibition**

Mice were randomized in 5 groups of treatment with 8 animals/group. 50 µL of either NaCl 0.9%, luciferase-siRNA solution, HA-lipoplexes prepared with nonspecific control siRNA, HA-lipoplexes prepared with luciferase siRNA or non-modified lipoplexes prepared with luciferase siRNA were

administered using a microsyringe (PennCentury) once a day for 3 days. The study was double-blinded. Total siRNA amount injected was 60 µg/mouse. Tumor imaging was performed before and after the treatment.

Statistical analysis

Statistical analysis of data was performed by analysis of variance (ANOVA) followed by Bonferroni test. Differences between groups were considered to be statistically significant at a level of $P < 0.05$.

Results

Physicochemical properties of lipoplexes

To test the ability of HA-lipoplexes to move through human airway mucus, we first modified the HA-lipoplexes formulations in attempt to obtain particles that were as hydrophilic as possible with a zeta potential being the closest to neutrality. For that reason, 10% and 12% mol of DPPE-PEG were added to plain and HA-modified liposomes, and the obtained liposomes were used to prepare lipoplexes at +/- ratios of 2, 4 and 8. The particles obtained were characterized in terms of mean diameter, polydispersity index (Pdl) and zeta potential (Table 1).

Liposomes mean diameter ranged from 106 nm to 132 nm, without significant differences between the plain and HA-modified particles ($p > 0.05$). PEGylated vesicles were slightly smaller, but the diameter decrease did not depend on the amount of PEG present on the formulation. Zeta potentials changes were significant with liposome surface modification, HA-liposomes having a decreased surface charge compared to the non-modified and PEGylated cationic liposomes.

Upon addition of siRNA to prepare the lipoplexes, a gradual decrease in the surface charge with increasing concentrations of complexed siRNA molecules was observed. Moreover, surface charge of PEGylated lipoplexes was significantly reduced, indicating the shielding of the siRNA and HA negative charges by the presence of neutrally charged PEG. An 'optimized formulation', in terms of surface neutrality, was obtained when siRNA was complexed to 10% PEG/HA-lipoplexes at a +/- ratio of 8 (Table 1).

Table 1. Characterization of non-modified, HA-modified, PEG-modified and HA/PEG-modified DE:DOPE liposomes and lipoplexes in terms of particle mean diameter (nm), polydispersity index (Pdl), and zeta potential (mV).

Preparation	Mean diameter (nm)	Pdl	Zeta Potential (mV)
Liposomes			
Non-modified	132.1 ± 2.4	0.263 ± 0,009	39.7 ± 1.3
HA-modified	130.3 ± 1.9	0.113 ± 0,006	29.6 ± 1.8
10% PEG liposomes	126.8 ± 2.6	0.371 ± 0.015	45.5 ± 1.2
10% PEG HA liposomes	106.4 ± 2.4	0.431 ± 0.032	21.1 ± 3.4
12% PEG HA liposomes	120.9 ± 3.9	0.284 ± 0.005	24.5 ± 0.7
Lipoplexes			
Non-modified +/- 2	158.1 ± 2.1	0.155 ± 0,020	33.6 ± 2.4
HA-lipoplexes +/- 2	154.5 ± 1.7	0.147 ± 0,028	-39.7 ± 0.5
10% PEG lipoplexes +/- 2	78.3 ± 1.5	0.386 ± 0.020	-13.1 ± 1.3
10% PEG lipoplexes +/- 4	126.6 ± 2.4	0.271 ± 0.004	12.9 ± 0.4
10% PEG lipoplexes +/- 8	116.8 ± 0.5	0.308 ± 0.042	18.5 ± 1.0
10% PEG HA lipoplexes +/- 2	86.3 ± 1.2	0.348 ± 0.014	-17.2 ± 2.9
10% PEG HA lipoplexes +/- 4	90.1 ± 1.4	0.341 ± 0.044	-15.8 ± 4.1
10% PEG HA lipoplexes +/- 8	97.4 ± 1.3	0.340 ± 0.042	-1.4 ± 0.6
12% PEG lipoplexes +/- 2	85.4 ± 1.4	0.381 ± 0.010	-24.7 ± 4.0
12% PEG HA lipoplexes +/- 2	92.4 ± 1.2	0.299 ± 0.033	-24.0 ± 1.7

Diffusion of lipoplexes in respiratory mucus

The movement of non-modified liposomes, non-modified lipoplexes (+/- ratio of 2), HA-liposomes and HA-lipoplexes (+/- ratio of 2) in respiratory mucus was studied. The formulation PEG/HA-lipoplexes (+/- ratio of 8) was also analyzed, since this was the preparation that presented the surface charge closest to neutrality and was therefore more likely to move through the mucus. Polystyrene nanoparticles (PS) of 100 nm internally labeled with a fluorescent dye, which were densely coated with PEG to minimize mucus adhesion and have neutral surface charge [31, 32], were used as a control for the mucus tracking experiments. Tracked trajectories over 20 s, distribution of individual particle mean squared displacement at a time scale of 1 s and the ensemble-averaged geometric mean squared displacement are illustrated in Figures 1 and 2.

As expected from their positive surface charge and reduced stability in physiological medium, the motion of HA-liposomes in mucus was strongly hindered, as was evidenced by their highly constrained, non-Brownian time-lapse traces (Figure 1). The geometric averaged mean square displacement (MSD) of HA-liposomes in four different mucus samples was $1.03 \times 10^{-3} \mu\text{m}^2$ at a time scale (τ) of 1 s (Fig. 2); which was ~1200-fold lower than the MSD of the control PS nanoparticles ($1.2 \mu\text{m}^2$). Non-modified

liposomes moved more freely in mucus compared to the HA-modified; with MSD only 20-fold lower than PS.

Interestingly, addition of siRNA to the formulations increased the mobility of particles, as was observed for lipoplex formulations, which displayed time-lapse trajectories that spanned markedly greater distances. Non-modified lipoplexes moved with a MSD 6.04-fold smaller than PS nanoparticles, while PEG/HA-lipoplexes and HA-lipoplexes moved with MSDs only 3.49 and 2.40-fold smaller than PS nanoparticles. These findings suggest that the presence of HA alone does not provide a muco-inert surface coating of cationic liposomes for efficient diffusion in respiratory mucus, but it is an important factor that increases the diffusion of the particles. HA presence together with the addition of siRNA allowed the preparation of two efficient mucus-penetrating lipoplexes formulations, the HA-lipoplexes and PEG/HA-lipoplexes. Also, modification of lipoplexes with HA allowed the preparation of more homogenous vesicles. The distribution of individual MSD for all samples was monomodal, but unlike non-modified formulations, HA-lipoplexes and PEG/HA-lipoplexes presented high fractions of population that rapidly penetrated respiratory mucus (Figure 3).

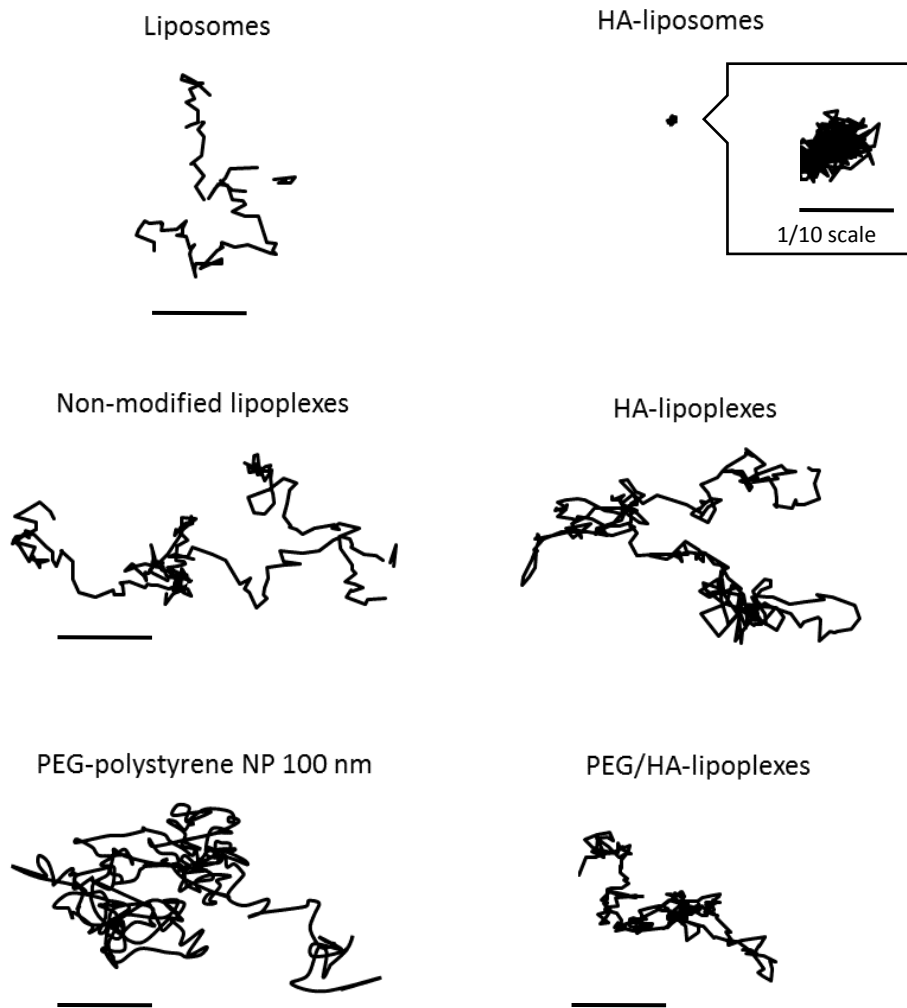


Figure 1. Representative trajectories of non-modified liposomes, non-modified lipoplexes (+/- ratio of 2), HA-liposomes, HA-lipoplexes (+/- ratio of 2), PEG-HA-lipoplexes (+/- ratio of 8) and the control PEG-polystyrene nanoparticles in airway mucus. Trajectories show 20 s of motion. Scale bar = 7 μ m.

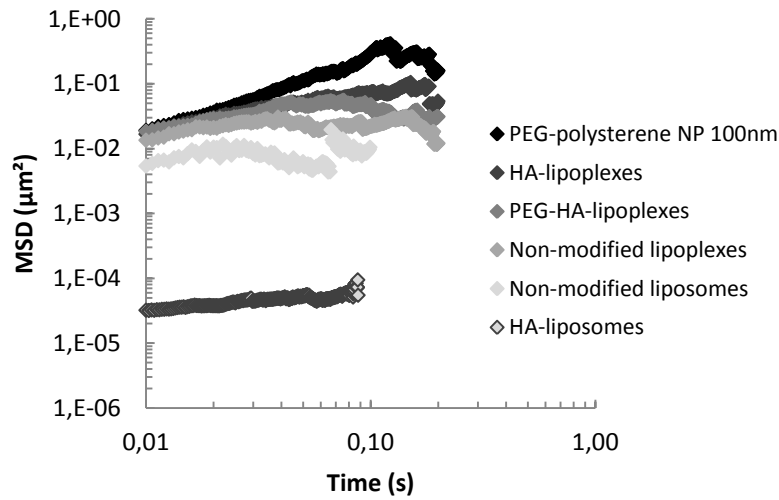


Figure 2. Ensemble-averaged geometric mean squared displacement (MSD) as a function of timescale for non-modified liposomes, non-modified lipoplexes (+/- ratio of 2), HA-liposomes, HA-lipoplexes (+/- ratio of 2), PEG-HA-lipoplexes (+/- ratio of 8) and control PEG-polystyrene nanoparticles in airway mucus.

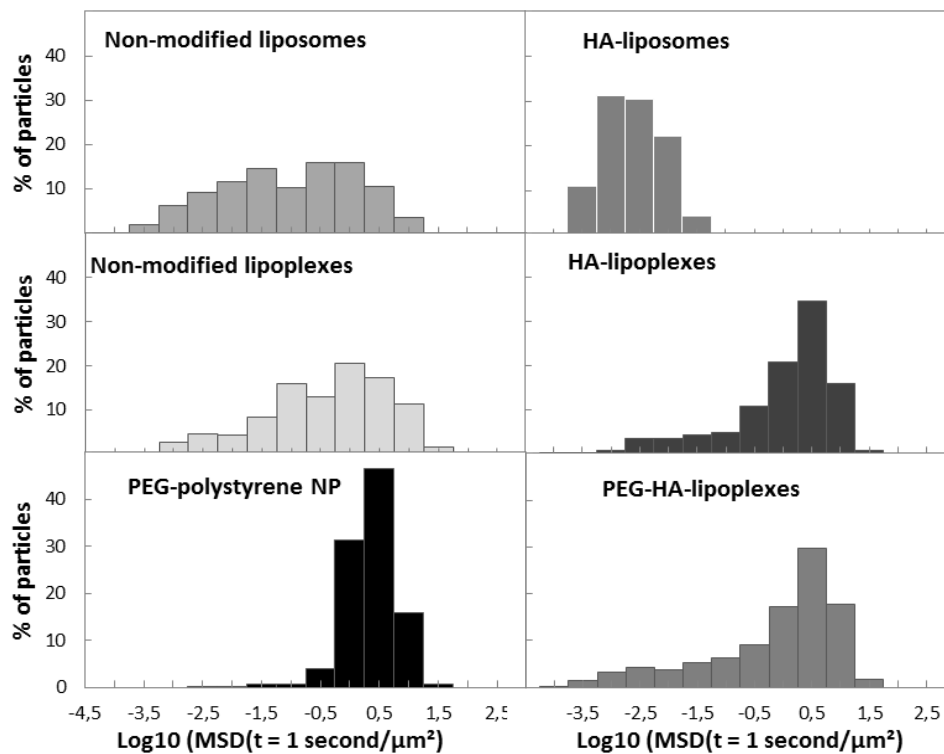


Figure 3. Distribution of individual particle mean squared displacements at a time scale of 1 s for the formulations: non-modified liposomes, non-modified lipoplexes (+/- ratio of 2), HA-liposomes, HA-lipoplexes (+/- ratio of 2), PEG-HA-lipoplexes (+/- ratio of 8) and the control PEG-polystyrene nanoparticles.

Distribution of lipoplexes in mucus of mouse lung

Liposomes and lipoplexes were administered to CF mice by the intrapulmonary route with a microsyringe, and particle distribution in the lungs was observed using fluorescence microscopy. Figure 4 shows representative images of the nanoparticles distribution in the lungs.

Thirty minutes following administration, HA-liposomes were found sparsely distributed in the lung airways, with the weakest fluorescence spots compared to the other analyzed samples. Increased fluorescence intensity on the lung tissue was observed for the non-modified lipoplexes, while HA-modified lipoplexes were even more intensely distributed. A different distribution pattern along the airway epithelium throughout the lungs was observed for the 10% PEG/HA-lipoplex formulation, for which an intense fluorescence was present and uniformly distributed.

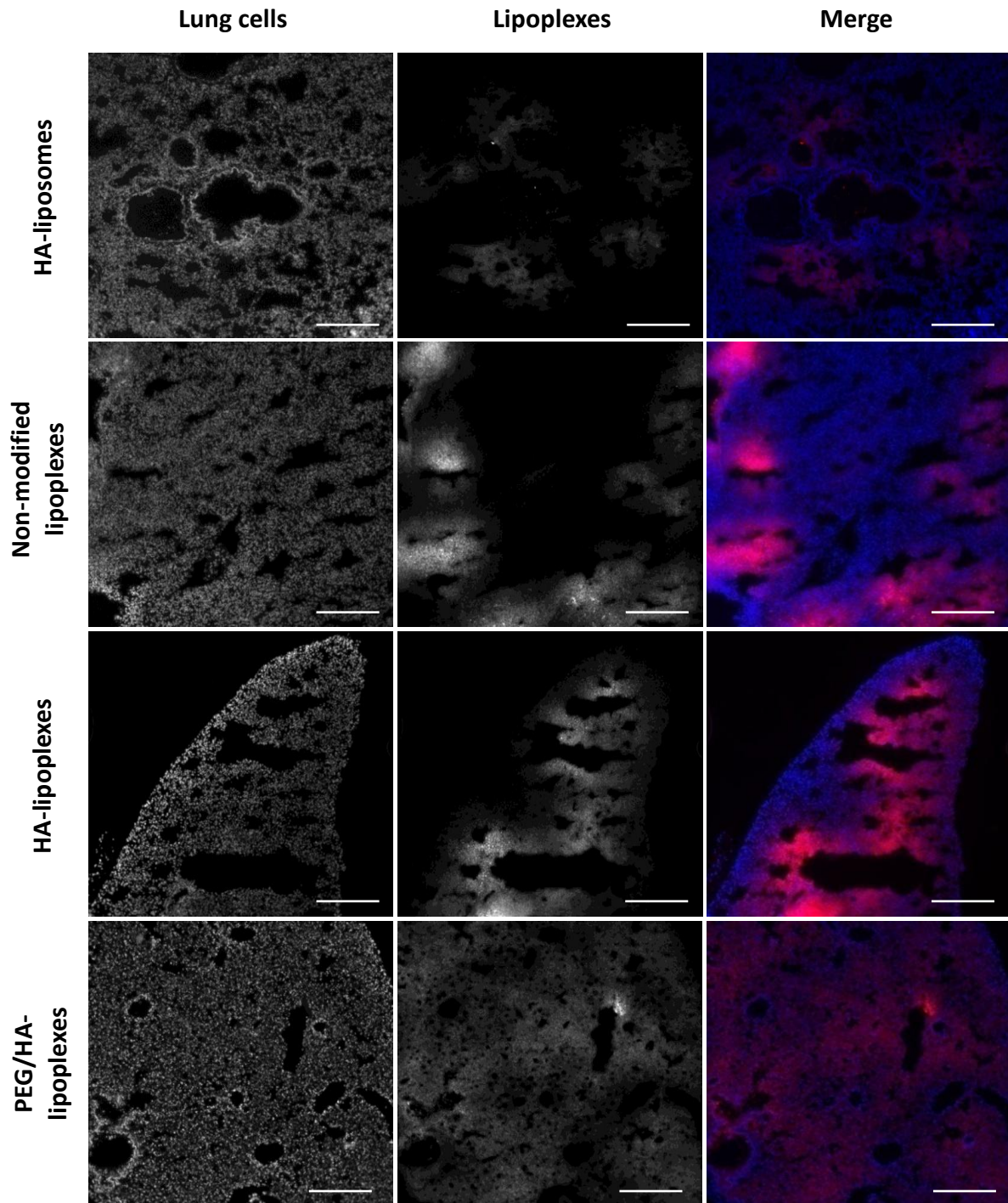


Figure 4. Representative image of distribution of nanoparticles in the lungs of mice. Pictures were taken with a 10x magnification. From left to right: on the first column, images recorded using the filter for DAPI staining (cells); second column, images recorded using the filter for rhodamine staining (lipoplexes); third column, merged images, showing lungs cells in blue and lipoplexes in red. Non-modified lipoplexes (+/- ratio of 2), HA-lipoplexes (+/- ratio of 2), PEG-HA-lipoplexes (+/- ratio of 8) and HA-liposomes were administered to the lungs using a microsyringe. Animals were euthanized and lungs were dissected and flash-frozen 30 minutes after treatment. Scale bars = 100 μ m.

In vivo luciferase inhibition

The ability of lipoplexes to carry siRNAs into the cell cytoplasm of cancer cells after intratracheal administration was evaluated by measuring the inhibition of luciferase activity of A549-luc-bearing mice (Figure 5). Treatment with non-modified or HA-modified lipoplexes did not inhibit the lung expression of luciferase, contrarily to what was observed previously after intravenous administration of HA-lipoplexes. To efficiently deliver siRNA on the cytoplasm of targeted lung cells after intrapulmonary administration, lipoplexes have several obstacles to transpose. Their site of deposition after administration, their ability to efficiently penetrate the mucus layer while protecting siRNA from degradation and their cell targeting properties will influence their success as a siRNA delivery system. To further understand which of these steps HA-lipoplexes are not overcoming, a detailed study of each of them is needed.

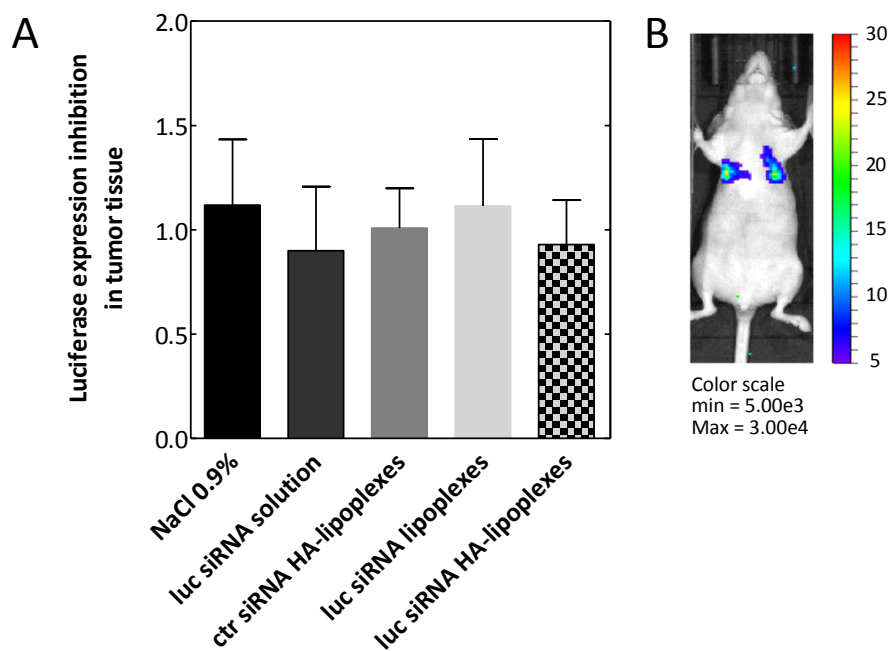


Figure 5. A. Luciferase expression inhibition in lungs of nude athymic mice. Representative image of a mouse with lung bioluminescence. B. Mice were inoculated intravenously with 1.5 million A549-luc cells. After 4 weeks, animals were treated once a day for 3 days by intrapulmonary administrations of NaCl 0.9%, luciferase-siRNA solution, HA-lipoplexes prepared with nonspecific control siRNA, HA-lipoplexes prepared with luciferase siRNA or non-modified lipoplexes prepared with luciferase siRNA. Data represent the mean \pm SD ($n \geq 6$).

Discussion

Local administration of siRNA to the lungs is a promising strategy for the treatment of lung diseases. To reach the cell cytoplasm where they will enter the pathway that leads to gene silencing, these small molecules have to overcome the mucus barrier, the primary defense mechanism of mucosal tissues, which traps and removes nano- and micron-sized objects. Mucus is a highly entangled, viscoelastic polymer network composed of secreted mucin proteins, cells, bacteria, nutrients, protective factors and waste [33]. The percentage of the components in the mucus varies between the different tissues and health conditions [13], as do the mesh spacing (~340 nm for human cervicovaginal mucus, ~145 nm for cystic fibrotic sputum, and ~150 nm for human chronic rhinosinusitis, for example) [29, 34, 35], but the major components of healthy human mucus are basically water (95%) and mucins (2%) [36].

To be able to cross these mucosal barriers, nanoparticles have to be small enough to pass through the mucus mesh spaces, and possess appropriate surface characteristics to avoid interaction with mucins. Surface-modified nanoparticles that undergo extensive interaction with negatively charged mucins and are able to cross the mucus barrier have been studied [37, 38]. For example, coating solid lipid nanoparticles (SLN) with poloxamer (Pluronic) increased their movement in cystic fibrosis sputum by 5 and 100 folds compared to tween- and PVA-coated SLNs, allowing efficient lung mucus penetration [39]. Pluronic-coated liposomes were able to penetrate the mucus layers to reach the intestinal epithelial surface and deliver encapsulated active substances [41, 42]. Imidazole-modified chitosan and trimethyl chitosan nanoparticles were also able to overpass the gastric mucus layer and deliver siRNA to the gastrointestinal mucosa [43]. Notably, polymeric PEGylated nanoparticles have shown significant progress as mucus-penetrating nucleotide delivery systems [44]. Coating polymeric PSA [45], PLGA [46], PCL [46] and latex [31] nanoparticles with PEG minimized protein adhesion at biomaterial surfaces. The hydrated PEG layer enthalpically resists the release of water molecules and entropically resists compression [47], thereby drastically increasing the ability of these nanoparticles to move through the mucus mesh.

The use of HA as a hydrophilic coating material has also been explored for the carrying of cargo through the mucus layer [48]. Modification of siRNA carriers with HA has been used for targeting and controlling particle surface properties [23-26]. In our previous work, we describe the structure of an optimized HA-lipoplex formulation, and its *in vitro* and *in vivo* applications for the targeting of CD44-overexpressing cells. Here, we investigate the impact of HA on lipoplexes fate in the lungs, especially regarding interaction with mucus, and the effect of PEG incorporation to improve this properties. To do so, we prepared HA-lipoplexes, notably negatively charged, and by modifying their formulation with PEG and different ratios of siRNA, we obtained 10% PEG/HA-lipoplexes with +/- ratio of 8 that had a global surface charge of -1.4 mV.

To visualize the diffusion of lipoplexes in human mucus, we labeled liposomes and lipoplexes with a fluorescent probe and quantified the translational motion of hundreds of particles in mucus freshly collected from patients using multiple particle tracking (MPT). HA-liposomes were almost completely immobilized in the mucus, which correlated with the results obtained for stability studies in physiological medium (Supplementary information, Chapter 2). The MSD of non-modified liposomes was slightly lower than that of the non-modified lipoplexes, implying that the addition of siRNA negative charges reduced adhesive (hydrophobic, electrostatic) interactions with mucus. Contrary to what could be expected [35], PEG-shielding was not fundamental for effective lipoplex diffusion in respiratory mucus. Rapid diffusion was observed for PEG/HA-lipoplexes as well as HA-lipoplexes, whose mean MSD values were very close to each other and to that of the mucus-penetrating PEG-polystyrene control nanoparticles [31]. This indicated that the presence of HA in the lipoplexes structure was able to reduce interactions with the mucus components. The modification of lipoplexes with HA also decreased vesicles heterogeneity, and allowed higher fractions of population to rapidly penetrate respiratory mucus. We hypothesize that, as for muco-inert viruses, that have high density of both cationic and anionic surface coating [37, 49], the presence of both densely negative siRNA molecules and HA moieties and positive DE charges on the surface of the HA-lipoplexes, together with the hydrophilic character of HA, are responsible for preventing adhesion to mucus constituents. It is important to note that particle movement in the mucus depends on multiple factors, and not only on their mean diameter and surface charge. Exact threshold of hydrophilic coverage needed to achieve mucoresistance depends on the specific system of interest [33].

We then compared the distribution of the particles in the lungs of CF-1 mice after intrapulmonary administration. Increasing amount of particles were observed in the lungs after administration of HA-liposomes < non-modified lipoplexes < HA-modified lipoplexes < 10% PEG/HA-lipoplexes, in agreement with the observations of their movement in lung mucus, confirming the importance of siRNA and HA presence in particle mobility. Instead of defined fluorescent regions, as observed for the other formulations, lungs of mice treated with PEGylated HA-lipoplexes showed intense fluorescence all over the tissue, evidencing that the *in vivo* mucus penetration of these particles was indeed more efficient compared to the non-PEGylated HA-lipoplexes. Thus, the similarity of the mucus-penetrating properties of HA-lipoplexes and PEG/HA-lipoplexes observed in MPT experiments was not confirmed *in vivo*, and the larger vesicle heterogeneity of the PEG/HA-lipoplexes may be the cause of this difference. PEG/HA lipoplexes had the highest Pdl index of all preparations (0.340). We can thus assume that although there is a part of this population that is not efficiently penetrating through the mucus mesh, the part that is actually moving in the mucus is able to travel greater distances, as evidenced *in vivo* and also on the tracked trajectories image. Dense PEG grafting on the lipoplexes

surface have been previously shown to effectively shield them against adhesive hydrophobic and electrostatic interactions and minimized protein binding [29].

To reach lung cells after administration in the respiratory system, nanoparticles have several obstacles to transverse, including coughing, dissolution, mucociliary clearance and phagocytosis by macrophages [50]. Already their site of deposition in the lungs will depend on the entry pathway. Considering that our HA-modified lipoplexes were administered directly to the lungs, we expect that their deposition extends from the bronchial to the alveolar region. Since they had reasonable mucus penetrating properties, as observed by MPT experiments, a reasonable mobility could also be expected for the alveolar lining fluid. It is possible, though, that their movement wasn't fast enough to reach the cells before being cleared. Also, it is possible that while crossing the mucus layer lipoplexes were removed by mucociliary clearance, especially in the case of HA-(non-PEGylated) lipoplexes. Although *in vitro* [51-56] and *in vivo* [57, 58] evidences suggest that cell-to-cell transfer of RNAs occurs, particles reaching the lung tissue through the intratracheal route will first encounter cells from the respiratory epithelium. In our tumor model, in which the lung carcinoma formation was observed after intravenous and not intratracheal administration of A549 cells, it is expected that the metastatic tumor is localized preferentially in the endothelial region of the lungs. Therefore, the fact that the possible main localization of the lipoplexes that reach the tissue after mucus penetration does not coincide with the tumor localization, is also a reason that could explain why gene silencing was not observed.

Conclusion and perspectives

HA-modified siRNA lipoplexes showed a promising mucus penetrating ability. The presence of HA and siRNA on the vesicles structure were equally important to prevent particle hindrance in the mucus and increase particle homogeneity and stability. Modification of lipoplexes with both HA and PEG increased showed the best results in improving particle diffusion in airway mucus, as confirmed in the lung distribution study using fluorescently-labeled lipoplexes. Further investigation regarding the macromolecular structure and siRNA stability could shine a light on the formation process of these lipoplexes. The investigation of the *in vivo* gene expression inhibition by this formulation would also be interesting, since PEG/HA-lipoplexes showed good potential as carriers for localized delivery of siRNA to the lungs.

References

1. Aagaard, L. and J.J. Rossi, *RNAi therapeutics: Principles, prospects and challenges*. *Adv Drug Deliv Rev*, 2007. **59**(2-3): p. 75-86.
2. Nascimento, T., H. Hillaireau, and E. Fattal, *Nanoscale particles for lung delivery of siRNA*. *Journal of drug delivery science and technology*, 2012. **22**(1): p. 99-108.
3. Zhang, X., et al., *Cucumber mosaic virus-encoded 2b suppressor inhibits Arabidopsis Argonaute1 cleavage activity to counter plant defense*. *Genes Dev*, 2006. **20**(23): p. 3255-68.
4. Siner, J.M., et al., *VEGF-induced heme oxygenase-1 confers cytoprotection from lethal hyperoxia in vivo*. *The FASEB Journal*, 2007. **21**(7): p. 1422-1432.
5. Huang, H., C. Lee, and B. Chiang, *Small interfering RNA against interleukin-5 decreases airway eosinophilia and hyper-responsiveness*. *Gene therapy*, 2008. **15**(9): p. 660-667.
6. Perl, M., et al., *Silencing of Fas, but not caspase-8, in lung epithelial cells ameliorates pulmonary apoptosis, inflammation, and neutrophil influx after hemorrhagic shock and sepsis*. *The American journal of pathology*, 2005. **167**(6): p. 1545-1559.
7. Lomas-Neira, J.L., et al., *In vivo gene silencing (with siRNA) of pulmonary expression of MIP-2 versus KC results in divergent effects on hemorrhage-induced, neutrophil-mediated septic acute lung injury*. *Journal of leukocyte biology*, 2005. **77**(6): p. 846-853.
8. Moschos, S.A., et al., *Targeting the lung using siRNA and antisense based oligonucleotides*. *Current pharmaceutical design*, 2008. **14**(34): p. 3620-3627.
9. Koli, U., et al., *siRNA-Based Therapies for Pulmonary Diseases*. *Journal of Biomedical Nanotechnology*, 2014. **10**(9): p. 1953-1997.
10. Vicentini, F., et al., *Delivery Systems and Local Administration Routes for Therapeutic siRNA*. *Pharmaceutical Research*, 2013. **30**(4): p. 915-931.
11. Gautam, A., J.C. Waldrep, and C.L. Densmore, *Aerosol gene therapy*. *Mol Biotechnol*, 2003. **23**(1): p. 51-60.
12. Griesenbach, U., et al., *In vivo imaging of gene transfer to the respiratory tract*. *Biomaterials*, 2008. **29**(10): p. 1533-40.
13. Sanders, N., et al., *Extracellular barriers in respiratory gene therapy*. *Advanced Drug Delivery Reviews*, 2009. **61**(2): p. 115-127.
14. Koshkina, N.V., et al., *Biodistribution and pharmacokinetics of aerosol and intravenously administered DNA-polyethyleneimine complexes: optimization of pulmonary delivery and retention*. *Molecular therapy*, 2003. **8**(2): p. 249-254.
15. Sham, J.O.H., et al., *Formulation and characterization of spray-dried powders containing nanoparticles for aerosol delivery to the lung*. *International journal of pharmaceutics*, 2004. **269**(2): p. 457-467.
16. Patton, J.S., *Mechanisms of macromolecule absorption by the lungs*. *Advanced Drug Delivery Reviews*, 1996. **19**(1): p. 3-36.
17. Soutschek, J., et al., *Therapeutic silencing of an endogenous gene by systemic administration of modified siRNAs*. *Nature*, 2004. **432**(7014): p. 173-8.
18. Braasch, D.A., et al., *Biodistribution of phosphodiester and phosphorothioate siRNA*. *Bioorg Med Chem Lett*, 2004. **14**(5): p. 1139-43.
19. Dykxhoorn, D.M. and J. Lieberman, *Knocking down disease with siRNAs*. *Cell*, 2006. **126**(2): p. 231-5.
20. Fattal, E. and G. Barratt, *Nanotechnologies and controlled release systems for the delivery of antisense oligonucleotides and small interfering RNA*. *British Journal of Pharmacology*, 2009. **157**(2): p. 179-194.
21. Arpicco, S., et al., *Synthesis, characterization and transfection activity of new saturated and unsaturated cationic lipids*. *Farmaco*, 2004. **59**(11): p. 869-78.
22. Pardue, E.L., S. Ibrahim, and A. Ramamurthi, *Role of hyaluronan in angiogenesis and its utility to angiogenic tissue engineering*. *Organogenesis*, 2008. **4**(4): p. 203-214.

23. Peer, D. and R. Margalit, *Tumor-targeted hyaluronan nanoliposomes increase the antitumor activity of liposomal Doxorubicin in syngeneic and human xenograft mouse tumor models*. *Neoplasia*, 2004. **6**(4): p. 343-53.
24. Peer, D. and R. Margalit, *Loading mitomycin C inside long circulating hyaluronan targeted nano-liposomes increases its antitumor activity in three mice tumor models*. *Int J Cancer*, 2004. **108**(5): p. 780-9.
25. Surace, C., et al., *Lipoplexes Targeting the CD44 Hyaluronic Acid Receptor for Efficient Transfection of Breast Cancer Cells*. *Molecular Pharmaceutics*, 2009. **6**(4): p. 1062-1073.
26. Wojcicki, A.D., et al., *Hyaluronic Acid-Bearing Lipoplexes: Physico-Chemical Characterization And In Vitro Targeting Of The CD44 Receptor*. *Journal of Controlled Release*, 2012.
27. Batzri, S. and E.D. Korn, *Single bilayer liposomes prepared without sonication*. *Biochim. Biophys. Acta*, 1973. **298**: p. 1015-1019.
28. Taetz, S., et al., *Hyaluronic Acid-Modified DOTAP/DOPE Liposomes for the Targeted Delivery of Anti-Telomerase siRNA to CD44-Expressing Lung Cancer Cells*. *Oligonucleotides*, 2009. **19**(2): p. 103-115.
29. Schuster, B.S., et al., *Nanoparticle diffusion in respiratory mucus from humans without lung disease*. *Biomaterials*, 2013. **34**(13): p. 3439-3446.
30. Suk, J.S., et al., *Lung gene therapy with highly compacted DNA nanoparticles that overcome the mucus barrier*. *Journal of Controlled Release*, 2014. **178**: p. 8-17.
31. Lai, S.K., et al., *Rapid transport of large polymeric nanoparticles in fresh undiluted human mucus*. *Proceedings of the National Academy of Sciences*, 2007. **104**(5): p. 1482-1487.
32. Suk, J.S., et al., *The penetration of fresh undiluted sputum expectorated by cystic fibrosis patients by non-adhesive polymer nanoparticles*. *Biomaterials*, 2009. **30**(13): p. 2591-2597.
33. Wang, Y.Y., et al., *Addressing the PEG Mucoadhesivity Paradox to Engineer Nanoparticles that "Slip" through the Human Mucus Barrier*. *Angewandte Chemie International Edition*, 2008. **47**(50): p. 9726-9729.
34. Lai, S.K., et al., *Nanoparticles reveal that human cervicovaginal mucus is riddled with pores larger than viruses*. *Proceedings of the National Academy of Sciences*, 2010. **107**(2): p. 598-603.
35. Yu, T., et al., *Liposome-based mucus-penetrating particles (MPP) for mucosal theranostics: Demonstration of diamagnetic chemical exchange saturation transfer (diaCEST) magnetic resonance imaging (MRI)*. *Nanomedicine: Nanotechnology, Biology and Medicine*, 2014. **11**(2): p. 401-405
36. Bansil, R. and B.S. Turner, *Mucin structure, aggregation, physiological functions and biomedical applications*. *Current Opinion in Colloid & Interface Science*, 2006. **11**(2): p. 164-170.
37. Lai, S.K., Y.Y. Wang, and J. Hanes, *Mucus-penetrating nanoparticles for drug and gene delivery to mucosal tissues*. *Advanced drug delivery reviews*, 2009. **61**(2): p. 158-171.
38. Lam, J.K.-W., W. Liang, and H.-K. Chan, *Pulmonary delivery of therapeutic siRNA*. *Advanced Drug Delivery Reviews*, 2012. **64**(1): p. 1-15.
39. Nafee, N., et al., *Antibiotic-free nanotherapeutics: Ultra-small, mucus-penetrating solid lipid nanoparticles enhance the pulmonary delivery and anti-virulence efficacy of novel quorum sensing inhibitors*. *Journal of Controlled Release*, 2014. **192**(0): p. 131-140.
41. Chen, D., et al., *Comparative study of Pluronic[®] F127-modified liposomes and chitosan-modified liposomes for mucus penetration and oral absorption of cyclosporine A in rats*. *International Journal of Pharmaceutics*, 2013. **449**(1): p. 1-9.
42. Li, X., et al., *Novel mucus-penetrating liposomes as a potential oral drug delivery system: preparation, in vitro characterization, and enhanced cellular uptake*. *International Journal of Nanomedicine*, 2011. **6**: p. 3151.
43. Sadio, A., et al., *Modified-Chitosan/siRNA Nanoparticles Downregulate Cellular CDX2 Expression and Cross the Gastric Mucus Barrier*. *PloS one*, 2014. **9**(6): p. e99449.
44. de la Fuente, M., B. Seijo, and M.J. Alonso, *Novel hyaluronic acid-chitosan nanoparticles for ocular gene therapy*. *Invest Ophthalmol Vis Sci*, 2008. **49**(5): p. 2016-24.

45. Tang, B.C., et al., *Biodegradable polymer nanoparticles that rapidly penetrate the human mucus barrier*. Proceedings of the National Academy of Sciences, 2009. **106**(46): p. 19268-19273.
46. Yang, M., et al., *Biodegradable nanoparticles composed entirely of safe materials that rapidly penetrate human mucus*. Angewandte Chemie International Edition, 2011. **50**(11): p. 2597-2600.
47. Valentine, M.T., et al., *Colloid Surface Chemistry Critically Affects Multiple Particle Tracking Measurements of Biomaterials*. Biophysical Journal, 2004. **86**(6): p. 4004-4014.
48. Sandri, G., et al., *Mucoadhesive and penetration enhancement properties of three grades of hyaluronic acid using porcine buccal and vaginal tissue, Caco-2 cell lines, and rat jejunum*. Journal of Pharmacy and Pharmacology, 2004. **56**(9): p. 1083-1090.
49. Cone, R.A., *Barrier properties of mucus*. Advanced Drug Delivery Reviews, 2009. **61**(2): p. 75-85.
50. Carafa, M., et al., *Novel Concept in Pulmonary Delivery*. In Chronic Obstructive Pulmonary Disease - Current Concepts and Practice, Chapter 16, InTech, 2012. 484 pages.
51. Dunoyer, P., et al., *Small RNA duplexes function as mobile silencing signals between plant cells*. Science, 2010. **328**(5980): p. 912-916.
52. Molnar, A., et al., *Small silencing RNAs in plants are mobile and direct epigenetic modification in recipient cells*. Science, 2010. **328**(5980): p. 872-875.
53. Valiunas, V., et al., *Connexin-specific cell-to-cell transfer of short interfering RNA by gap junctions*. The Journal of physiology, 2005. **568**(2): p. 459-468.
54. Hosoda, T., et al., *Human cardiac stem cell differentiation is regulated by a mircrine mechanism*. Circulation, 2011. **123**(12): p. 1287-1296.
55. Lim, P.K., et al., *Gap Junction–Mediated Import of MicroRNA from Bone Marrow Stromal Cells Can Elicit Cell Cycle Quiescence in Breast Cancer Cells*. Cancer Research, 2011. **71**(5): p. 1550-1560.
56. Katakowski, M., et al., *Functional microRNA is transferred between glioma cells*. Cancer Research, 2010. **70**(21): p. 8259-8263.
57. Pan, Q., et al., *Hepatic cell-to-cell transmission of small silencing RNA can extend the therapeutic reach of RNA interference (RNAi)*. Gut, 2012. **61**(9), p. 1330-1339.
58. McCaskill, J., et al., *Efficient biodistribution and gene silencing in the lung epithelium via intravenous liposomal delivery of siRNA*. Molecular Therapy-Nucleic Acids, 2013. **2**(6): p. e96.

Discussion générale

General discussion

Context

The increasing knowledge of the molecular mechanisms related to the pathogenesis of cancers has allowed the development of new strategies to improve the treatment of these diseases. Due to their high selectivity and efficiency, much effort has been made on using siRNAs as a therapeutic tool in the treatment of cancer and other severe diseases. These small molecules can be designed to specifically interfere with the production of mRNA and consequently with the translation of proteins. Presently, specific delivery of siRNA molecules to target cells remains the major handicap for the use of these small hydrophilic molecules in cancer therapy, since they lack stability in serum and targeting properties. Various delivery systems have been developed to overcome these obstacles and to promote an efficient delivery of siRNA to diseased cells. These nanocarriers are designed to protect siRNA from degradation, access to the tumor cells and deliver siRNA molecules to the cytoplasm. They are broadly divided into two categories, viral and non-viral. In part due to the potential toxicities associated with viral vectors, non-viral vectors have become increasingly popular alternatives. Non-viral siRNA vectors typically involve complexing siRNA with a positively charged vector (e.g., cationic cell penetrating peptides, cationic polymers and dendrimers, and cationic lipids); conjugating siRNA with small molecules (e.g., cholesterol, bile acids, and lipids), polymers, antibodies, and RNAs; and encapsulating siRNA in nanoparticulate formulations[1].

A high molecular weight HA-modified lipoplex formulation has been developed in our laboratory which allowed the selective *in vitro* delivery of DNA plasmids to CD44-overexpressing MDA breast cancer cells[2] and A549-luc cells[3]. These particles were prepared by conjugating DOPE lipid molecules to high molecular weight HA, followed by the preparation of lipoplexes by the incubation with DNA. The formulation strategy of these particles relies on the overexpression of the CD44 receptor in various cancer cells, particularly metastasis-developing primary tumors. These tumors include a larger fraction of cancer stem cells, which are rare cells with indefinite proliferative potential that dictate the formation and growth of tumors[4] and present a CD44+ overexpressing phenotype[5, 6]. The constitutive binding between HA and CD44 would give HA-lipoplexes the ability to enter the cells via the interaction with these receptors. Also, the modification of the lipoplexes surface with the long hydrophilic chains of HA would promote particle stealth properties, increasing plasmatic circulation time and passive targeting to the tumor region by the EPR effect.

In this thesis, the hypotheses regarding the applicability of the lipoplex system to the targeted delivery of siRNA molecules to CD44-overexpressing cells were tested. We first studied the formation of siRNA lipoplexes and analyzed the influence of the HA-modification on the particle structure combining

particle diameter and surface charge analysis, capillary electrophoresis, cryo-TEM microscopy, surface plasmon resonance and small angle X-ray scattering techniques. The effects of the modification of lipoplexes with HA on cell internalization were then evaluated. The cellular viability, uptake kinetics, lipoplexes cellular localization and *in vitro* gene expression inhibition were studied using a luciferase-expressing A549 cell model. Then, the ability of the lipoplexes to carry intact siRNA to the cytoplasm of cancer cells *in vivo* was studied. For this, an A549 luciferase-expressing metastatic cancer model was developed. Bioluminescence signals from the lungs of animals before and after treatment were compared to evaluate expression inhibition. At last, we studied the diffusion of the HA-modified siRNA lipoplexes in human airway mucus, in order to evaluate the viability of administering these particles by the pulmonary route to treat lung diseases. The diffusion of lipoplexes was studied using the multiple particle tracking (MPT) technique, and the distribution of HA-modified siRNA lipoplexes in the mouse lung after pulmonary administration was analyzed.

The HA-DOPE conjugate

In order to insert HA on liposome structure, we used a conjugate of HA and DOPE lipid molecules, which act as anchors of HA on the bilayer structure. The choice of high molecular weight HA for the preparation of the conjugate was based on literature reports that indicate that these large molecules, being ubiquitous, do not induce expression of genes involved in proliferation or inflammation[7] and counteract proangiogenic effects of the HA oligomers[8]. The HA-DOPE conjugate preparation was based on a reaction described by Yerushalmi and Margalit[9]. In this reaction, the carboxylic groups of hyaluronic acid are activated to react with the amine groups from the DOPE lipid molecules (Figure 1). The efficiency of the conjugation reaction was calculated by the Stewart assay [32] as $1.1 \pm 0.5\%$, meaning that each HA molecule (composed of 6320 D-glucuronic acid and N-acetyl-D-glucosamine dimers) had 250 molecules of DOPE attached to its structure.

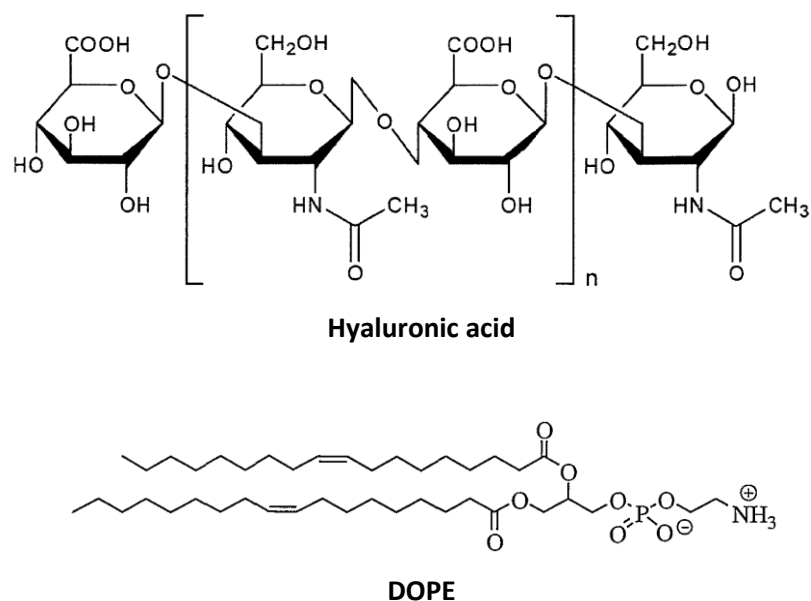


Figure 1. Structures of hyaluronic acid (HA) and 1,2-dioleoyl-sn-glycero-3-phosphoethanolamine (DOPE).

Preparation and structure of HA-modified liposomes and lipoplexes

The cationic lipid [2-(2-3didodecyloxypropyl)hydroxyethyl]ammonium bromide (DE, Figure 2), which has demonstrated improved transfection efficiency in different cell lines[10], was used for the preparation of the cationic liposomes.

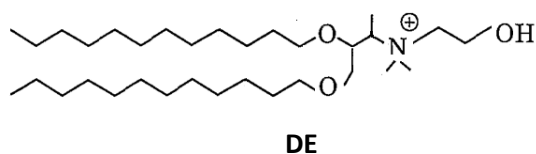


Figure 2. Structure of [2-(2-3didodecyloxypropyl)hydroxyethyl]ammonium bromide (DE) lipid.

DOPE was used as helper lipid on account of its well documented ability to adopt an inverted hexagonal phase and attach itself to and rapidly fuse with anionic membranes, resulting in the release of the liposome content into the cytoplasm[11-13], and to destabilize the endosomal membrane at acidic pH and assist liposomes in delivering their contents into the cytoplasm[14].

The obtained liposomes presented a variable polydispersity index (PDI) as a consequence of using the ethanol injection for their preparation without a subsequent size calibration using extrusion. As observed by Cryo-TEM microscopy, the population of liposomes was composed mainly, but not

exclusively, of unilamellar vesicles. The presence of HA on the surface of these particles was indicated by the increase of liposomes diameter proportionally to the amount of HA added to the formulation, from around 90 for non-modified liposomes to around 140 nm for liposomes containing 15% (w/w) HA-DOPE. Zeta potential measurements confirmed the presence of HA dimers on the surface of liposomes, observed as a proportional reduction from +55 mV to +30 mV for non-modified to liposomes containing 15% HA-DOPE.

Previous studies by Wojcicki et al.[3] using differential scanning calorimetry (DSC) had already revealed a different behavior between unconjugated HA and HA conjugated to DOPE upon interaction with the liposomes membrane. The analysis of DOPE demonstrated that the endotherm of gel to liquid crystal phase transition shifted from -10.30 °C with water or unconjugated HA to -8.97 °C with HA-DOPE (Figure 3). This suggested that DOPE covalently linked to HA interacts with DOPE in the liposomes, being therefore able to play the role of anchor in the lipid membrane.

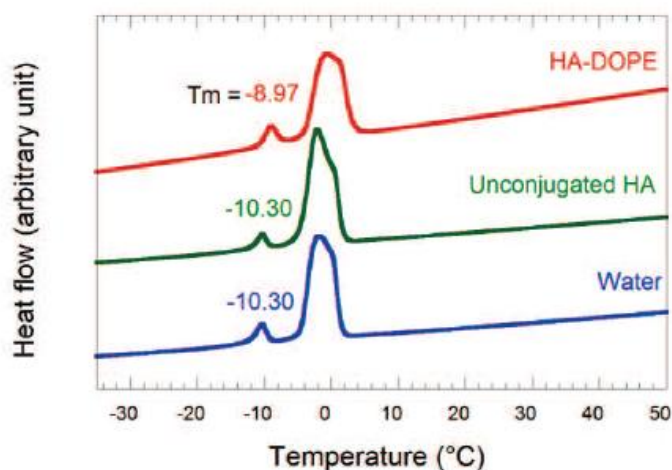


Figure 3. Study of the transition temperature from gel to liquid crystalline phase of DOPE hydrated by different solutions (HA-DOPE, unconjugated HA and water) by differential scanning calorimetry. The first peak of each thermogram corresponds to the transition temperature (T_m) of hydrated DOPE and the second to the water melting. The three curves correspond (from top to bottom) to DOPE film hydrated by an aqueous solution of HA-DOPE 10%, DOPE film hydrated by an aqueous solution of unconjugated HA 10% and to DOPE film hydrated by water. Adapted from Wojcicki et al.[15].

We searched for further evidences of the interaction between the HA-DOPE conjugate and the lipid bilayers in our studies using SAXS. Analysis of liposomes modified with different concentrations of the conjugate revealed that its presence causes the reorganization of unilamellar vesicles into oligolamellar ones. Between 10 and 15% HA-DOPE, an increase in hydration of the lamellar phase was observed, indicating a more important steric repulsion between bilayers caused by the presence of HA molecules. Because multiple DOPE molecules are linked to one chain of HA, conjugate insertion by

multiple lipid anchors favors the presence of HA between lipids bilayers of the liposomes. The structures obtained are therefore different from the previously suggested brush or mushroom conformations [16].

The complexation with siRNA for the formation of lipoplexes originated vesicles with, as for the HA modification, increasing diameters and decreasing surface charges. The rearrangement of lipid vesicles resulted in the formation of a more homogeneous population of oligolamellar structures of around 230 nm and -40 mV for lipoplexes of $+/-$ charge ratios of 1 and 2. This was evidenced by Cryo-TEM microscopy and SAXS analysis, and is in agreement with the multiple small unilamellar vesicles fusion observed for DNA lipoplexes [17-19]. This is a favorable characteristic when siRNA stability is considered, since the packing of the bilayers around siRNA molecules represent a barrier from degradation of plasmatic RNAses. This lipoplex structure could furthermore increase lipoplex efficiency, since as it has been described in the literature that MLV lipoplexes are generally better transfecting agents than SUV lipoplexes [20-22]. It was evidenced by ITC experiments that lipoplexes contained no more lipid than the necessary for a complete neutralization of siRNA charges. Therefore, the maximal $+/-$ ratio possible for complexation was 1. At this siRNA concentration, the maximal capacity of the lipids for siRNA binding was reached. Revealed by the end point of the ITC titration, this value is in agreement with the maximal possible final $+/-$ ratio obtained in the association studies using radiolabeled siRNA for liposome binding. The complete association of siRNA to liposomes at $+/-$ ratio 2 was also visualized by gel electrophoresis. As shown in Figure 4, complete siRNA association was confirmed for lipoplexes diluted in water and in cell culture medium.

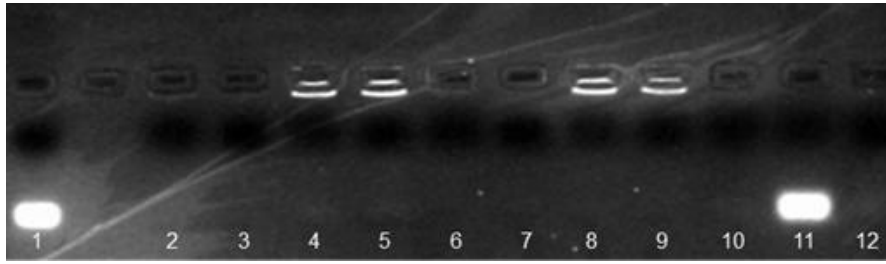


Figure 4. Agarose gel electrophoresis of siRNA lipoplexes at \pm ratios 134 and 2. Lipoplexes were prepared and diluted in water or cell culture medium before analysis. 1. Free siRNA correspondent to the \pm ratio 2 concentration; 2. Lipoplexes 0% HA-DOPE \pm ratio 134 diluted in cell culture medium; 3. Lipoplexes 0% HA-DOPE \pm ratio 134 diluted in water; 4. Lipoplexes 0% HA-DOPE \pm ratio 2 diluted in cell culture medium; 5. Lipoplexes 0% HA-DOPE \pm ratio 2 diluted in water; 6. Lipoplexes 10% HA-DOPE \pm ratio 134 diluted in cell culture medium; 7. Lipoplexes 10% HA-DOPE \pm ratio 134 diluted water; 8. Lipoplexes 10% HA-DOPE \pm ratio 2 diluted in cell culture medium; 9. Lipoplexes 10% HA-DOPE \pm ratio 2 diluted in water; 10. Free siRNA correspondent to the \pm ratio 134 concentration diluted in cell culture medium; 11. Free siRNA correspondent to the \pm ratio 2 concentration diluted in cell culture medium; 12. Free siRNA correspondent to the \pm ratio 134 concentration diluted in water.

Based on the liposome concentration (estimated from lipid concentration and liposome size) and siRNA loading (13.84%), each lipoplex at \pm ratio 2 would have approximately 1054 siRNA molecules. This estimation considers that all vesicles are unilamellar. In the case of our oligolamellar HA-modified lipoplexes, the cargo capacity is more important since vesicles have a much higher lipid density. This is comparable to highly charged and efficient siRNA carriers described in the literature[23]. As far as HA is concerned, the concentration of the polymer in the liposome suspension (that has a conjugate association of 71%) is 0.14 mg/ml, corresponding to 5.9 HA molecules/liposome. When siRNA is added at \pm ratio 2, charge competition with strongly interacting siRNA molecules and steric hindrance caused by the bilayers rearrangement decrease the HA-DOPE concentration to 37%, that represents 0.024 mg/ml and 2.21 HA molecules/lipoplex. Despite the fact that this concentration is smaller than the ones described by Quattal et al.[16] and Landesman-Milo et al.[24], for example, it was proven effective for CD44 binding using surface plasmon resonance experiments and *in vitro* binding and internalization and gene expression inhibition experiments.

***In vitro* activity of lipoplexes**

The A549-luc human lung carcinoma cell line was used to evaluate the biological activity of HA-lipoplexes. This cell line is commonly used as a CD44-targeting cell model because of the high and homogeneous CD44 membrane receptor expression, as we confirmed by flow cytometry. The luminescence analysis revealed, on the other hand, that these cells did not homogeneously express luciferase. Therefore, a selection protocol using gentamicine (G418, Geneticin®, Thermo Fisher Scientific Inc., USA) was optimized, and cells were treated with 75 µg/ml for 12 days before each experiment.

A549-luc viability studies showed that the modification by hyaluronic acid did not change lipoplex toxicity, as expected due to the well known biocompatibility of HA[25]. The low cytotoxicity observed after incubation with high concentrations of lipoplexes regardless of the +/- ratio suggested that this effect was not related to the changes in particle surface charge, but probably to the type and amount of lipids in the formulation[26, 27]. Nevertheless, the uptake and gene silencing inhibition of the lipoplexes was not compromised. Flow cytometry experiments showed a progressive uptake, with lipoplexes containing the HA-DOPE conjugate being taken up by the cells at a higher rate when compared to the plain lipoplexes. This difference was clearly observed for the ratio +/- 134. Lipoplexes at +/- 2 were internalized more rapidly compared to all other analyzed particles, and a plateau of the uptake of these lipoplexes was reached after 2 h. Confocal laser microscopy confirmed that the lipoplexes were localized at the cell cytoplasm, as were siRNA molecules.

After identifying the cellular localization of the siRNA, it was important to check if these molecules were intact and able to bind RISC and form the RNA-induced silencing complex that would lead to gene silencing. With this aim, we tested the lipoplexes luminescence inhibition using a luciferase-targeted siRNA. Previous studies of Surace et al.[2] and Wojcicki et al.[15] demonstrated that 10% HA-DOPE (w/w) is the optimal concentration for transfection of CD44-overexpressing MDA-MB231 and A549 cells with plasmid DNA lipoplexes. We performed a gene expression inhibition test with lipoplexes at +/- ratio 2 modified with 5, 10 and 15% of conjugate, in which we confirmed this result for the siRNA lipoplexes formulation (Figure 5).

Specific inhibition by the luciferase-siRNA compared to the control siRNA was observed, which validated the model chosen. Higher luciferase expression was observed for lipoplexes modified by HA, at both +/- ratios 134 and 2, in agreement with the uptake experiments, being the highest luciferase expression observed after treatment with HA-lipoplexes at +/- ratio 2.

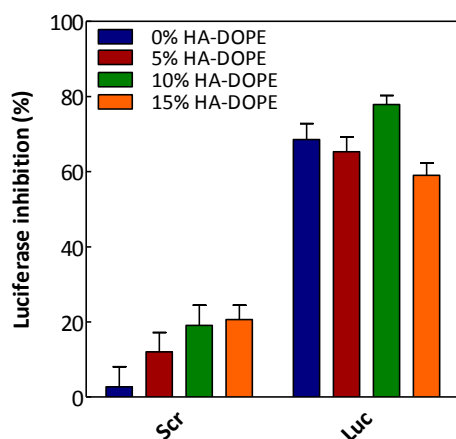


Figure 5. Luciferase expression inhibition in A549-luc cells by siRNA lipoplexes at +/- ratio 2 prepared with 0, 5, 10 or 15% HA-DOPE conjugate and scramble (scr) or luciferase-siRNA (luc). Cells were incubated with lipoplexes for 48 h before luminescence measurements (n=8).

***In vivo* activity of lipoplexes**

The results obtained using the A549-luc model *in vitro* demonstrated the relevance of the siRNA delivering system that we developed. The increased internalization of the lipoplexes, cytoplasm localization and luciferase inhibition results encouraged the evaluation of the *in vivo* activity of the HA-lipoplexes. It was our interest to use a model that could mimic as best as possible the biological conditions of a tumor, and with this in mind, we developed a metastatic lung tumor model using the A549-luc cell line. Tumor-bearing mice were treated for 3 consecutive days with HA-lipoplexes +/- ratio 2, and luminescence signals were quantified using the In Vivo Image System (IVIS), an instrument that allows the measurement of the bioluminescence in living animals. This feature brings the important advantage of sensibly reducing the number of animals and following the behavior on the same individual at any time point. Images of the thoracic region of each animal before and after treatment were compared. The effect of HA-lipoplexes on luciferase expression inhibition, although modest, was clearly demonstrated in comparison to the controls. At this point we were interested in observing the effect of the modification of lipoplexes with HA in the lung distribution after intravenous administration of the lipoplexes. For this, we treated healthy CF-1 mice with fluorescently labeled lipoplexes, and analyzed by microscopy the lung distribution of both plain and HA-lipoplexes at +/- ratio 2. A clear difference in tissue distribution was observed between these two types of particles, which evidenced the advantage of the HA modification of the lipoplexes. While a more intense and homogenous lipoplex-related fluorescence was found in the airway tissue of animals treated with HA-lipoplexes, only weak fluorescence spots were observed for the non-modified lipoplexes. This clearly showed that the presence of HA on the surface of lipoplexes improved the distribution in the lung

tissue. This result correlates with the siRNA expression inhibition measured by the decrease in luminescence and in the expression of luciferase mRNA in the lungs. They indicate that after intravenous administration, the increase in hydrophilicity of lipoplexes promoted by their modification with HA favors a prolonged circulation time and accumulation in the lungs, where lipoplexes can interact with tumor CD44 receptors. Together, these results demonstrate the ability of HA-lipoplexes of carrying siRNA *in vivo* to tumor cells, being therefore relevant candidates for CD44-targeted siRNA therapy.

Mucus diffusion of lipoplexes after endotracheal administration

This last part of my thesis was motivated by many studies that discuss the possibility of using HA as an alternative to PEG[27-30] as biocompatible hydrophilic coating of nanoparticles, and the coating of particles with hydrophilic polymers (e.g., PEG, pluronic) as a strategy to develop mucus-penetrating particles (MPP). We were interested in evaluating the viability of administering our lipoplexes through the endotracheal route for the eventual targeting of CD44 overexpressing lung cancerous cells. The direct administration of lipoplexes to the lungs could allow a higher efficiency of the treatment with possibly less amount of particles and siRNA being administered. With this aim, we studied the diffusion of lipoplexes in mucus using the multiple particle tracking (MPT) technique. A PEGylated formulation of the lipoplexes, PEG/HA-lipoplexes (10% HA, +/- ratio 8), with a neutral surface charge and therefore theoretically more prone to move through the mucus mesh, was also studied. Both HA-lipoplexes (10% HA-DOPE, +/- 2) and PEG/HA-lipoplexes (10% HA, +/- 8) presented a rapid diffusion in the mucus compared to the non-modified particles, which indicated that the presence of HA on lipoplex surface reduced the interactions with mucus components. The analysis of the distribution of these lipoplexes in the mouse lung after pulmonary administration showed that HA-lipoplexes had a larger distribution than the plain lipoplexes, with defined fluorescent regions being observed, while PEG/HA-lipoplexes were intensely distributed in a homogenous pattern throughout the lung tissue. Contrarily to the results after intravenous administration, a luciferase expression inhibition was not observed after the *in vivo* administration of HA-lipoplexes through the endotracheal route. We hypothesized several explanations that could be likely related to this observation, including particle clearance, phagocytosis by mucus macrophages and the impossibility to reach endothelial lungs cells, since the distribution of airway-instilled lipoplex may involve different regions of the lung than that of intravenously injected material [31]. Nevertheless, we believe that the further investigation of the PEGylated HA-lipoplex formulation is of interest, since they showed promising mucus penetrating properties and *in vivo* lung distribution, and can thus offer a combination of both CD44-targeting and mucus penetration properties.

Conclusions and Perspectives

An efficient CD44-targeting lipoplex system for gene expression inhibition using siRNA was developed. Lipoplexes modified with HA were easy to prepare, and thanks to their oligolamellar structure, they were able to achieve high siRNA loading. The interest of the HA-DOPE conjugate for the modification of the lipoplexes was demonstrated in terms of improving stability in physiological media and providing affinity to CD44 receptors. Receptor-mediated internalization was confirmed *in vitro*, as lipoplexes were shown to effectively transport siRNA to the cytoplasm of the targeted cells, where they actively inhibited gene expression. HA-lipoplexes were also able to deliver *in vivo* a dose of intact siRNA to the CD44-overexpressing lung cancer cells, and promote gene silencing in the tumor.

HA-modified siRNA lipoplexes showed promising mucus penetrating ability and the addition of PEG to their structure further improved lipoplexes diffusion in the lungs. Taken together, these results confirm that HA-lipoplexes are able to efficiently release siRNA within the cell cytoplasm *in vitro* and *in vivo*.

Capillary electrophoresis studies allowed the quantification of the HA-DOPE conjugate attached to the lipoplexes. A further exploration of the supramolecular structure of these particles could be performed, with the quantification of the amount of HA present on the surface of the particles. The distinction between the HA portion on the surface and the portion inside the lipoplexes would be of interest and could be related to the binding to CD44 receptors. This measurement would be possible after exposure of HA-lipoplexes to hyaluronidases, which would separate the portion of the HA localized at the surface of the lipoplexes.

An important future goal would be to study lipoplexes biodistribution after intravenous administration. This analysis would elucidate the contribution of the active CD44-targeting promoted by HA and of the furtivity promoted by the hydrophilic coating of the lipoplexes to the gene silencing effect observed.

The PEGylated HA-lipoplexes showed promising mucus diffusion *in vitro* and after endotracheal administration. Therefore, an investigation of their macromolecular structure and organization in comparison to (non-PEGylated) HA-lipoplexes should be carried out, as well as their *in vivo* gene expression inhibition. This further modification of the lipoplex surface could also represent an improvement in terms of particle stability when the intravenous administration of the particles is considered. PEGylation would help decrease HA-lipoplexes interaction with plasma components and improve tumor accumulation and receptor targeting, and consequently gene silencing activity.

References

1. Wang, J., et al., *Delivery of siRNA therapeutics: barriers and carriers*. Aaps j, 2010. **12**(4): p. 492-503.
2. Surace, C., et al., *Lipoplexes targeting the CD44 hyaluronic acid receptor for efficient transfection of breast cancer cells*. Molecular Pharmaceutics, 2009. **6**(4): p. 1062-1073.
3. Wojcicki, A.D., et al., *Hyaluronic acid-bearing lipoplexes: Physico-chemical characterization and in vitro targeting of the CD44 receptor*. Journal of Controlled Release, 2012.
4. Reya, T., et al., *Stem cells, cancer, and cancer stem cells*. Nature, 2001. **414**(6859): p. 105-11.
5. Abraham, B.K., et al., *Prevalence of CD44+/CD24-/low cells in breast cancer may not be associated with clinical outcome but may favor distant metastasis*. Clin Cancer Res, 2005. **11**(3): p. 1154-9.
6. Tiezzi, D.G., et al., *CD44+/CD24- cells and lymph node metastasis in stage I and II invasive ductal carcinoma of the breast*. Med Oncol, 2012. **29**(3): p. 1479-85.
7. Noble, P.W., *Hyaluronan and its catabolic products in tissue injury and repair*. Matrix Biol, 2002. **21**(1): p. 25-9.
8. Deed, R., et al., *Early-response gene signalling is induced by angiogenic oligosaccharides of hyaluronan in endothelial cells. Inhibition by non-angiogenic, high-molecular-weight hyaluronan*. Int J Cancer, 1997. **71**(2): p. 251-6.
9. Yerushalmi, N. and R. Margalit, *Hyaluronic acid-modified bioadhesive liposomes as local drug depots: effects of cellular and fluid dynamics on liposome retention at target sites*. Arch Biochem Biophys, 1998. **349**(1): p. 21-6.
10. Arpicco, S., et al., *Synthesis, characterization and transfection activity of new saturated and unsaturated cationic lipids*. Farmaco, 2004. **59**(11): p. 869-78.
11. Koltover, I., et al., *An inverted hexagonal phase of cationic liposome-DNA complexes related to DNA release and delivery*. Science, 1998. **281**(5373): p. 78-81.
12. Mönkkönen, J. and A. Urtti, *Lipid fusion in oligonucleotide and gene delivery with cationic lipids*. Advanced Drug Delivery Reviews, 1998. **34**(1): p. 37-49.
13. Hirsch-Lerner, D., et al., *Effect of "helper lipid" on lipoplex electrostatics*. Biochimica Et Biophysica Acta-Biomembranes, 2005. **1714**(2): p. 71-84.
14. Filion, M.C. and N.C. Phillips, *Toxicity and immunomodulatory activity of liposomal vectors formulated with cationic lipids toward immune effector cells*. Biochimica et Biophysica Acta (BBA) - Biomembranes, 1997. **1329**(2): p. 345-356.
16. Qhattal, H.S.S. and X.L. Liu, *Characterization of CD44-Mediated Cancer Cell Uptake and Intracellular Distribution of Hyaluronan-Grafted Liposomes*. Molecular Pharmaceutics, 2011. **8**(4): p. 1233-1246.
17. Gershon, H., et al., *Mode of formation and structural features of DNA-cationic liposome complexes used for transfection*. Biochemistry, 1993. **32**(28): p. 7143-7151.
18. Mok, K.W. and P.R. Cullis, *Structural and fusogenic properties of cationic liposomes in the presence of plasmid DNA*. Biophys J, 1997. **73**(5): p. 2534-45.
19. Gonçalves, E., R.J. Debs, and T.D. Heath, *The effect of liposome size on the final lipid/DNA ratio of cationic lipoplexes*. Biophysical Journal, 2004. **86**(3): p. 1554-1563.
20. Felgner, J.H., et al., *Enhanced gene delivery and mechanism studies with a novel series of cationic lipid formulations*. Journal of Biological Chemistry, 1994. **269**(4): p. 2550-2561.
21. Liu, Y., et al., *Factors influencing the efficiency of cationic liposome-mediated intravenous gene delivery*. Nat Biotechnol, 1997. **15**(2): p. 167-73.
22. Ross, P.C. and S.W. Hui, *Lipoplex size is a major determinant of in vitro lipofection efficiency*. Gene Ther, 1999. **6**(4): p. 651-9.
23. Peer, D., et al., *Systemic leukocyte-directed siRNA delivery revealing cyclin D1 as an anti-inflammatory target*. Science, 2008. **319**(5863): p. 627-630.

24. Landesman-Milo, D., et al., *Hyaluronan grafted lipid-based nanoparticles as RNAi carriers for cancer cells*. Cancer Letters, 2013. **334**(2): p. 221-227.
25. De Rosa, G., et al., *Novel cationic liposome formulation for the delivery of an oligonucleotide decoy to NF-kappaB into activated macrophages*. Eur J Pharm Biopharm, 2008. **70**(1): p. 7-18.
26. Lonez, C., M. Vandenbranden, and J.-M. Ruysschaert, *Cationic lipids activate intracellular signaling pathways*. Advanced Drug Delivery Reviews, 2012. **64**(15): p. 1749-1758.
27. Jiang, T., et al., *Dual-functional liposomes based on pH-responsive cell-penetrating peptide and hyaluronic acid for tumor-targeted anticancer drug delivery*. Biomaterials, 2012. **33**(36): p. 9246-9258.
28. Peer, D. and R. Margalit, *Loading mitomycin C inside long circulating hyaluronan targeted nano-liposomes increases its antitumor activity in three mice tumor models*. Int J Cancer, 2004. **108**(5): p. 780-9.
29. Peer, D. and R. Margalit, *Tumor-targeted hyaluronan nanoliposomes increase the antitumor activity of liposomal Doxorubicin in syngeneic and human xenograft mouse tumor models*. Neoplasia, 2004. **6**(4): p. 343-53.
30. Mizrahy, S., et al., *Hyaluronan-coated nanoparticles: the influence of the molecular weight on CD44-hyaluronan interactions and on the immune response*. Journal of Controlled Release, 2011. **156**(2): p. 231-238.
31. Uyechi, L.S., et al., *Mechanism of lipoplex gene delivery in mouse lung: binding and internalization of fluorescent lipid and DNA components*. Gene therapy, 2001. **8**(11): p. 828-836.
32. Stewart, J.C.M. *Colorimetric determination of phospholipids with ammonium ferrothiocyanate*. Analytical biochemistry, 1980. **104**(1): p. 10-14.

Remerciements / Acknowledgements / Agradecimentos

A la fin de ces années de thèse, j'adresse mes plus vifs remerciements à mon directeur de thèse, Prof. Elias Fattal, pour l'accueil chaleureux, pour m'avoir donné la possibilité de travailler dans un cadre de travail pluridisciplinaire, dynamique, agréable et amusant, facteurs très importants pour le bon déroulement de ce projet. Merci pour la confiance à mon travail, pour la disponibilité et ouverture professionnel et personnel.

Je tiens également à remercier mon co-encadrant de thèse, Dr. Herve Hillaireau, pour les précieux conseils scientifiques, patience et motivation, qui m'ont permis de grandir en tant que chercheur et d'aiguiser mes sens scientifiques.

Un grand merci à Dr. Nicolas Tsapis, pour la disponibilité, les conseils scientifiques et personnels. Pour l'exemple de simplicité et efficacité de gérer les situations. Je remercie également le Dr. Amélie Bochot, pour l'aide au début de la thèse, la disponibilité et les discussions toujours pertinentes. Merci aussi à Juliette Vergnaud pour son aide avec les expériences *in vitro*, la disponibilité et les conseils.

Je remercie le Docteur Silvia Arpicco pour la gentil collaboration pour la préparation du lipide DE et d'avoir accepté d'examiner mon travail. De même, je remercie aux Professeurs Nathalie Mignet et Didier Betbeder de m'avoir fait l'honneur d'être les rapporteurs de ce travail. Je remercie également le Professeur Myriam Taverna pour son encadrement lors des expériences d'électrophorèse capillaire, ainsi que pour sa participation à ce jury.

Un merci particulier à Magali Noiray pour son importante aide manuelle et scientifique avec les manip d'interactions moléculaires (BIACORE et ITC), les conseils et discussions. Merci beaucoup à Delphine Courilleau pour son aide avec les expériences de quantification de luminescence *in vitro*. Merci à Helene Chacun, pour ses conseils lors des expériences en radioactivité et sa gentillesse. Merci à Claudine Delomenie pour son précieuse aide avec les expériences de PCR. Merci à Donato Cosco pour les échanges scientifiques et les conseils lors de la caractérisation du conjugué HA-DOPE.

Merci à toute l'équipe 5 et l'institut Galien Paris-Sud pour les échanges scientifiques et les bons moments passés ensemble pendant mon séjour à Châtenay.

Je tiens à remercier particulièrement aussi Letícia Aragão Santiago, Sabrina Valetti, Giovanna Giacalone, Rachel Ouvinha de Oliveira e Acarília Eduardo da Silva pour leur précieuses amitiés. À Alice Gaudin, Vianney Delplace, Romain Canioni et Tanguy Boissenot pour les bons moments passés ensemble. À Duy Pham, Naila Elkechaj, Patricia Calleja, Ludivine Mousnier, Chantal Al Sabbagh, Rosana Simón, Adam Bohr et Guilherme Picheth, pour la compagnie pendant ces années de thèse. À Walhan Alshaer pour les discussions, scientifiques ou non. À Dominique pour sa gentillesse et aide lors des affaires administratifs. À Andrey Maksimenko pour les conseils sur les manip *in vivo* et les histoires amusantes.

Un immense merci à Melania Rivano, pour son enthousiasme et dédicace lors de son stage de master, et son aide avec les expériences *in vivo*. Aussi à Barbara Tessier pour l'expérience d'enseignement.

My sincere thanks also go to Professor Justin Hanes, for having received me in his laboratory for the multiple particle tracking and lung distribution experiments. I am very thankful as well to Jung Soo Suk for his guidance and Gregg Duncan for his help with the experiments, the discussions and the pleasant moments spent in the lab.

Finalmente, agradeço à minha família pelo apoio durante esses anos de tese.